

**EXPERIMENTAL VERIFICATION
OF DYNAMIC OPERATION OF
CONTINUOUS AND MULTIVESSEL
BATCH DISTILLATION COLUMNS**

by
Bernd Wittgens

A Thesis Submitted for the Degree of Dr. Ing.

The Norwegian University of Science and Technology

Submitted September 1999

ERRATA

22. November. 1999

Some results in Chapter 2 were unfortunately omitted in the final editing of the Chapter. The reader is referred to the paper "Evaluation of Dynamic Models of Distillation Columns with Emphasis on the Initial Response" by Bernd Wittgens and Sigurd Skogestad, presented at: DYCORDER'95, 7-9 June 1995, Helsingør, Danmark (see Appendix F). In sections three to six of the paper and also Appendix B and C of the thesis, methods to determine operational parameters from experiment are presented. Further results concerning the importance of linearized tray hydraulics which were omitted in the thesis are given.

In Table B.11, page 201, the coefficients of Equation B.53 are:

Procedure	π_1	π_4	π_3
D	-11.44	0.63	1.0
D2R	-24.17	0.73	1.0
D2S	-7.03	0.61	1.0

Abstract

Distillation is probably the most important unit operation in chemical industries for the separation of liquid mixtures into pure products. In a single batch distillation column, multicomponent mixtures can be separated into a number of product fractions, whereas in continuous distillation a sequence of columns is necessary to perform the same task. Batch distillation columns offer greater flexibility with respect to variations of feed mixtures, feed composition, relative volatilities and product specification. However, batch distillation columns in general require more energy input compared to a continuous distillation column. A newly developed batch distillation column, for the simultaneous separation of a multicomponent mixture might represent a process which combine the energy consumption of continuous distillation and the flexibility of conventional distillation.

In recent years research on the dynamics of distillation column was focused on the development of models suitable for dynamic simulation of the composition dynamics. The purpose of research was on *e.g.* the selection of control structures. Few of these models were verified experimentally on distillation columns. A rigorous model based on first principles of a staged high purity continuous distillation column is presented and experiments are performed to verify the model. The importance of the tray hydraulics to obtain good agreement between simulation and experiment is demonstrated. Further, analytical expressions are derived for hydraulic time constants for the application in models with simplified liquid and vapor dynamics.

Over the last centuries, chemical industries has more and more changed from conventional batch columns to continuous distillation columns, because of the lower energy demand. However, this trend is about to change especially in the production of fine chemicals or pharmaceuticals where batch distillation is recently becoming more important. The production of fine chemicals is characterized by small amounts of product and frequent changes with respect to feedstock and product specifications. With this renewed interest, investigations on the operation of batch distillation processes are needed or alternatively, new column configurations should be considered.

The newly developed multivessel batch distillation column consists of a reboiler, intermediate vessels and a condenser vessel and provides a generalization of previously proposed batch distillation schemes. The total reflux operation of the multivessel batch distillation column was presented recently, a simple feedback control structure based on temperature measurements has been developed. The feasibility of this strategy is demonstrated by simulations and verified on a laboratory scale multivessel column. The experiments show very good agreement with the simulations, and confirm that the multivessel column can be easily operated with simple temperature controllers. A simple procedure to determine the setpoint of the temperature controller is presented and show that final product compositions are independent on the feed composition.

The multivessel batch distillation column is compared to a conventional batch column, both operated under feedback control. It is found that the energy consumption for separation of a multicomponent mixtures into high purity product requires considerably less energy in a multivessel column compared to a conventional batch distillation column. Besides the reduction in energy consumption the much simpler operation of the new column is established.

Acknowledgement

I am grateful to my supervisor, Sigurd Skogestad, for his great encouragement and guiding me into the scientific world. The numerous discussions with him have always been fruitful and inspiring. Further, I am grateful for his patience and moral support throughout the work.

Thanks to all present and past members of the staff of the Department of Chemical Engineering, especially the process control group at NTNU for a good time and many interesting discussions, both on research projects as well as on less serious matters. In particular, I would like to thank Eva Sørensen who endured me during the first years of this study.

Many friends have been important to me over the years. In particular I have shared lots of good time with Jørn & Trude Skogø and Christian Steinebach who shared both ups and downs with me. Thanks also to all members of “Trondhjem’s Kajakk Klubb” of Trondheim for the mostly exciting and usually time consuming kajak-trips in Norway.

Most of all I would like to thank the one which has suffered the most during the final “phase” of this work, Ann Elisabet Østvik, she gave me all the support I needed through this rather demanding time.

My family has always been important to me. Nevertheless, I am most off all grateful to my very first teacher, who has always supported me and I therefore dedicate this thesis to my mother.

Financial support from the Royal Norwegian Council for Scientific and Industrial Research (DEMINEX-Program) and the Norwegian University of Science and Technology is gratefully acknowledged.

Contents

1	Introduction and Literature Review	3
1.1	Motivation	3
1.2	Distillation dynamics and modeling	5
1.2.1	Rigorous Models	6
1.2.2	Simplified models	8
1.2.3	Constant molar flow model	9
1.2.4	Simplification of the liquid dynamics	9
1.3	Continuous Distillation	10
1.3.1	Initial response in Continuous distillation columns	11
1.3.2	Experimental determination of operational parameters	11
1.4	Batch Distillation	12
1.4.1	Conventional batch column	13
1.4.2	Heat integrated batch columns	14
1.4.3	Middle Vessel Column	15
1.4.4	Multiple-effect Batch Distillation System	15
1.4.5	Multivessel Batch Distillation Column	16
1.5	Thesis overview	18
	Bibliography	18
2	Evaluation of Dynamic Models of Distillation Columns with Emphasis on the Initial Response	23
2.1	Introduction	23
2.2	Modelling	24
2.2.1	Rigorous Tray Model	24
2.3	Simplified Model with Linearized Tray Hydraulics	28
2.3.1	Tray Model	29
2.3.2	Linearized Tray Hydraulics	29
2.4	Obtain operational parameters from experiment	32
2.4.1	Liquid holdup and distribution on tray M_l and M_d	32
2.4.2	Liquid hydraulic time constant τ_l	33
2.4.3	Vapor constant λ	34
2.5	Results	34
2.5.1	Holdup estimation	34
2.5.2	Hydraulic time constant	35

2.5.3	Comparison of initial time constant of Experiment and Simulation	36
2.6	Conclusion	39
	Bibliography	39
	Notation	40
3	Multivessel Batch Distillation	43
3.1	Introduction	43
3.2	Simulation model	46
3.3	Total reflux operation with constant vessel holdups	47
3.4	Feedback control of multivessel column	49
3.5	Achievable separation	51
3.6	Discussion	52
3.7	Conclusions	53
	Bibliography	57
	Notation	58
	Appendix	58
4	Closed Operation of Batch Distillation - Experimental Verification	61
4.1	Introduction	61
4.2	Multivessel Batch Distillation Pilot Plant	62
4.3	Experimental Results	65
4.3.1	Experiment 12: Feed initially in reboiler	67
4.3.2	Experiment 4: Feed initially distributed	67
4.3.3	Experiment 2: Product composition trajectory	67
4.4	Simulation of experiment 12	71
4.5	Discussion	74
4.5.1	Main lessons from the experiments	74
4.5.2	Suggestions for controller tunings	75
4.5.3	Justification for column temperature control	77
4.5.4	Alternative control variables	78
4.5.5	Optimal operation	79
4.5.6	Closed operation of conventional batch distillation	79
4.6	Conclusions	80
	Bibliography	81
	Notation	81
5	Alternative Control Structure of Multivessel Batch Distillation	83
5.1	Introduction	83
5.2	Total Reflux Operation	85
5.3	Composition control by feedback	88
5.3.1	Feedback from vessel composition	89
5.3.2	Feedback from control tray composition	92
5.3.3	Feedback control based on tray temperatures	94

5.4	Alternative Start-up Procedure	103
5.5	Discussion	108
5.6	Conclusions	109
	Bibliography	109
	Notation	110
6	Comparison of Multivessel and Conventional Batch Distillation	113
6.1	Introduction	114
6.2	Column configurations	114
6.2.1	Conventional batch distillation	114
6.2.2	Multivessel batch distillation	115
6.3	Simulation model	116
6.4	Operation policies	116
6.4.1	Conventional batch distillation	116
6.4.2	Multivessel batch distillation	118
6.4.3	Operation conditions	118
6.5	Results	120
6.5.1	Conventional batch distillation: Production rate	120
6.5.2	Multivessel batch distillation: Production rate	120
6.5.3	Multivessel batch distillation: Achievable separation	123
6.5.4	Multivessel batch distillation: Influence of the controller setpoint	124
6.6	Discussion	126
6.7	Conclusions	129
	Bibliography	129
	Notation	130
	Appendix	131
7	Discussion, Conclusions and Future Work	133
7.1	Discussion	133
7.2	Conclusions	134
7.3	Future work	136
7.3.1	Continuous distillation	136
7.3.2	Multivessel batch distillation	136
A	Experimental facilities	139
A.1	Continuous distillation tower	139
A.1.1	Tray design	139
A.1.2	Reboiler	142
A.1.3	Total condenser and accumulator	142
A.1.4	Peripheral equipment	143
A.1.5	Instrumentation	144
A.1.6	Data acquisition and control	146
A.1.7	Control of manipulated variables	146
A.2	Multivessel batch distillation unit	147

A.2.1	Instrumentation	147
A.2.2	Control structure	149
A.2.3	Design and operation data	149
A.2.4	Data Acquisition and control	150
A.3	Product composition analysis	151
A.4	Distilled system	154
B	Obtain operational parameters of a distillation column	157
B.1	Initial temperature response	159
B.1.1	Definition of the initial time constant	159
B.1.2	Hydraulic time constant estimated from experiment	159
B.1.3	Experimental procedure to obtain the initial temperature response	161
B.1.4	Results initial temperature response	162
B.1.5	Estimation of the tray holdup from initial temperature response	173
B.1.6	Results tray holdup estimation	175
B.2	Experiments to obtain the hydraulic time constant	178
B.2.1	Results	178
B.2.2	Discussion	181
B.3	Experimental determination of the residence time	182
B.3.1	Experimental procedure of tracer injection experiments	182
B.3.2	Results	182
B.3.3	Discussion of experimental procedure	187
B.3.4	Modeling of tracer experiment	187
B.4	Obtain column holdup	194
B.4.1	Dumping of the column	194
B.4.2	Modeling of the column pressure drop	194
B.4.3	Parameter Estimation for the simulation model	200
B.4.4	Results	203
B.4.5	Holdup prediction	204
B.4.6	Discussion	205
B.5	Summary of experiments	205
	Bibliography	208
	Notation	209
C	Linearized Tray Hydraulics	211
C.1	Tray hydraulics	211
C.2	Estimation of hydraulic time constants from column design data	213
C.3	Linearization of hydraulics	216
C.4	Summary: Hydraulic time constants	220
C.4.1	Comparison: Experiment - Simulation	223
D	Multivessel Batch Distillation, Modeling aspects	225
D.1	Introduction	225

D.2	Simulation model	225
D.2.1	Mass and Component Balance	225
D.2.2	Vapor Liquid Equilibrium	227
D.2.3	Thermodynamic model	227
D.3	Comparison simulation models	229
D.4	Design of the experimental system	234
D.5	Discussion	236
D.6	Conclusions	238
	Bibliography	239
E	Experiments: Multivessel Batch Distillation	241
E.1	Experiment 1	241
E.2	Experiment 2, 06.december.1995	248
E.3	Experiment 3, 22. march. 1996	251
E.4	Experiment 4, 03. april. 1996	253
E.5	Experiment 7, 04. october. 1996	255
E.6	Operation with three components	257
F	Evaluation of Dynamic Models of Distillation Columns with Emphasis on the Initial Response	259
F.1	Introduction	259
F.2	Tray Modeling	261
F.2.1	Rigorous Tray Model	261
F.2.2	Tray hydraulics	263
F.3	Linear Tray Hydraulics	265
F.3.1	Linear flow relationships for column sections	267
F.4	Obtaining parameters from experiments	268
F.4.1	Liquid holdup	268
F.4.2	Liquid hydraulic time constant τ_l	269
F.4.3	Vapor constant λ	269
F.5	Results	269
F.5.1	Pressure drop	270
F.5.2	Liquid holdup	270
F.5.3	Liquid hydraulic time constant τ_l	272
F.5.4	Vapor constant λ	273
F.6	Discussion and Conclusion	274
	Bibliography	275
	Notation	276

Chapter 1

Introduction and Literature Review

Abstract

This chapter give a brief description of the two types of distillation columns considered in this thesis. The remainder of this chapter is divided into two major parts; first an overview of the literature concerning modeling of the initial response of distillation columns, the second part is focused on the control of a newly developed distillation arrangement, the multivessel batch distillation column. The introductory chapter concludes with a description of the following chapters of the thesis.

1.1 Motivation

Distillation is an essential unit operation in chemical industries, *e.g.* for the purification of final products or for the recovery of components due to environmental aspects. The distillation of chemical mixtures can be performed both by means of batch or continuous operation. A schematic of a continuous distillation column including a control structure is shown to the left in Figure 1.1. A generalized batch distillation column (further called multivessel batch distillation column) with a feedback control structure is shown to the right of Figure 1.1.

During the last decades, the academic research community have focused their activities more on the energy consumption of the process by improving the operation of this process in general and its design. In the chemical industries distillation columns are high energy consumers with up to 40 % of the total energy consumption of the plant.

Continuous distillation columns are used for the separation of bulk chemicals where high throughput and few feed or product changes are expected. The design of the processes concerns rather often one feed mixture which is about to be separated, the unit is then optimized with respect to productivity and energy consumption. Batch distillation with its inherent flexibility becomes increasingly important in the production of fine chemicals and pharmaceuticals, where product is characterised by small amounts and high added value. Batch distillation is able to recover a number of different products from one multicomponent feed charge, a wide range of feed compositions and relative volatilities can be handled in one sin-

gle column. In a conventional batch distillation, one component at a time is separated from the mixture when multicomponent mixtures are separated. Generally, batch distillation is applied for low throughput operations where the higher capital costs of a continuous distillation unit are not justified.

A generalization of the conventional batch distillation column is the multivessel batch distillation column, in its most flexible form, a superstructure for batch distillation columns with an energy consumption comparable to a continuous distillation for a given separation.

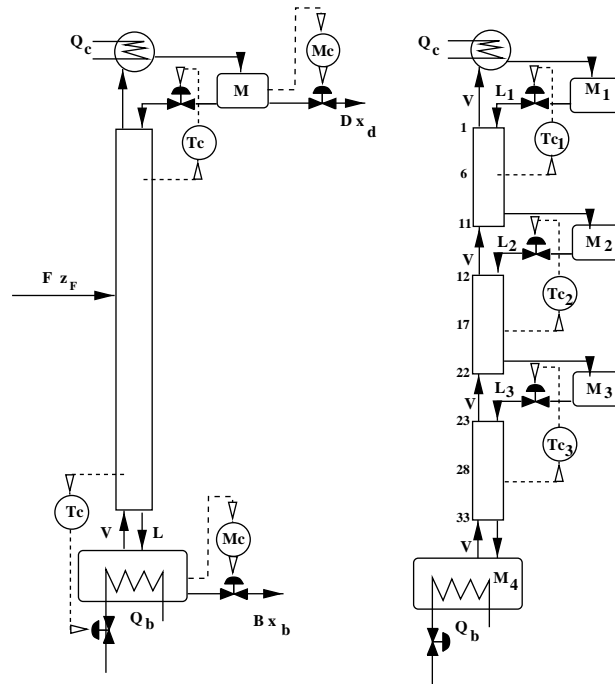


Figure 1.1: Flowsheet of a continuous (left) and multi vessel batch distillation column (right)

Although distillation is one of the most intensively studied processes in the chemical industry, still it represents an interesting field for research:

- The academic research in distillation is primarily directed towards the optimization of the operation and the process itself. Further, dynamic studies are performed concerning the control of this process, which is characterized by excessive control interaction of the manipulated variables. For this purpose models of different complexity are developed and applied with satisfactory accuracy for simulation studies, both with respect to the dynamic and steady state behavior of the process. However, few of these models are validated experimentally on distillation plants.
- Batch distillation is probably the “oldest” unit operation in chemical industries. The operation policy of industrial installations is not fundamentally different from laboratory equipment, which means that rather simple operation policies are applied. Increasing demand for efficiency, both with respect to energy consumption and product

recovery, opens for research focused on new operation policies. Further, the combination of several units to some kind of “superstructure” which combines flexibility with respect to feed mixtures, ease of operation and reduced energy consumption is an important research area.

1.2 Distillation dynamics and modeling

Review articles in the area of distillation column dynamics and control are published quite frequently and give a rather good insight in ongoing research. Early articles consider mainly steady state operation of distillation columns, the introduction of digital computing enable the investigation of the dynamics in the early 1950's. The pioneering work in distillation dynamics is reviewed in the work by Rosenbrok (1962). The book by Rademaker (1975) includes a detailed investigation on the material and energy balance of staged distillation column, further the influence of the flow dynamics on the composition dynamics is considered. Reviews on dynamics and control were published by Tolliver and Waggoner (1980), McAvoy and Wang (1986) and Skogestad (1997). Practical recommendations for the control of distillation columns are published by Shinskey (1984) and Luyben (1992) considering dual composition control, including the issue of control configurations selection.

There is a continuous development of rigorous models of distillation columns for process control and dynamic studies. Nevertheless, few of these models solve the material and energy balance on each plate using models which incorporate plate hydraulics and the downcomer dynamic. Further, the performance of the process can seldom be predicted by models which exclude fluid hydraulics and change of physical properties.

However, the application of highly complex models for control studies is not always necessary. The existence of a rigorous model of the system enables the study of the relative importance of different features and can verify simplifications of simplified models. The objective of a model is to describe a dynamic system as precise as necessary and the complexity of the model considered is strongly dependent on the intended use of the model. Models with neglected tray hydraulics are sufficient for the steady state optimization of an entire plant, while they are insufficient in the selection process of a new control system.

For the development, validation and verification of a control system, the model has to represent the initial response of a given unit to step changes of the manipulated variables or disturbances correctly, since the control system is supposed to limit deviations from the intended point of operation. Further, the process of modeling has to consider the design data of a particular tray, the operation point of the plant and will often encounter the use of empirical functions to describe some phenomena. Correct modeling of *e.g.* the hydraulic time constant of the liquid flow is important in this respect. The liquid lag over a staged column decouples the composition response of the column, which is from a control point of view an advantage, since it opens for somewhat slower composition measurements.

Low order dynamic models can be used for several purposes, for example for the derivation of analytical expressions to gain deeper insight into the dynamic behavior of a process. Further, low order model can be applied for simulation and controller design. However, the derivation of low order models from rigorous models by combining sub-models (one for the

dominant composition dynamics, one for the holdups) may result in inconsistent models. Jacobsen *et al.* (1991) suggested to derive low order linear models from (numerical) linearizing the nonlinear rigorous model combined with subsequent model reduction.

1.2.1 Rigorous Models

Models are often classified as “rigorous” or “simplified” models. Rigorous models for equilibrium stages consist of mass and energy balance which include some kind of flow and pressure dynamic as well as the thermodynamic relations. The flow dynamic describe the changes in liquid holdup on a stage because of variations in liquid and vapor flow, while the pressure dynamic primary influence the vapor holdup on a stage. Considering the stage design (see Figure 1.2) of a column the liquid holdup has (sometimes) to be split into liquid on the tray and downcomer which result in twice as much states per stage. Nevertheless, even in the most rigorous model certain simplifications as thermal and mechanical equilibrium or assumption of perfect mixing in the phases are introduced. The thermodynamic equilibrium (vapor liquid equilibrium) can be corrected by introducing a simple Murphree tray efficiency for each component. Commonly, the effect of heat losses to the surroundings and the dynamic of the column structure are neglected.

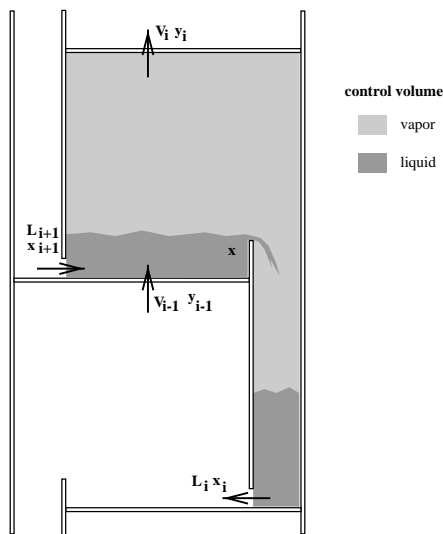


Figure 1.2: Control volume on a stage

Assumptions for an equilibrium based stage model:

- A1 perfect mixing in both liquid and vapor phase
- A2 thermodynamic and mechanical equilibrium (assume 100 % tray efficiency)
- A3 neglect heat loss and thermal capacity of column structure
- A4 consider only normal operation (*e.g.* no flooding, weeping)

Assumptions A3 and A4 can be removed easily by extending the model.

The differential-algebraic system of equations to describe a “staged” distillation column (see Figure 1.2) based on a UV-flash, consist of the component-mass balance:

$$\begin{aligned} \frac{dM_i}{dt} = & L_{i+1} \cdot x_{i+1,j} - L_i \cdot x_{i,j} \\ & + V_{i-1,j} \cdot y_{i-1,j} - V_i \cdot y_{i,j} \end{aligned} \quad (1.1)$$

where $M_i = M_{l,i} + M_{v,i}$ with $M_{i,j}$ as component holdup of component j on stage i . This are $N_c - 1$ independent component balances since $M_i = \sum_i^{N_c} M_{i,j}$. $M_{l,i}$ represents the entire liquid holdup (tray and downcomer) and $M_{v,i}$ the molar holdup of the vapor phase. Both liquid and vapor phase are subjected to some dynamics because of changes in liquid and vapor flow (flow dynamics, see Equations 1.3 and 1.4).

The energy balance over the stage

$$\frac{dU_i}{dt} = L_{i+1} \cdot h_{l,i+1} - L_i \cdot h_{l,i} + V_{i-1,j} \cdot h_{v,i-1} - V_i \cdot h_{v,i} \quad (1.2)$$

with $U_i = M_{l,i} \cdot (h_{l,i} - p/\rho_l) + M_{v,i} \cdot (h_{v,i} - p/\rho_v)$. The flow dynamics of the liquid leaving the tray and downcomer are described by algebraic and empirical equations which link hydraulic and stage design, determined by

$$L_i = f(M_{l,i}, V_{st}, \Delta p_i, geometry) \quad (1.3)$$

and the vapor dynamic

$$V_i = f(M_{v,i}, V_{st}, \Delta p_i, geometry) \quad (1.4)$$

These correlations consider the design of a stage and can be found in *e.g.* Bennett *et al.* (1983), Lockett (1986), Rademaker *et al.* (1975), or Stichlmair (1978). Additionally, thermodynamic relations to describe the flash relation (VLE) given by

$$(U_i, V_{st}, M_i) \rightarrow (x_i, y_i, T_i, p_i, h_{l,i}, h_{v,i}, M_{l,i}, M_{v,i}) \quad (1.5)$$

between liquid and vapor phase are necessary.

Given the above assumption and the constant stage volume implies that a UV-flash has to be solved. The definition of a UV-flash is: Given the internal energy U , volume of a stage, V_{st} and the component holdup $M_{i,j}$, a flash calculation is performed computing the ratio of vapor and liquid on the stage ($M_{l,i}$ $M_{v,i}$ or phase split), composition of vapor and liquid phase (x_i and y_i), as well as pressure p and temperature T . In a recent review paper on distillation (Skogestad, 1997) are almost no references listed which apply this approach. Papers by Gani *et al.* (1990) on design a simulation of complex chemical process and Flatby *et al.* (1994) seems to be the exception.

An alternative model by Retzbach (1986), propose a rate based mass transfer correlation between phases, including hydraulic and pressure drop correlations. The rigorous model of Retzbach is primarily developed for the nonlinear simulation of a multi-component mixture in a distillation column with side stripper. The tray hydraulic models applied are extensively described by Stichlmair (1978), simplifications are introduced to simplify for application of the model in a control structure synthesis.

1.2.2 Simplified models

Solving a dynamic distillation column with a that complicated model (see outline in section 1.2.1) often requires a considerable amount of both time and resources (computer power) to solve the set of differential-algebraic equations.

Neglecting the vapor holdup

The most common simplification is to neglect the vapor holdup ($M_{V,i} = 0$), which is valid for moderate pressure (1 - 10 Mpa) distillation, nevertheless for applications were the (molar) vapor holdup exceed 20 %, Choe and Luyben (1987) recommend that the vapor phase is included in mass and energy balance.

The assumption that the vapor phase can be neglected result in somewhat unrealistic responses of the model to a step in vapor flow. The vapor flow change will propagate immediately through the column, this is a step in the flow leaving the reboiler will change the vapor flow at the uppermost stage instantaneous.

Simplified models in the above described manner for nonlinear simulations of distillation columns are developed by *e.g.* Ruiz *et al.* (1986) and Gani *et al.* (1986). The work of Gani *et al.* (1986) is focused on the development of a general dynamic model including tray hydraulics, heat transfer, vapor-liquid equilibrium and prediction of the physical properties which is numerically robust. The most important modeling assumption were the neglection of the vapor holdup and that reboiler and condenser/accumulator are represented through their component mass-balances. These models have been used primary for the simulation of the open- and closed-loop response of distillation columns, investigation of start-up and shut-down procedures and the verification of plate hydraulic design.

The energy and mass balance over a stage are similar to these presented in Equations 1.1 and 1.2, except for where $M_i = M_{l,i}$ and $U_i = M_{l,i} \cdot h_{l,i}$ since the vapor phase is neglected. The liquid hydraulic is given in equation 1.3. The thermodynamic flash calculation performed is a bubble point flash with known component holdup $M_{i,j}$ and specific liquid enthalpy $h_{l,i}$ on each stage.

$$(U_i, V_{st}, M_i) \rightarrow (x_i, y_i, T_i, p_i, h_{l,i}, h_{v,i}, M_{l,i}, M_{v,i}) \quad (1.6)$$

Commonly used is the assumption of constant pressure and negligible vapor holdup in a distillation columns, because pressure is tightly controlled in most applications such that assuming constant pressure seems reasonable.

Simplified energy balance

A common assumption is the approximation of $u_i \approx h_{l,i}$ in cases where the vapor holdup is neglected. The energy balance given in equation 1.2 is reduced to

$$\frac{dU_i}{dt} = \frac{dM_i \cdot h_{l,i}}{dt} = M_i \cdot \frac{dh_{l,i}}{dt} + h_{l,i} \cdot \frac{dM_i}{dt} \quad (1.7)$$

combining Equation 1.7 with the mass balance on a stage (see Equation 1.1) results in

$$M_{l,i} \cdot \frac{dh_{l,i}}{dt} = L_{i+1} \cdot (h_{l,i+1} - h_{l,i}) + V_{i-1} \cdot (h_{v,i-1} - h_{l,i}) + V_i \cdot (h_{l,i} - h_{v,i}) \quad (1.8)$$

This simplification will be reasonable correct even for more extensive holdup changes, since the term dM_i/dt is considered in the energy balance (see Eq. 1.7).

Further simplification of the energy balance is achieved by assuming $dh_l/dt \simeq 0$ and constant liquid enthalpy on all stages, $h_{l,i} = h_l$. This assumption can be used by definition of the correct reference state, which should be the pure component as saturated liquid at a given reference pressure. Applying this definition give different reference temperatures (components boiling points at *e.g.* column pressure).

$$M_i \cdot \frac{dh_{l,i}}{dt} = 0 = V_{i-1} \cdot (h_{v,i-1} - h_{l,i}) + V_i \cdot (h_{l,i} - h_{v,i}) \quad (1.9)$$

from this algebraic energy balance, the vapor flow leaving a stage can be computed for cases where the heat of vaporization of the components is considerably different at the column pressure.

1.2.3 Constant molar flow model

For similar heat of vaporization of the components and the above defined reference states the equimolar flow assumption can be derived, such that the energy balance is finally reduced to

$$V_{i+1} = V_i \quad (1.10)$$

The vapor flow over the entire column is constant, except at places where vapor is introduced or withdrawn from the column. Finally, the mass balance is reduced to

$$\frac{dM_i}{dt} = L_{i+1} - L_i \quad (1.11)$$

The component balance is identical to Equation 1.1. Dynamically, the tray holdup $M_{l,i}$ varies such that the liquid flow over the column is not constant. The liquid dynamic can be described by means of a linearized tray hydraulic (see Eq. 1.12) to model effects of liquid and vapor flow changes on the overall composition response.

In some cases an energy balance as given in equation 1.10 will give a reasonable model in cases where the heat of vaporization of the components are similar. In the opposite case, the internal flow will affect the composition through the composition material balance, while the compositions affect the flow through the energy balance.

1.2.4 Simplification of the liquid dynamics

Details on the flow dynamics for trayed distillation columns are published by Rademaker *et al.* (1975). For models utilized for the development of an *e.g.* feedback control system of a distillation column a linearized tray hydraulics is often suitable. Linearized tray hydraulics are presented by Rademaker *et al.* (1975) and Skogestad (1988)

$$\Delta L_i = \lambda \Delta V_i + \frac{1}{\tau_l} \Delta M_i \quad (1.12)$$

The coefficient λ represent the vapor constant, the initial effect of a vapor flow change on the liquid flow and τ_l is the liquid hydraulic time constant. If we assume constant molar flows, the mass and "energy" balance shown in Equations 1.10 and 1.11 are valid and the flow dynamics is decoupled from the composition dynamic. Laplace transformation of the mass balance 1.11 and repeated combination with equation 1.12 (Rademaker *et al.* 1975) give for disturbances in reflux flow ΔL_T and vapor flow ΔV_B

$$\Delta L_B = g_L \Delta L_T + (1 - g_L) \Delta V_B \quad (1.13)$$

$$g_L = \frac{1}{(1 + \tau_{l,T})^{N_T} \cdot (1 + \tau_{l,B})^{N_B}} \quad (1.14)$$

where $\tau_l \simeq \theta_L/N$.

With N_T and N_B as the number of stages in the rectifier and stripper section respectively. The vapor constant λ and the liquid hydraulic time constant τ_l are dependent on the column loading, such that in general they are different for the individual sections. A more detailed discussion on the hydraulics of a distillation column is given in chapter 2.

1.3 Continuous Distillation

The literature on continuous distillation is extensive, so an indepth review on distillation will not be given in this thesis, the focus will be on aspects of modeling and dynamics important for composition control of continuous distillation.

The dynamics and control of distillation columns involves a multitude of issues. The modeling process of a distillation column involves the choice of a suitable model structure which describe the investigated system sufficiently well for a certain purpose; *e.g.* model used in investigations concerning the control of a distillation unit should consider the flow dynamics. First principle models will be used for the composition dynamics, empirical correlations, considering the design data of a unit, are often applied to take care of flow dynamics.

The identification of model parameters and the verification of models from available operation and design data require an iteration between modeling, simulation and experiment. Determination of model parameters based on simple experiments which can be performed during normal operation of a distillation column will simplify this process. These experiments include *e.g.* traditional step response analysis were one manipulated variable is stepped at a time, tracer injection at the top to determine the liquid holdup and pressure drop measurements over the column sections.

Based on a rigorous model, which is validated on experimental data, model simplifications can be introduced and their influence on the composition response will be investigated. The hydraulics of the liquid and vapor flow could be linearized to achieve low order models, which later aid as a basis for the selection of controller types and structure. In the thesis, the initial response of a distillation column to changes in manipulated variables will be investigated.

1.3.1 Initial response in Continuous distillation columns

Detailed knowledge of the initial response of a distillation column is necessary for the design of a control system. The fast response of a control system rely on the initial behavior of the process. For automatic control the gain from an initial steady state to a final steady state is not that important compared to the shape of the initial response, since deviations from the steady state (set point) are never allowed to become to extensive. Severe control limitations are encountered for responses which have an initial inverse response, in these cases the control system has to “wait” until the response changes direction towards the new steady state.

The transient response and their modeling was the topic of an extensive research program by Baber *et al.* (1961), they investigated the responses of a five tray stripping column to step disturbances. Baber *et al.* (1961, 1962) done experiments on feed composition changes, vapor and liquid flow step changes and investigate the influence of the liquid holdup on the stage on the composition response of the column.

During the modelling phase Baber *et al.* (1961) found that the liquid holdup in the downcomer could not be neglected, to keep the model simple they combined the liquid holdup of tray and downcomer. Baber *et al.* (1962) report an error in the initial reponse of up to 32 % of the initial time constant when the downcomer holdup is neglected. Further on reboiler holdup dependent tray responses were reported (Baber, 1962). Overall they conclude that the relative simple linearized model from Lamb *et al.* (1961) may be used to characterize the transient behavior of the investigated pilot plant. Sproul and Gerster (1963) continued the research and focus on the initial response and accept the observed steady state error as acceptable.

In the paper by Wittgens *et al.* (1995) a pilot plant distillation column is modelled. The model, based on first principles was tuned to describe the initial response of the unit. Similar research was presented by Betlem *et al.* (1998) presenting an investigation of the influence of the tray hydraulics on the dynamics of a trayed column. The resulting dynamic behavior of a staged distillation column is investigated by linearizing the rigorous tray model, especially the influence of changes in the vapor flow on the column dynamics is considered.

1.3.2 Experimental determination of operational parameters

Experimental determination of the initial responses of a pilot plant do not necessary lead to general correlations of the transient behavior of distillation columns. This limited generalization of the results is due to the limited range of operational conditions and liquid and vapor holdup in a given system. A further limitation is the influence of auxiliary equipment such as accumulator, condenser and reboiler, which influence the initial response of the overall system significantly. Nevertheless, we can determine the most important hydraulic parameters and the interior design as well as their influence on the dynamics of a given system. Results from a pilot plant can give insight into the modeling of the system by a set of differential algebraic equations, combination with empirical relations give an indications to perform the fitting of parameters to match the observed responses as close as necessary for a given task. Further, we gain insight in the necessary structure of a model and which operational and design parameters determine the hydraulics.

From an experimental point of view several different types of measurements are available. The operation of distillation units, both continuous and batch wise, depends on the reliability and availability of measurements for the material balance (flow, level and pressure) and composition balance (composition by gas chromatograph or estimated from temperature). The measurement of pressure and level can be performed by *e.g.* differential pressure sensors (Shinsky, 1984 and Buckley *et al.* 1985), liquid flows are measured by variable area flow sensors and temperatures by thermocouples.

Measuring the composition of product flows is a more complicated process, a selection of measurement devices is presented by *e.g.* Rademaker *et al.* (1975). These include boiling and flash point analyzers, refractive index, ultraviolet and infrared light analyzers and mass spectrometers. The most common on-line instrument in industries is the gas chromatograph. Numerous operational difficulties characterize these instruments, Kister (1990) mention the following problems for gas chromatographs: sampling and sample time, frequent recalibration, plugging of sampling lines and sensitivity of the sensor to impurities. These require intensive maintenance of the analyzer and increase the operation costs. Sampling time of a gas chromatograph can be in the range of 10 - 30 minutes and give rise to severe control limitations. The long sampling time is caused by time consuming analysis and transport delay from the process to the analyzer. Temperature measurements along the column have proven to be a reliable, fast, easy to maintain and cheap sensor type. The continuous recording of temperature inside a column and a suitable estimation procedure give a good indication for product composition changes (Mejdell, 1991).

1.4 Batch Distillation

In batch distillation the focus is on the operation and implementation of a newly developed multivessel batch distillation unit. This process enable the separation of a multicomponent mixture in one single unit. The design of the process is an extended combination of conventional, inverted and middle vessel batch distillation column. There is not that much literature in this particular area, nevertheless extensive research is done on the operation of conventional batch distillation columns. Some of these research activities focus on the optimization of the reflux flow to the column to either keep the top product composition constant or minimize energy consumption.

The multivessel batch distillation is useful for the separation of multicomponent mixtures frequently found in the chemical process industries. The regeneration of multicomponent mixtures of solvent is only one example for the utilization of this new process. Splitting the mixture into pure components allow the recirculation of solvents even to processes which require an accurate quality control of the feedstock in *e.g.* the production of pharmaceuticals.

Although batch distillation generally is less energy efficient than continuous distillation, it has received increased attention in the last few years because of its simplicity of operation, flexibility and lower capital cost. For many years academic research on batch distillation was focused primarily on optimizing the reflux policy (Sørensen and Skogestad, 1994). However, in most cases the difference to the simple-minded constant reflux policy usually is small. In practice, other issues are usually more important, such as the recycling of off-spec prod-

ucts, separation of azeotropic mixtures and pressure swing operation. More recently, one has started re-examining the operation of batch distillation as a whole. For example, for mixtures with a small amount of light component, a cyclic operation where the operation is switched between total reflux operation and dumping the product (*i.e.* the condenser holdup is introduced as an additional degree of freedom) may be better (Sørensen and Skogestad, 1994). The total reflux operation of a distillation column solve a given separation problem with a unit which consists of a minimum number of stages. The distance between operation line and vapor-liquid equilibrium line determines how easy the separation is or how many stages are necessary for a given separation with a given reflux (Perry 1984). The larger the distance between operation line and vapor liquid equilibrium in a *McCabe-Thiele* diagram the easier is the separation of two components. The total reflux operation is from the viewpoint of separation efficiency the most efficient operation mode of a distillation column. Traditionally, this operation policy does not provide any product, since we recirculate all of the condensed vapor to the column and no product is withdrawn (Coulson *et al.* 1985). Nevertheless, applying the above described cyclic operation policy (Sørensen, 1994) batchwise withdrawal of a product is possible.

1.4.1 Conventional batch column

In conventional batch distillation columns, a multicomponent mixture is separated by removing one component at a time, either the most volatile is drawn over top (Figure 1.3) or alternatively the least volatile component is removed first through the bottoms (See Figure 1.4). The most common operation policy of a conventional batch distillation column is performed with constant reflux, frequently optimal reflux policies to reduce energy consumption and total batch time are employed, too.

More recently, one has started re-examining the operation of batch distillation as a whole. The total reflux operation of a conventional batch distillation (or batch rectifier) was suggested independently by Bortolini and Guarise (1970) and Treybal (1970). Treybal writes that he first learned about the technique from Gustison in 1958, and “has found it most useful” and that it “practically runs the distillation by itself”. For mixtures with a small amount of impurities, Sørensen and Skogestad (1994) suggest a cyclic operation procedure which is an extension of the procedure proposed by Treybal (1970). The operation is switched between total reflux operation and dumping the product into separate product tanks (Figure 1.3), for this configuration the condenser (or more correct accumulator) holdup is introduced as an additional degree of freedom. The simplest operation strategy is with only one cycle, that is, the column is operated under total reflux and the final products are collected in the condenser drum and in the reboiler. The products are accumulated in accumulator and reboiler, and removed when both the desired product specifications are achieved (Figure 1.3 with $D = 0$). By introducing a variable accumulator holdup we enable the accumulation of product and can withdraw the product frequently by dumping the accumulator (Sørensen and Skogestad, 1994 and Noda *et al.* 1999). Composition control of this configuration is enabled by *e.g.* controlling a temperature (secondary measurement) in the column section and let the holdup in the reboiler and accumulator float.

Another alternative for this type of mixture is to “invert” the column by charging the

feed to the top and removing a heavy product in the bottom (Robinson and Gilliland, 1950; Sørensen and Skogestad, 1995). This configuration is shown in Figure 1.4 and is often called batch stripper. Investigations by Sørensen and Skogestad (1995) showed that an inverted column is more economical to operate compared to a conventional batch distillation column for mixtures containing only a small amount of light component.

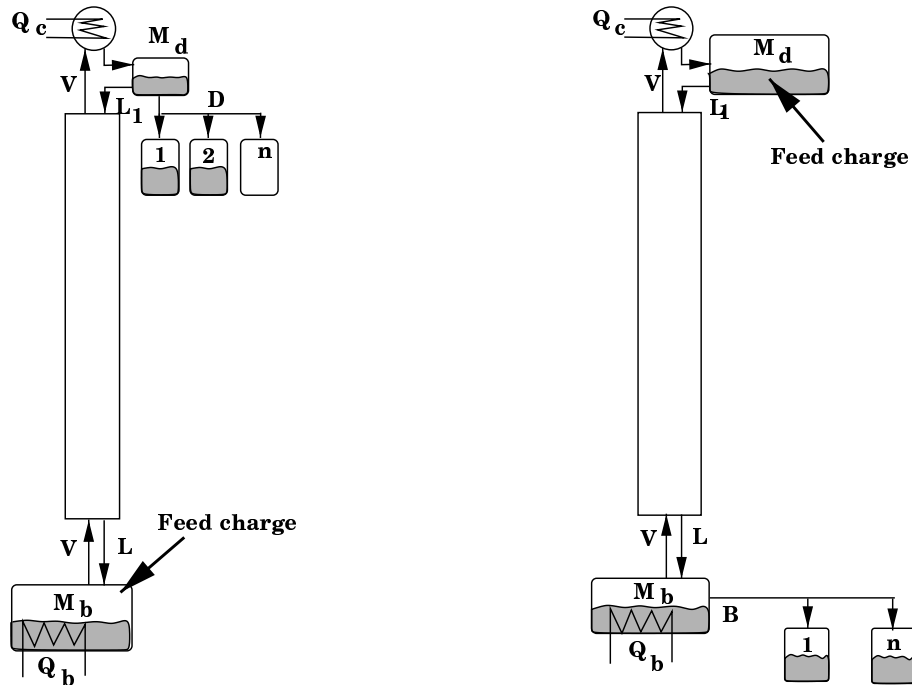


Figure 1.3: Conventional batch distillation, feed charged to the reboiler

Figure 1.4: Inverted batch distillation column, feed charged to the accumulator

1.4.2 Heat integrated batch columns

The effectiveness of batch distillation columns operated under total reflux can be increased by heat integration of several batch columns, where the condenser of one column is interconnected to the reboiler of the next column (see Figure 1.5). This column interconnection is used to minimize energy consumption, but requires that a sufficient temperature difference in the intermediate heat exchangers (condenser/reboiler combination) exists and is applied in separations where the chemicals have different properties or should not get in contact to each other.

This scheme can be simplified considerably by combining the columns such that vapor/liquid from one column is fed directly to the next column. This is facilitated by replacing the intermediate condenser and reboiler in Figure 1.5 by an intermediate vessel where liquid and vapor are in direct contact, which enables the efficient use of the latent heat of the vapor.

1.4.3 Middle Vessel Column

Combining the previous presented schemes, conventional and inverted batch distillation column and the heat integrated batch distillation columns lead to the design of a middle vessel column (see Figure 1.6). This type of column consists of a stripping and rectifying section, such that products both from the top and bottom can be withdrawn; the feed is charged to the middle of the column (Bortolini and Guarise, 1970). For binary separations, two operation procedures are possible. First, a frequent recharging of the middle vessel keep the concentration in the middle vessel almost constant (rather close to an continuous distillation column). Second, the middle vessel is filled in the beginning and the operation is terminated when the middle vessel is empty (Barolo *et al.*, 1996). Separation of a ternary mixture was suggested by Hasebe (1992), the mixture is charged to the middle vessel and a light and heavy fraction are withdrawn simultaneously from the top and bottom, respectively. The operation of the system is stopped when the desired product purity in the middle vessel is achieved.

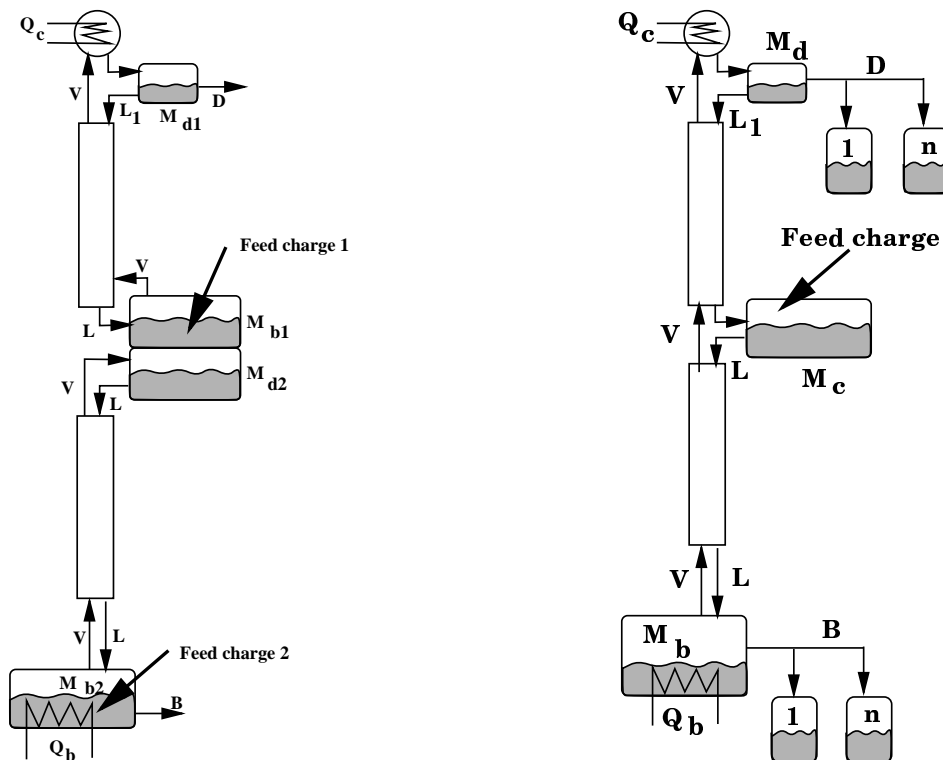


Figure 1.5: Heat integrated batch distillation column, feed charges to reboiler and intermediate heat exchanger

Figure 1.6: Middle vessel batch distillation column, feed charge to the center tank

1.4.4 Multiple-effect Batch Distillation System

A generalisation of the previous presented column types is a multivessel batch distillation column proposed by Hasebe *et al.* (1995). They proposed a process based on total reflux operation where one can separate more than two components, they denote this process a

“multiple-effect batch distillation system” (MEBAD, see Figure 1.7). The separation products are accumulated in vessels placed along the column and their holdups are introduced as additional degrees of freedom.

There are at least two advantages with this multivessel column compared to regular batch distillation where the products are taken over the top, one at a time. First, one can avoid off-spec products and recycling of these. Second, the energy requirement may be much less due to the multi-effect nature of the operation, where the heat required for the separation is supplied only to the reboiler and cooling is done only at the top. In fact, Hasebe *et al.* (1995) show that for some separations with many components the energy requirement may be less than for continuous distillation using $N - 1$ columns.

Hasebe *et al.* (1995) propose to control the multivessel batch distillation column by calculating in advance the final holdup in each vessel and then using a level control system to keep the holdup in each vessel constant. For cases where the feed composition is not known exactly they propose to, after a certain time, adjust the holdup in each vessel based on composition measurements. This scheme, involving the optimization of the vessel holdups and their adjustment based on composition measurement in these vessels is rather complicated to implement and requires an advanced control structure to implement the control law.

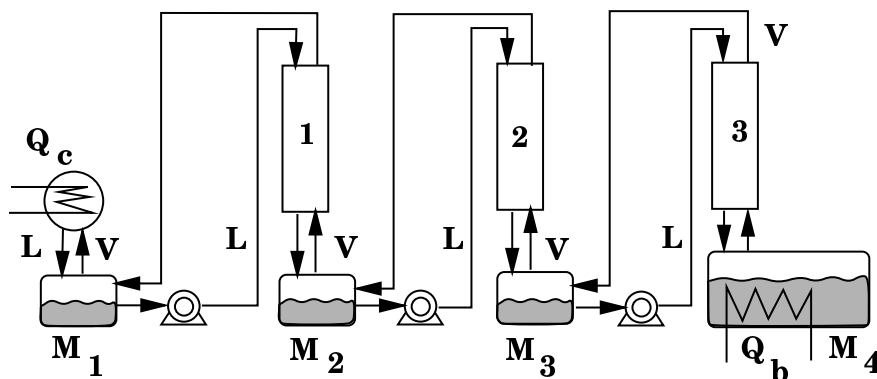


Figure 1.7: Multiple Effect Batch Distillation column

A possible implementation of the Multiple Effect Batch Distillation column is shown in Figure 1.7 where the columns are placed besides each other, this scheme requires pumps to bring the reflux flow from a vessel to an adjacent column top. A simplified version of a multiple effect distillation column is shown in Figure 1.8 where the columns are stacked on top of each other, the reflux flow out of the vessels is controlled by valves and gravity replaces the pumping action. Nevertheless, this scheme is less flexible than the scheme presented in Figure 1.7. The scheme proposed by Hasebe is more easy to adapt to separations with changing number of components and difficulty (change in relative volatilities) since the reflux and vapor flow can easily be rerouted through the process.

1.4.5 Multivessel Batch Distillation Column

All the above described operation policies may be realized in a multivessel batch distillation column with both holdups, M_i , and product flows, D_i , as additional degrees of freedom.

A simplified flowsheet of the multivessel batch distillation column is shown in Figure 1.8. The interconnection of vessels and column sections forms a superstructure of the columns shown in Figures 1.3 to 1.7 and their operation strategies. The previous presented columns can be synthesized by changing the vapor and liquid paths through the system, *e.g.* vessels can be removed from the path such that liquid or vapor from one column enters the column below/above directly.

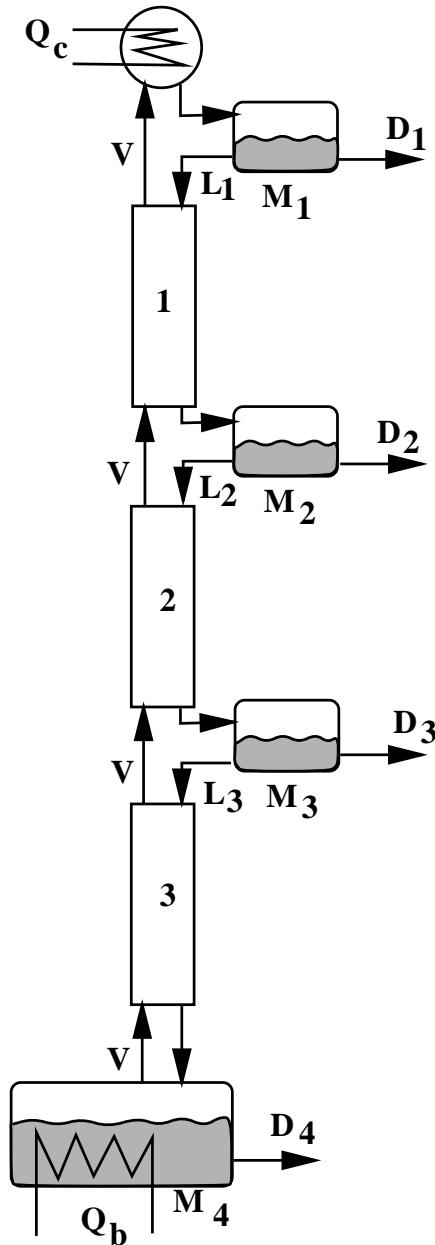


Figure 1.8: General multivessel batch distillation column

With N_c vessels along the column and with given pressure and heat input, this column has $2N_c - 1$ degrees of freedom for optimization; namely the $N_c - 1$ holdups (*e.g.*, controlled by the $N_c - 1$ reflux streams) and the N_c product rates. The simplest operation form of the proposed multivessel column, is the *total reflux operation* where the N_c product rates are set to zero ($D_i = 0$).

Compared to the more traditional column configurations, where the products are withdrawn over the top, one at a time and the use of off-cut fractions to fulfill product quality specifications, there are at least two advantages with the multivessel column. First, the operation is simpler since no product changeovers are required during operation. Second, the energy requirement may be much less due to the multi-effect nature of the operation, where the heat required for the separation is supplied only to the reboiler and cooling is done only at the top.

Hasebe *et al.* (1995) propose to “control” the total reflux operation of the multi-effect batch distillation column by an optimization of the vessel holdups and their adjustment based on composition measurement. The here presented control structure is based on the idea to adjust the reflux flow out of each of the upper $N_c - 1$ vessels by controlling the temperature at some location in the column section below. There is no explicit level control, rather the holdup in each vessel is adjusted indirectly by varying the reflux flow to meet the temperature specifications.

Performing the separation of a multi-component mixture under total reflux individual

components will accumulate according to their boiling points along the column, provided sufficient storage capacity (*e.g. by intermediate vessels*) is available and a non-azeotropic mixture is separated. Assume that the number of stages is large enough in each section, a pseudo-binary separation takes place between two adjacent vessels. Based on the composition-temperature relation Skogestad *et al.* (1997) propose a feedback control structure based on $N_c - 1$ temperature controllers (see Figure 4.1). The feasibility of the proposed control structure was verified by simulation. Initial experimental results of the operation of the multivessel batch distillation column were presented by Wittgens *et al.* (1997 and 1999). The operation of the multivessel batch distillation column opens for some degrees of freedom for optimizing of start-up and operation, these include initial distribution of holdup (Skogestad *et al.* 1997), setpoint temperatures and controller tunings (Furlonge *et al.* 1999).

1.5 Thesis overview

The study presented in this work is focused on dynamic issues in batch and continuous distillation. From industrial perspective, the choice of distillation process depends primarily on the amount of feed to be processed, other aspects include the complexity of the mixture or if a flexible multi-purpose facility is required. In general, continuous distillation column will be chosen for separating large feed flows, conventional batch distillation is used in small scale production, where flexible units are required to solve a variety of separation problems in one multi-purpose plants.

The introductory chapter gave an overview over distillation in general. The modeling of the distillation process and determination of parameters in a given model will be presented in the first part of this thesis accompanied by the experimental verification of a model developed for a continuous distillation column. From a control point of view we will stress the importance of the initial response and may accept steady state deviations when we compare simulated and experimental data. In the second part of the thesis, the newly developed multivessel batch distillation column will be investigated. The total reflux operation policy and a new feedback control strategy for the multivessel batch distillation columns will be presented followed by the experimental verification of the simulation study. Finally the presented results are discussed and the conclusions of this work are given.

All simulation studies are performed in the SPEEDUP (1993) environment, the thermodynamic properties of the components are computed by means of the ASPEN Properties Plus package (1988). For simplified models where a thermodynamic package was not necessary, simple correlations based on experimental data were used, *e.g.* constant relative volatility replace the vapor liquid equilibrium or a linear relation between liquid composition and temperature instead of an equation of state to compute the temperature.

Bibliography

1. ASPEN PROPERTIES PLUS, User Guide, Release 8 , Aspen Technology, Inc., Cambridge, USA, 1988
2. Baber, M.F., L.L. Edwards, W.T. Harper, M.D. Witte, and J.A. Gerster; “Experimental Transient Resonse of a Pilot Plant Distillation Column”, *Process Dynamics and Control*, 1961, No. 36, Vol.57, pp. 149-159.
3. Baber, M.F. and J.A. Gerster, “Experimental Transient Resonse of a Pilot Plant Distillation Column: Part II, response to Liquid and Vapor Rate Pertubations”, *A. I. Che. Journal*, 1962, No. 3, Vol.8, pp. 407-415.
4. Barolo, M., G.B. Guarise, N. Ribon, S. Rienzi, A. Trotta and S. Machietto, “Some issues in the design and operation of a batch distillation column with middle vessel”, Proc. ESCAPE-6, *Computers & Chemical Engineering*, Rhodes, Greece, May 1996
5. Bennett, D.L., R. Agrawal, and P.J. Cook, “New Pressure Drop Correlations for Sieve Tray Distillation Columns”, *AIChE Journal*, Vol.29, No. 3, pp. 434-443, 1983
6. Betlem, B.H.L., Rijnsdorp, J.E. and R.F. Azink, ”Influence of tray hydraulics on tray column dynamics”, *Chem. Eng. Sci.*, Vol. 53, No. 23, pp. 3991-4003, 1998
7. Bortolini, P. and G.B. Guarise, “Un nuovo metodo di distillazione discontinua; (A new method of Batch Distillation)” (in italian), *Ing. Chim. Ital.*, Vol. 6, No. 9, Sep. 1970
8. Buckley, P.S., W.L. Luyben and F.S. Shunta, “Design of Distillation Column Control Systems”, *Instrument Society of America*, Research Triangle Park, USA, 1985
9. Choe, Y.S. and W.L. Luyben, “Rigorous dynamic models of distillation columns”, *Ind. Eng. Chem.*, Vol. 26, pp. 2158-2161, 1987
10. Coulson, J.M., Richardson, J.F. and R.K. Sinnott, “Chemical Engineering, Volume 6, Design”, *Pergamon Press*, 1985
11. Flatby, P., S. Skogestad and P. Lundström, “Rigorous Dynamic Simulation of Distillation Columns based on UV-Flash”, *IFAC-Symposium, ADCHEM’94*, Kyoto, Japan, May 25-27, 1990
12. Furlonge, H.I., C. C. Pantelides and E. Sørensen, “ Optimal Operation of Multivessel Batch Distillation Columns”, *AIChE-Journal*, Vol 45, No. 4, 781-802, 1999
13. Gani,R., Ruiz, C.A. and T. Cameron, “A Generalized Model For Distillations - I: Model Description and Applications”, *Comp & Chem. Eng*, Vol. 10, No. 3, pp 181-198, 1986
14. Gani, R., J. Perregaard and H. Johansen, “Simulation strategies of complex chemical processes”, *Trans. IChemE.*, Vol 68, pp. 407-417, 1990
15. Hasebe S., B. Abdul Aziz, I. Hashimoto and T. Watanabe, “Optimal design and operation of complex batch distillation Column”, *Preprint of the IFAC Workshop on Interaction between Process Design and Process Control* , London 1992
16. Hasebe, S., T. Kurooka and I. Hashimoto, “Comparison of the separation performances of a multi-effect batch distillation system and a continuous distillation system”, *Proc. IFAC-symposium DYCORN’95*, Denmark, June 1995.

17. Jacobsen, E.W., P. Lundström and S. Skogestad, "Modeling and Identification for robust control of ill-conditioned plants - a distillation case study", *Proc. American Control Conference*, Boston, pp 242-248, 1991
18. Kister, H.Z., "Distillation Operation", McGraw-Hill, New York, USA, 1990
19. Lamb, D.E., R.L. Pigford and D.W. Rippin, "Dynamic characteristics and analogue simulation of distillation columns" *Chem. Eng. Progr. Symposium Series*, No. 36, Vol. 57, p 132, 1961
20. Lockett, M.J., "Distillation tray fundamentals", *Cambridge University Press*, 1986
21. Luyben, W.L. (Ed.), "Practical Distillation Control", Von Nostrand Reinhold, New York, 1992
22. McAvoy, T.J. and Y.H. Wang, "Survey of recent distillation control results", *ISA Transactions*, Vol. 21, No. 1, pp. 5 - 21, 1986
23. Mejdell T. and S. Skogestad, "Estimation of Product Compositions from Temperature Measurements by Multivariable Calibration", *Ind. & Eng. Chem. Res.*, 1991
24. Noda M., A. Kato, S. Hasebe and I. Hashimoto, "Optimal Structure of Batch Distillation Column", *Comp. & Chem. Eng.*, Supplement, Vol. 23, S 105-108, 1999
25. Perry, H.P. and D. Green (Ed.), "Perry's Chemical Engineers' Handbook", *McGraw-Hill Chemical Engineering Series*, 50th edition, 1984 Chapter 18
26. Rademaker, O., J.E. Rijnsdorp and A. Maarleveld, "Dynamics and Control of Continuous Distillation Units", *Elsevier, Amsterdam*, 1975
27. Retzbach, B., "Mathematisches Modell von Distillationskolonnen zur Synthese von Regelungskonzepten", *VDI Fortschrittberichte*, Reihe 8: Mess-, Steuerungs- und Regelungstechnik (in German), Nr. 126, 1986
28. Robinson, C.S. and E.R. Gilliland, "Elements of Fractional Distillation", *McGraw Hill Book Company*, New York, 4th ed., 1950
29. Rosenbrock, H.H., "The transient behaviour of distillation columns and heat exchangers. A historical and critical review." *Trans. Instn. Chem. Engrs.*, Vol. 40, pp. 376-384, 1962
30. Ruiz, C.A. and R. Gani, "Simulation and Design of Distillation Columns, Part 1: Hydraulic model and dynamic behavior", *Lat. Am. J. Chem. Appl. Chem.*, Vol. 16, pp 277-305, 1986
31. Shinskey, F.G., "Distillation Control", 2nd Edition, McGraw-Hill, New York, USA, 1984
32. Skogestad, S. and M. Morari, "Understanding the Dynamic Behavior of Distillation Columns", *Industrial and Engineering Chemistry Research*, No. 10, Vol. 27, pp. 1848-1862, 1988
33. Skogestad, S., "Dynamics and Control of Distillation Columns - A critical Survey", *Modeling, Identification and Control*, Vol. 18, No. 3, pp. 177-217, 1997

34. Skogestad, S., B. Wittgens, R. Litto and E. Sørensen, "Multivessel Batch Distillation", *AIChE Journal*, Vol. 43, No. 4, pp 971-978, 1997
see also chapter 3
35. Sproul, J.S. and J.A. Gerster, "Experimental Transient Response of a Pilot-Plant Distillation Column: Part III, Condensing and Reboiling Systems", *Process Systems Engineering, Chemical Engineering Progress Symposium Series*, Vol. 59, No. 59, pp. 21-31, 1963
36. Stichlmair, J., "Grundlagen der Dimensionierung des Gas/Flüssig Kontaktapparates Bodenkolonnen" (in german), *Verlag Chemie*, Weinheim, New York, 1978
37. SPEEDUP Release 5.4 User Manual, Prosys Technology Ltd., 1993
38. Sørensen, E. and S. Skogestad, "Optimal operating policies of batch distillation", *Proc. Symposium PSE'94*, Kyongju, Korea, June 1994, 449-456, 1994 a
39. Sørensen, E. and S. Skogestad, "Comparison of Inverted and Regular Batch Distillation", *Proc. IFAC-symposium Dycord'95*, Denmark, June 1995
40. Tolliver, T.L. and R.C. Waggoner, "Distillation column control: A review and perspective from the CPI", *ISA*, Vol. 35, pp 83-106, 1980
41. Treybal, R.E., "A Simple Method of Batch Distillation", *Chemical Engineering*, pp. 95-98, Oct. 1970
42. Wittgens, B. and S. Skogestad, "Evaluation of Dynamic Models of Distillation Columns with Emphasis on the Initial Response", 4th IFAC Symposium, Dycord+ '95, Helsingør, pp. 261-268, 1995
see also chapter 2
43. Wittgens, B., R. Litto, E. Sørensen and S. Skogestad, "Total Reflux Operation of Multivessel Batch Distillation", *ESCAPE-96, Comp. Chem. Engng.*, Vol. 20, S1041-1046, 1996
44. Wittgens, B. and S. Skogestad, "Multivessel Batch Distillation - Experimental Verification", *Distillation and Absorption '97, IChemE Symposium*, Maastricht, The Netherlands, 8-10 September, 1997, pp 239-248, 1997
45. Wittgens, B. and S. Skogestad, "Closed Operation of Multivessel Batch Distillation - Experimental Verification", submitted to *AIChE-Journal*, June 1999
see also chapter 4

Chapter 2

Evaluation of Dynamic Models of Distillation Columns with Emphasis on the Initial Response

Bernd Wittgens and Sigurd Skogestad

Extended version of paper presented at the symposium:
DYCORD+'95, 7-9 June 1995, Helsingør, Denmark

Abstract

A rigorous model for trayed high purity distillation based on first principles is developed. The importance of the tray hydraulics to obtain good agreement between simulation and experiment is demonstrated. Analytical expressions to derive the hydraulic time constants τ_l , τ_v and the vapor constant λ for models with simplified tray hydraulics are presented. The validity of these key parameters is verified by comparison to experimental data. In the model we assumed the liquid exiting the tray is clear liquid. We find that it is very important to include the downcomer design.

Key Words Distillation dynamics; Initial time constant

2.1 Introduction

Simplified models which simplify or neglect tray hydraulics and energy balance are often used for studies of distillation column dynamics and control. However, the applicability of such simple models for this purpose is often questioned by practitioners. This critique is indeed reasonable as one knows that the tray hydraulics are crucial in determining the initial dynamic response, which is of key importance for control.

The objective of the paper is to derive models that are as simple as possible while at

the same time match the behavior of real columns. We consider two kinds of models: 1) Simplified models where the tray hydraulics is taken care by simple parameters such as the hydraulic time constant τ_L and the vapor constant λ ; and 2) Models with detailed description of the tray hydraulics.

The most important parameters from an operational point of view are the liquid holdup M_l , the hydraulic time constant τ_l , the parameter λ for the initial effect of a change in vapor flow on liquid flow, the fraction of vapor on the tray and the pressure drop. These key parameters may be determined from either 1) experiments, 2) simulation or 3) estimated from analytical expressions based on linearizing the detailed model equations. One problem is to get consistent results from the different methods.

In this paper we compare the dynamics of a laboratory-scale high purity distillation column with those of a rigorous and simplified dynamic process model. We find that a very detailed model is needed to match closely the responses of the real experimental column. The objective of the experimental work was to evaluate the theoretical simulation results and gain further insight into the complexity of the required model.

2.2 Modelling

The rigorous model has a separate mass and energy balance for holdups on tray and downcomer. The holdup on the stage is computed from pressure drop correlations and the geometry. The downcomer is modelled as a mixing tank. The flash calculation is performed as a UV-flash.

For the second model the molar liquid holdup of the stage is the combined holdup of tray and downcomer, the vapor holdup is neglected. The tray hydraulics is linearized with one hydraulic time constant for the liquid flow and a vapor constant to describe the vapor hydraulics. Since the flash calculation is reduced to a p,x-flash, pressure is not longer the driving force of the system. The liquid flow from the stage is computed by a linear function, while a steady state energy balance is applied to determine the vapor flow from the stage. The liquid time constant τ_L and the vapor constant λ are constant for each section. To allow the thermodynamic package to compute liquid enthalpy, equilibrium constant and temperature, the pressure on each stage has to be set.

2.2.1 Rigorous Tray Model

Assumptions The total holdup of the tray consists of liquid and vapor holdup. According to the geometry of the interior of the distillation column, see Figure 2.1, the liquid holdup on the tray is divided into liquid on the active tray area and liquid in the downcomer. The following assumptions are made:

- R1 two-phase system in thermal and mechanical equilibrium
- R2 perfect mixing in vapor and liquid phases
- R3 no heat losses to the surroundings

the component balance:

$$M_d = \sum_{i=1}^n M_{dc,i} \quad ; \quad M_{dc,i} = M_d x_{out} \quad (2.7)$$

the energy balance of the tray:

$$\frac{U_{dc}}{dt} = L_t h_{l,t} - L_{out} h_{l,out} \quad (2.8)$$

and the total internal energy:

$$U_{dc} = M_d h_{l,out} \quad (2.9)$$

where we neglect the pressure dependent part.

Vapor-Liquid Equilibrium

The thermodynamic equilibrium of vapor and liquid, is described by Raoult's law.

$$y_{out,i} = K_i x_{out,i} \quad ; \quad \sum_{i=1}^n y_{out} = \sum_{i=1}^n x_{out} \quad (2.10)$$

The composition of the vapor leaving the tray is computed by the Murphree tray efficiency coefficient

$$\eta_i = \frac{y_{out,i} - y_{in,i}}{y_{eq,i} - y_{in,i}} \quad (2.11)$$

with $y_{eq,i}$ as the equilibrium vapor composition at given tray temperature and pressure. The composition of the vapor that would be in equilibrium, $y_{eq,i}$, with the liquid leaving the tray.

Holdup Distribution

The liquid and vapor molar holdup on the tray is related to the total tray volume by:

$$V_{tray} = \frac{M_{tray}}{\rho_l} + \frac{M_v}{\rho_v} + \frac{M_{dc}}{\rho_l} \quad (2.12)$$

The molar volume on tray is computed by

$$M_{tray} = \frac{h_{cl} A_{active} \rho_{ml,t}}{MW_{l,t}} \quad (2.13)$$

and of the downcomer

$$M_{dc} = (h_{dc} A_{dc} + V_{dc0}) \frac{\rho_{ml,d}}{MW_{l,d}} \quad (2.14)$$

Froth Density

We have chosen to use the correlation presented by Bennett (1983) to compute the froth

density and thus the liquid holdup on the tray. The velocity of the vapor through the active tray area is:

$$v_{active} = \frac{V_{in} MW_v}{A_{active} \rho_{mv}} \quad (2.15)$$

and the free (hole) area of the sieve tray.

$$v_{hole} = v_{active} \frac{A_{active}}{A_{hole}} \quad (2.16)$$

the dimensionless (superficial) velocity factor

$$K_s = v_{active} \sqrt{\frac{\rho_{mv}}{\rho_{ml} - \rho_{mv}}} \quad (2.17)$$

the froth density ϕ is expressed by

$$\phi = \exp(\pi_1 K_s^{\pi_2}) \quad (2.18)$$

with these parameters the clear liquid height h_{cl} on the tray is

$$h_{cl} = \phi \left(h_{weir} + \left(\frac{h_{ow}}{\phi} \right)^{\pi_3} \right) \quad (2.19)$$

The parameter π_1 to π_3 are empirical constants determined from experiments. If the computed froth height, $h_{cl}/\phi \leq h_{weir}$, the liquid leaving the tray is set to zero.

Hydraulic Model

The modeling of the tray hydraulic is based on empirical correlation selected from the literature. These correlations are not necessarily the best available. The applied correlations allow fairly accurate predictions and are easy to implementation in the model.

Flow over outlet weir

The liquid flowing over the circular weir from the tray to the downcomer, is computed with a modified Francis weir formula (Perry *et.al.*, 1984). Note that we assume the liquid exiting the tray over weir is clear liquid. Since the outlet weir is placed off center towards the column wall, the liquid height above the weir h_{ow} will not be constant. There are no existing correlations which deal with the converging flow over outlet weirs in distillation column (Lockett, 1986). Taking the design into consideration, we choose to correct the weir length with a factor of 0.5.

$$h_{ow} = 44300 \left(\frac{q}{0.5 d_{weir}} \right)^{0.704} \quad (2.20)$$

Downcomer

The pressure drop over the downcomer (Perry *et. al* 1984) from the surface of the liquid

exiting the downcomer to the surface of the downcomer level is identical to the total pressure drop over a plate. The flow under the downcomer apron is modelled by an instationary Bernoulli equation. The computation takes the pressure loss due to friction and the acceleration of the liquid under the downcomer apron into consideration.

$$\frac{dp_{plate}}{\rho_{ml}} = g h_{dc} - \zeta v_{dc}^2 - L \frac{v_{dc}}{dt} \quad (2.21)$$

where the velocity under the apron is

$$v_{dc} = \frac{q_t}{A_{apron}} \quad (2.22)$$

and the characteristic length L is chosen to be equal to the height of the downcomer apron.

Pressure drop correlation

The total pressure drop dp_{plate} over a plate is the difference of the pressure of the vapor entering the tray and the vapor leaving the tray:

$$dp_{plate} = p_{v,in} - p_{v,out} = dp_{static} + dp_{dry} \quad (2.23)$$

This is equal to the sum of the liquid head on the tray, dp_{static} and the dry pressure drop dp_{dry} . The pressure drop due to the liquid head on the tray is

$$dp_{static} = g h_{cl} \rho_{ml} \quad (2.24)$$

According to Lockett (1986) the hydraulic gradient for sieve tray distillation column of small diameter (less than 0.5 m) is negligible. Numerous correlations for the dry pressure drop are available (*e.g.*: Liebson *et al.* 1957) we have chosen:

$$dp_{dry} = \rho_{ml} \frac{51}{C_o^2} \frac{\rho_{mv}}{\rho_{ml}} v_{hole}^2 \quad (2.25)$$

Thermodynamic Properties

The thermodynamic properties of the components are calculated by the ASPEN PROPERTIES PLUS (1988) package.

2.3 Simplified Model with Linearized Tray Hydraulics

Modern control system synthesis is based on the state variable representation of the plant model. In applying these tools to higher order systems, such as distillation column, practical reasons during controller design require an order reduction. This is, the large number of state variables obtained by models based on first principle has to be replaced by a considerably smaller set of suitable state variables. The preferred model is obvious one with a first order plus dead time characteristic for the stage model. During model reduction the hydraulic lag (of the liquid flow) has to be preserved. Models with linearized tray hydraulics are most common in practical use (Rademaker, 1975 and Skogestad, 1988) as this simplifies the model considerably.

2.3.1 Tray Model

The holdup of tray and downcomer are combined to one liquid holdup which is similar to the total liquid holdup of the rigorous model. The linearization of the tray hydraulics (Equation 2.27) is done based on the hydraulic relationships of the rigorous model (see Equation 2.12 to 2.25). The energy balance is done over the entire stage holdup. Additionally to the assumption R1 to R5 for the rigorous model the following assumptions are made:

SH1 vapor holdup neglected

SH2 combine tray and downcomer to one liquid holdup

SH3 assume $u_l \approx h_l$, $\frac{dh_{l,out}}{dt} \approx 0$, this is a rather rough assumption, especially since the reference state for the thermodynamic is $25^\circ C$

SH4 linearized tray hydraulics

SH5 $p = \text{const}$ on each tray

Under consideration of assumption SH1 to SH2 the material balance is similar to Equation 2.1 to Equation 2.3. Assumption SH3 simplifies the energy balance, which is now used to compute the vapor flow leaving the tray:

$$V_{out} = \frac{1}{h_{v,out} - h_{l,out}} (V_{in} (h_{v,in} - h_{l,out}) + L_{in} (h_{l,in} - h_{l,out})) \quad (2.26)$$

The vapor-liquid equilibrium is described by Equation 2.10. The tray hydraulics is expressed by:

$$L_{out} = L_{out,0} + \lambda (V_{in} - V_{in,0}) + \frac{1}{\tau_l} (M_l - M_{l,0}) \quad (2.27)$$

2.3.2 Linearized Tray Hydraulics

In this section we use the simplified tray hydraulics which is proposed by Rademaker (1975) and Skogestad (1988). Simple expressions for the key parameters describing the hydraulics, namely the hydraulic time constant τ_l and the effect of vapor flow on liquid flow the vapor constant λ will be derived. For simplicity, the vapor holdup is neglected and constant molar flow is assumed $V_{in} = V_{out}$.

Linearization

It is assumed that the liquid flow, L_{out} , from a stage is directly affected through the vapor flow in, V_{in} , (indirectly through its effect on the liquid level) and by the holdup (mass) on the tray M . Linearizing this relation yields (Rademaker *et al.* 1975, Skogestad and Morari 1988)

$$\begin{aligned} dL_{out} &= \left(\frac{\delta L_{out}}{\delta V_{in}} \right)_M dV_{in} + \left(\frac{\delta L_{out}}{\delta M} \right)_V dM \\ &= \lambda dV_{in} + \frac{1}{\tau_L} dM \end{aligned} \quad (2.28)$$

Note that this relationship is assumed to hold dynamically. We want to obtain λ and τ_l from steady state relationships for the liquid holdup on the stage found from design data of the column. The liquid holdup can be expressed by the following relations $M = f(L, V, dp)$ with pressure drop $dp = f(L, V)$. Linearize these expressions and assume $L_{in} = L_{out}$ yields:

$$\begin{aligned} dM &= \left(\frac{\delta M}{\delta L_{out}} \right)_V dL_{out} + \left(\frac{\delta M}{\delta V_{in}} \right)_L dV_{in} \\ &= \tau_L dL_{out} + \tau_V dV_{in} \end{aligned} \quad (2.29)$$

Note that this equations only holds at steady state. After obtaining τ_l and τ_v we may express λ by

$$\lambda = -\frac{\tau_V}{\tau_L} \quad (2.30)$$

This follows by setting $dM = 0$ in Equation 2.28 and 2.29 and rearrange to get $(\delta L_{out}/\delta V_{in})_M$.

Estimation of hydraulic time constants from column design data

The liquid holdup distrubution on the stage (tray plus downcomer) is shown in Figure 2.1. To simplify the derivation the vapor holdup is neglected and all liquid holdup is in terms of clear liquid. The liquid holdup depends on geometry, liquid and vapor flow. The liquid holdup of a stage can be split up into liquid on the tray M_{tray} and in the downcomer M_d . The liquid holdup on the tray can be divided into liquid under, M_{uw} , and over, M_{ow} , weir. The holdup in the downcomer consists of the liquid in the seal pan M_{seal} (or behind the inlet weir), holdup due to hydrodynamic losses under the downcomer apron, M_{loss} , holdup due to dry pressure drop M_{dry} and the amount of liquid corresponding to the clear liquid height on the tray, M_{dc} . The liquid holdup in the seal pan is independent of the vapor or liquid flow. Since the height of clear liquid on the tray and the corresponding height of liquid in the downcomer (denoted h_{cl} in Figure 2.1) depend equally on liquid and vapor flow, these holdups are combined to M . To simplify the computation of the partial derivatives we combine the liquid holdups on the stage dependent on the vapor flow to M_{cl} and consider the liquid flow dependent part M_{ow} separately.

The holdup is related to geometry and flows by the following relations:

$$M = f(L_{out}, V_{in}) \quad ; \quad M = M_{tray} + M_{dc} \quad (2.31)$$

$$M_{tray} = M_{uw} + M_{ow} = A_{active} \rho_l h_{cl} \quad (2.32)$$

$$M_{dc} = A_{dc} \rho_l h_{cl} \quad (2.33)$$

$$M_{ow} = f(L_{out}) \quad ; \quad M_{ow} = A_{active} \rho_l h_{ow} \quad (2.34)$$

$$M_{dry} = f(V_{in}) ; M_{dry} = A_{dc} \frac{dp_{dry}}{g MW_l} \quad (2.35)$$

$$M_{loss} = f(L_{out}) ; M_{loss} = A_{dc} \rho_l \zeta \frac{v_{dc}^2}{g} \quad (2.36)$$

The clear liquid height is defined in Equation 2.19. The height over weir h_{ow} is obtained from Equation 2.20, finally the dry pressure drop is computed from Equation 2.25.

Assuming constant molar flows over the tray we can express the hydraulic time constant of vapor τ_v and liquid τ_l of Equation 2.29 by changes in liquid holdup on the stage.

$$\tau_V = \left(\frac{\delta M_{dry}}{\delta V} \right)_L + \left(\frac{\delta M_{cl}}{\delta V} \right)_L \quad (2.37)$$

$$\tau_L = \left(\frac{\delta M_{loss}}{\delta L} \right)_V + \left(\frac{\delta M_{ow}}{\delta L} \right)_V \quad (2.38)$$

Express the holdups with correlations 2.32 to 2.36 and linearize the nonlinear equations yields:

$$\frac{\delta M_{cl}}{\delta V} = M_{cl} \frac{\phi(\ln\phi)^2}{V_{in}} \quad (2.39)$$

$$\frac{\delta M_{dry}}{\delta V} = 2 \frac{M_{dry}}{V_{in}} \quad (2.40)$$

$$\frac{\delta M_{loss}}{\delta L} = 2 \frac{M_{loss}}{L_{out}} \quad (2.41)$$

$$\frac{\delta M_{ow}}{\delta L} = 0.704 \frac{M_{ow}}{L_{out}} \quad (2.42)$$

Combining Equations 2.39 to 2.42 with 2.37 and 2.38 yields:

$$\tau_V = 2 \frac{M_{dry}}{V_{in}} + M_{cl} \frac{\phi(\ln\phi)^2}{V_{in}} \quad (2.43)$$

$$\tau_L = 2 \frac{M_{loss}}{L_{out}} + 0.704 \frac{M_{ow}}{L_{out}} \quad (2.44)$$

$$\lambda = -\frac{\tau_V}{\tau_L} = -\frac{2M_{dry} + \phi(\ln\phi)^2 M_{cl}}{2M_{loss} + 0.704M_{ow}} \frac{L_{out}}{V_{in}} \quad (2.45)$$

2.4 Obtain operational parameters from experiment

2.4.1 Liquid holdup and distribution on tray M_l and M_d

The liquid holdup and its distribution on the tray can be estimated by the following means:

- i) From geometric data and pressure drop measurement over the column the amount of liquid stored on a stage will be the sum of liquid on the tray itself and the liquid stored in the downcomer. From the column design we know the area of the tray A_{active} and downcomer A_{dc} and the volume of the downcomer seal $V_{dc,0}$. For simplicity we neglect the hydrodynamic pressure drop under the downcomer apron, such that $h_{dc} = h_{tot}$. Pressure drop measurement will give the clear liquid height h_{cl} on the tray and the backup in the downcomer (see Figure 2.1).

$$M_l / \rho_l \approx A_{tray} h_{cl} + A_{dc} h_{tot} + V_{dc,0} \quad (2.46)$$

$$h_{tot} = dp_{plate} / (\rho_{ml} g) \approx h_{dry} + h_{cl} \quad (2.47)$$

The liquid height corresponding to the dry pressure drop h_{dry} , is determined from Equation 2.25 and the clear liquid height h_{cl} from Equation 2.19.

- ii) Measuring the initial temperature response to a step change in reflux ΔL or vapor flow ΔV enable the estimation of the liquid holdup. The initial response of the composition, Δx_i on the tray is independent on the magnitude of the applied step change (Skogestad, 1988). From a mass balance over a stage it will be possible to estimate the tray holdup. The following assumptions are made:

OP1 vapor holdup is negligible

OP2 neglect the energy balance, which results in equimolar flows, that is $L_i = L_{i-1}$ and $V_i = V_{i+1}$

OP3 constant molar liquid holdup M

$$\frac{dM_i}{dt} = L_{i-1} - L_i + V_{i+1} - V_i \quad (2.48)$$

$$M \frac{dx_i}{dt} = L_i (x_{i-1} - x_i) + V_i (y_{i+1} - y_i) \quad (2.49)$$

For a step change in L_i and V_i the internal flows are $L_i = L_i^o + \Delta L$ and $V_i = V_i^o + \Delta V$. Subtracting the steady state solution of Equation 2.48 from Equation 2.49 and assuming that immediately after the step change the tray composition to be unchanged, yields a linear equation in ΔL and ΔV :

$$M \frac{d\Delta x_i}{dt} = \Delta L_i (x_{i-1}^o - x_i^o) + \Delta V_i (y_{i+1}^o - y_i^o) \quad (2.50)$$

To facilitate the use of the installed measurements on the investigated distillation column we assume:

OP4 vapor-liquid equilibrium described by $y_i = K_i x_i$

OP5 a linear relation between liquid composition and temperature, *i.e.* $x_i = T_i k_i$
further assume that k_i is constant for trays next to each other

Apply assumptions OP4 and OP5 and rearrange Equation 2.50 yields:

$$M_i \frac{d\Delta T_i}{dt} = \Delta L (T_{i-1}^o - T_i^o) + \Delta V K_i (T_{i+1}^o - T_i^o) \quad (2.51)$$

From Equation 2.51 it is possible to estimate the molar holdup on stage for a step change in reflux and vapor respectively.

- iii) Determine the liquid volume inside the distillation column by empty the column. Liquid evaporating from the column interior is collected in the accumulator. The combined holdup change of accumulator and reboiler is the amount of liquid stored under operation in the column.

2.4.2 Liquid hydraulic time constant τ_l

The hydraulic time constant τ_l describe the dependency of the internal liquid flows dL on the manipulated variables dL_T . Under the assumption of constant molar flows, the flow dynamics in a distillation column can be approximated by (Rademaker *et al.* 1975, Skogestad *et al.* 1988):

$$dL_N \approx \frac{1}{(1 + \tau_l s)^N} dL_T + \left(1 - \frac{1}{(1 + \tau_l s)^N}\right) \lambda dV \quad (2.52)$$

Equation 2.52 is derived by repeated combination of the massbalance Equation 2.48 assuming $V_{in} = V_{out}$ and the tray hydraulics Equation 2.28 for each tray (Rademaker *et al.* 1975) The response of the liquid flow on stage N is a cascade of first-order responses, one for each tray. Introduce the following approximation:

$$(1 + \tau_L s)^{-N} \approx e^{-N\tau_L s} = e^{-\theta s} \quad (2.53)$$

yields:

$$dL_N \approx e^{-\theta s} dL_T + (1 - e^{-\theta s}) \lambda dV \quad (2.54)$$

From Equation 2.54 we can estimate the hydraulic time constant from the measurement of the delay between a change in external reflux until the liquid outflow of tray N changes $\theta_L \approx \tau_l N$. Determining the liquid hydraulic time constant experimentally can be done by observing the reboiler level after a step change in external reflux. A second method is the observation of the temperature response to an increase in L_T . The initial response will indicate the time a reflux flow change needs to propagate through the column.

2.4.3 Vapor constant λ

The vapor constant λ represents the initial effect of a change in vapor flow on liquid flow from a stage. Experimentally we can obtain λ by the following means.

- i) Recording the temperature response for an increase in vapor flow V . In case of $\lambda \leq -0.5$ we will have an increase in tray temperature in the upper part of the column earlier than in the lower part. Earlier response of trays in the top section than in the bottom section is due to liquid pushed from the trays such that the internal reflux increase temporarily. This effect will be more extensive in the lower part of the column than in the upper part.
- ii) Observation of the reboiler holdup after an increase in heat supply where the bottom flow is kept constant. Observing an inverse response indicate $\lambda \leq -0.5$.
- iii) The estimation of λ from differential pressure drop measurement under application of Equation 2.37 to Equation 2.45.

2.5 Results

2.5.1 Holdup estimation

For the estimation of holdup and time constants we assume that ρ_{ml} and MW_l is constant and we have chosen the conditions of a 50/50 mixture of ethanol and butanol at boiling point and 1 bar, which gives $\rho_{ml} = 727.6 \text{ kg/m}^3$, $MW_l = 60.1 \text{ kg/kmol}$ on each tray and $\Delta h_{vap} = 41320 \text{ kJ/kmol}$. The K-value in Equation 2.51 is taken from a simulation of the vapor-liquid equilibrium at 1 bar at the initial steady state conditions.

Table 2.1 list the experimental conditions of experiment 2 and 3. The liquid volume in the distillation column is determined by dumping the distillation column after the experiment. The liquid volume determined by this method is denoted $V_{l,d}$. A second method to estimate the liquid volume, $V_{l,dp}$, in the column is to compute the amount of liquid on the trays from the differential pressure drop over the column under consideration of the downcomer holdup. The estimation of the liquid holdup (denoted M_3 and M_9) by measuring the **initial time constant** for a step in external reflux (Figure 2.4) and a step in heat supply (Figure 2.5) is done by applying Equation 2.51 with $\Delta V = 0$ and $\Delta L = 0$, respectively.

The liquid holdup estimated by the rigorous model (M_R) and determined experimental M_{exp} agree very well. The holdup estimated from the initial time constant M_{init} and from the simplified model M_{simp} show an extensive mismatch.

The holdup estimation from the initial time constant of the experiment relies on the accuracy in determination of the temperature derivatives. Determining the temperature derivative from e.g. Figure 2.5 will give inaccurate results due to noise. In conjunction with the rough approximation of the physical properties an estimation of the holdup will be unreliable.

From simulation we get app. 200 ml (rectifier) and 300 ml (stripper) liquid on the trays, this give a total liquid volume in the column of approximate 2.7 liter, which is a rather good

result compared to the dumping experiment $V_{l,d}$ and the computation based on the pressure drop.

Table 2.1: Data for holdup estimation for experiment 2 and 3

	dim.	Exp. 2	Exp. 3
F	ml/min	250	250
z_F		0.54	0.56
d_p	$mbar$	22.3	26.1
$Q_{t=0}$	kJ/s	3.60	4.50
$Q_{t>0}$	kJ/s	4.05	4.50
$L_{t=0}$	ml/min	250	350
$L_{t>0}$	ml/min	250	380
$V_{l,d}$	l	2.94	3.18
$V_{l,dp}$	l	2.81	2.79
M_{exp}	mol	3.24	3.51
T_2	$^{\circ}C$	79.11	80.96
T_3	$^{\circ}C$	79.49	84.80
T_4	$^{\circ}C$	80.45	90.07
$\Delta T_3/dt$	$^{\circ}C/s$	0.0018	0.0133
$M_{init,3}$	mol	6.16	2.96
$M_{simp,3}$	mol	1.2	1.2
$M_{R,3}$	mol	3.05	2.80
T_8	$^{\circ}C$	90.87	109.79
T_9	$^{\circ}C$	104.68	113.73
T_{10}	$^{\circ}C$	111.15	115.81
$\Delta T_9/dt$	$^{\circ}C/s$	0.0252	0.0045
$M_{init,9}$	mol	8.65	9.06
$M_{simp,9}$	mol	1.5	1.5
$M_{R,9}$	mol	3.00	2.85

The slightly different gradient in the response is due to the modelling of the bottom product valve. In the experiment the valve position is set, while in the simulation the volumetric liquid flow was set constant.

Vapor

Results of the estimation of τ_v from Equation 2.37, τ_l from Equation 2.38 and λ from Equation 2.45 for experiment 6 are shown in Table 2.3. Parameters are computed for the initial flows stated in Table 2.2. In Figure 2.4 the response of the tray temperature a step change in heat input is shown. The numerical results indicate an an inverse response for the simulation.

2.5.2 Hydraulic time constant

Liquid

The hydraulic lag between the increase in reflux until the reboiler level changes is shown in Figure 2.2 and found to be $\theta_M = 21s$. The response of the reboiler level to a change in the heat supply is shown in Figure 2.3. The operational parameters are stated in Table 2.2.

Applying Equation 2.54 to the measured delay from changing the control signal of the reflux pump until the reboiler level start to change is incorrect. Inspecting Figure 2.2, it is seen that the experimental response is approximately 5 seconds delayed to the simulated response. We have to consider that it take app. 5 sec from changing the signal of the reflux pump until the flow changes. Take this into consideration, the liquid lag for the entire column is in the range of 16 seconds, which give an average hydraulic time constant of approximately $\tau_l = 1.5s$. Applying Equation 2.38 to this set of operational conditions a time constant of $\tau_l = 0.9s$ for the rectifier and $\tau_l = 1.18s$ for the stripper is computed (see Table 2.3)

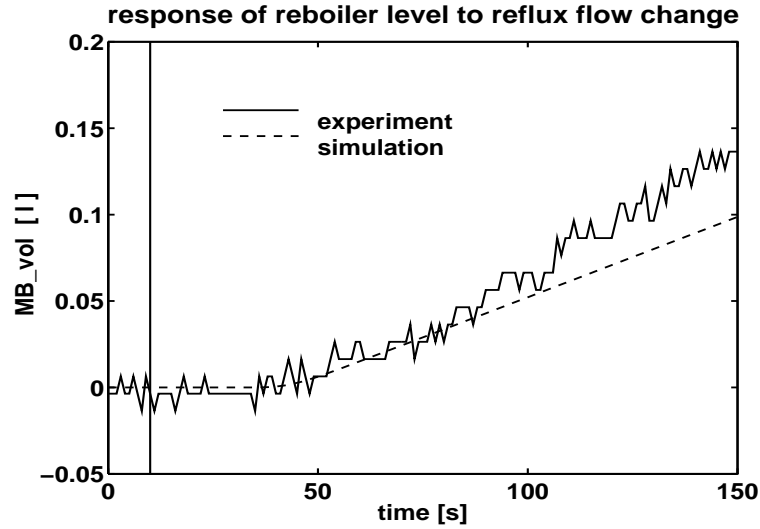


Figure 2.2: Response of reboiler level to a step in reflux flow at $t = 20$ s

Table 2.2: Experimental conditions of experiments 5 and 6 and the key parameters found

	dimen.	Exp. 5	Exp. 6
F	ml/min	350	350
z_F		0.56	0.45
$L_{t=0}$	ml/min	470	470
$L_{t \geq 0}$	ml/min	557	470
$Q_{t=0}$	kJ/s	5.8	6.5
$Q_{t \geq 0}$	kJ/s	5.8	8.0
Θ_M	s	21	5

Table 2.3: Parameters estimated from data for Exp. 6 for $Q_{b,t=0} = 6.5 kJ/s$

		Q_b	
		rectifier	stripper
M_{dry}	mol	0.13	0.26
h_{dry}	mm	34.4	34.4
M_{cl}	mol	1.09	2.10
h_{cl}	mm	9.8	18.7
ϕ		0.23	0.49
τ_v	s	5.19	6.56
τ_l	s	1.18	0.99
λ		-4.41	-6.62

The simulated inverse response of the reboiler volume of maximum 0.05 liter corresponds to a change in the real reboiler of approximately 5mm, which is approximately the resolution of the level measurement. The predicted change in the column holdup is app. 1.5 mol, which is less than 5 % of the reboiler holdup. Some liquid is pushed from the trays since the initial decrease in reboiler level slows down after 20 seconds. Nevertheless the extensive mismatch of experiment and rigorous model for the reboiler level has to be investigated and the model has to be corrected, it is not fully understood which effect of the real system is overestimated in the rigorous model.

2.5.3 Comparison of initial time constant of Experiment and Simulation

Step changes in the manipulated variables (reflux and heat input) were performed and the responses of the models and the real process are compared. The inventory of the distillation

column is controlled by PI-controllers acting on the distillate and bottom flow, except for experiments 5 and 6 where the product flows are set manually. The presented responses are simulated with a tray efficiency of 0.85 in the rectifier section and 0.8 for the stripping section. The efficiency of the reboiler is set to 0.6. The deviation from the steady state temperature is plotted to compare simulation by means of the rigorous model and the experimental data.

In **Experiment 2** the heat supply to the reboiler is increased at $t = 10\text{s}$. The temperature response of tray 3 and 9 is shown in Fig. 2.4.

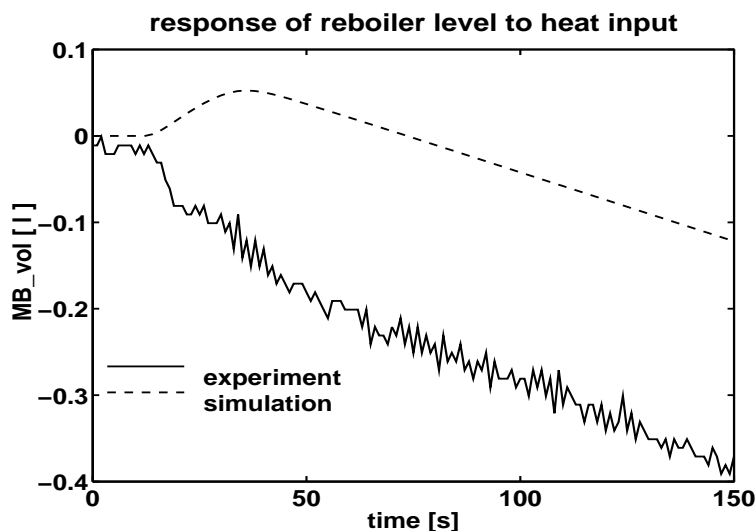


Figure 2.3: Response of reboiler level to a step in heat supply at $t = 10\text{ s}$

A thorough inspection of the first 100 seconds show an inverse response with a magnitude of -0.25°C in the response of the rigorous model. Since the noise level of the experimental data is $\pm 0.25^{\circ}\text{C}$ it is rather difficult to identify this from the set of experimental data. The experimental data were recorded at a sampling time of one second, without filtering of the signal, such that the inverse response should not be removed from the data set. Nevertheless the size and the duration of the inverse response is at a that high frequency that it is of only limited importance for control of the distillation column. Nevertheless it is not fully understood which effect of the real system was overestimated and initiate the inverse response.

The reflux flow is increased in **Experiment 3**, the temperature response of trays 3 and 9 are shown in Figure 2.5.

The responses of the rigorous model agree well with the recorded experimental data. The delays and initial time constants of the tray temperatures to the steps in heat input and reflux are in good agreement. In Figure 2.6 the response of the rigorous model (denoted with T3 R and T9 R) and the model with linearized tray hydraulics (T3 L, T9 L) are compared for a step change of the reflux flow.

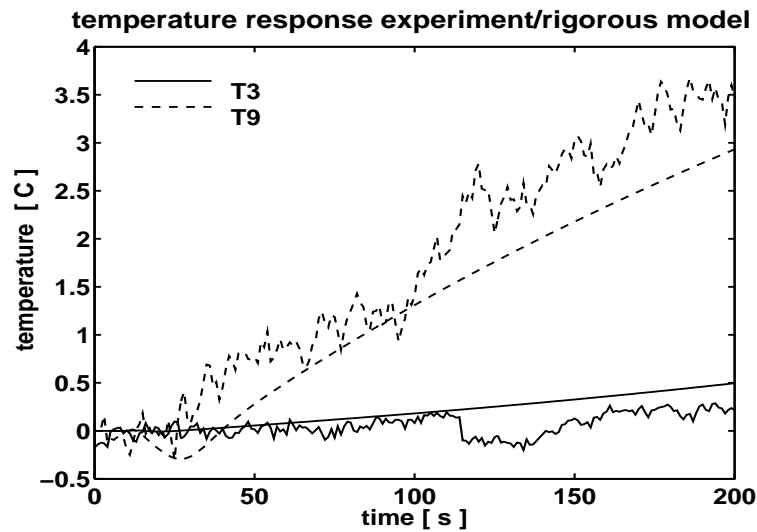


Figure 2.4: Initial response of temperatures on trays 3 and 9 to a step change in heat input at $t = 10$ s.

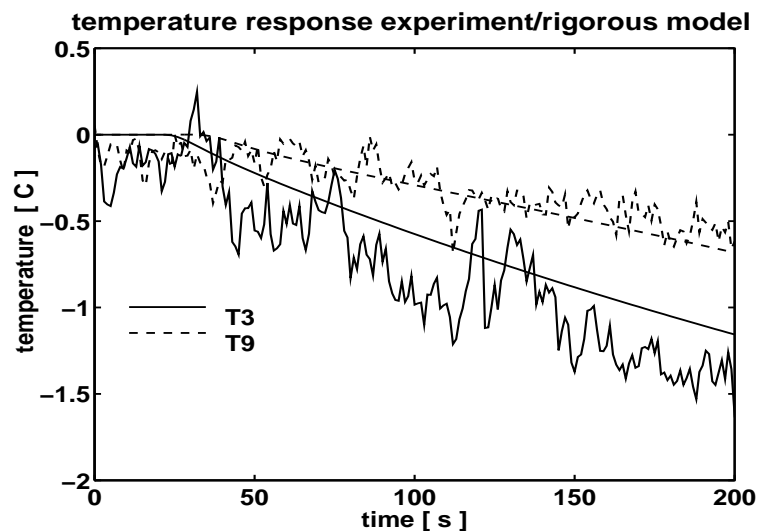


Figure 2.5: Initial response of temperatures on trays 3 and 9 to a step change in reflux flow at $t = 20$ s.

The essential difference between the two models is the method used to determine the holdup and the tray hydraulics. Although the liquid holdup for the linearized model was determined from experiment an extensive mismatch in the initial time constant was observed (see Table 2.1). The hydraulic time constant τ_l and the vapor constant λ are taken from Table 2.3. Iteration on the liquid holdup in the linearized model to match the experimental initial time constants give a liquid holdup of 1.2 mol in the rectifier section and 1.5 in the stripper section. This holdup was used in to obtain the data shown in Figure 2.6. The liquid holdup of the rigorous model is 2.8 and 2.85 mol in the rectifier and stripper respectively. The difference in holdup is approximately the amount of liquid in the downcomer.

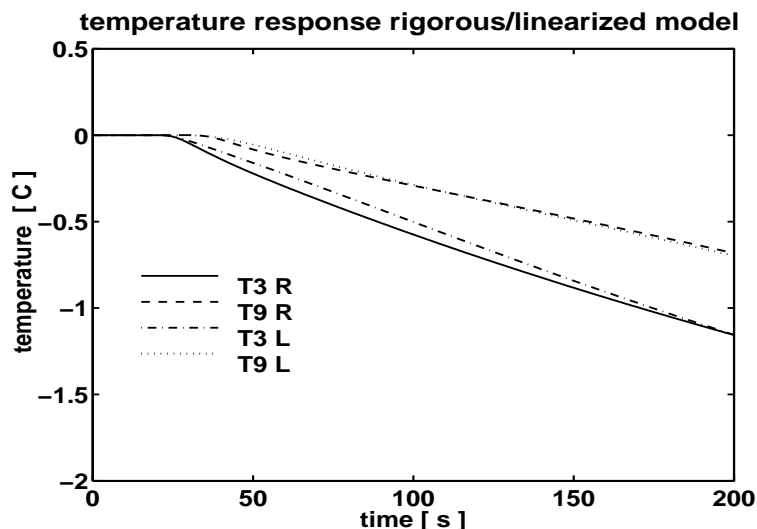


Figure 2.6: Initial response of temperatures on trays 3 and 9 to a step change in reflux flow. Step at $t = 20$ s.

2.6 Conclusion

The validity of the model has been demonstrated through the comparison of experimental and simulation results of the open-loop operation of the investigated distillation column. Nevertheless the model does not represent the reboiler holdup dynamics correctly.

It is fairly straight forward to generalize the results to other sieve tray distillation columns, since no for the investigated system specific correlations were utilized. The presented results demonstrate the importance of realistic modelled tray hydraulics for the proper operation of the process.

The transient responses of the hydraulic variables show the important role they have in the design process of a control system.

From the analysis of the simplified model we see that even if we use simple dynamic models for the composition dynamics the hydraulic dynamics should still be considered and modelled in an appropriate manner. Especially care has to be taken to obtain good estimates for the hydraulic time constants and the liquid holdup on the stage.

Bibliography

1. ASPEN PROPERTIES PLUS; User Guide; Release 8 , Aspen Technology, Inc., Cambridge, USA, 1988
2. Bennett, D.L., R. Agrawal and P.J. Cook, "New Pressure Drop Correlations for Sieve Tray Distillation Columns", *AiChe Journal*, Vol.29, No. 3, pp. 434-443, 1983
3. Lockett, M.J., "Distillation tray fundamentals", *Cambridge University Press*, 1986
4. Liebson, I., R.E. Kelly and L.A. Bullington, "How to design perforated trays", *Petrol. ref.*, Vol. 36, No. 127, 1957
5. Perry, H.P. and D. Green (Ed.), "Perry's Chemical Engineers' Handbook", *McGraw-Hill Chemical Engineering Series*, 50th edition, 1984 Chapter 18
6. Rademaker, O., J.E. Rijnsdorp and A. Maarleveld, "Dynamics and Control of Continuous Distillation Units", *Elsevier, Amsterdam*, 1975
7. Skogestad, S. and M. Morari, "Understanding the Dynamic Behavior of Distillation Columns", *Ind. & Eng. Chem. Research*, 1988, No. 10, Vol. 27, pp. 1848-1862
8. SPEEDUP Release 5.3 User Manual, Prosys Technology Ltd., 1992

Notation

A	active area	m^2
C_0	discharge coefficient	
dp	dry pressure drop over tray	N/m^2
d	diameter	mm
F_i	molar feed flow of component i	$kmol/h$
g	standard acceleration of gravity	m/s^2
h	molar enthalpy	$GJ/kmol$
h	height	mm
K_s	dimensionless velocity	
L_i	molar liquid flow of component i	$kmol/h$
M	molar holdup of liquid	$kmol$
MW	molecular weight	$kg/kmol$
p	pressure	$bar, N/m^2$
q	liquid flow	m^3/s
T	temperature	$^{\circ}C$
v	velocity	m/s
V	molar vapor flow of component i	$kmol/h$

$y_{eq,i}$	equilibrium mole fraction of component i in vapor
y_i	mole fraction of component i in vapor
x_i	mole fraction of component i in liquid
z_i	mole fraction of component i in feed

Greek Symbols

η	Murphree tray efficiency	
ρ_m	liquid mass density	kg/m^3
ρ	liquid molar density	$kmol/m^3$
ϕ	froth density	

Subscripts

active	active tray area
apron	downcomer apron
d,dc	downcomer
i	identifier
in	flow into the system volume
n	dummy index for number of components
l	liquid phase
out	flow out of the system volume
t	tray
v	vapor phase

Chapter 3

Multivessel Batch Distillation

**SIGURD SKOGESTAD, BERND WITGENS,
EVA SØRENSEN¹ and RAJAB LITTO**

Norwegian University of Science and Technology (NTNU),
Department of Chemical Engineering,
7034 Trondheim, Norway

Published in: AIChE Journal, Volume 43, No.4, 1997

Abstract

The multivessel batch column consists of a reboiler, several column sections and intermediate vessels and a condenser vessel. This configuration provides a generalization of previously proposed batch distillation schemes, including the inverted column and the middle vessel column. The total reflux operation of the multivessel batch distillation column was presented recently, and the main contribution of this paper is to propose a simple feedback control strategy for its operation. We propose to adjust the vessel holdups indirectly, by manipulating the reflux flow out of each vessel to control the temperature at some location in the column section below. The feasibility of this strategy is demonstrated by simulations.

3.1 Introduction

Although batch distillation generally is less energy efficient than continuous distillation, it has received increased attention in the last few years because of its simplicity of operation, flexibility and lower capital cost. For many years academic research on batch distillation

¹Department of Chemical and Biochemical Engineering, University College London, London WC1E 7JE, UK

was focused primarily on optimizing the reflux policy for the conventional batch distillation column (also called the batch rectifier) where the feed is charged to the reboiler and the products are drawn from the top of the column. However, more recently, there has been renewed interest in re-examining the operation of batch distillation as a whole.

A total reflux strategy, where two final products are collected in the condenser drum and in the reboiler, was suggested independently by Treybal (1970) and Bortolini and Guarise (1971). Sørensen and Skogestad (1994) found the total reflux operation to be better for separations with a small amount of light component. A generalization of the total reflux strategy is the cyclic operation described by Sørensen and Skogestad (1994). Here, the operation is switched between total reflux operation and dumping of the product (*i.e.* the condenser holdup is introduced as an additional degree of freedom).

Robinson and Gilliland (1950) proposed an inverted batch column, also called the batch stripper, where the feed is charged to the top and the heavy products are drawn from the bottom of the column. Sørensen and Skogestad (1995) found that, also in this case, the inverted column is better than the conventional column for separations with a small amount of light component. Bernot *et al.* (1991) studied the use of this column for separating azeotropic mixtures.

A further generalization of the inverted column is the middle vessel column, which has both a rectifying and stripping section. This configuration was first mentioned by Robinson and Gilliland (1950, p. 388) and was first analyzed for binary mixtures by Bortolini and Guarise (1971) and later studied in the Russian literature (e.g. Davidyan *et al.* 1991; see the updated English translation in Davidyan *et al.* 1994). The middle vessel column is also sometimes referred to as the “complex” batch distillation column (Mujtaba and Macchietto, 1992). Bortolini and Guarise (1971) proposed to charge a *binary* feed mixture to the middle vessel and draw products from both the top and the bottom, such that the composition in the middle vessel was approximately constant during the operation, and operation stops when the middle vessel is empty. This mode of operation is found to be optimal in some cases (Meski and Morari, 1995).

Hasebe *et al.* (1992) proposed to charge a *ternary* mixture to the middle vessel, and let the light and heavy impurities be drawn from the top and the bottom of the column. In this case the operation stops when the intermediate component in the middle vessel has reached its desired purity. Mujtaba and Macchietto (1992, 1994) studied the case where a chemical reaction takes place in the middle vessel, and conversion can be increased by removing the products.

A further generalization is the multivessel column suggested by Hasebe *et al.* (1995). They proposed a total reflux operation where the products are collected in vessels along the column. Because one may view this column as a stacking of several columns on top of each other, they denote this process a “multi-effect batch distillation system” (MEBAD).

All the above designs and strategies can be realized in the *multivessel batch distillation column* shown in Figure 3.1, where both the holdups, $M_i(t)$, and product flows, $D_i(t)$, are degrees of freedom. With N_c vessels along the column and with given pressure and heat input, this column has $2N_c - 1$ degrees of freedom for optimization; namely the $N_c - 1$ holdups $M_i(t)$ (*e.g.* controlled by the $N_c - 1$ reflux streams) and the N_c product rates $D_i(t)$.

Further generalizations are possible, for example, by adding feed streams (semi-batch

operation), by taking out liquid or vapor streams other places in the column, or by using intermediate heaters or coolers.

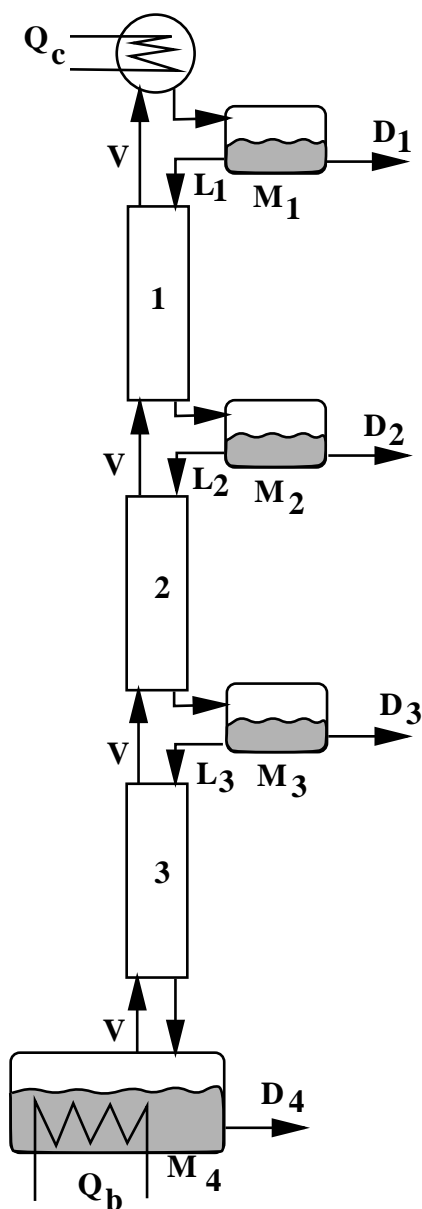


Figure 3.1: General multivessel batch distillation column for a case with 4 vessels

The main contribution of our paper is to propose, for the total reflux operation of the multivessel column, a feedback control structure based on $N_c - 1$ temperature controllers (see Figure 3.2). The idea is to adjust the reflux flow out of each of the upper $N_c - 1$ vessels by controlling the temperature at some location in the column section below. There is no explicit level control, rather the holdup, M_i , in each vessel is adjusted indirectly by varying the reflux flow to meet the temperature specifications.

In addition to the dynamic simulations which show the feasibility of the proposed scheme,

The simplest strategy for operating the multi-vessel column, which is the focus of this paper, is the *total reflux operation* suggested by Hasebe *et al.* (1995) where the N_c product rates are set to zero ($D_i = 0$). There are at least two advantages with this multivessel column compared to conventional batch distillation where the products are drawn over the top, one at a time. First, the operation is simpler since no product change-overs are required during operation. Second, the energy requirement may be much less due to the multi-effect nature of the operation. In fact, Hasebe *et al.* (1995) found that for some separations with many components the energy requirement may be similar to that for continuous distillation using $N_c - 1$ columns.

Hasebe *et al.* (1995) propose to “control” the total reflux multivessel batch distillation column by calculating in advance the final holdup in each vessel and then using a level control system to keep the holdup in each vessel constant. For cases where the feed composition is not known exactly they propose to, after a certain time, adjust the holdup in each vessel based on composition measurements. Their scheme, involving the optimization of the vessel holdups and their adjustment based on composition measurement in these vessels, is rather complicated to implement and it requires an advanced control structure to implement the control law.

we present the steady-state values which would be achieved if we were to let the batch time approach infinity ($t \rightarrow \infty$). Of course, in practice we want the batch time to be as short as possible, and we would terminate the batch when the specifications are met or the improvement in purity is small. Nevertheless, the steady-state values are interesting because they give the achievable separation for a given case.

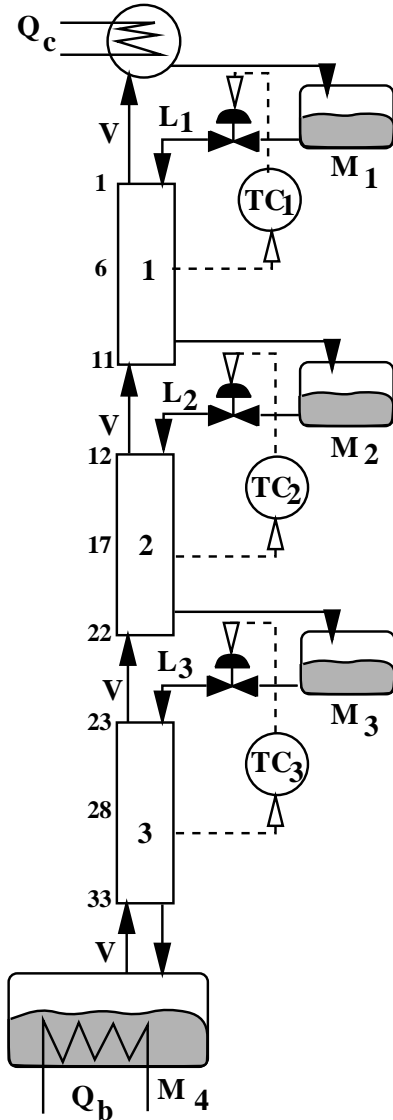


Figure 3.2: Feedback control structure for multivessel batch distillation column under total reflux

3.2 Simulation model

All the results in this paper are based on simulations using the dynamic model described in the Appendix. We have made a number of simplifying assumptions, such as constant molar flows, constant relative volatility, linear boiling point curve, constant stage holdup and constant pressure. These assumptions are introduced to simplify the model similar results are obtained when the assumptions are relaxed. The dynamic model is implemented using the SPEEDUP software package (Speedup, 1993). In all simulations we neglect the time to heat up the column and feed mixture to the boiling temperature (i.e. “hot” startup is assumed).

In the simulations we consider a four-component mixture, and use a column with three sections and four vessels (including reboiler and condenser). The data for the mixture and the column are summarized in Table 3.1. The numerical values of the relative volatility are chosen to be close to those of the system methanol-ethanol-propanol-butanol. As mentioned, we assume the mixture temperature, T_k , on stage k to be the molar average of the boiling temperatures of the pure components²

$$T_k = \sum_{j=1}^{N_c} x_j \cdot T_{b,j} \quad (3.1)$$

where $T_{b,j} = [64.7, 78.3, 97.2, 117.7]^\circ\text{C}$.

²The linear boiling point curve assumption may seem very crude. However, we have performed simulations where temperatures are computed from *Raoult's* law for ideal mixtures, $p_{tot} = \sum_{j=1}^{N_c} x_j \cdot p_j^{sat}(T)$, and the *Clausius-Clapeyron* equation for the pure component vapor pressures, $p_j^{sat}(T) = \exp\left(-\frac{\Delta H_{vap,j}}{R} \left(\frac{1}{T} - \frac{1}{T_{b,j}}\right)\right)$, and the results show only minor deviations. See Appendix D for more details.

In the simulations we consider two feed mixtures; one equimolar (z_{F1}), and one with smaller amounts of components 2 and 4 (z_{F2}). In all cases, except in Figure 3.6, the initial (at $t = 0$) vessel holdup is the same ($M_i = 2.5 \text{ kmol}$) in all four vessels, and the initial composition in all vessels is equal to that of the feed mixture. In all simulations, the vapor flow is kept constant at $V = 10 \text{ kmol/h}$.

Table 3.1: Summary of column data and initial conditions

Number of components	$N_c = 4$
Relative volatility	$\alpha_j = [10.2, 4.5, 2.3, 1]$
Total number of stages	$N_{tot} = 33$
Number of sections	3
Number of stages per section	$N_i = 11$
Vessel holdups	$M_{i,0} = 2.5 \text{ kmol}$
Tray holdups (constant)	$M_k = 0.01 \text{ kmol}$
Total initial charge	$M_{tot} = 10.33 \text{ kmol}$
Reflux flows	$L_{i,0} = 10 \text{ kmol/h}$
Vapor flow (constant)	$V = 10 \text{ kmol/h}$

3.3 Total reflux operation with constant vessel holdups

In this section we follow Hasebe *et al.* (1995) and present simulations which demonstrate the feasibility of the multivessel batch distillation under total reflux. The holdup of each vessel is calculated in advance by taking into account the amount of feed, feed composition and product specifications. After feeding the predescribed amount of raw material to the vessels, total reflux operation with constant vessel holdup is carried out until the product specifications are achieved, or until the improvement in product purity with time is too slow to justify further operation.

The simulated composition profiles as a function of time are shown in Figure 3.3 for the equimolar feed mixture

$$z_{F1} = [0.25, 0.25, 0.25, 0.25] \quad (3.2)$$

The holdup in each vessel is kept constant at $M_i = 2.5 \text{ kmol}$ during the simulation. The purity of the main component in each of the vessels is seen to improve nicely and levels off after about 2 hours. As time goes to infinity the steady-state compositions presented in Table 3.2 are achieved. The steady state purity of the main component is better than 99% in the top and bottom vessels, and is about 96% in the two intermediate vessels.

However, in practice, it may be difficult to keep the vessel holdups constant, and the composition of the feed mixture may be uncertain. The results may be sensitive to holdup errors as is illustrated by considering a case where the actual feed composition is

$$z_{F2} = [0.30, 0.10, 0.40, 0.20] \quad (3.3)$$

but the holdup of each vessel is kept constant at $M_i = 2.5 \text{ kmol}$, which are the vessel holdups corresponding to the equimolar feed composition, z_{F1} . This results in large changes in the final vessel compositions as seen from Table 3.3. For example, the purity in vessel 2 is reduced from about 96% to 40%, whereas the purity in vessel 3 is improved from 96% to 99.9%.

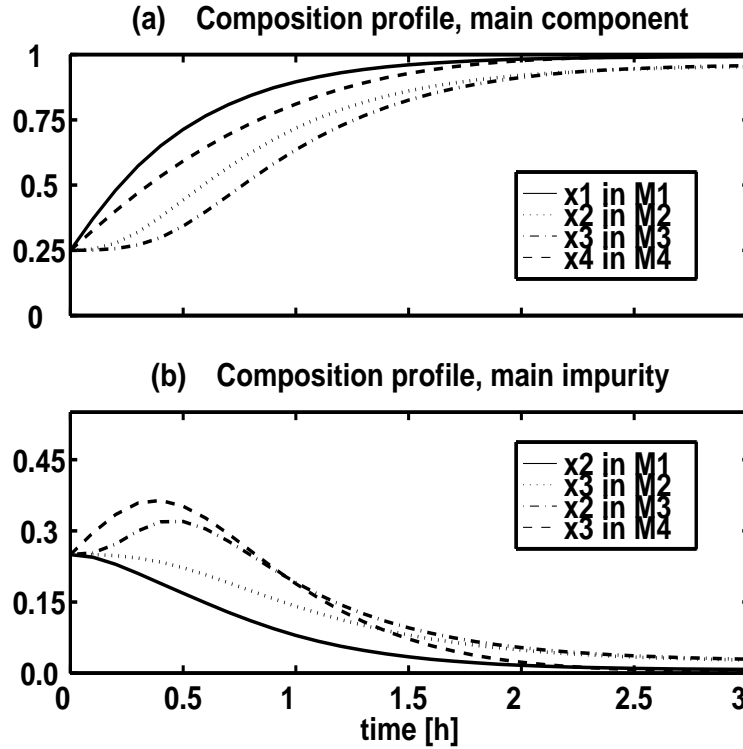


Figure 3.3: Constant vessel holdup for feed mixture z_{F1} : Composition response in accumulator (1), vessel 2, vessel 3 and reboiler (4)

Table 3.2: Constant vessel holdups for feed mixture z_{F1} : Steady-state compositions

	Vessel 1	Vessel 2	Vessel 3	Vessel 4
$M_i \text{ [kmol]}$	2.5	2.5	2.5	2.5
x_1	0.993	0.017	0.0	0.0
x_2	0.007	0.959	0.025	0.0
x_3	0.0	0.024	0.963	0.004
x_4	0.0	0.0	0.012	0.996

To compensate for these feed variations Hasebe *et al.* (1995) propose a rather complicated algorithm for adjusting the holdup based on measuring the composition in the vessels. We propose a much simpler feedback scheme which is discussed in the next section.

Table 3.3: Constant vessel holdups for feed mixture z_{F2} : Steady-state compositions

	Vessel 1	Vessel 2	Vessel 3	Vessel 4
M_i [kmol]	2.5	2.5	2.5	2.5
x_1	0.999	0.203	0.0	0.0
x_2	0.001	0.404	0.001	0.0
x_3	0.0	0.393	0.999	0.180
x_4	0.0	0.0	0.0	0.820

3.4 Feedback control of multivessel column

We now present results for our proposed control structure for the total reflux operation; see Figure 3.2. The separation of a mixture containing N_c components requires N_c vessels and $N_c - 1$ temperature controllers. The i 'th temperature controller (TC_i) controls the temperature (T_i) in the middle of the i 'th column section, using as a manipulated input the reflux flow (L_i) out of the vessel above that column section. This enables an indirect control of the holdup (M_i) in that vessel. Note that there is no level controller or level measurement, although some minimum and maximum level sensors may be needed for safety reasons.

The simplest strategy is to let the setpoint for each temperature controller be set as the average boiling temperature of the two components being separated in that column section. This simple strategy is used in the simulations. Alternatively, to reduce the batch time for a specific separation, the setpoints may be obtained from steady-state calculations corresponding to the desired separation, or they may even be optimized as functions of time. However, it is believed that in most cases, except when the number of stages in the column is close to the minimum for the desired separation, the simple strategy will be acceptable.

To demonstrate the feasibility of our proposed control scheme we consider the same column as studied in the previous section (see Table 3.1). To prove that the scheme is insensitive to the initial feed composition we consider two different initial feed compositions, z_{F1} (Eq. 3.2) and z_{F2} (Eq. 3.3).

We use simple proportional temperature controllers to manipulate the reflux flow

$$L_i = K_c \cdot (T_{s,i} - T_i) + L_{i,0} \quad (3.4)$$

where we selected the controller bias as $L_{i,0} = V = 10 \text{ kmol}/h$. The numerical values of the controller gain, K_c and temperature setpoints, $T_{s,i}$, are given in Table 3.4. The controller gains were selected such that an offset in the temperature of $\Delta T_i = 10^\circ C$ yields a change in the corresponding reflux flow of $\Delta L_i = 2.5 \text{ kmol}/h$ (25% of the nominal flowrate). The temperature sensors are located in the middle of each column section, and, as already mentioned, the setpoint, $T_{s,i}$, for each section is the average boiling temperature of the components being separated in that section.

With these temperature controllers (see Table 3.4), we achieve for *both* feed mixtures the same steady-state compositions ($t \rightarrow \infty$) given in Table 3.5. These steady state compositions are very close to those found earlier for feed mixture z_{F1} with constant vessel holdups of $M_i = 2.5 \text{ kmol}$; compare Tables 3.2 and 3.5.

Table 3.4: Data for temperature controllers

	$T_{s,i}$ [$^{\circ}C$]	K_c [$kmol/(^{\circ}Ch)$]	location *
TC_1	71.5	-0.25	6
TC_2	87.75	-0.25	17
TC_3	107.2	-0.25	28

* stage numbered from top of column

Table 3.5: Temperature control (independent of feed composition): Steady-state compositions

	Vessel 1	Vessel 2	Vessel 3	Vessel 4
x_1	0.993	0.016	0.0	0.0
x_2	0.007	0.967	0.034	0.0
x_3	0.0	0.017	0.960	0.007
x_4	0.0	0.0	0.006	0.993

As expected, for feed mixture z_{F1} , the steady-state vessel holdups are close to 2.5 kmol; see the first row in Table 3.6. The composition time responses for feed mixture z_{F1} are shown in Figure 3.4 (a) and (b). The responses are similar to those with constant vessel holdups shown in Figure 3.3 (a) and (b); the difference is that the approach to steady state is faster in vessels 1 and 4 and slower in vessels 2 and 3 for the control structure employing temperature control.

In Figures 3.4 we also present for feed mixture z_{F1} the time responses for the holdups in the vessels (c), the reflux flows out of the vessels (d), and the controlled temperatures (e). The simulations demonstrate how the action of the temperature controllers adjust the reflux flows, which indirectly adjust the vessel holdups such that the final products are of high purity.

Similar results for feed mixture z_{F2} are shown in Figure 3.5. The initial vessel holdups are as for feed mixture z_{F1} , and the simulations demonstrate how the temperature controllers indirectly adjust the vessel holdups such that the steady-state vessel compositions are the same as for feed mixture z_{F1} . From the second row in Table 3.6 we see that the steady state holdups with feed mixture z_{F2} vary from 0.788 kmol in vessel 2 to 4.159 kmol in vessel 3.

Two remarks about the results are in order.

1. From Figures 3.4(e) and 3.5(e) we observe that the controlled temperatures reach their setpoint with no offset ($T \rightarrow T_s$ as $t \rightarrow \infty$), even though only proportional controllers are used. The reason is that the model from L_i to T_i contains an integrating element, since the system is closed. More specifically, consider the reflux L_i to a column section and the temperature T_i in that section. We know that we can change the steady-state value of T_i by changing L_i . We also know that a steady-state change in L_i is not allowed, since we must have $L_i \rightarrow V_i$ as $t \rightarrow \infty$ (total reflux operation).

Table 3.6: Temperature control for feed mixtures z_{F1} and z_{F2} : Steady-state vessel holdups

	Vessel 1	Vessel 2	Vessel 3	Vessel 4
feed	M_1 [kmol]	M_2 [kmol]	M_3 [kmol]	M_4 [kmol]
z_{F1}	2.506	2.452	2.512	2.530
z_{F2}	3.053	0.788	4.159	2.000

Thus the transfer function from L_i to T_i must contain an integrator.

2. With temperature control we achieve the same steady-state compositions in the vessels independent of the initial feed composition (only the vessel holdups differ at steady state). The reason is that the column has only three degrees of freedom at steady state and if we fix three temperatures at three locations in the column, then the temperature profile over the column at total reflux is determined. (This assumes that we do not have multiple steady states. Multiple solutions are not likely when temperatures are specified, but may be encountered if we specify the composition of a given component.)

We have also performed some simulations to study the start-up for the case when the entire feed mixture is charged to the reboiler (and not distributed to the vessels as in Figure 3.5). The composition responses for feed mixture $z_{F,2}$ are presented in Figure 3.6 (a) and (b). The results indicate that the temperature controllers can be activated immediately after start-up; possibly with some strategy to ensure that the vessels are not emptied. The vessels are then slowly filled up by action of the temperature controllers which reduce the reflux flows for a transient period (see Figure 3.6 (c) and (d)). The simulations indicate that, the required time to reach a desired separation is similar to that found when the feed is initially distributed to the vessels (see Figure 3.5).

3.5 Achievable separation

The achievable separation is limited by the number of theoretical stages in the column sections. Or, stated in another way, if there are no thermodynamic limitations caused by azeotropes etc., then we can achieve any desired purity in a multivessel column if we have a sufficient number of stages. This is demonstrated in Table 3.7 where we present the steady-state product compositions for different numbers of theoretical stages, N_i , in the three column sections. The total number of stages is $3 \cdot N_i$. We use the same components as before (the feed composition does not matter), and use temperature controllers with the setpoints given in Table 3.4. With 7 stages in each section we achieve a purity of about 86% in vessels 2 and 3, with 11 stages (base case used in rest of paper) about 96%, with 15 stages about 99%, and with 25 stages about 99.97%.

Table 3.7: Temperature control (independent of feed composition): Steady-state vessel compositions (main component) as a function of number of stages N_i in each section.

N_i	Vessel 1	Vessel 2	Vessel 3	Vessel 4
	x_1	x_2	x_3	x_4
7	0.965	0.864	0.856	0.965
9	0.984	0.932	0.923	0.984
11 (base case)	0.993	0.967	0.960	0.993
15	0.998	0.992	0.990	0.999
19	0.9997	0.9982	0.9974	0.9997
25	0.9999	0.9998	0.9997	0.9999

3.6 Discussion

One justification for using multivessel distillation instead of conventional batch distillation is to save energy, or equivalently, for a given heat input the batch time may be significantly shorter. Another advantage is the simple operation of the multivessel column under total reflux. A third advantage is that it may be easier to operate the column close to optimum with the multivessel column. In conventional batch distillation the optimal operation may depend on the reflux policy and quite strongly on the use of off-cuts to achieve the desired product composition. On the other hand, in the multivessel batch column there are fewer degrees of freedom and this simplifies the operation considerably; the reflux flow is adjusted with simple temperature controllers such that the desired products are accumulated in the vessels.

One disadvantage with the multivessel column compared with the conventional batch distillation is that the column itself is more complicated. Also, whereas in a conventional batch column one only has to make decision on the length of one single column section, one has to decide on the number of sections and their length for a multivessel column. The design of the multivessel columns is therefore more closely linked to a specific feed mixture, in particular the relative volatility and the product specifications. Thus, the design process of a multivessel column is similar to the design of a sequence of continuous distillation columns.

A simple practical implementation, which is used in our lab-scale column, is to place the sections and stages on top of each other as indicated in Figure 3.1. The liquid then flows by the influence of gravity and there is no need for pumps. However, this design is rather inflexible, and it cannot be used if a large number of stages is required. For an industrial multi-purpose separation facility, it is probably better to place the column sections in series with the vessels at ground level as indicated by Hasebe *et al.* (1995). Reflux pumps are then needed to bring the liquid from the vessels to the column sections. In this case, one can quite easily put several column sections in series to meet the separations requirements for a given feed mixture.

Although the results presented in this paper on the temperature controlled multi-vessel column are most encouraging, a number of questions are open for further research.

1. The simulations need to be verified experimentally. This work is in progress, and preliminary results (Wittgens *et al.* 1996) show very good agreement with the simulations.
2. The start-up procedure needs to be studied in more detail, including the initial distribution of the feed mixture.
3. In this study the setpoints for the temperature controllers were set such that the temperature in the middle of the section should equal the average of the boiling points of the components separated in that section. In general, this is not optimal, especially if the requirements for product purities are very different.
4. It should be established for what type of mixtures and conditions the new multivessel batch column is most suited.
5. Reasonable criteria for aborting the total reflux operation should be established, that is, when is the improvement in product purity too slow to justify further operation, and how should this be detected.
6. Finally, the total reflux operation may be generalized by also allowing withdrawal of products (continuous or discontinuous) from the vessels. In this way the multivessel column forms a “super structure” which has as special cases all the previously proposed batch schemes mentioned in the introduction.

3.7 Conclusions

A general multivessel batch distillation column is proposed, along with a new control strategy for its total reflux operation. It is shown that the proposed control scheme is easy to implement and operate, in particular, for widely varying feed compositions.

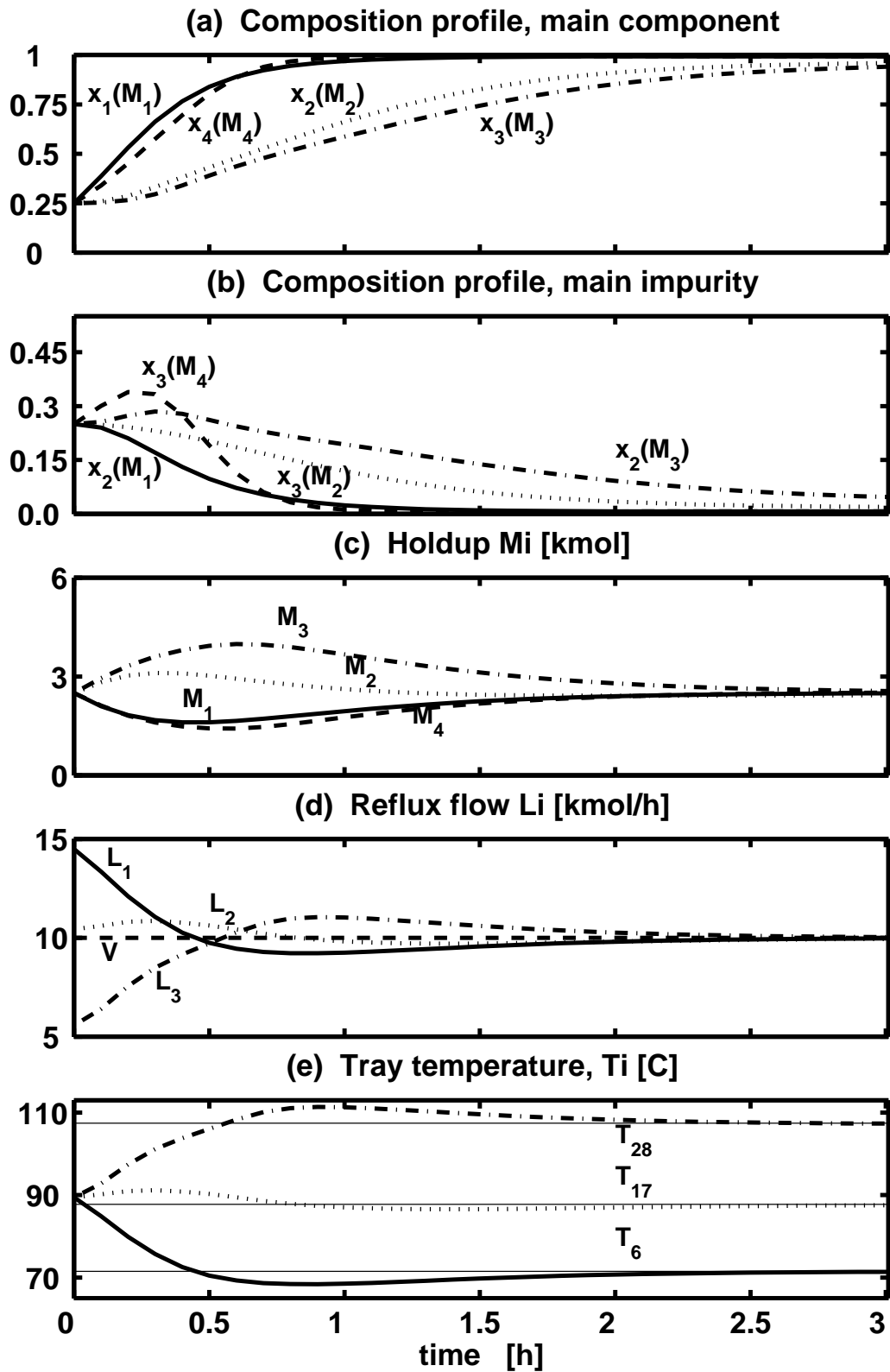


Figure 3.4: Temperature control for feed mixture $z_{F,1}$: Vessel compositions (a), impurities (b), holdups (c), reflux flows (d) and tray temperatures (e) as a function of time

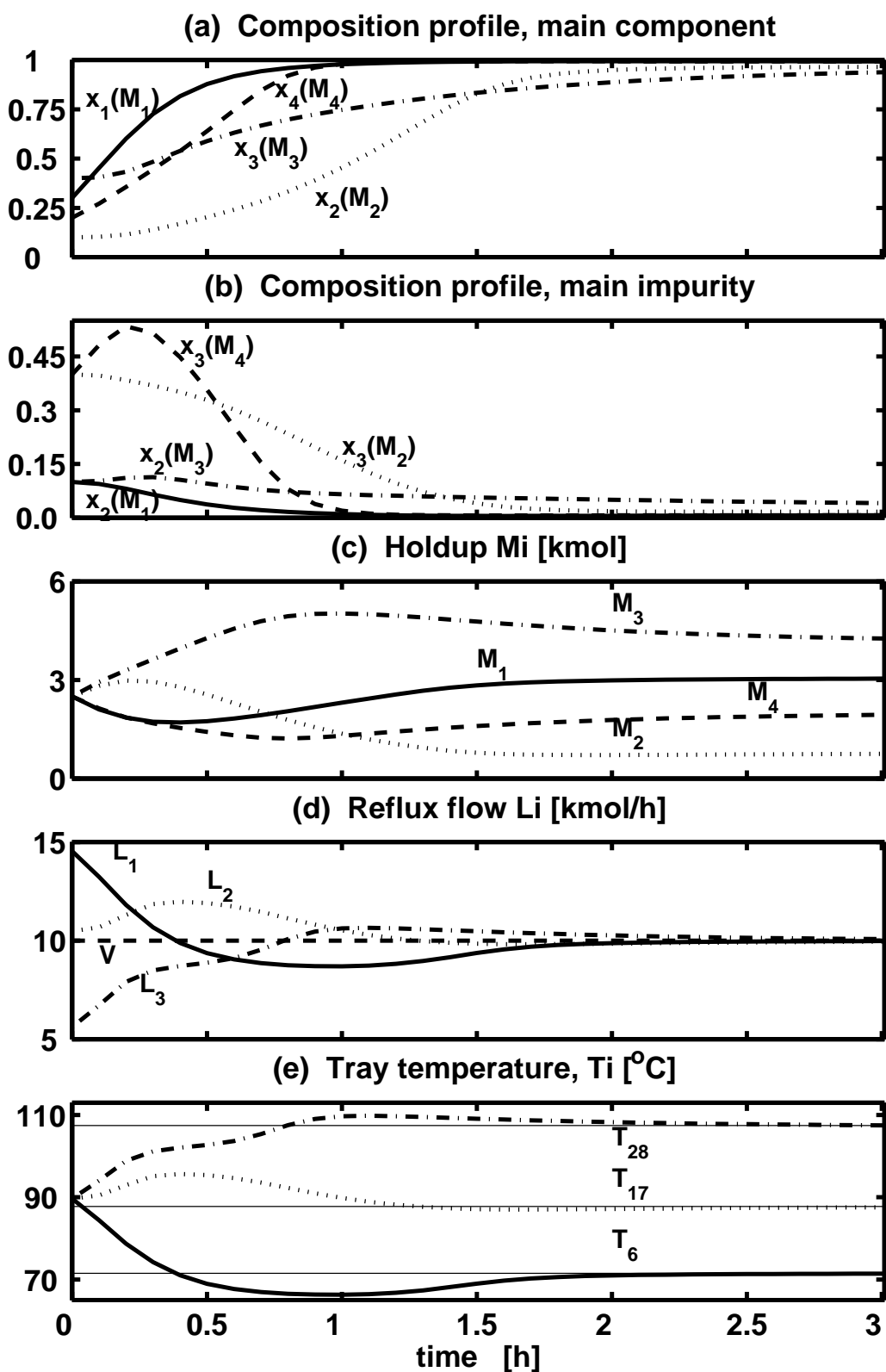


Figure 3.5: Temperature control for feed mixture $z_{F,2}$: Vessel compositions (a), impurities (b), holdups (c), reflux flows (d) and tray temperatures (e) as a function of time

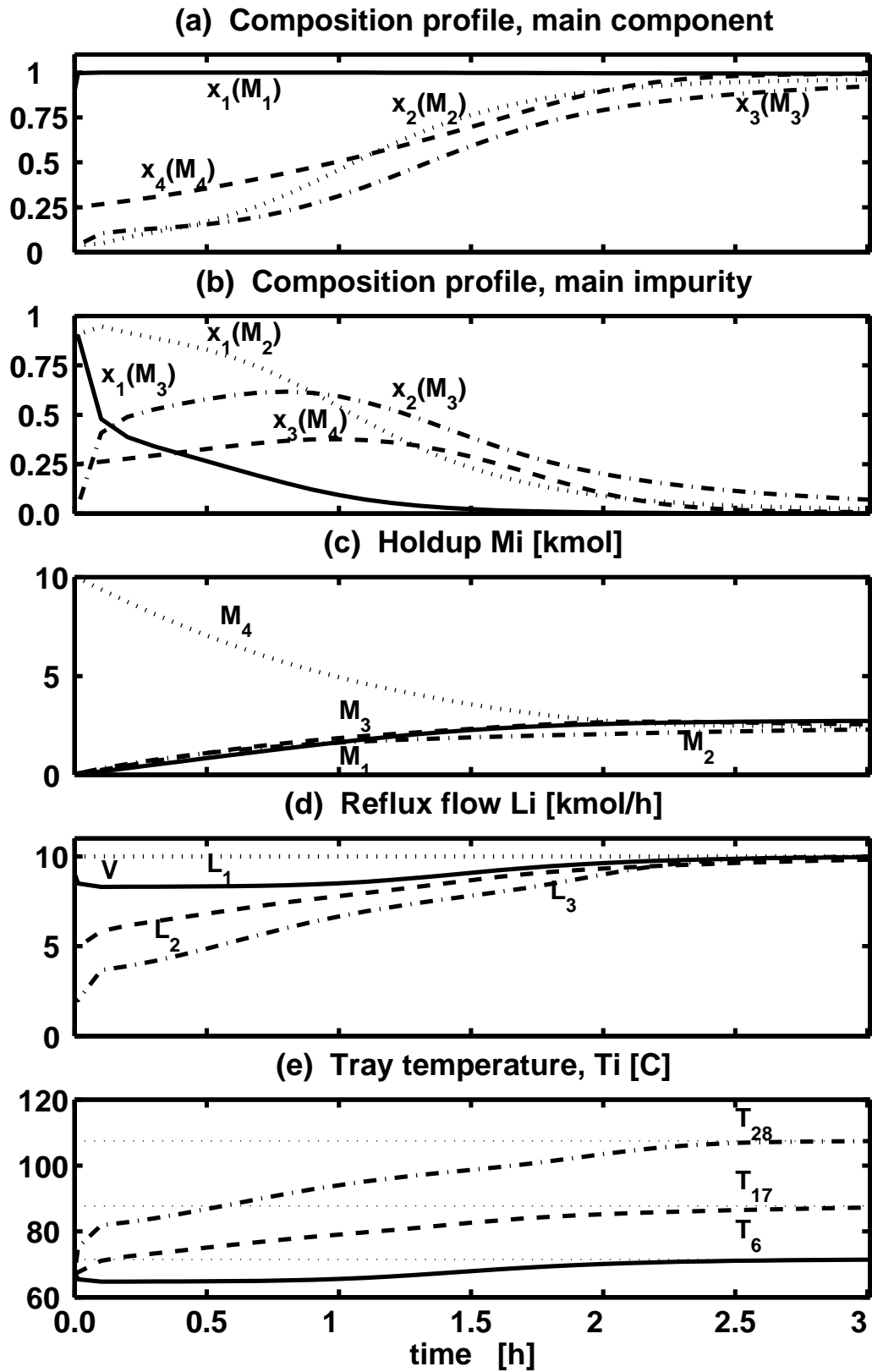


Figure 3.6: Temperature control for feed mixture $z_{F,2}$ with all liquid initially in the reboiler: Vessel compositions (a), impurities (b), holdups (c), reflux flows (d) and tray temperatures (e) as a function of time

Bibliography

1. Bernot, C., M.F. Doherty and M.F. Malone, "Feasibility and Separation Sequencing in Multicomponent Batch Distillation", *Chem. Eng. Sci.*, 1311-1326, 1991
2. Bortolini, P. and G.B. Guarise, "Un nuovo metodo di distillazione discontinua (In Italian; A new practice of Batch Distillation)", *Quad. Ing. Chim. Ital.*, Vol. 6, No. 9, 150-159, 1970
3. Davidyan, A.G., V.N. Kiva, V.M. Platonov, "Batch Distillation in Column with Middle Reservoir", *Theo. Found. of Chem. Eng.* (In Russian), Vol. 25, No. 4, 467-475, 1991
4. Davidyan, A.G., V.N. Kiva, V.M. Platonov, "Batch Distillation in Column with Middle Reservoir", *Theo. Found. of Chem. Eng.* (In Russian), Vol. 25, No. 6, 771-781, 1991
5. Davidyan, A.G., V.N. Kiva, G.A. Meski and M. Morari, "Batch distillation in a column with a middle vessel", *Chem. Eng. Sci.*, Vol. 49(18), 3033-3051, 1994
6. Hasebe, S., B. Abdul Aziz, I. Hashimoto and T. Watanabe, "Optimal Design and Operation of Complex Batch Distillation Column", *Preprint of the IFAC Workshop on Interaction between Process Design and Process Control*, London, 177-182, 1992
7. Hasebe, S., T. Kurooka and I. Hashimoto, "Comparison of the Separation Performances of a Multi-effect Batch Distillation System and a Continuous Distillation System", *Proc. IFAC-symposium DYC'D'95*, Denmark, June 1995, 249-255, 1995
8. Meski, G.A. and M. Morari, "Design and operation of a batch distillation column with a middle vessel", *Comp. Chem. Engng.*, Vol. 19, S597-S602, 1995
9. Mujtaba, I.M. and S. Macchietto, "Optimal operation of reactive batch distillation", *AICHE 1992 Annual Meeting*, Miami Beach, November 1992.
10. Mujtaba, I.M. and S. Macchietto, "Optimal operation of multicomponent batch distillation - a comparative study using conventional and unconventional columns", *Preprints IFAC Symposium ADCHEM'95*, Kyoto (Japan), 415-420, May 1994.
11. Robinson, C.S. and E.R. Gilliland, "Elements of Fractional Distillation", *McGraw Hill Book Company*, New York, 4th ed., 1950
12. SPEEDUP Release 5.4 User Manual, Prosys Technology Ltd., 1993
13. Sørensen, E. and S. Skogestad, "Optimal Operating Policies of Batch Distillation", *Proc. Symposium PSE'94*, Kyongju, Korea, 449-456, June 1994
14. Sørensen, E. and S. Skogestad, "Comparison of Inverted and Regular Batch Distillation", *Proc. IFAC-symposium DYC'D'95*, Denmark, 141-146, June 1995

15. Treybal, R.E., "A Simple Method of Batch Distillation", *Chemical Engineering*, 95-98, 1970
16. Wittgens, B., R. Litto, E. Sørensen and S. Skogestad, "Total Reflux Operation of Multivessel Batch Distillation", *ESCAPE-96, Comp. Chem. Engng.*, Vol. 20, S1041-1046, 1996

Notation

D	Distillate flow	$kmol/h$
K_c	Controller gain	
L	Reflux flow	$kmol/h$
M	Holdup	$kmol$
N_c	Number of components	
N_i	Number of stages in section i	
t	time	h
T	Temperature	$^{\circ}C$
T_b	Boiling temperature	$^{\circ}C$
TC_i	Temperature controller	
V	Vapor flow	$kmol/h$
x	Liquid composition	
y	Vapor composition	
z_F	Feed composition	
α	Relative volatility	

Subscripts

i	section identifier
j	component identifier
k	stage identifier
s	setpoint

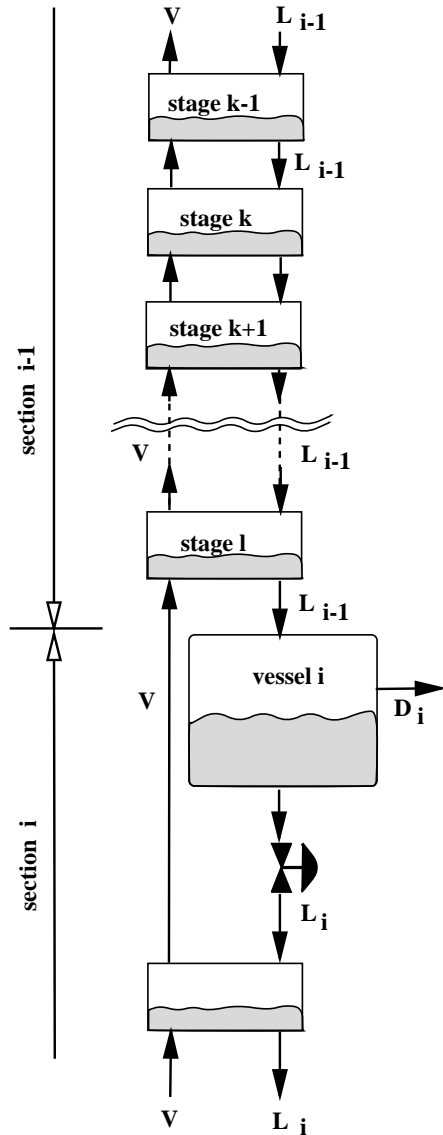
Appendix: Mathematical model of multivessel column

The model used in the simulations is based on the following assumptions:

- constant relative volatility
- constant molar liquid holdups on the stages (liquid flow dynamics neglect)
- constant molar vapor flows V_i (energy balance neglected)
- constant pressure
- constant tray efficiency (100 %)
- negligible vapor holdup

- perfect mixing on all trays and in all vessels
- total condenser

The distillation column is modeled as a stack of stages (counted from the top) as shown in Figure 3.7. Note that the vapor flow V does not pass through the intermediate vessels so these do not contribute to the number of theoretical stages. The model for stage k in section i consists of a material balance for each component j (Note M_k is assumed constant)



$$M_k \frac{d x_{j,k}}{dt} = L_i (x_{j,k-1} - x_{j,k}) + V (y_{j,k+1} - y_{j,k}) \quad (3.5)$$

and the vapor liquid equilibrium

$$\alpha_j = \frac{y_{j,k}/x_{j,k}}{y_{H,k}/x_{H,k}} \quad (3.6)$$

where H denotes the heaviest component in the mixture.

The material balance for the condenser ($i = 1$) is

$$\frac{d (M_i x_{j,i})}{dt} = V y_{j+1,i} - L_i x_{j,i} \quad (3.7)$$

and its mass balance

$$\frac{d M_i}{dt} = V - L_i \quad (3.8)$$

For intermediate vessels (i)

$$\frac{d (M_i x_{j,i})}{dt} = L_{i-1} x_{j-1,i} - L_i x_{j,i} \quad (3.9)$$

with

$$\frac{d M_i}{dt} = L_{i-1} - L_i \quad (3.10)$$

Figure 3.7: Connection of trays and vessels

where x_i is the composition in vessel i and $x_{j-1,i}$ is the liquid composition at the bottom of the section above. The liquid flow L_i leaving vessel i is set by a control valve.

The reboiler ($i = R$)

$$\frac{d(M_i x_{j,i})}{dt} = L_{i-1} x_{j,i} - V y_{j,i} \quad (3.11)$$

where

$$\frac{dM_i}{dt} = L_{i-1} - V \quad (3.12)$$

where again the vapor liquid equilibrium is described by Equation 3.6.

Chapter 4

Closed Operation of Batch Distillation - Experimental Verification

submitted to AIChE-Journal, 21. june 1999

Bernd Wittgens and Sigurd Skogestad

Chemical Engineering Department,
Norwegian University of Science and Technology,
N-7491 Trondheim, Norway

Abstract

The multivessel batch distillation column, as well as conventional batch distillation, may be operated in a closed (total reflux) mode where the products are collected in vessels along the column. We have previously proposed and simulated a feedback control strategy for the closed operation, where the idea is to indirectly adjust the vessel holdups by using the reflux flow out of the vessel to control the temperature at some location in the column section below. The feasibility of this scheme is here demonstrated experimentally on a laboratory scale multivessel column. The experimental column consists of a reboiler, two intermediate vessels and accumulator, where we separate a mixture of methanol-ethanol-propanol-butanol into almost pure components.

The paper presents the first published experimental work on the closed operation of batch distillation, as well as the first published results on the operation of a multivessel column.

4.1 Introduction

In this paper we study the closed ("total reflux", "redistributive") operation of a multivessel batch distillation column with temperature control. The aim is to confirm experimentally the feasibility of this method of operation which was proposed by Skogestad *et al.* (1997), some

early experimental results were presented in Wittgens *et al.* (1996). Since the multivessel column provides a generalization of a conventional batch distillation column, the results in the paper also demonstrate how a conventional column may be operated in a closed mode. We refer to Skogestad *et al.* (1997) for a more detailed review of the literature.

For conventional bath distillation, the closed operation, where the two final products are collected in the condenser drum (accumulator) and reboiler, was suggested independently by Treybal (1970) and Bortolini and Guarise (1970). Treybal writes that he first learned about the technique from Gustison in 1958, and “has found it most useful” and that it “practically runs the distillation by itself”.

The generalization of the closed operation of conventional batch distillation to the case with several vessels along the column (the multivessel column) was proposed by Hasebe *et al.* (1995). With N_c vessels along the column (including reboiler, condenser and intermediate vessels), it is possible in the multivessel column to obtain N_c pure products in a single batch, and it was also found that the energy efficiency of this scheme is very good.

Treybal (1970) proposes, as do all other authors except Skogestad *et al.* (1997) that, following the initial startup period, the accumulator holdup (level) should be kept constant during the operation using a level control system. However, this way of operation is sensitive to errors in the feed composition (from which the level setpoint is precomputed) and to errors in the control of the level. To correct this, one may introduce a correction on the level setpoint based on composition measurements (Bortolini, 1970 and Hasebe *et al.*, 1995), but this makes the control system complicated and requires on-line composition measurements. To avoid these problems, Skogestad *et al.* (1997) suggest to *indirectly* adjust the accumulator holdup (level) by using the reflux to control the temperature at some location in the column section below (see Figure 4.1).

They show through simulations that this simple way of operation works very well, but there has been raised concerns about whether it would work in practice, especially for the multivessel column. The main contribution of this paper is therefore to demonstrate the practicability of the closed operation with indirect level control on a laboratory scale multivessel batch distillation column.

4.2 Multivessel Batch Distillation Pilot Plant

A laboratory scale multivessel batch distillation unit (see Figure 4.2) was build to perform the experiments needed to verify the proposed control strategy. The chemical system studied is methanol (boiling point $T_{b1} = 64.7^\circ C$), ethanol ($T_{b2} = 78.3^\circ C$), n-propanol ($T_{b3} = 97.1^\circ C$) and n-butanol ($T_{b4} = 117.7^\circ C$). This mixture is fairly ideal with a relatively high relative volatility ($\alpha_{i,j} \geq 1.7$).

The objective was to make the apparatus as simple as possible, and to avoid auxiliary equipment such as reflux pumps. Therefore the column sections and intermediate vessels are placed on top of each other. The unit was built in glass and carefully insulated to reduce heat loss to the surroundings during operation. The apparatus is operated at atmospheric pressure.

The unit consists of a reboiler vessel (4 l volume), two intermediate vessels (1 l volume each), and a condensate accumulator (1 l volume). The four vessels are connected by three

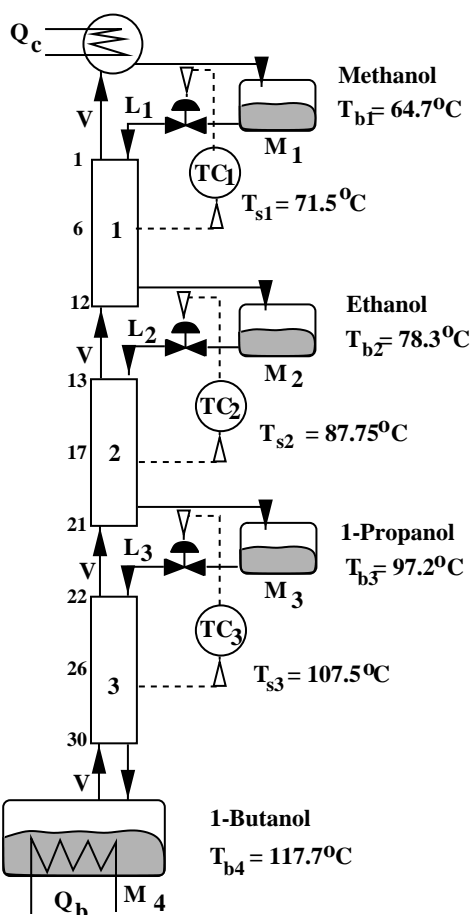


Figure 4.1: Control scheme for closed operation of multivessel batch distillation column with two intermediate vessels for mixture methanol - ethanol - propanol - butanol.

packed column sections of 420 mm length and 30 mm diameter which are filled with double-wound wire mesh rings of 3 x 3 mm made from stainless steel by Normschliff. The normal heat input to the reboiler is about 350 W, which at steady state results in liquid and vapor flows of about 0.5 mol/min¹.

Each column section is equipped with three chromel-alumel-thermocouples placed in the center of the column cross section. Two thermocouples are placed 5 cm from each end and a third in the middle of the column section. The latter temperature measurement was used for control purposes. The reflux into each of the column sections can be adjusted by means of a two-way solenoid (on-off) valve operated by solid-state relays². The reflux is introduced to the center of the column, slightly above the packing material.

The reflux into each section was used to control the temperature in the middle of the section below (as shown in Figure 4.1). For simplicity the setpoint of the temperature controllers

¹Because of variations in molecular weight the volumetric liquid flows varies from about 25 ml/min (vessel 1 from top) to 50 ml/min (vessel 3).

²The reflux flow is estimated based on the control signal to the solenoid valve. The relation between opening frequency of the valve and liquid flow has been established by calibration.

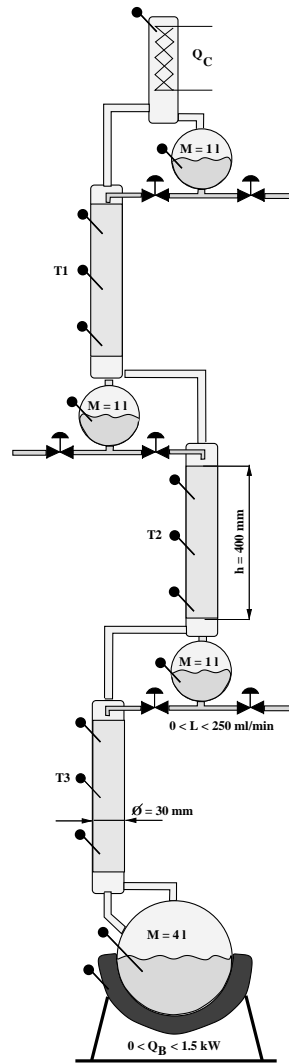


Figure 4.2: Pilot plant scale distillation column

were set to the arithmetic mean of the boiling points of the two components to be separated in the section $T_{s,i} = \frac{1}{2} \cdot (T_{b,i} + T_{b,i+1})$. The chosen controller type for the experiments is a standard PI-controller, which were tuned to be rather slow to avoid excessive control action during start-up and in the presence of disturbances.

Thermocouples are also placed in the liquid phase of the intermediate vessels and in the reboiler for monitoring purposes. A second thermocouple installed in the reboiler measures the surface temperature of the heating element, and the reboiler duty is adjusted by controlling the temperature difference between reboiler holdup and heating mantle. The process is interfaced to a PC-based control system with a sampling frequency of 1 Hertz. Product composition analysis is performed off-line by means of a gas chromatograph. The intermediate vessels are supplied with heating tapes, but after properly insulating the apparatus these were not used from experiment 4 onwards. Start-up of the experimental system is always from a column at room temperature such that the liquid holdup in the reboiler has to be heated up

to its boiling point.

After some initial experiments, the following start-up procedure was used from experiment 5 and onwards:

- The three temperature controllers (linking column temperature and reflux to a section) are activated as soon as vapor reaches the top of the column and liquid starts condensing.
- The reflux flow at the top of the column (L_1) is set to a minimum value of 5 ml/min to ensure a minimum degree of separation and to avoid emptying the reboiler. Further, due to condensation of vapor in the intermediate vessels during the start-up period, liquid is recycled to the column sections.
- For similar reasons we require at any time that $L_3 \geq L_2 \geq L_1$ on a volumetric basis.
- The following PI-settings were used for the temperature controllers: $K_c = 2.88 \frac{ml}{minK}$, $\tau_{I,1} = 7 \text{ min}$, $\tau_{I,2} = 10 \text{ min}$ and $\tau_{I,3} = 7 \text{ min}$.

4.3 Experimental Results

The experimental results verify that the closed operation with temperature control indeed works in practice. A summary of the experiments are given in Table 4.1. In the table we give the initial feed composition, as well as the mole fraction of the main component in each vessel and the impurity ratio in the intermediate vessels 2 and 3 at the end of the experiment. The impurity ratio gives an indication of in which direction we have to change the temperature setpoint in the section adjacent to a vessel to achieve a certain product quality.

For our mixture with similar relative volatilities, we conjecture that the degree of separation for a component in the intermediate vessel is maximized (*i.e.* x_i for the main component i is maximized) when the impurity ratio x_{i-1}/x_{i+1} is reasonably close to 1.

All experiments were performed with a total liquid feed of approximately 4 liter. Most of the experiments were performed with the liquid charged to the reboiler (start-up procedure 1), except for experiment 4, 10, 11 and 14 were approximately 1.5 liter of the initial feed mixture was distributed evenly to the two intermediate vessels and accumulator (start-up procedure 2).

In Figures 4.3 to 4.5 we present temperature trajectories in product vessels, controlled temperatures in column sections, volumetric liquid reflux flows and the heat input to the reboiler for three selected experiments; no. 4, 7 and 12. Experiments 7 and 12 use start-up procedure 1 whereas experiment 4 uses start-up procedure 2. To illustrate the operation these experiments are discussed in some detail below.

Table 4.1: Summary of experiments

Experiment date	reboiler duty [$\frac{J}{s}$]	feed composition z_F	batch time t_f [h]	product composition				impurity ratio		
				$x_1(M_1)$	$x_2(M_2)$	$x_3(M_3)$	$x_4(M_4)$	$\frac{x_1(M_2)}{x_3}$	$\frac{x_2(M_3)}{x_4}$	
0	27.nov.'95	350	[.24, .22, .21, .33]	5.0	0.982	0.960	0.924	0.947	0.57	1.28
1	28.nov.'95	350	[.26, .21, .20, .33]	4.5	0.969	0.547	0.943	0.910	17.45	6.76
2	06.dec.'95	450	[.26, .18, .16, .40]	4.6	0.940	0.886	0.884	0.934	4.39	11.79
3	22.mar.'96	380	[.20, .15, .21, .43]	4.9	0.975	0.915	0.926	0.910	0.890	6.00
4*	03.apr.'96	390	[.27, .19, .20, .34]	6.8	0.936	0.919	0.907	0.993	13.91	49.50
5	24.sept.'96	375	[.18, .13, .10, .59]	6.9	0.978	0.915	0.962	0.925	7.50	0.52
6	01.oct.'96	385	[.12, .13, .14, .61]	7.1	0.969	0.937	0.950	0.959	3.50	0.67
7	04.oct.'96	370	[.40, .04, .07, .49]	10.8	0.971	0.922	0.945	0.961	5.00	0.35
8	17.oct.'96	380	[.17, .16, .16, .51]	6.0	0.960	0.929	0.941	0.961	4.96	0.67
9	18.oct.'96	375	[.20, .15, .15, .50]	6.2	0.963	0.923	0.941	0.966	3.76	0.74
10*	19.oct.'96	350	[.18, .15, .14, .53]	6.1	0.969	0.914	0.933	0.962	5.71	0.69
11*	20.oct.'96	355	[.18, .15, .14, .53]	6.3	0.970	0.931	0.939	0.958	3.60	0.59
12	07.nov.'96	360	[.26, .12, .18, .44]	8.3	0.971	0.931	0.945	0.949	5.18	0.81
13	18.nov.'96	370	[.18, .16, .16, .52]	6.4	0.963	0.924	0.937	0.957	3.97	1.27
14*	19.nov.'96	360	[.18, .16, .14, .52]	6.5	0.972	0.928	0.933	0.967	3.55	0.73

Note: The liquid was initially charged to the reboiler vessel, except for the experiments marked with * where the feed was initially distributed to all four vessels. Temperature setpoints in all cases are $T_{s,i} = [71.5, 87.75, 107.2]^{\circ}\text{C}$

4.3.1 Experiment 12: Feed initially in reboiler

In Figure 4.3 we show as a function of time, the temperatures in the vessels (a) and in the column sections (b), the reboiler heat input (c) and the liquid flows to each column section (d) for experiment 12. Note that the time axis is defined such that $t = 0$ when the first liquid starts flowing ($L_1 \geq 0$).

The start-up and operation of the column is explained by referring to Figure 4.3 and is as follows: The feed charge is filled to the reboiler and heated to its boiling point by an electrical heater. The boiling point of the feed mixture is reached at about $t = -0.15$ h, indicated by the increase in the column temperatures T_i . When liquid starts collecting in the uppermost vessel ($t = 0$) the three temperature controllers TC_i are activated and reflux L_i is recycled to the column sections.

Since the implemented override on the reflux flow control require $L_3 \geq L_2 \geq L_1$, the reflux flows follow each other for approximately 0.5 h. For $t \geq 1$ h, the reflux flow controllers manipulate the flows and the column temperature T_i (Fig. 4.3 b) approach their setpoints $T_{S,i}$. The control action of the temperature controllers indirectly adjust the level in vessels M_1 to M_3 (not measured). Operation is continued for a pre-specified time (at least 3 h) until the column approaches a steady state³.

4.3.2 Experiment 4: Feed initially distributed

Experiment 4, presented in Figure 4.4 was performed with start-up procedure 2, that is liquid distributed over the column; approximately 60 % of the feed charge was fed to the reboiler, the rest was added to accumulator (M_1) and intermediate vessels (M_2 and M_3). The initial (feed) composition was identical in all vessels. The start-up was performed in the following order: All heating elements were activated simultaneously, after establishing vapor flow through the column and continuous condensate flow into the accumulator, reflux flow was set manually. Manual reflux control was necessary to avoid that a large amount of subcooled reflux enter the column and cause flooding. From Figure 4.4 we see that vessel temperatures (a) and controlled column temperatures (b) level out at about $t \geq 2$ h. Experiment 4 was performed with PI-control tunings $K_C \simeq 5.2 \frac{ml}{min.K}$ and $\tau_I = 5$ min; these somewhat aggressive tunings are responsible for the oscillatoric reflux flow from $t \geq 2.7$ h. The experiment was stopped at $t \approx 5$ h and samples from the products were taken and analyzed.

4.3.3 Experiment 2: Product composition trajectory

Experiment 2 was performed with a feed mixture similar to experiment 12 and with the feed charged to the reboiler. The PI-control tunings are the same as in experiment 4.

The compositions of the main component in the vessels and the most important impurities from experiment 2 are shown in Figure 4.6. From composition analysis can be seen that the primary purification is finished after approximately 3.5 h for this experiment.

³With a holdup of about 500 ml in each vessel and a reflux flow in excess of 15 ml/min, the vessel composition time constant on volumetric basis is about $\tau_c = 500ml/15ml/min = 33min$.

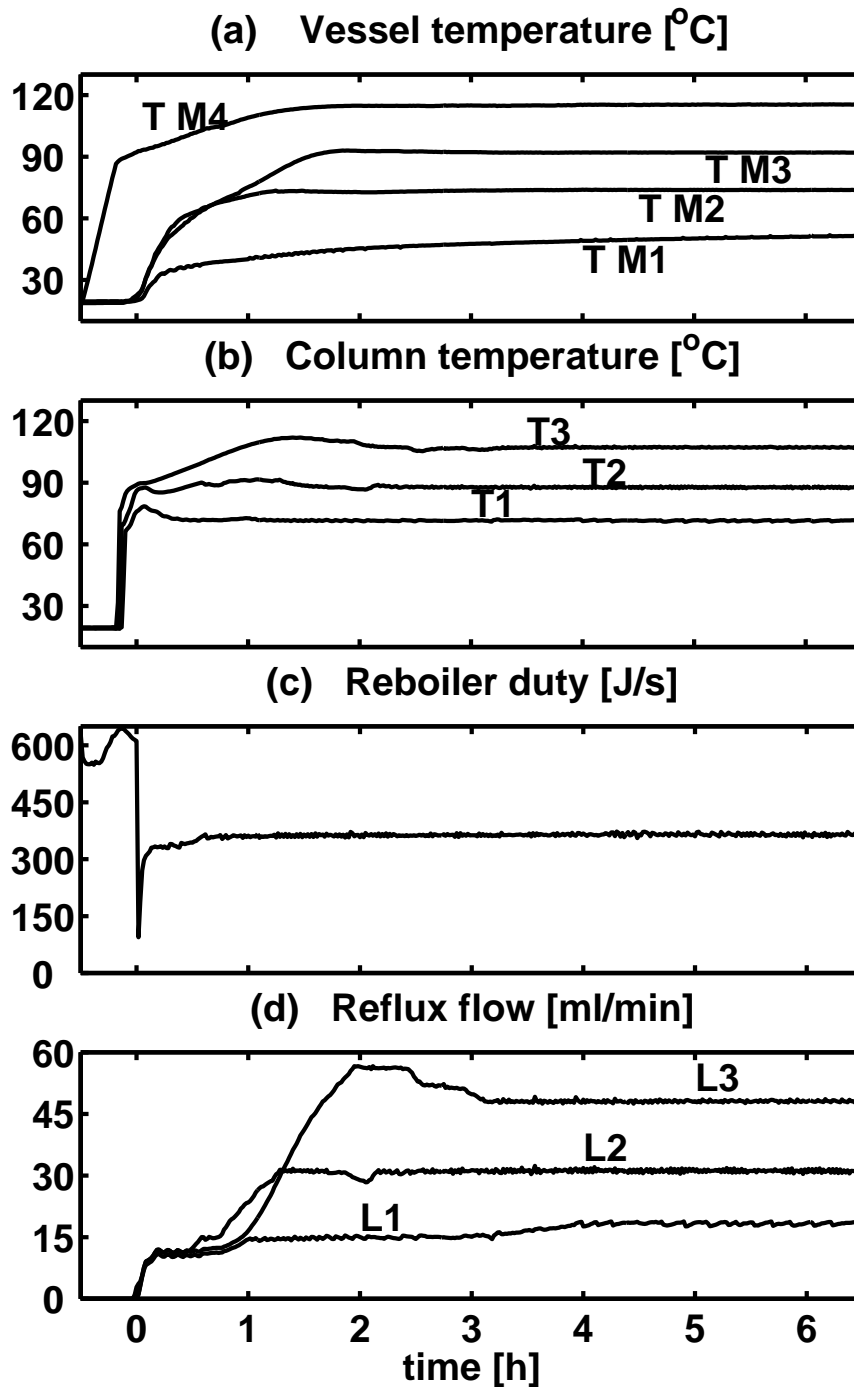


Figure 4.3: Experiment 12: Temperature responses in vessels (a), in column sections (b), reboiler heat input (c) and volumetric reflux flows as function of time recorded from experiment 12

Comparing the trajectories of the main components in the vessels (Figure 4.6, top) with the simulation (Figure 4.9, top), we see that the trajectories are similar in shape for the purification of the main components in accumulator, intermediate vessels and reboiler. Compara-

ble trajectories for the impurities in the vessel holdup are found for accumulator, intermediate vessel 2 and reboiler.

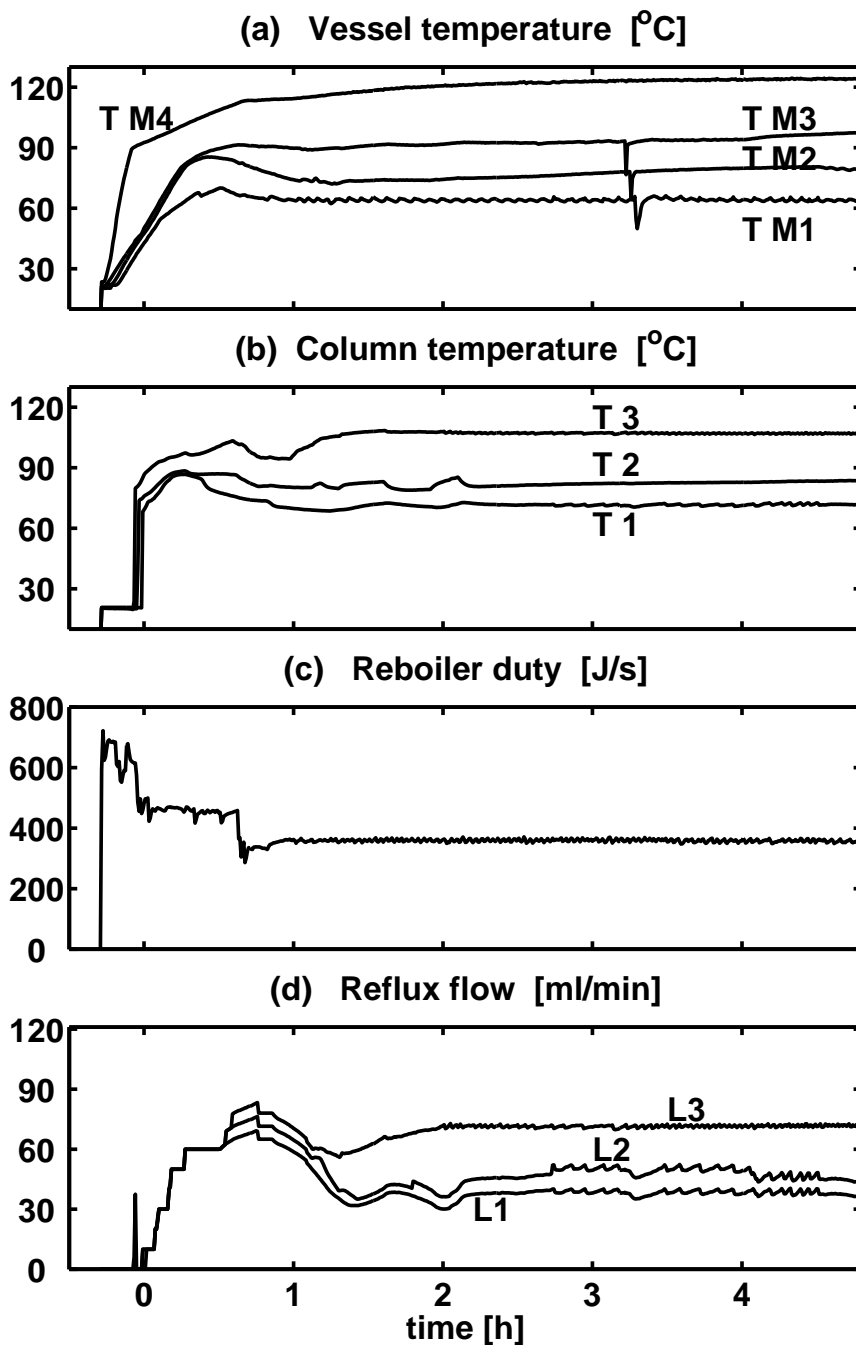


Figure 4.4: Experiment 4: Temperature responses in vessels (a), in column sections (b), reboiler heat input (c) and volumetric reflux flows as function of time recorded from experiment 4

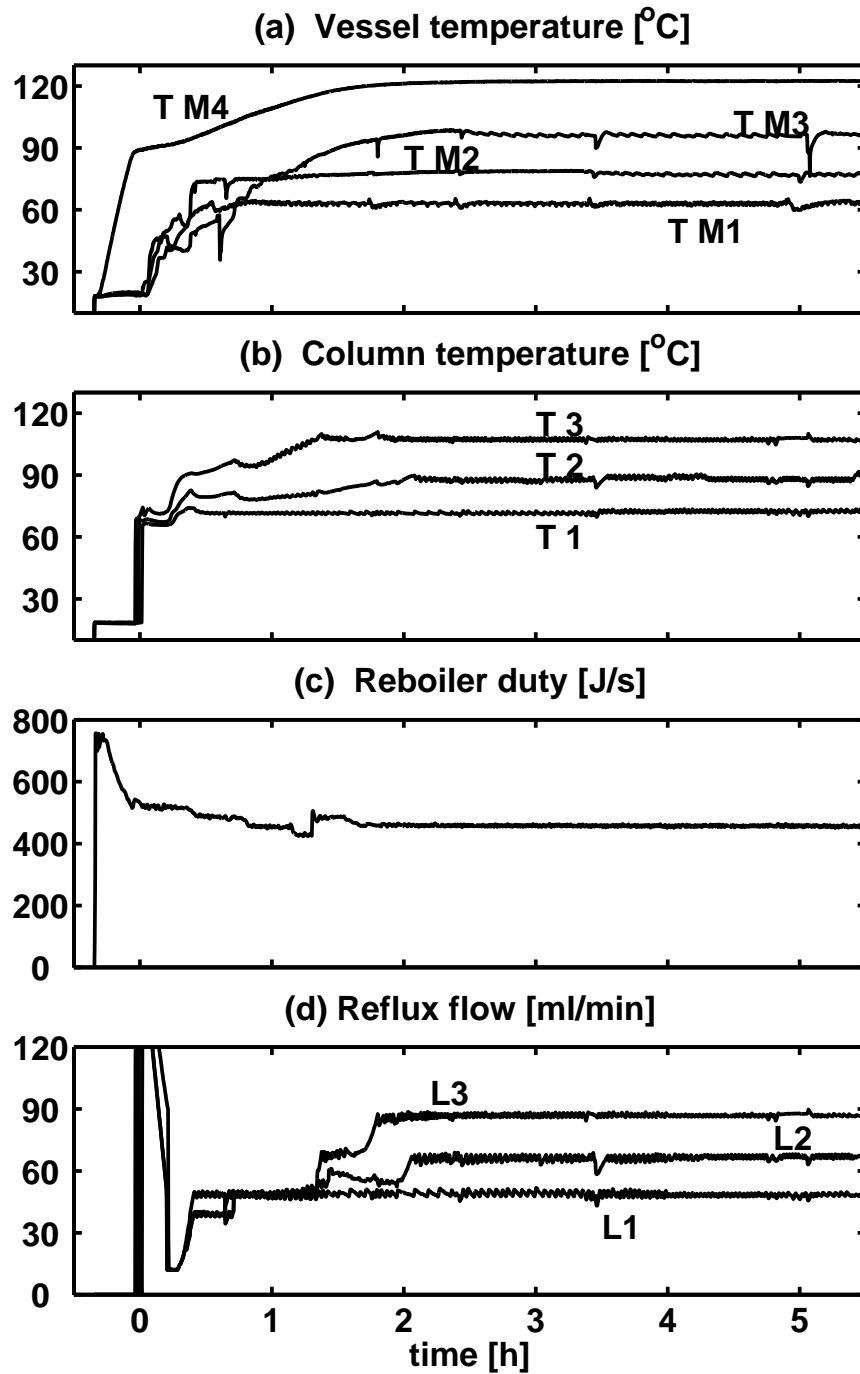


Figure 4.5: Experiment 2: Temperature responses in vessels (a), in column sections (b), reboiler heat input (c) and volumetric reflux flows as function of time recorded from experiment 7

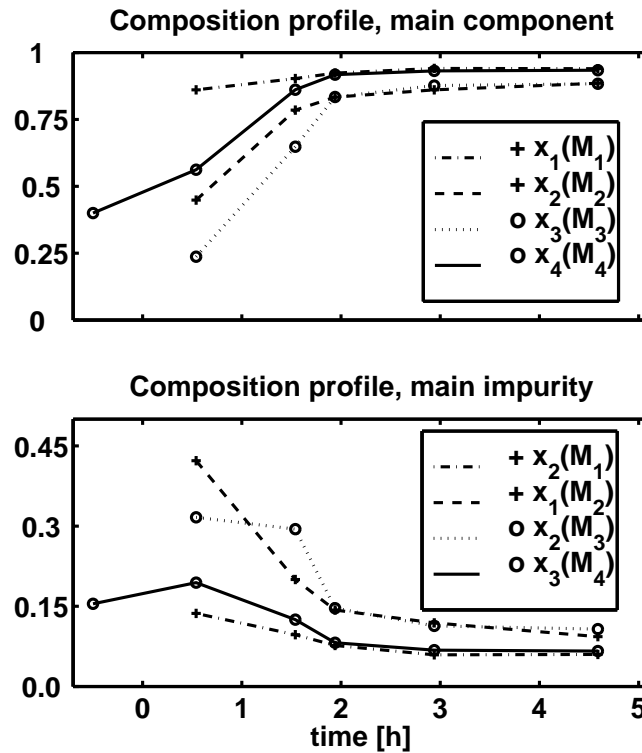


Figure 4.6: Experiment 2: Compositions of main components (top) and the largest impurity (bottom) determined from experiment 2

4.4 Simulation of experiment 12

In this section we present simulation results for a simple equilibrium stage model with conditions similar to those in experiment 12. The data used for the simulations are given in Table 4.2. The number of theoretical stage was adjusted to match the observed compositions at the end of the experiment.

At start-up all liquid is fed to the reboiler and we assume the column is “hot”. The initial reflux flow is set to $L = 0$ mol/h. We use PI-temperature controllers with an override action were the minimum reflux flow are $L_3 \geq L_2 \geq L_1$ on volumetric basis as described in the experimental section.

The feed mixture contains methanol, ethanol, n-propanol and n-butanol with boiling points of the pure components of $T_{b,i} = [64.7, 78.3, 97.2, 117.7]^\circ C$. For simplicity the column temperature is computed to be the average of the boiling temperatures $T = \sum_{i=1}^{N_c} x_i \cdot T_{b,i}$ (this seemingly crude simplification has little effect on the computed temperatures). As described in the experimental section, the setpoints for each temperature controller was set as the mean boiling temperature of the two components being separated in that column section, $T_{s,i} = [71.5, 87.75, 107.2]^\circ C$.

We use proportional-integral temperature controllers to manipulate the reflux flow,

$$L_i = K_c \cdot (T_i - T_{s,i}) + \frac{1}{\tau_i} \int_0^\infty (T_i - T_{s,i}) dt$$

with controller gain is $K_c = -2.88 \frac{ml}{minK}$ and an integral time $\tau_i = [7, 10, 7] \text{ min}$ as in the experiment. The temperature sensors for control purpose are located close to the middle of each column section. In the simulation we use an “integer” number of trays, numbered from the top, the control trays in the simulation are T_6, T_{17} and T_{26} , which correspond to trays T1, T2 and T3 in the experiment.

Table 4.2: Simulation of experiment 12: column data and initial conditions

	Simulation	Experiment
Number of components	$N_c = 4$	
Relative volatility	$\alpha_j = [7.8, 4.5, 2.3, 1]^1$	
Total number of stages	$N_{tot} = 30^2$	
Number of sections	3	3
Number of stages per section	$N_i = [12, 9, 9]^2$	
Initial Vessel holdups	$M_0 = 0.01 \text{ mol}$	$M_0 = 0 \text{ mol}$
Tray holdups	$M_k = 0.01 \text{ mol}$	<i>unknown</i>
Initial composition	$x_{i,0} = [0.99, 0.007, 0.002, 0.001]$	<i>unknown</i>
Initial reflux flows	$L_{i,0} = 0 \text{ mol/h}$	$L_{i,0} = 0 \text{ mol/h}$
Final reflux flow	$L_{i,\infty} = 30 \text{ mol/h}$	$L_{1,\infty} \simeq 27 \pm 2 \text{ mol/h}$ $L_{2,\infty} \simeq 28 \pm 2 \text{ mol/h}$ $L_{3,\infty} \simeq 33 \pm 2 \text{ mol/h}$
Vapor flow	$V_{t=0+}^3 = 32 \text{ mol/h}$ $V_{t \rightarrow \infty} \simeq 30 \text{ mol/h}$	$V_{t=0+} \simeq 32 \pm 2 \text{ mol/h}$ $V_{t \rightarrow \infty} \simeq 30 \pm 2 \text{ mol/h}$
Total initial reboiler charge	$M_4 = 55 \text{ mol}$	$M_4 \simeq 55 \text{ mol}$
Initial reboiler composition	$z_F = [0.26, 0.12, 0.18, 0.44]$	$z_F \simeq [0.26, 0.12, 0.18, 0.44] \pm 0.01$
Final reboiler holdup	$M_4 = 25 \text{ mol}$	$M_4 \simeq 24 \pm 2 \text{ mol}$

¹ *Approximated data for mixture: methanol - ethanol - n-propanol - n-butanol;*

² *Determined from experimental data (rounded to the next integer) excluding reboiler (note that the reboiler is a theoretical stage)*

³ *The steady state vapor flow is computed from $V \simeq Q_b / \Delta H_{vap,i}$*

The simulated responses for vessel (a) and column (b) temperatures presented in Figure 4.7 are in good agreement with the experimental data in Figure 4.3. One major cause for differences are the neglected heat loss from the intermediate vessels in the simulation. Furthermore we do not compensate for possible subcooling of the reflux flow. The volumetric reflux flows (see Fig. 4.7 c) show a somewhat different response with respect to the initial increase in reflux flow L_3 compared to the experiment (see Figure 4.3 d), however the overall trajectories are similar.

With the temperature setpoints given, we achieve for a feed charge of $M_{init} = 55 \text{ mol}$ and a composition of $z_F = [0.26, 0.12, 0.18, 0.44]$ the steady-state liquid holdup and compositions ($t \rightarrow \infty$) given in Table 4.3. The achieved product compositions compare well with the experimental result presented in Table 4.1; the differences in composition are at maximum $x = 0.026$ mole fraction units. Nevertheless, considerable differences between experiment and simulation are found for the impurity ratio x_{i-1}/x_{i+1} . Those differences can be partly explained because we use an integer number of stages in the simulations.

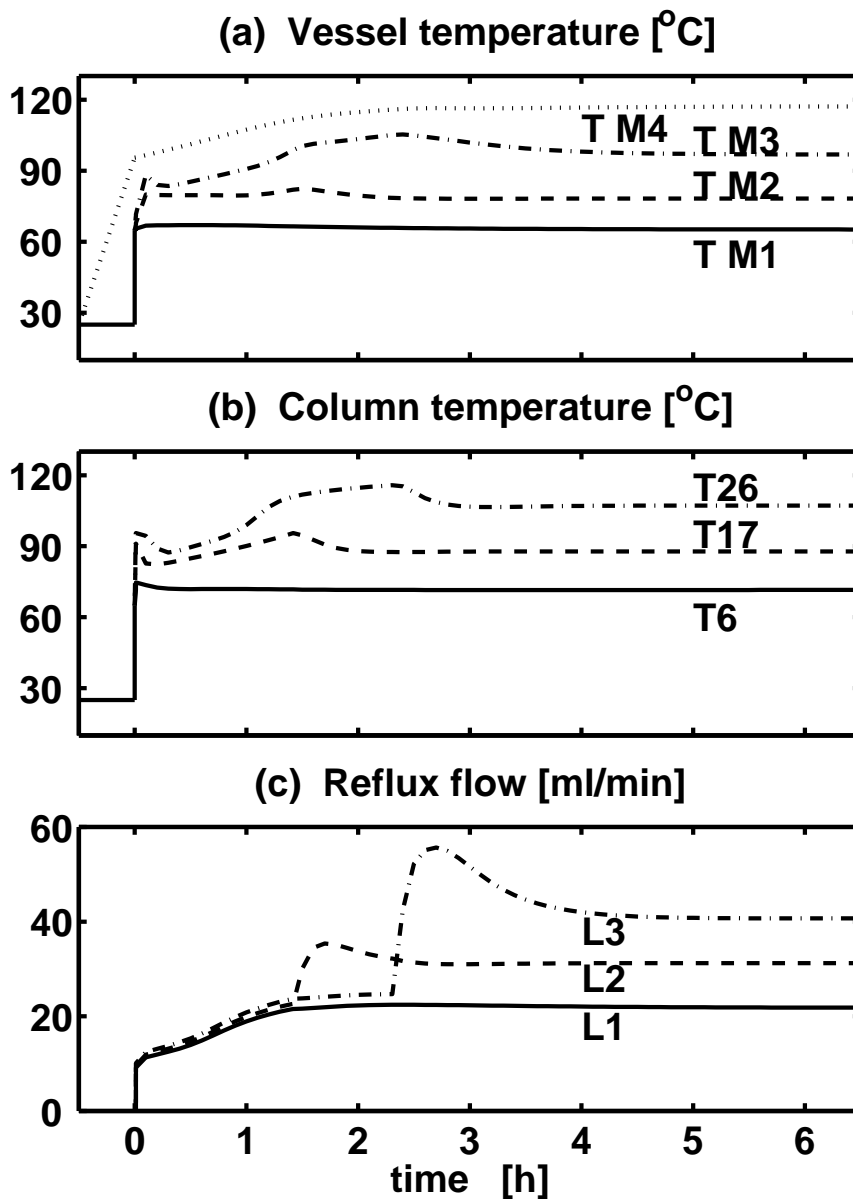


Figure 4.7: Simulation of experiment 12: Vessel temperature (a) and tray temperature (b) and volumetric reflux flow (c) as a function of time (to be compared with experimental results in Figure 4.3)

In Figure 4.9, we present composition time responses of the main components and impurities in the vessels for the simulation of experiment 12.

In Figure 4.10 we plot simulated composition profiles over the column for the four components for times $t = [0.5, 1, 2, 3, 6]h$. These profiles show nicely how the individual components accumulate along the the column during operation. The simulated temperature profile over the column is presented in Figure 4.11. A pronounced gradient in temperature is observed close to the center of each column section, which results in a temperature measurement with sufficient sensitivity for control purposes.

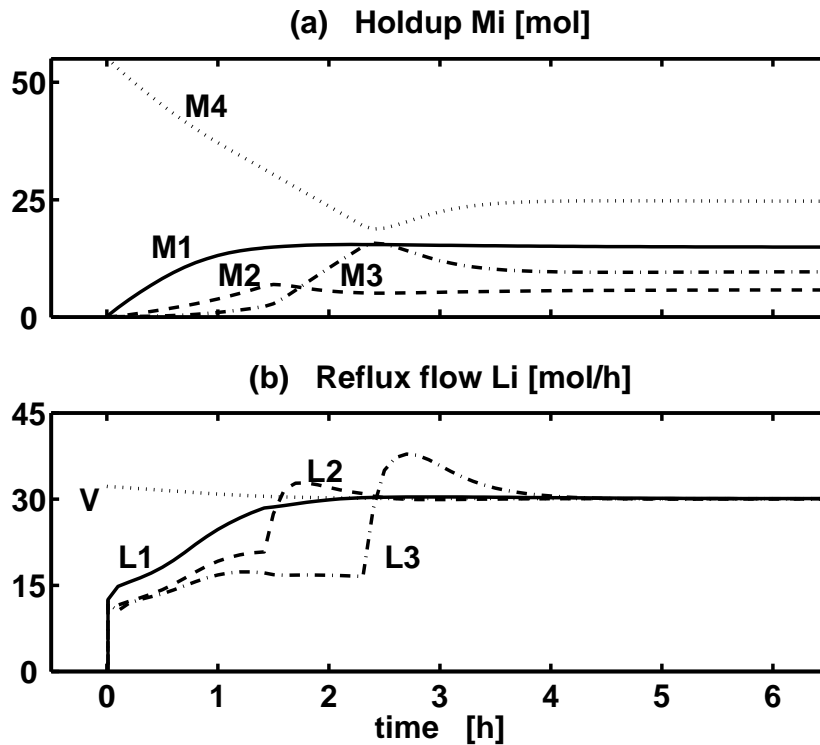


Figure 4.8: Simulation of experiment 12: molar vessel holdup (a), molar vapor flow and molar reflux flow (b) as a function of time

4.5 Discussion

4.5.1 Main lessons from the experiments

Following our initial proposal for closed operation with indirect level adjustment based on temperature control (Skogestad *et al.* 1997), concerns were raised that this would not work in practice, for example, due to the possibility of non-uniqueness in the specifications or other unforeseen reasons. The aim of this study was therefore to confirm experimentally the feasibility of the proposed method for operation.

The conclusion is that the experiments almost completely verify what was found in the simulations and we find that it is very easy to operate the column in this way. Except for some initial monitoring during start-up to make sure that the reboiler is not emptied, the column essentially “runs itself”. The only modifications made compared to the simulations in Skogestad *et al.* (1997) were to include some minimum liquid flows during the startup period, and to add integral action to the controller. The integral action is needed to adjust the bias term for liquid flows (in the simulations we used a P-controller and set the bias equal to the vapor flow, $L_{i,0} = V[\text{mol/s}]$, but this does not work in practice, because we do not have a perfect model and a constant and known value of the boilup).

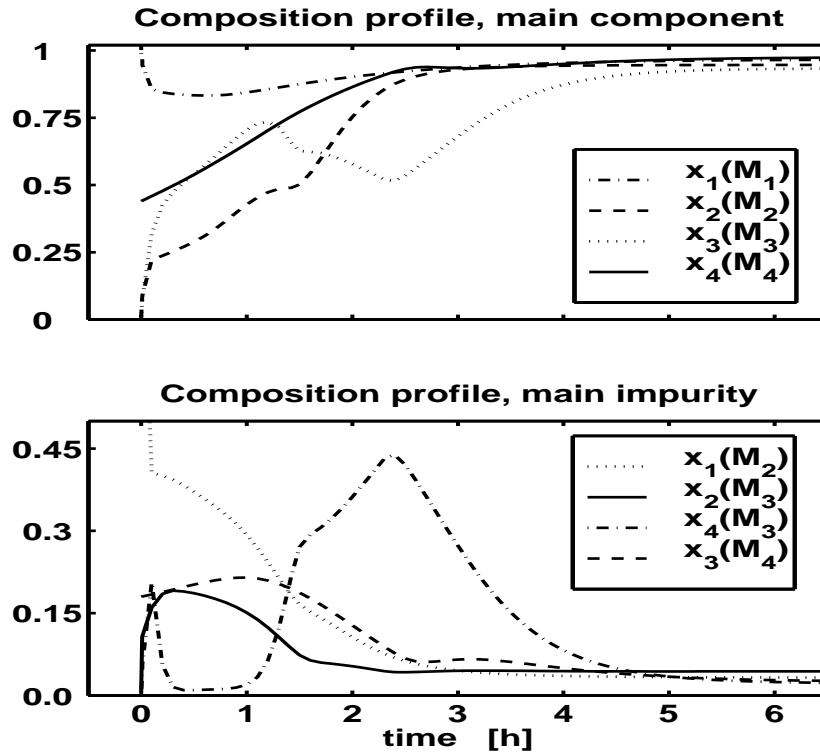


Figure 4.9: Simulation of experiment 12: vessel compositions (a) and major impurities (b) as a function of time

Table 4.3: Simulation of experiment 12: Steady-state holdups and compositions

	Vessel 1	Vessel 2	Vessel 3	Vessel 4
M	14.91	5.83	9.69	24.66
x_1	0.967	0.032	0.0	0.0
x_2	0.033	0.947	0.044	0.0
x_3	0.0	0.021	0.934	0.025
x_4	0.0	0.0	0.022	0.975
x_{i-1}/x_{i+1}	-	1.52	2.00	-

4.5.2 Suggestions for controller tunings

PI-controllers were used to manipulate the liquid flow to keep the column temperature in the middle of the section below at its setpoint. The operation depends somewhat on the controller tunings; a higher controller gain may give a somewhat faster response, but may result in a noisy response and problems with saturation of the manipulated variables. As a starting point for the controller gain we suggest the value

$$K_c = -\frac{L}{\Delta T_b}$$

where L is the nominal liquid flowrate and ΔT_b is the difference in boiling points of the components to be separated in the section. With this controller gain a change in composition corresponding a full boiling point difference is needed to make a liquid flow change of 100 %. For example, for our experimental column we have at the top of the column (vessel 1) $L/\Delta T_b = -20/13.6 \frac{ml}{minK} = -1.47 \frac{ml}{minK}$, and at the bottom (vessel 3) $L/\Delta T_b = -50/20.5 \frac{ml}{minK} = -2.45 \frac{ml}{minK}$. In the experiments we used a somewhat higher controller gain of $K_c = -2.88 \frac{ml}{minK}$ (in all vessels). Also, recall from experiment 4 that a gain of $K_c = -5.3 \frac{ml}{minK}$ was found to be too high as it gave a somewhat oscillatory response.

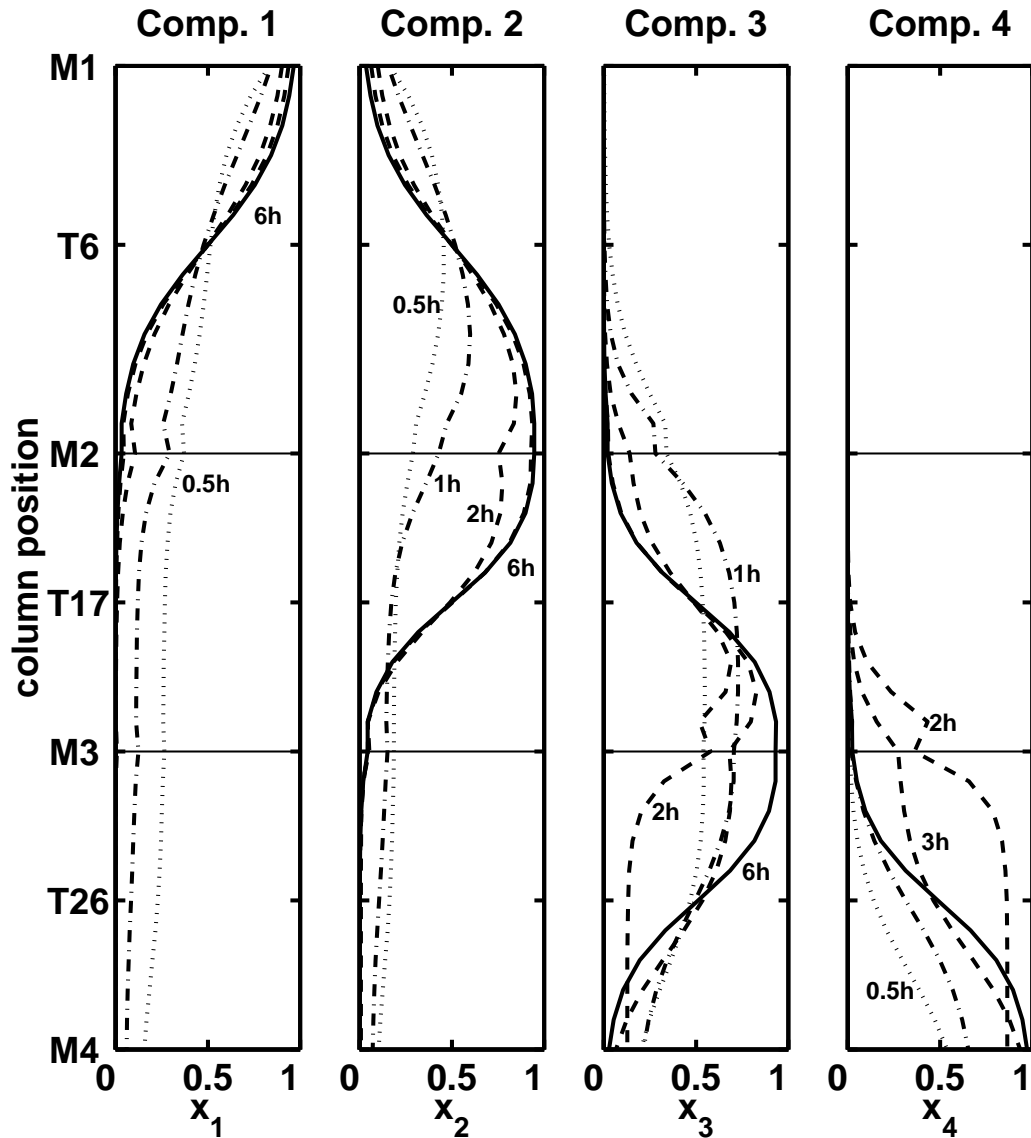


Figure 4.10: Simulation of experiment 12: Evolution composition profile over column

The integral time used in the experiments was about 5-10 minutes. This is about 1/15 of the time to evaporate the entire feed mixture (internal circulation time) which was about 2

hours in our experiments.

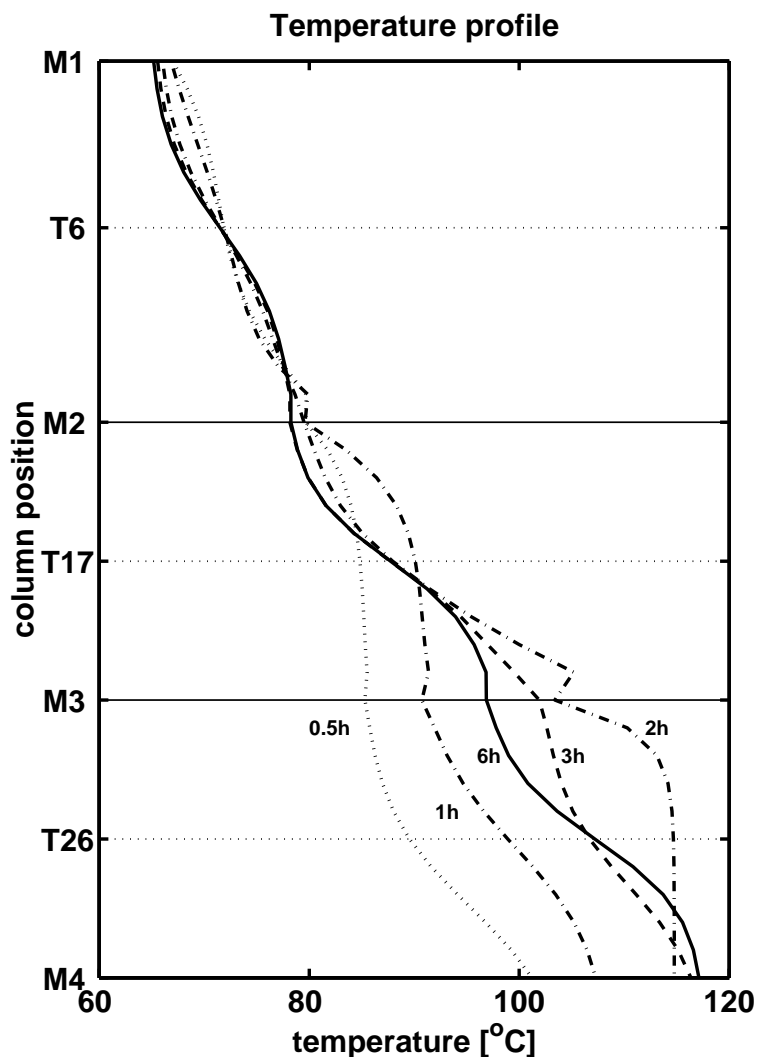


Figure 4.11: Simulation of experiment 12: Evolution temperature profile over column

4.5.3 Justification for column temperature control

In the experiments we keep the temperature in the middle of each column section at a given setpoint value by manipulating the liquid reflux into the section. The setpoint value is essentially the cut-point temperature between the components (fractions) to be separated. This control strategy has proven to work very well, both in simulations and experiments.

At first this may seem somewhat surprising. For example, if we specify $T_{S2} = 87.75^{\circ}\text{C}$ (middle of the column), then there is clearly an infinite number of possible mixtures of methanol-ethanol-propanol-butanol with this boiling temperature. However, there is only one binary mixture of ethanol-propanol with this boiling temperature, so provided we are able to establish some initial profile in the column, the relationship between temperature and composition is unique.

Thus, there seems to be at least two reasons why the control strategy based on column temperature control works in practice:

1. **Steady-state uniqueness.**

Consider a column with $n-1$ sections (and thus with $n-1$ temperature setpoints) separating a mixture of n given components in a column with a fixed number of theoretical stages. We conjecture that there is then a unique steady-state relationship between the temperature setpoints and the vessel compositions. Furthermore, this relationship is independent of the initial feed composition, except for some azeotropic mixtures where there may be several regions (Hilmen *et al.* 1999).

The conjecture has been confirmed by simulations and the experiments presented in this paper. It is also confirmed by the thermodynamic analysis of Hilmen *et al.* (1999) for ternary mixtures who point out that the steady state temperature profile will be identical to the *distillation lines* (which are closely related to the *residue curves*).

2. **Unique dynamic response (no inverse response behavior).**

We conjecture that the dynamic response from the reflux (manipulated input) to the temperature in the section below (controlled output) has no inverse response behavior (unstable zero dynamics; RHP-zeros) which may cause control difficulties. This is based on the assumption that the temperature decreases as we go up the column. An increase in liquid reflux will then result in decrease in temperature in the column section below.

4.5.4 Alternative control variables

We have established that column temperature control works well. We argue here that some of the alternative schemes *e.g.* based on vessel compositions or vessel temperature, will not work in practice.

Composition measurement of main component in vessel

This is of course what we really want to control. However, there are two serious problems if composition is used for feedback control:

1. Steady state considerations.

Most seriously, the composition specifications may not be achievable because there are too few theoretical stages. In another case, a given specification may be “too easy” compared to the number of stages, and we may quickly meet the specification in one vessel. However, if we have not yet reached the specifications in the other vessels, then we will have difficulty trying to keep the composition at this “easy” value (as confirmed by simulations).

2. Dynamic considerations

The dynamic response is not unique and inverse response behavior may result because the effect of a change in reflux on composition of the main component in the vessel

will depend on the distribution of the impurities. If the impurities are mostly heavy component, then we need to “move” some of the vessel holdup down to the vessel below, and an increase in reflux (i.e. the flow out of the vessel) will increase the purity of main component. However, if the impurities are mostly light component, then we need to “move” some of the vessel holdup up to the vessel above, and an increase in reflux will only make the situation worse by transferring the main component to the vessel below. Thus, the sign of the gain from reflux to composition depends on the operating point, and such a system is almost impossible to control.

These difficulties have been confirmed in simulations (Wittgens, 1999).

Temperature measurement in vessel

This variable has the same problem with respect to inverse response behavior as just mentioned for the composition of the main component. In addition, we will have the “usual” problem of sensitivity to measurement error and noise which is always encountered when we use temperature as an indicator of composition for a high-purity product.

In conclusion, use of column temperatures is simple and also seems to be the best measurement to use for controlling the multivessel column.

4.5.5 Optimal operation

There are some degrees of freedom for optimizing the operation. These include initial distribution of holdup setpoint temperatures, and controller tunings.

Simulations and experiments have shown that the exact value of the setpoint temperature is not important as long as the column has sufficient number of stages for the desired separation. Thus using the average between the boiling points is a good choice in most cases. Also, note that with a sufficient number of stages we may achieve any desired purity in the intermediate vessels (see Skogestad *et al.* 1997).

The initial holdup distribution has some effect, and it seems from simulations (Furlonge *et al.* 1999 and Hasebe *et al.* 1999) that in most cases it is best in terms of minimum batch time to charge the feed to the reboiler. In addition we have found experimentally that it is easier to establish a good initial composition profile with light component in the top if we charge the feed to the reboiler.

4.5.6 Closed operation of conventional batch distillation

Our experimental work is for a multivessel column, but obviously it also “simplifies” the closed operation of a conventional batch column where we include a top product vessel (see Figure 4.12).

The closed mode of operation based on a single temperature measurement is very simple and requires minimal operator intervention and monitoring. For example, one can leave the column by itself without having to worry that we will get breakthrough of heavy component. Simulations also indicate that it compares well with conventional batch distillation from an

energy point of view. It is therefore very surprising that there is no previous mention of this mode of operation (see Figure 4.12) in the literature, at least to our knowledge.

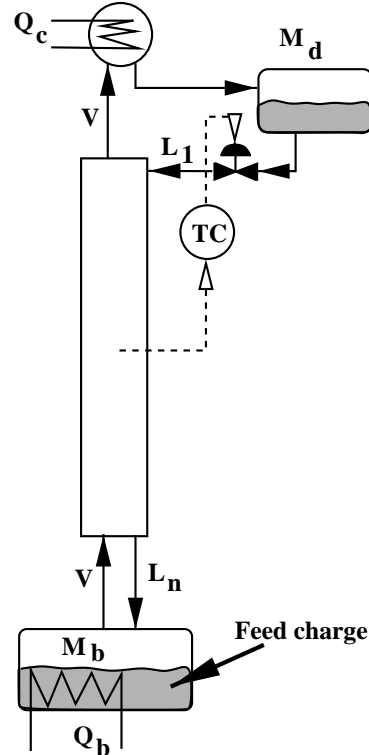


Figure 4.12: Control scheme for closed operation of conventional batch distillation column (two-vessel column)

4.6 Conclusions

The experiments show very good agreement with the simulations, and confirm that the multivessel column can be easily operated with a simple temperature controllers, where the holdups are only controlled indirectly. For a given set of temperature setpoints, we confirm that the final product compositions are independent of the initial feed composition.

Acknowledgements

The authors would like to thank students Stig Selberg, Kristian Aas and Berhanu D. Assefa for their assistance on some of the experiments.

Bibliography

1. Bortolini, P. and G.B. Guarise, "Un nuovo metodo di distillazione discontinua (In Italian; A new practice of Batch Distillation)", *Quad. Ing. Chim. Ital.*, Vol. 6, No. 9, 150-159, 1970
2. Furlonge, H.I., C. C. Pantelides and E. Sørensen, "Optimal Operation of Multivessel Batch Distillation Columns", *AIChE-Journal*, Vol 45, No. 4, 781-802, 1999
3. Hasebe, S., T. Kurooka and I. Hashimoto, "Comparison of the Separation Performances of a Multi-effect Batch Distillation System and a Continuous Distillation System", *Proc. IFAC-symposium DYCORD'95*, Denmark, 249-255, June 1995
4. Hilmen, E.K., V. Kiva and S. Skogestad, "Analysis of closed multivessel batch distillation of ternary azeotropic mixtures using elementary VLE cells", *Comp. & Chem. Eng.*, Supplement, Vol. 23, S 347-350, 1999
5. Noda, M., A. Kato, S. Hasebe and I. Hashimoto, "Optimal Structure of Batch Distillation Column", *Comp. & Chem. Eng.*, Supplement, Vol. 23, S 105-108, 1999
6. Skogestad, S., B. Wittgens, R. Litto and E. Sørensen, E. "Multivessel Batch Distillation", *AIChE-Journal*, Vol. 43, No. 4, 971-978, 1997
7. Treybal, R.E., "A Simple Method of Batch Distillation", *Chemical Engineering*, 95-98, 1970
8. Wittgens, B., R. Litto, E. Sørensen and S. Skogestad, "Total Reflux Operation of Multivessel Batch Distillation", *ESCAPE-96, Comp. Chem. Engng.*, Vol. 20, S1041-1046, 1996
9. Wittgens, B., PhD.-Thesis: "Experimental Verification of Dynamics Operation of Continuous and Multivessel Batch Distillation", Norwegian University of Science and Technology, 1999

Notation

K_c	Controller gain	$\frac{kmol}{h^\circ C} \frac{ml}{min^\circ C}$	L	Reflux flow	$\frac{kmol}{h} \frac{ml}{min}$
M	Holdup	$kmol, l$	N_c	Number of components	
N_i	Number of stages in section i		Q_B	reboiler heat duty	$\frac{kJ}{h}$
t	time	h	T	Temperature	$^\circ C$
T_b	Boiling temperature	$^\circ C$	TC_i	Temperature controller	
V	Vapor flow	$\frac{kmol}{h}$	x	molar liquid composition	
y	molar vapor composition		z_F	molar feed composition	
α	Relative volatility				
i	section identifier		j	component identifier	

Chapter 5

Alternative Control Structure of Multivessel Batch Distillation

Abstract

The multivessel batch column presented in the previous chapter provides a generalization of previously proposed batch distillation schemes. Composition control of this scheme is necessary if varying feed compositions are distilled in one column. A simple feedback control strategy, based on temperature measurements on the column is presented. The feasibility of this strategy for widely varying feed compositions is demonstrated by simulations and its performance is compared to control structures based on composition measurements. Initial investigations on the start-up procedure of the process will be presented which demonstrate the versatility of the column and its control system.

5.1 Introduction

The multiple heat-integrated batch distillation column, or “multi-effect batch distillation system” (MEBAD) (Hasebe *et al.* 1995) was suggested as an alternative to a train of continuous columns for the separation of a multicomponent mixture. A control scheme of this configuration was suggested by Hasebe *et al.* (1992 and 1995). The proposed operation is characterized by total reflux, in addition frequent product composition measurement and re-optimization of the vessel holdup is performed. An off-line optimization of the vessel holdup, and thus product composition will not cope sufficiently well with disturbances in feed composition or amount.

In its most general case, the multivessel column designed for the separation of N_C -components will consist of N_C -vessels and $N_C - 1$ column sections which interconnect the vessels. The column has $N_C - 1$ -degrees of freedom, that is if we specify $N_C - 1$ holdups (Hasebe *et al.*, 1995) all product compositions are specified, however, this open loop operation is not robust concerning feed-disturbances. A generalized feedback control structure of this column configuration is shown in Figure 5.1, the manipulated variables are the reflux

flows out of vessels 1 to 3, note that measured variables are omitted in Figure 5.1.

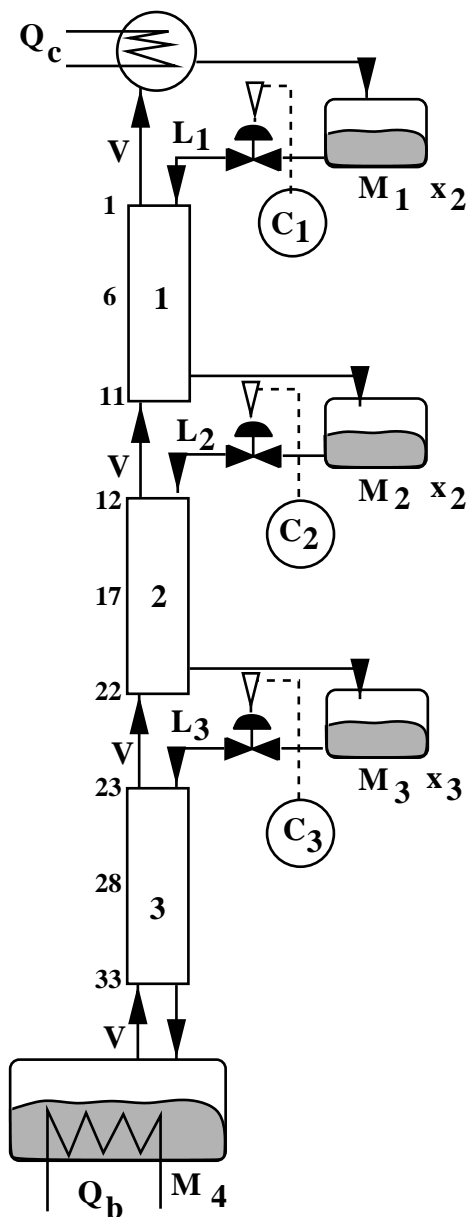


Figure 5.1: Multivessel batch distillation column

Composition control of the multivessel batch distillation column is not as straightforward as expected from conventional batch distillation. Direct composition control will consist of specifying the concentration of the main component in $N_C - 1$ vessels simultaneously, and apply *e.g.* controllers which adjust the reflux flow to a column section. Previous work on multicomponent distillation, show that a single composition specification in a multicomponent system not necessarily give a unique solution with respect to product composition if single loop controllers are applied (Jacobsen and Skogestad, 1991).

Alternative to a direct composition control, product composition estimation or control based on secondary measurements is suggested. Secondary measurements are frequently used in distillation column control (Kister, 1990; Mejdell, 1990) primarily cascaded to product composition analysis, these schemes in general speed-up the responses such that a better control performance is achieved. Application of secondary measurements on the multivessel column is straight forward, instead of specifying $N_C - 1$ holdup, $N_C - 1$ temperatures are specified (Skogestad *et al.* 1997). Of course this does not apply during start-up, nevertheless if time increases a binary separation is performed in each section of the multivessel column, thus specification of the temperature of a binary mixture (assumed constant pressure) result in a unique composition.

This chapter will outline the development of the control structure, starting from an initially proposed policy (Hasebe *et al.* 1995) where the initial feed composition and its amount is well known, thus the final product compositions can be determined by infrequent measurements of holdups and their product composition. In section 5.2 we outline the proposed implementation of the multivessel column and present dynamic simulation results of its open loop (uncontrolled) operation, this is, we keep the vessel holdups constant. Control strategies based on the direct control of the composition by adjusting the reflux flow are presented

and compared to the feedback control system presented by Skogestad *et al.* (1997). We demonstrate the feasibility of the feedback control structure and demonstrate that the final product composition is independent of feed compositions. Finally, a start-up procedure more oriented on the practical implementation on a pilot plant is considered. For an introduction to the process and a review of the literature we refer to chapters 1.4 and 3.

5.2 Total Reflux Operation

In this section we follow Hasebe *et al.* (1995) and present simulations which demonstrate the feasibility of the multivessel batch distillation under total reflux. This basic operation policy keeps the vessel holdup constant. In practice this can be achieved by fixing the height of an outlet weir¹.

The model applied is presented in the appendix to chapter 3. A summary of data for the column and feed mixture for the simulation example are given in Table 5.1.

Table 5.1: Summary of column data and initial conditions

Number of components	$N_c = 4$
Total number of stages	$N_{tot} = 33$
Number of sections	$N_s = 3$
Number of stages per section	$N_t = 11$
Vessel holdup	$M_m = 2.5 \text{ kmol}$
Tray holdup	$M_t = 0.01 \text{ kmol}$
Total initial charge	$M_{tot} = 10.33 \text{ kmol}$
Reflux flow	$L = 10 \text{ kmol/h}$
Vapor flow	$V = 10 \text{ kmol/h}$

The numerical value of ratios of the relative volatilities is chosen to be close to the experimental system in the pilot plant. Constant molar flows are assumed.

The holdup of each vessel is calculated in advance by taking into account the amount of feed, feed composition and product specifications. After feeding the predescribed amount of raw material to the vessels (identical holdups and compositions in each vessel), total reflux operation with constant vessel holdup is carried out until the compositions in all vessels satisfy their specifications.

The distribution of liquid over the vessels corresponds to a start-up from a “hot” column, this is, an initial composition profile over the entire column as well as flows and holdups are established².

¹Note we assume constant molar volume and density.

²Basically we assume that the entire column is filled with a feed mixture at boiling point. One might argue that this is a rather crude assumption since the light component are supposed to accumulate in the upper part of the column, while the heavier tend to accumulate in the bottom. Nevertheless the simulations show that the transient phase from assumed start-up condition to operation (initialization phase of the simulation) is short compared to the duration of the simulated operation.

Typical simulated composition profiles as a function of time are shown in Figure 5.2 for a four-component mixture with an initial feed composition of

$$z_{F,1} = [0.25, 0.25, 0.25, 0.25] \quad (5.1)$$

The simulation is terminated when either the product specifications in all vessels are fulfilled, that is

$$x_{spec} \geq [0.99, 0.95, 0.95, 0.99] \quad (5.2)$$

or the derivative of all compositions is less than $dx/dt = 10^{-6}$, which is defined as steady state condition. As time goes to infinity the steady state compositions presented in Table 5.2 are achieved, additionally the composition profile of the four components over the distillation column is shown in Figure 5.3. The operation policy of keeping the holdup of the vessels constant may be difficult to achieve in practice and also is very sensitive to errors in the assumed feed composition.

Considering a case where the actual feed composition is

$$z_{F,2} = [0.30, 0.10, 0.40, 0.20] \quad (5.3)$$

but the holdup of each vessel is equal to the example with feed composition $z_{F,1}$ in Eq. 5.1. This results in large changes in the final vessel compositions as seen from Table 5.3. For example, the purity in vessel 2 is reduced from $x_2 = 0.959$ to $x_2 = 0.404$. The composition profile for feed mixture $z_{F,2}$ over the distillation column at steady state is shown in Figure 5.4 for the constant holdup policy.

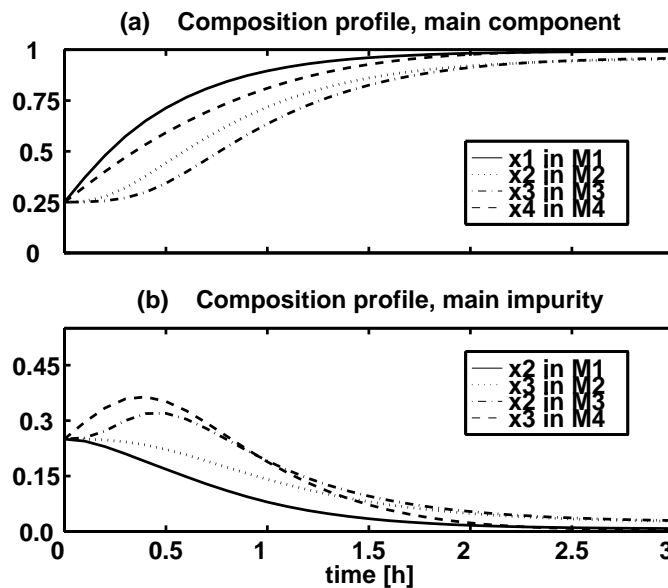


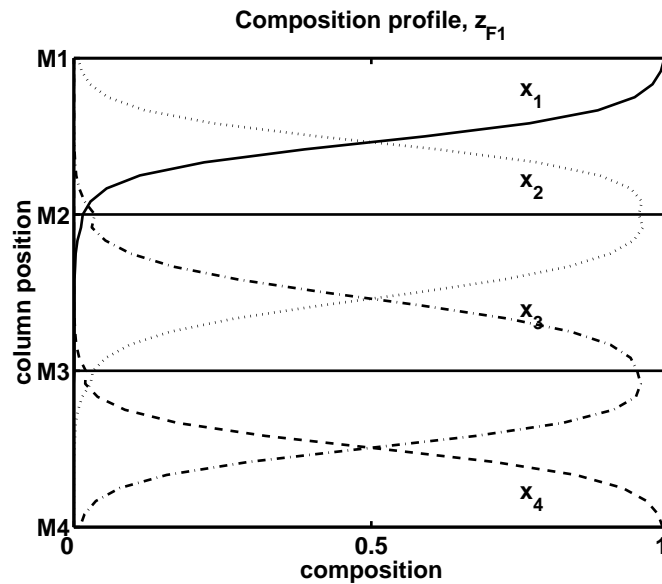
Figure 5.2: Constant vessel holdup (open loop): Composition response in accumulator (M1), vessel 2 (M2), vessel 3 (M3) and reboiler (M4) for feed mixture $z_{F,1}$

Table 5.2: Constant vessel holdup (open loop): Steady state ($t = \infty$) composition for initial feed composition $z_{F,1}$

	Vessel 1	Vessel 2	Vessel 3	Vessel 4
M_i [kmol]	2.5	2.5	2.5	2.5
x_1	0.993	0.017	0.0	0.0
x_2	0.007	0.959	0.025	0.0
x_3	0.0	0.024	0.963	0.004
x_4	0.0	0.0	0.012	0.996

Table 5.3: Constant vessel holdup (open loop): Steady state ($t = \infty$) composition for initial feed composition $z_{F,2}$

	Vessel 1	Vessel 2	Vessel 3	Vessel 4
M_i [kmol]	2.5	2.5	2.5	2.5
x_1	0.999	0.203	0.0	0.0
x_2	0.001	0.404	0.001	0.0
x_3	0.0	0.393	0.999	0.180
x_4	0.0	0.0	0.0	0.820

Figure 5.3: Constant vessel holdup (open loop): Steady state ($t = \infty$) composition profile over column for feed composition $z_{F,1}$

To compensate for these feed variations Hasebe *et al.* (1995) propose a rather complicated algorithm for adjusting the holdup based on measuring the composition and holdup in the vessels. An off-line optimization is performed to compute new setpoints for the vessel

holdup, these are then implemented subsequently by temporarily adjusting the reflux flow. Total reflux operation is resumed for a predefined time and the cycle of measuring the vessel composition, setpoint computation and implementation is repeated until the product composition requirements are fulfilled.

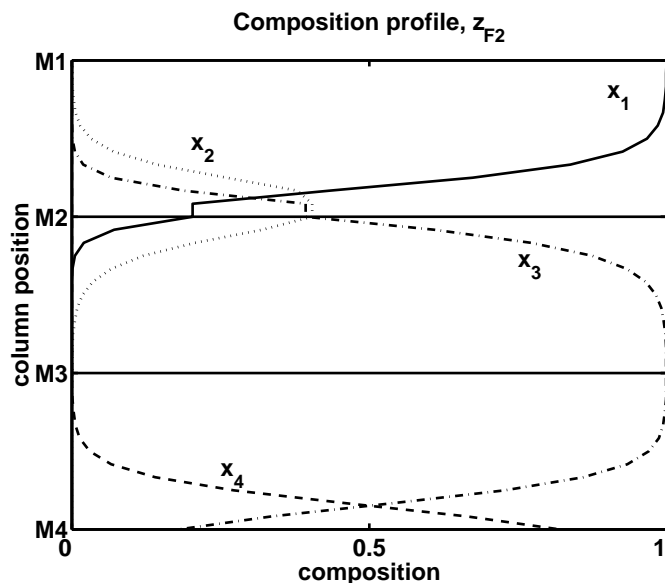


Figure 5.4: Constant vessel holdup (open loop): Steady state ($t = \infty$) composition profile over column for feed composition $z_{F,2}$

It is shown (Table 5.3 and Figure 5.4) that the fixed vessel holdup policy will not work if the initial feed composition is different from the design feed and an open loop control scheme is implemented (fixed vessel holdup). A composition control has to be implemented to ensure that product composition requirements are fulfilled. The above proposed scheme of indirect composition control (Hasebe *et al.* 1995) is rather complex, it requires, level and reflux control loops, instrumentation for composition analysis as well as an off-line optimization.

5.3 Composition control by feedback

The need of a reliable and simple to implement composition control has been demonstrated by the introductory example (see section 5.2). In the following sections we choose some means of feedback control of the product composition, namely by temporary adjusting the reflux flow out of the vessels based on some on-line measurement. Feedback control structures employing product composition control are presented in section 5.3.1 and 5.3.2. In section 5.3.3 and 5.4 control schemes with indirect composition control are presented.

An example of a flowsheet of the multivessel batch distillation column with feedback control structure is shown in Figure 5.1. The separation of a mixture containing N_c components require N_c vessels and $N_c - 1$ control loops. The controllers (C_i) adjust the reflux

flows (L_i) out of the vessels (M_i) above that column section. This enables an indirect control of the holdups in the vessels³

The operation of the column has to be performed such that operational problems, *e.g.* a reflux flow is reduced to $L_i = 0$ or draining of the vessels are avoided. The requirement, that all reflux flows $L_i \geq 0$, ensures that light components are removed from the vessels (constant draining) and propagate towards the top of the column while heavy component are moved towards the bottom of the column.

5.3.1 Feedback from vessel composition

A direct composition control scheme for the multivessel batch distillation column is shown in Figure 5.5, for simplicity only one of the intermediate vessels is presented, the entire column with an alternative feedback control scheme is presented in Figure 5.1.

The proposed feedback control scheme consists of composition analysis (*e.g.* gas chromatograph), a reflux controller (CC_i) and a reflux valve. The setpoint of the three necessary reflux flow controllers CC_i ⁴ are given by the first three product compositions (see Eq. 5.2).

It is assumed that each gas chromatograph has a sampling time of $\theta = 0.2 h$ ⁵. The column is initialized with the following start-up conditions: feed composition z_{F2} and liquid feed at boiling point evenly distributed over the column ($M_{i,0} = 2.5 kmol$).

For the presented simulations, single loop PI-controllers are chosen, the control algorithm is:

$$L_i = K_c \cdot \left((x_{s,i} - x_i) + \int_0^t \frac{1}{\tau_I} (x_{s,i} - x_i) dt \right) + L_{i,0} \quad (5.4)$$

where $L_{i,0}$ is the steady state reflux flow to a section. The control parameters are summarized in Table 5.4

³Note, we conjecture that no level controller or level measurement is necessary, even though it has to be ensured that vessels are not emptied during operation.

⁴The closed process has three degrees of freedom, such that, if three product compositions specified the entire system is specified.

⁵Note, the analysis time of the gas chromatograph is chosen according to the equipment which was used during the experimental work, see section 4

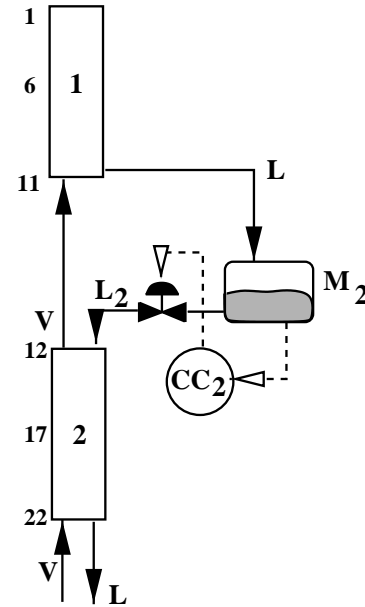


Figure 5.5: Feedback control structure for multivessel batch distillation, Composition control in product vessel M_i

Table 5.4: Vessel composition control: Data for composition controllers

composition controller	Component	setpoint	gain	reset	bias	location composition sensor
		$x_{s,i}$	K_c	time	L_∞	
			$kmol/h$	$1/h$	$kmol/h$	
CC_1	1	0.99	0.5	2	10	M_1
CC_2	2	0.95	0.5	2	10	M_2
CC_3	3	0.95	0.5	2	10	M_3

The controller gain was chosen to $K_C = 0.5 \text{ kmol/h}$ (for a deviation of $x_i = 0.1$ from the setpoint, the reflux flow is changed by $\Delta L = 0.05 \text{ kmol/h}$). The controller reset time (integral time) was set to $\tau_I = 2 \text{ h}$ (estimated from $\tau_I \geq 8 \cdot \theta$), and a controller bias $L_0 = 10 \text{ kmol/h}$ which is identical to the vapor flow. The controller tuning was determined from trial and error, primarily to avoid oscillations of the control loops.

In Figure 5.6 the vessel compositions (a), main impurities (b), vessel holdup (c) and reflux flows (d) as functions of time are presented. The simulation gave infeasible results, at $t > 4.2 \text{ h}$ negative holdup in vessel 2 are observed (see Figure 5.6c), because of the reflux flow out of vessel 2 and 3 (L_2 and L_3 , respectively) are at all times larger than the reflux flow L_1 from vessel 1 (see Figure 5.6 d).

In Figure 5.7 the composition trajectories of all four components in vessel 2 (top) and 3 (bottom) are shown. Inspecting the trajectories in vessel 3 at $t \approx 2 \text{ h}$ show that the controller gain has to change sign during the course of operation. The vessel compositions close to this point are presented in Table 5.5. From a control point of view the reflux flow controller has to change sign at $t = 1.9 \text{ h}$:

- $t < 1.9 \text{ h}$: the approach to setpoint is described by $\Delta x = x_s - x_3 > 0$ with $x_4 > x_2$: an increase in reflux L ($\Delta L > 0$) is required since heavier than key component has to be removed from this vessel
- $t > 1.9 \text{ h}$ still $\Delta x = x_s - x_3 > 0$ but with $x_4 < x_2$ a temporary decrease in reflux L ($\Delta L < 0$) is required

Even if in both cases ($t \neq 1.9 \text{ h}$) a positive deviation from the setpoint is observed, reflux flow has to be changed in opposite directions, which in turn requires a change in the controller gain from $K_C > 0$ to $K_C < 0$.

Table 5.5: Vessel composition control: Composition in vessel 3

time [h]	L_3 [kmol/h]	M_3 [kmol]	Comp. 1 x_1	Comp. 2 x_2	Comp. 3 x_3	Comp. 4 x_4
1.4	10.161	2.842	0.009	0.031	0.897	0.063
1.9	10.123	3.037	0.002	0.021	0.951	0.026
2.4	10.124	3.259	0.001	0.060	0.929	0.010

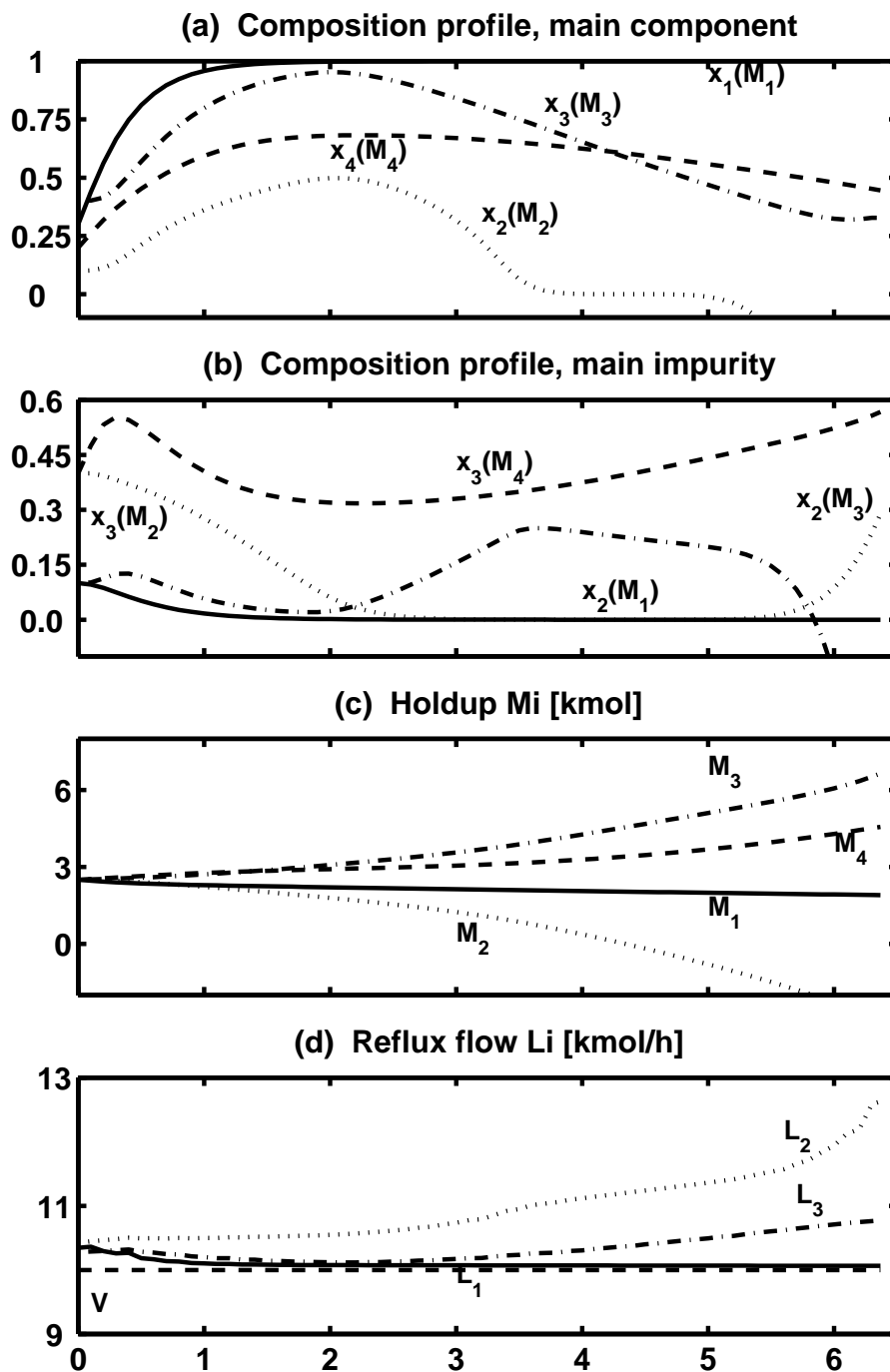


Figure 5.6: Vessel composition control for feed mixture $z_{F,2}$, vessel composition (a), impurities (b), holdup (c) and reflux flow (d) as a function of time

Similar conditions apply to vessel 2 (see Figure 5.6 top), at $t > 1$ h, concentration of component 1 is still increasing. The reflux flow out of vessel 2 should temporarily decrease to allow for heavier components to enter column section 2 and finally accumulate in vessel 2. Further, it can be seen from Figure 5.6 that with the now implemented reflux flow controller,

$L_2 > L_1$, such that vessel 2 is emptied. Note, that a cascade controller consisting of an inner-loop adjusting the holdup of the vessel by temporary adjusting the reflux flow and an outer control loop with an on-line composition measurement adjusting in the setpoint of the level controller will have similar performance problems.

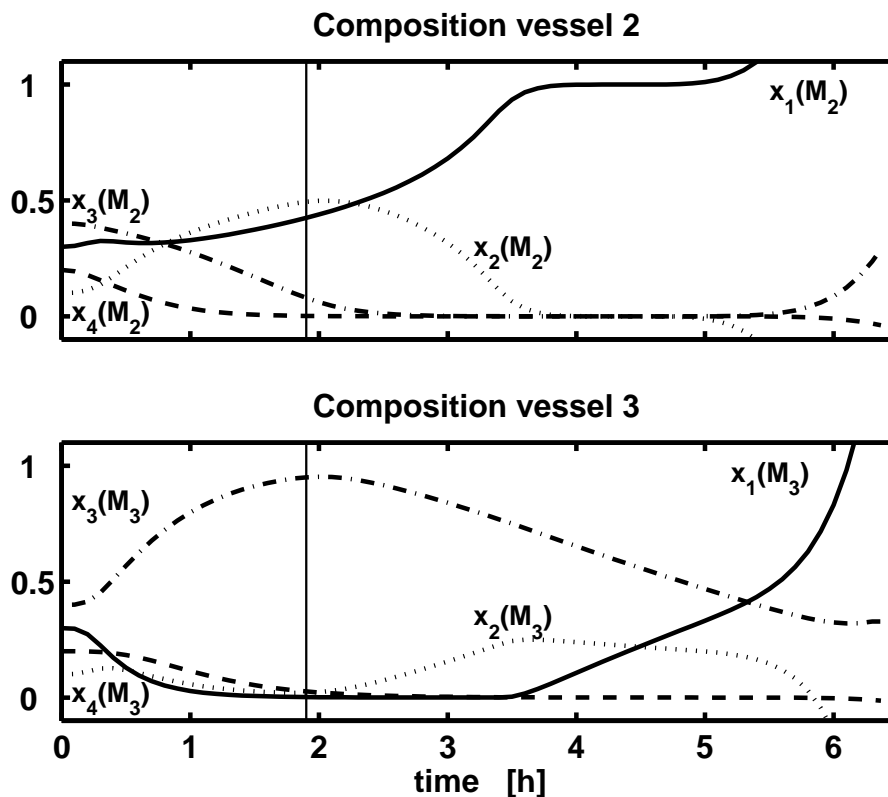


Figure 5.7: Vessel composition control: Compositions in vessel 2 and 3 as a function of time

5.3.2 Feedback from control tray composition

A control structure where tray composition from the center of each column is applied to adjust the reflux flow is investigated. In Figure 5.8 a control structure with direct measurement of the (liquid) tray composition is presented. A liquid sample is taken from trays 6, 17 and 28 (see Figure 5.1 for the column configuration) and on-line analyzed by means of a gas chromatograph. The composition measurement has a time delay of $\theta = 0.2h$. The control parameters are given in Table 5.6.

In Figure 5.9 the composition of the main components (a) and main impurities (b) in the vessels as function of time are presented. The product compositions are satisfied at $t = 3.07 h$, distillation has to be stopped in the interval $3.07 \leq t \leq 3.4 h$. At $t > 3.4 h$ the product compositions of vessel 2 and 3 are not longer satisfying the specifications, distillation has to proceed until $t = 10.88 h$, at this time all four product compositions are fulfilled again.

Table 5.6: Tray composition control: Data for composition controllers

composition controller	location composition sensor	Component	setpoint	gain	reset	bias
			$x_{s,i}$	K_c	time	L_∞
				$kmol/h$	$1/h$	$kmol/h$
CC_1	6	1	0.5	0.5	2	10
CC_2	17	2	0.5	0.5	2	10
CC_3	28	3	0.5	0.5	2	10

* location of control tray, counted from top to bottom.

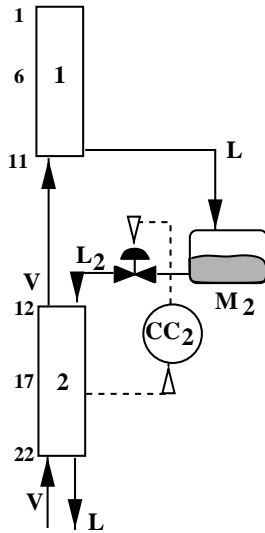


Figure 5.8: Tray composition control: Feedback control structure applying measurement on control trays 6 (x_1), 17 (x_2) and 28 (x_3)

In Figure 5.9 the trajectories of holdup (c), reflux flow (d) and control tray compositions (e) are presented. The trajectories of the tray compositions (see Figure 5.9 e) show extensive changes in tray compositions, due to the fact that a considerable amount of components has to be moved between vessels. The extensive changes on the control tray (time interval $0.2 \leq t \leq 3$) have similar control implications as an inverse response, which will limit the speed of control considerably. Thus a rather slow controller tuning has to be chosen which allow for a settling of the control tray compositions towards the setpoints. An increase in controller gain, alternative reduction in integral time constant result in draining of vessel 2 (see Figure 5.9 c).

The composition profiles over the column at times $t = [0, 0.5, 2, 3.1] h$ are shown in Figure 5.10. Note, for simplicity the composition profile at $t = 10.88 h$ is omitted since it is close to the steady state profile shown in Figure 5.3. The simulation results show that purification of the four components along the column is feasible, provided a suitable control system is applied.

Composition control by measuring the product composition in the center of the column and adjusting the reflux based on this measurement is possible. Nevertheless, the rather tight time interval where all four product compositions are satisfied requires a careful procedure to determine the shutdown of the facility. Comparing Figures 5.9 (a) and (e) shows that additional to the tray composition measurements used for control, composition measurements placed in each vessel are necessary to determine the exact time when all product composition specifications are satisfied. If product withdrawal is not performed in the time-window $3.07 < t < 3.4 h$, distillation has to proceed until $t = 10.88 h$, which correspond to an approximately threefold energy consumption.

Table 5.7: Tray composition control: Product composition for initial feed composition z_{F2} at $t = 3.07h$ and at steady state $t = 10.88 h$

time		Vessel 1	Vessel 2	Vessel 3	Vessel 4
$t = 3.07h$	$M_i [kmol]$	3.07	0.87	4.12	1.94
	x_1	0.991	0.011	0.0	0.0
	x_2	0.009	0.950	0.015	0.0
	x_3	0.0	0.039	0.970	0.003
	x_4	0.0	0.0	0.015	0.997
$t = 10.88h$	$M_i [kmol]$	3.06	0.74	4.21	1.99
	x_1	0.993	0.016	0.0	0.0
	x_2	0.007	0.970	0.044	0.0
	x_3	0.0	0.014	0.95	0.007
	x_4	0.0	0.0	0.006	0.993

Due to the difficulty to determine the correct time for shutdown of the facility and the extensive control signal variations, temperature measurements are introduced. In Figure 5.11 the temperature profile over the column at times $t = [0, 0.5, 2, 3.1] h$ is presented. The temperature profile show three regions with rather steep temperature gradients near the center of each column section⁶.

5.3.3 Feedback control based on tray temperatures

From the introductory example (see Figure 5.3 in section 5.2) we see that a pseudo-binary separation is performed in each column section. Assuming a binary separation, a unique solution of the relation between composition in a column section and measured temperature is given. The need for a more robust, reliable and faster control system was established in section 5.3.2 and temperature measurements where introduced.

In the feedback control structure (see Figure 5.12) temperature sensors provide the input signal for the individual reflux control loops, these sensors are located in the middle of each column section. The setpoints, $T_{s,i}$, for each temperature controller may be, in the simplest case, set as the average boiling temperature of the two components being separated in that column section, these setpoints are used in the simulations presented below. Alternatively, they may be obtained by steady-state calculations to get a desired separation, or they may be optimized with respect to minimum batch time or energy consumption.

⁶The tray temperatures are computed from $T_i = \sum_i^{N_c} x_i \cdot T_{B,i}$ with $T_B = [64.7, 78.3, 97.2, 117.2]^\circ C$ as boiling points of the pure components, see chapter 3 for details on the model.

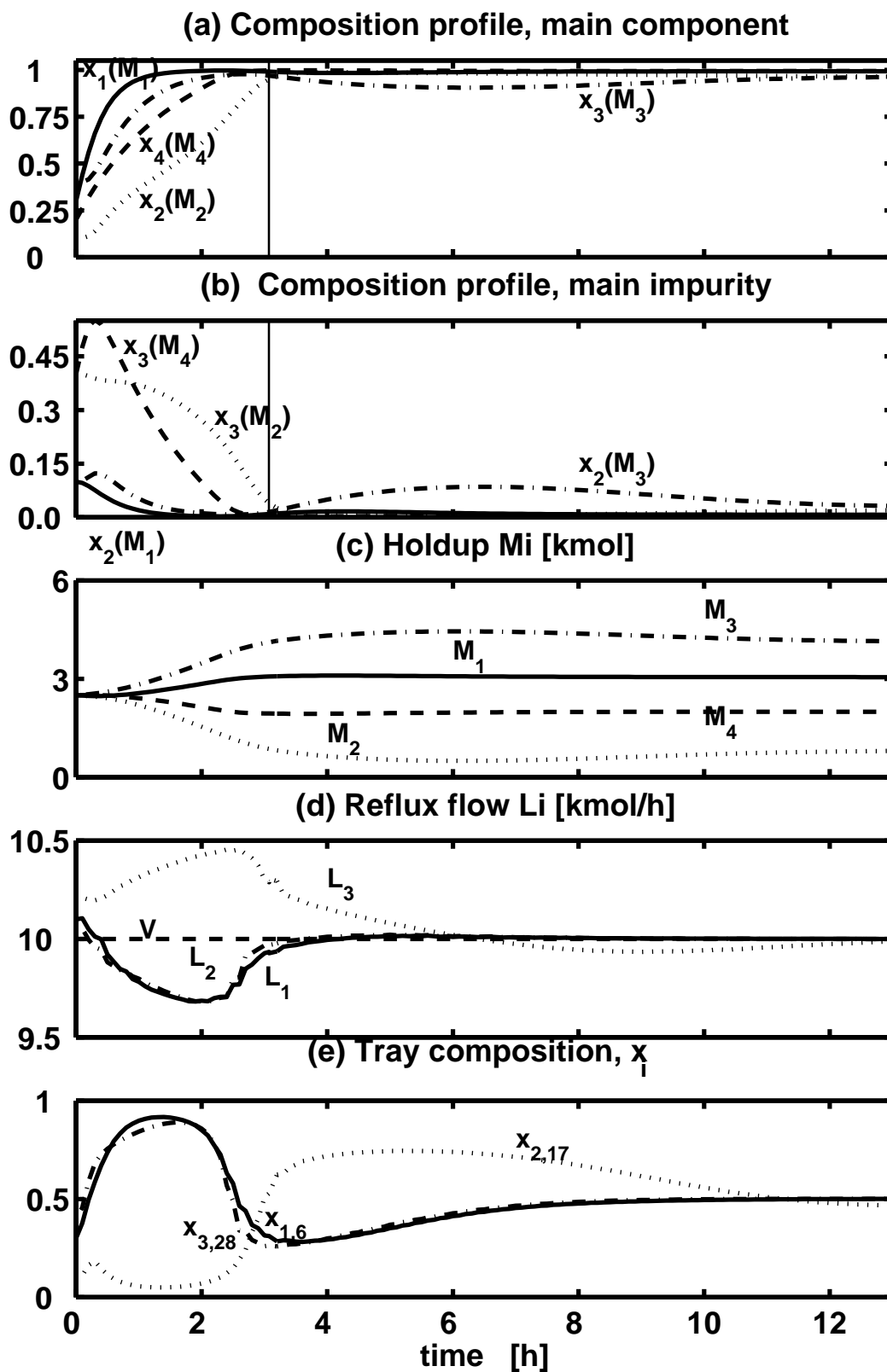


Figure 5.9: Tray composition control for feed mixture $z_{F,2}$: Vessel compositions (a), main impurities (b), holdup (c), reflux flow (d) and tray compositions (d) as a function of time

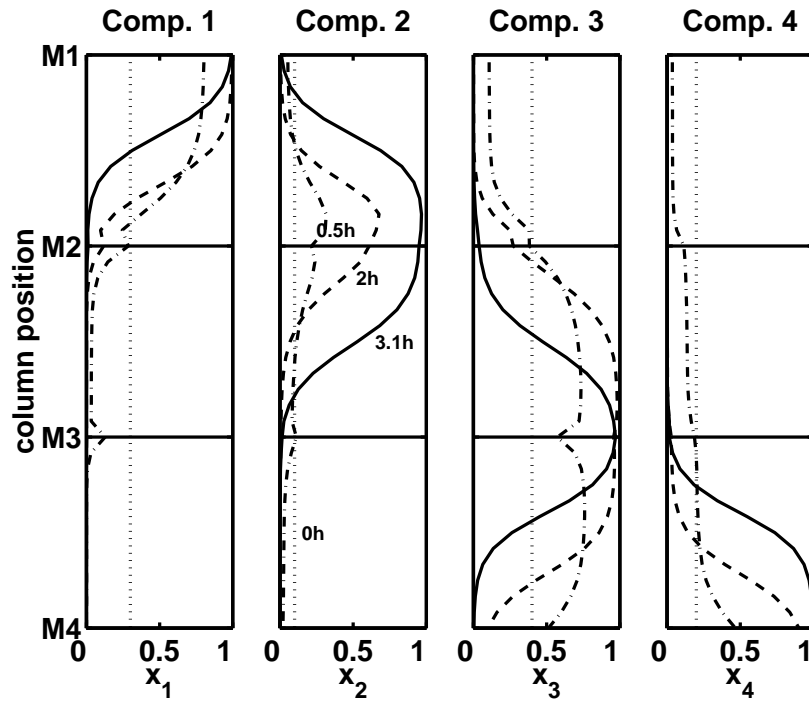


Figure 5.10: Tray composition control: Composition profile over column for component 1 to 4, $z_{F,2}$ at $t = [0, 0.5, 2, 3.1]h$

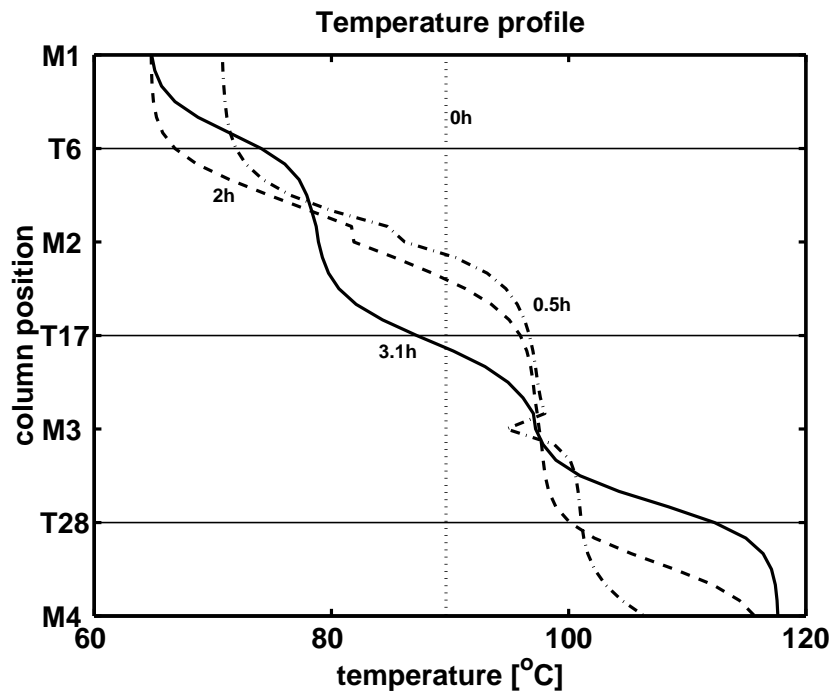


Figure 5.11: Tray composition control: Temperature profile over column at $t = [0, 0.5, 2, 3.1]h$

The feasibility of our proposed control scheme is demonstrated by the same column configuration as studied above (see Table 5.1). The utilized controllers are simple proportional controllers as given in Table 5.8. The controller gain K_c is chosen such that an off-set of 10 °C results in a change of 2.5 kmol (25 % of the steady state flow).

The proportional control algorithm is:

$$L_i = K_c \cdot (T_{s,i} - T_i) + L_{i,0} \quad (5.5)$$

where $L_{i,0}$ is the steady state reflux flow to a section.

Table 5.8: Tray temperature control: Data for temperature controllers

temperature controller	setpoint	gain	bias	location
	$T_{s,i}$	K_c	$L_{i,0}$	
	°C	kmol/(°C h)	kmol/h	*
TC_1	71.50	-0.25	10	6
TC_2	87.75	-0.25	10	17
TC_3	107.20	-0.25	10	28

* counting top to bottom

To demonstrate that the proposed control scheme is insensitive to the initial feed composition we use two different initial feed compositions, $z_{F,1}$ (Eq. 5.1) and $z_{F,2}$ (Eq. 5.3). With the given controller settings and chosen setpoints (see Table 5.8), in *both* cases the same steady state compositions are reached as $t \rightarrow \infty$ (see Table 5.9). These steady state compositions are very close to those found earlier for feed mixture $z_{F,1}$ for a constant vessel holdup of $M_i = 2.5 \text{ kmol}$, compare Tables 5.2 and 5.9. However the resulting holdups in the vessels are different in each case, as shown in Table 5.10. The new feedback policy ensures that the required product qualities are achieved irrespective of the initial feed composition by redistribution of the liquid holdup along the column. For feed mixture $z_{F,2}$ the vessel holdup varies from 0.788 kmol for vessel 2 to 4.159 kmol for vessel 3.

In Figures 5.13 and 5.14 the vessel compositions (a), main impurities (b), the vessel holdups (c), the reflux flows (d) and controlled tray temperatures (e) are shown as a function of time.

The composition profiles as a function of time for feedback control with tray temperature control are shown for mixture $z_{F,1}$ (Figure 5.13, a and b) and $z_{F,2}$ (Figure 5.14, a and b). The composition responses for feed mixture $z_{F,1}$ for the feedback control operation policy are quite similar to those for the case with constant holdup (see Figure 5.2). The approach to steady state is somewhat faster in vessel 1 and 4 and slower in vessel 2 and 3 for the control structure employing temperature control. On the other hand with feed composition $z_{F,2}$ the new policy ensures that the required product qualities are achieved. This is seen from Table 5.9 and is further demonstrated in Figures 5.14 (a) and (b) which show the composition profiles in the vessels.

For feed mixture $z_{F,2}$, the purification of the holdup in vessels 2 and 3 is considerably slower than in the accumulator (M_1) and reboiler (M_4) compared to feed mixture $z_{F,1}$ (see

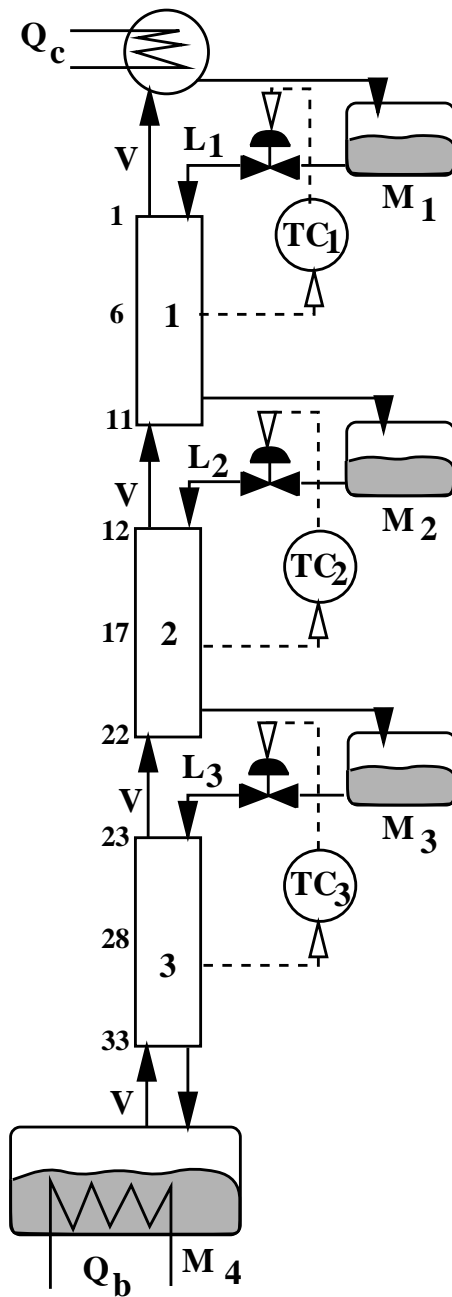


Figure 5.12: Tray temperature control: feedback control structure

Figure 5.14 a and b). The slower approach to steady state in the case of the feedback control structure is caused by temporary changes in reflux (compared to its steady state value) during the initial time of operation. The feedback controllers are activated on start-up and the initial temperature in the column (average boiling point of the mixture) is rather high/low in the upper/lower column section compared to its intended final temperature. This temperature profile results in a rather high reflux flow in the upper most column section (reflux L_1 see Figure 5.13 d and 5.14 d) such that light component is forced downwards towards vessel 2.

Table 5.9: Tray temperature control: Steady state compositions for feed mixtures $z_{F,1}$ and $z_{F,2}$

	Vessel 1	Vessel 2	Vessel 3	Vessel 4
x_1	0.993	0.016	0.0	0.0
x_2	0.007	0.967	0.034	0.0
x_3	0.0	0.017	0.960	0.007
x_4	0.0	0.0	0.006	0.993

Table 5.10: Tray temperature control: Steady state holdup distribution for feed compositions $z_{F,i}$

	Vessel 1	Vessel 2	Vessel 3	Vessel 4
feed	M_1	M_2	M_3	M_4
	[<i>kmol</i>]	[<i>kmol</i>]	[<i>kmol</i>]	[<i>kmol</i>]
$z_{F,1}$	2.506	2.452	2.512	2.530
$z_{F,2}$	3.053	0.788	4.159	2.000

A similar situation exist for vessel 3, where the rather low temperature in column section 3 results in low reflux flow L_3 , such that the holdup in vessel 3 increases. The excess liquid in vessel 2 and 3 has to be redistributed to vessel 1 and 4 which can be seen in Figure 5.14 e.

Three remarks about the results:

- In Figures 5.13 (e) and 5.14 (e) it is observed that the controlled temperatures reach their setpoint $T \rightarrow T_s$ as $t \rightarrow \infty$, even though only proportional controllers are used. This is possible since we know the steady state vapor and liquid flow exactly, thus we can set the controller bias such that $L_\infty = V_\infty$. With the applied control algorithm (see Eq. 5.5) we have $L_i = K_c \times (T_{s,i} - T_i) + L_{i,0}$ with $T_{s,i} - T_i \approx 0$ for $t \rightarrow \infty$ and $L_\infty = V_0$ ⁷.

Providing that the steady state flows are unknown, alternatively on a pilot plant were volumetric or mass flows are used for control purposes ($L \neq V$) a PI-controller will be necessary, this will be shown in section 5.4 as well as in the experimental verification presented in chapter 4.

- With temperature control we achieve the same steady state compositions in the vessels independent of the initial feed composition (only vessel holdups differ at steady state). The reason is that the column has only three degrees of freedom at steady state and if we fix three temperatures at three locations in the column, then the temperature profile over the column at total reflux is determined (if we assume that we do not have multiple steady states). Multiple solutions are not likely when temperatures are specified, but may be encountered if we specify the composition of a given component.

⁷This is a correction of the statement made in chapter 3

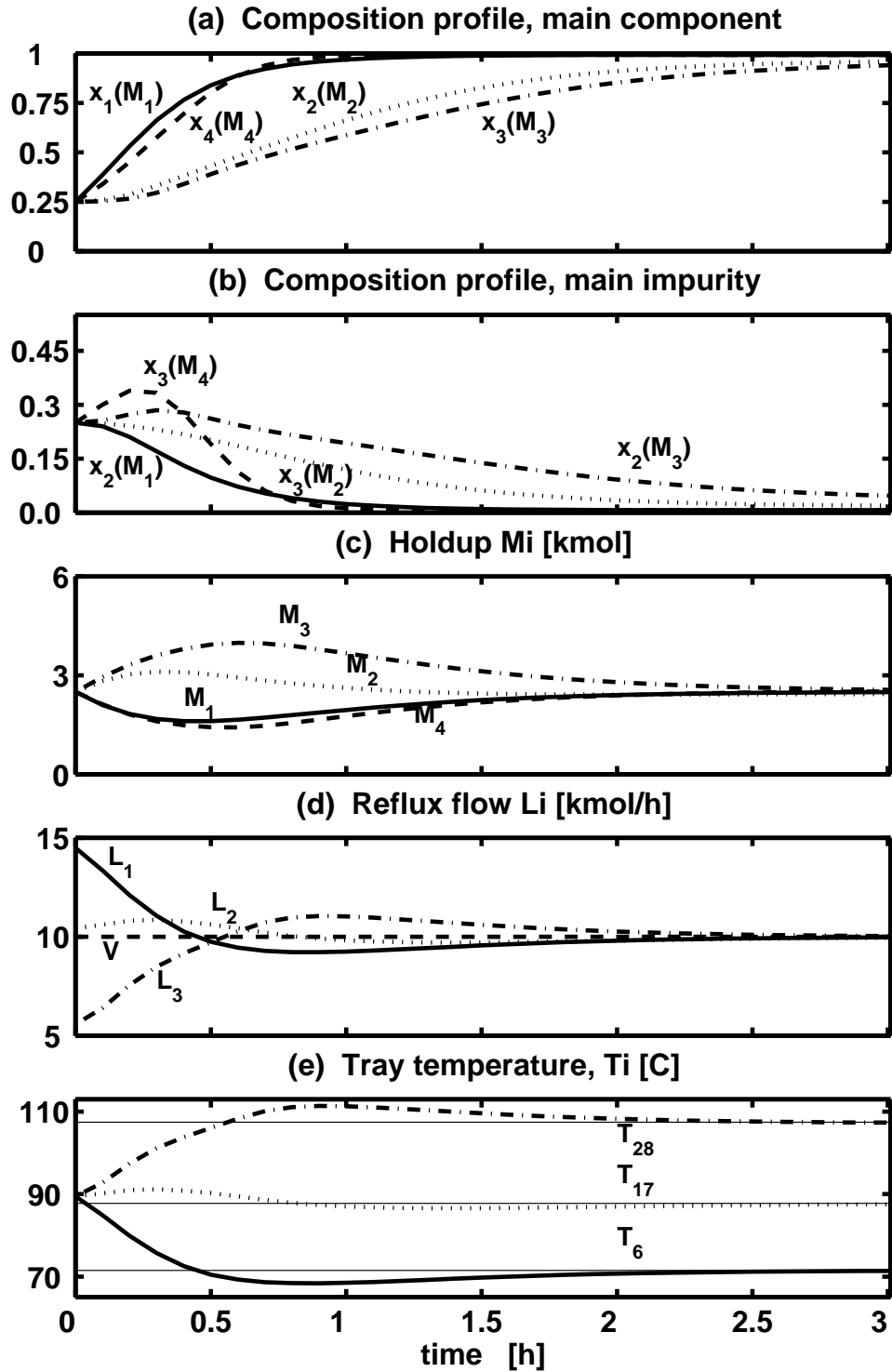
Feed composition z_{F1} 

Figure 5.13: Tray temperature control, feed mixture $z_{F,1}$: Vessel compositions (a), impurities (b), holdups (c), reflux flows (d) and tray temperatures (e) as a function of time

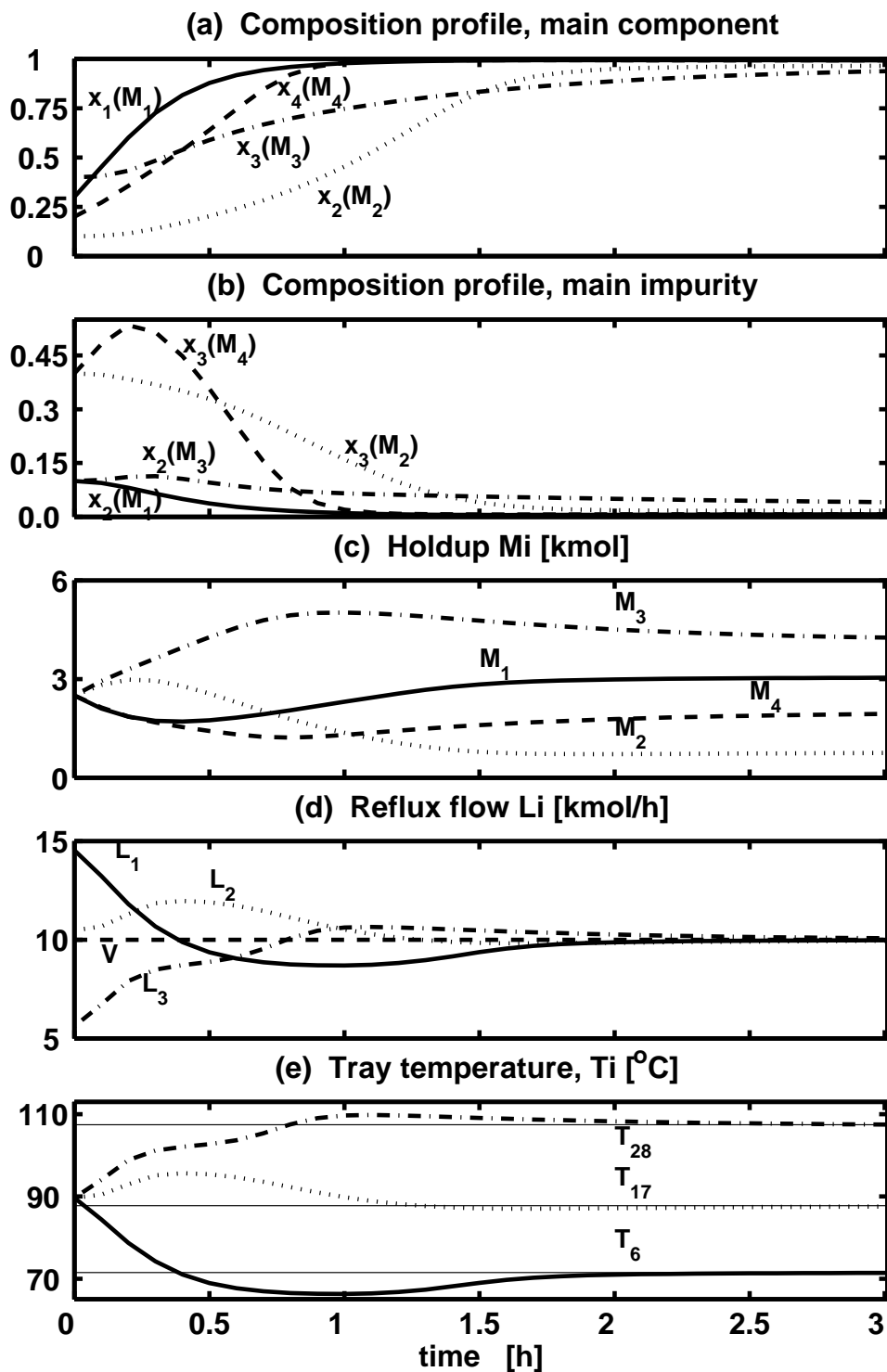
Feed composition z_{F2} 

Figure 5.14: Tray temperature control, feed mixture z_{F2} : Vessel compositions (a), impurities (b), holdups (c), reflux flows (d) and tray temperatures (e) as a function of time

- Inspecting the temperature trajectories on tray 17, shown in Figures 5.13 (e) and 5.14 (e), a slight inverse response is observed. This inverse response is dependent on the ratio of the lighter to heavier than the component which is purified in this section. In section 2, the steady state tray composition is supposed to be $x_{17} \approx [0.0, 0.5, 0.5, 0.0]$. The initial tray compositions are $z_{F1} = [0.25, 0.25, 0.25, 0.25]$ and $z_{F2} = [0.30, 0.10, 0.40, 0.20]$. Considering the chosen initial liquid distribution, for feed mixture z_{F1} approximately 1.25 kmol of component 3 have to be moved from vessels 1 and 2 to vessel 3. For feed mixture z_{F2} this amount is in the order of 2 kmol, approximately 60 % higher. Since the transport of component is performed in a similar time span, the inverse response in T_{17} for z_{F2} is more pronounced than for z_{F1} . Considering a feed mixture were the initial concentrations of component 2 and 3 are exchanged, the trajectory of T_{17} will be the mirror image as the one shown in Figure 5.14 (e).

In Figure 5.15 the composition profile over the column for feed composition z_{F2} are shown for times $t = [0, 0.5, 1.5, 3.5]h$. The composition profiles presented in Figure 5.3 (constant holdup policy with design feed z_{F1}) are close to those presented in Figure 5.15 for feed composition z_{F2} with tray temperature control.

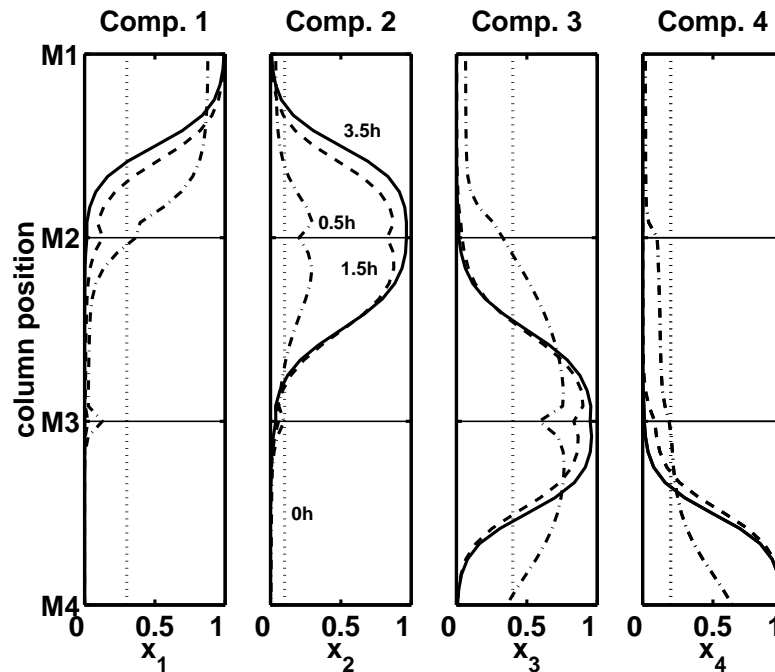


Figure 5.15: Tray temperature control, feed mixture z_{F2} : Composition profile over column at $t = [0, 0.5, 1.5, 3.5]h$

Figure 5.16 shows the temperature profile over the column for times $t = [0, 0.5, 1.5, 3.5]h$. The S-shape of the temperature profile in each section, with a rather steep temperature gradient at the center of the column sections, confirm that a sensor positioned in the center of each column section enable sensitive control of the vessel composition. The composition

in the vessel can be adjusted by keeping the sensor location and changing the temperature setpoint, which will move the profile accordingly.

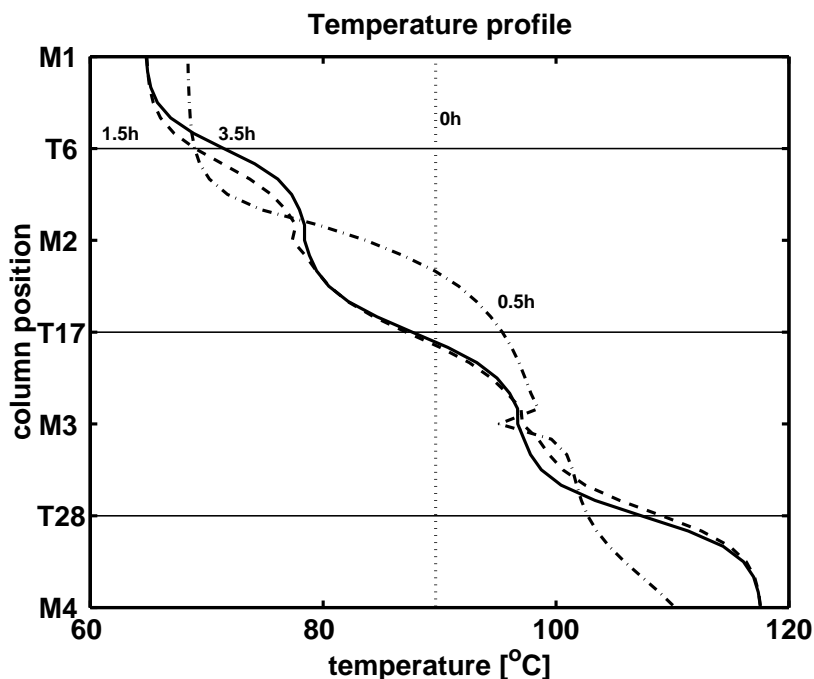


Figure 5.16: Tray temperature control, feed mixture z_{F2} : Temperature profile over column at $t = [0, 0.5, 1.5, 3.5]h$

5.4 Alternative Start-up Procedure

We have also performed some simulations to study the start-up for the case when the entire feed mixture is charged to the reboiler (and not distributed to the vessels as used in the previous sections). Investigations on the start-up of conventional batch distillation columns were presented by Sørensen and Skogestad (1994). They found that different start-up procedures for a batch distillation column are only of limited influence on the total batch time. Further, the non-unique relation between composition and temperature of a multi-component mixture might rise to operational problems. Especially during start-up of the unit, temperature in the column sections is subjected to considerable changes, such that some care has to be taken to avoid excessive control action.

The initial conditions for the start-up investigations, are summarized in Table 5.11, all remaining specifications are shown in Table 5.1.

The start-up of the multivessel batch distillation column was performed as follows. The reboiler was filled with an initial feed charge of $M_f = 10 \text{ kmol}$ with a composition of z_{F2} (see Eq. 5.3). The accumulator M_1 , the intermediate vessels and all trays were filled with $M_i = 0.01 \text{ kmol}$ with a initial composition of x_{init} (see Table 5.11). The vapor flow leaving

the reboiler was set to a constant value of $V = 10 \text{ kmol}/h$ over the whole simulation time⁸.

Table 5.11: Tray temperature control with alternative start-up: Summary of initial conditions for the start-up of multivessel batch distillation column under PI-control ($t = 0 \text{ h}$)

Reboiler holdup	$M_4 = 10 \text{ kmol}$
Reboiler feed composition	$z_{F2} = [0.3, 0.1, 0.4, 0.2]$
Vessel holdup	$M_{1:3} = 0.01 \text{ kmol}$
Tray holdup	$M_t = M_{t,i} \quad N_t = 0.33 \text{ kmol}$
Initial composition	$x_{init} = [0.90, 0.04, 0.04, 0.02]$

Start-up from “empty” vessels is performed with PI-controllers with the tuning parameters and setpoints presented in Table 5.12, the location of the temperature sensors is identical to the one given in Table 5.8. The rather long reset time τ_I of the integral action is chosen to achieve a smooth start-up and avoid extensive control action (*e.g.* saturation of manipulated variable or draining of the vessels). The control action of the PI-controllers is limited to be in the interval of $2 \text{ kmol}/h \leq L_{min} \leq 20 \text{ kmol}/h$. The lower limit on the reflux flow is chosen to prevent draining of the reboiler.

Table 5.12: Tray temperature control with alternative start-up: data for temperature controllers

temperature controller	setpoint	gain	reset time	bias	location sensor
	$T_{s,i}$	K_c^*	τ_I	L_∞	
	$^\circ\text{C}$	$^\circ\text{C}/\text{kmol}$	$1/h$	kmol/h	
TC_1	71.5	-0.25	1	10	6
TC_2	87.75	-0.25	1	10	17
TC_3	107.2	-0.25	1	10	28

* counted from top to bottom

The results indicate that the temperature controllers can be activated immediately after start-up or possibly after a short period with total reflux. The vessels are then slowly filled up by action of the temperature controllers which reduce the reflux flows for a transient period. Nevertheless, the simulations indicate that one should exercise some care to avoid emptying the reboiler (see Figure 5.17 c).

In Figure 5.17 we present the composition profiles in the vessels (a), main impurities (b), holdup response (c), the reflux flow (d) and the controlled tray temperatures (e) under start-up. The PI-controllers are activated at start up, with an initial reflux flow of $L_i = 10 \text{ kmol}/h$,

⁸Note, as in the previous presented simulations, see Section 5.3.3, we neglect an extensive total reflux period during start-up and assume that we start from a column filled with boiling liquid of some initial composition (x_{init}). Starting from a “cold” column would require time to heat up the feed mixture plus a certain time of total reflux operation to establish holdup in intermediate vessels and on all trays. This time will be identical for all simulations regardless of the chosen start-up procedure. For simplicity we have neglected this period of time.

the controller action adjust the reflux flow immediately after start-up and the intermediate vessels are filled slowly. The tuning of the PI-controllers (especially integral time) is chosen such that overshoot in the controlled column temperature (T_i in Figure 5.17 e) is small, such that only minor amount of heavier component, with respect to the main-component in a given section, are carried upwards. In Figure 5.18 the composition profiles over the column are shown for $t = [0, 0.5, 1, 4]h$, the specified product composition are achieved after approximately 4 hours, steady state is achieved at approximately 10 hours.

Temperature profiles over the multivessel batch distillation column with the alternative start-up procedure are presented in Figure 5.19.

The two control schemes where temperature is used as controller input signal are significantly different with respect to the start-up procedure and controller types, further different methods of initialization are applied.

- Proportional-only controllers are sufficient for the case where liquid is distributed over the column during start-up, provided the controller bias is chosen identical to the steady state reflux flow and boiling liquid with identical composition is distributed over all vessels and trays. Because of the chosen initial composition, rather extensive deviations between computed temperature and the setpoint in the section is observed for temperatures T_6 and T_{28} . The intermediate vessels build a buffer between liquid entering from a section and reflux leaving the vessels (Figures 5.14 and 5.17) where reflux flow $L_1 \geq V$ for $t \leq 1 h$. Clearly, if such an extensive control action caused by a proportional-only controller occurs during start-up from empty vessels, vessel M_1 will be drained and loss of the manipulated variables would be the result.

During start-up from an empty column, primarily light component is present in the column (see Figure 5.18). Choosing a proportional-only controller will reduce the reflux flow to $L_i = 0.0 kmol/h$ due to the deviation of setpoint and column temperature (see Figure 5.17 e). Thus, no liquid would reach the lower intermediate vessels, especially draining of the reboiler will be detrimental to the separation. Proportional only controllers are insufficient in respect to ensure a certain minimum liquid holdup in the vessels, further very low gains during start-up will result in extensive batch times.

- A proportional-integral controller give the opportunity to “adjust” the controller output changes without introducing hard bounds on the control action (minimum/maximum range) and provide a smooth transition from operation where $L \neq V$ towards total reflux operation, provided the integral time is chosen long enough. The control action of the PI-controller with long integral time has approximately the same control performance, with an in-build (slow) bias adjustment. Thus, the requirement made earlier that the steady state vapor and liquid flows have to be known (identical for molar flows) can be relaxed. Further, a robust operation is possible.

A slow integral action is chosen since we control the product composition in the vessel by means of a secondary measurement some distance away. The control is performed by moving the entire composition profile over the column, such that products with the desired composition can accumulate in the vessel (compare Figures 5.15 and 5.18). A trade-off in the controller gains has to be considered involving total batch time and the reduction in probability that the intermediate vessels or reboiler are drained.

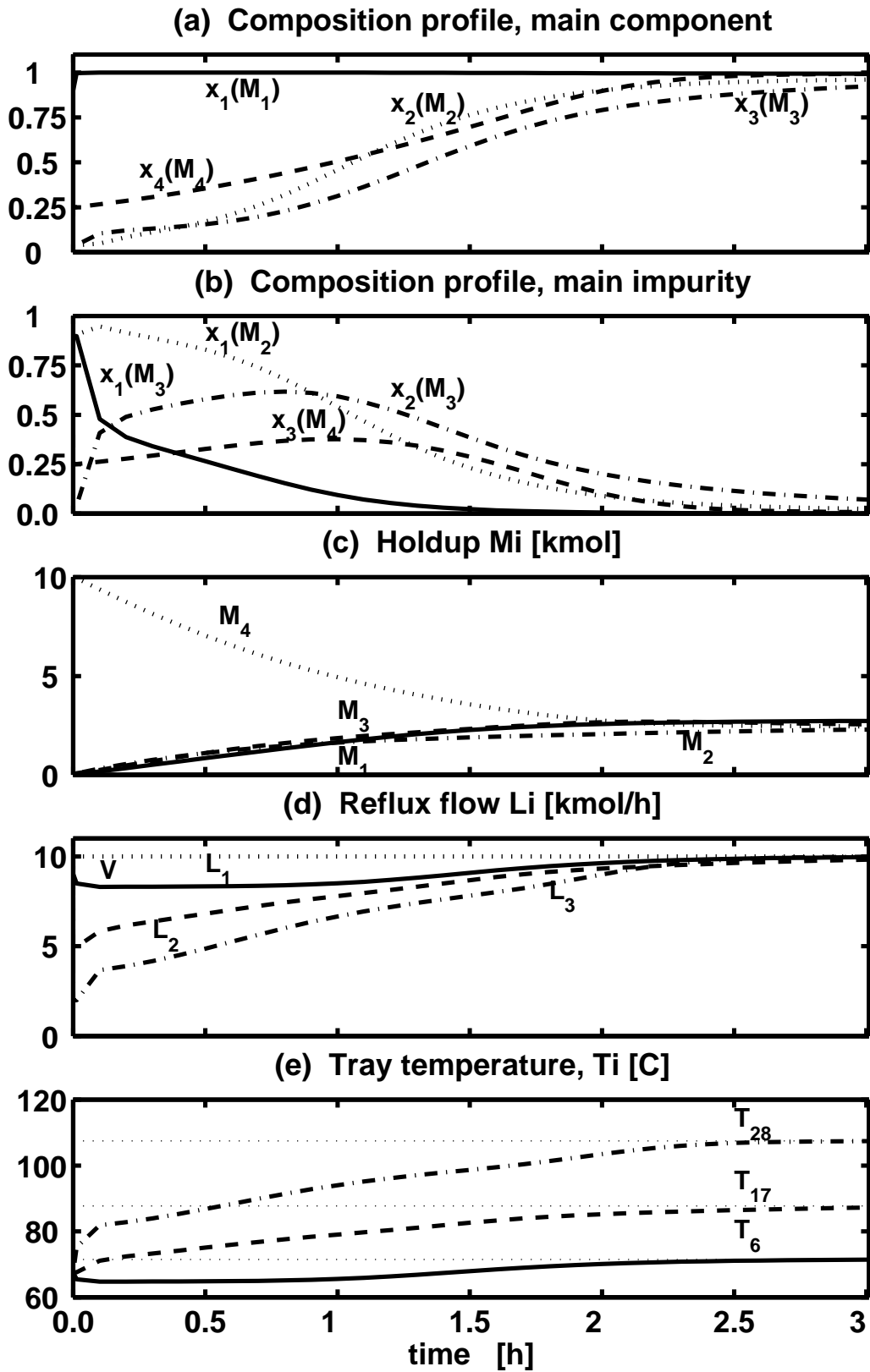


Figure 5.17: Tray temperature control with alternative start-up procedure for feed mixture $z_{F,2}$ with all liquid initially in the reboiler: Vessel compositions (a), impurities (b), holdups (c), reflux flows (d) and tray temperatures (e) as a function of time

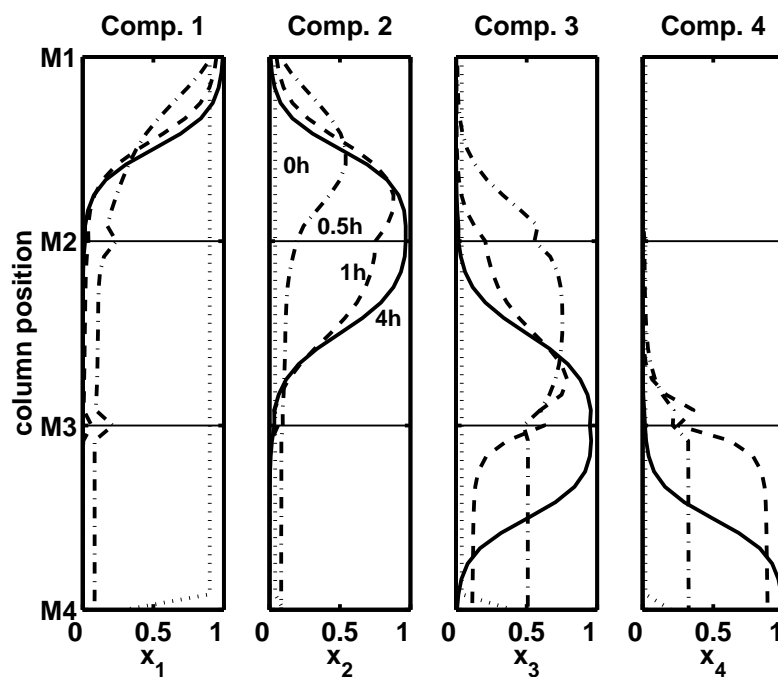


Figure 5.18: Tray temperature control with alternative start-up procedure, feed mixture z_{F2} : Composition profile over column at $t = [0, 0.5, 1, 4]h$

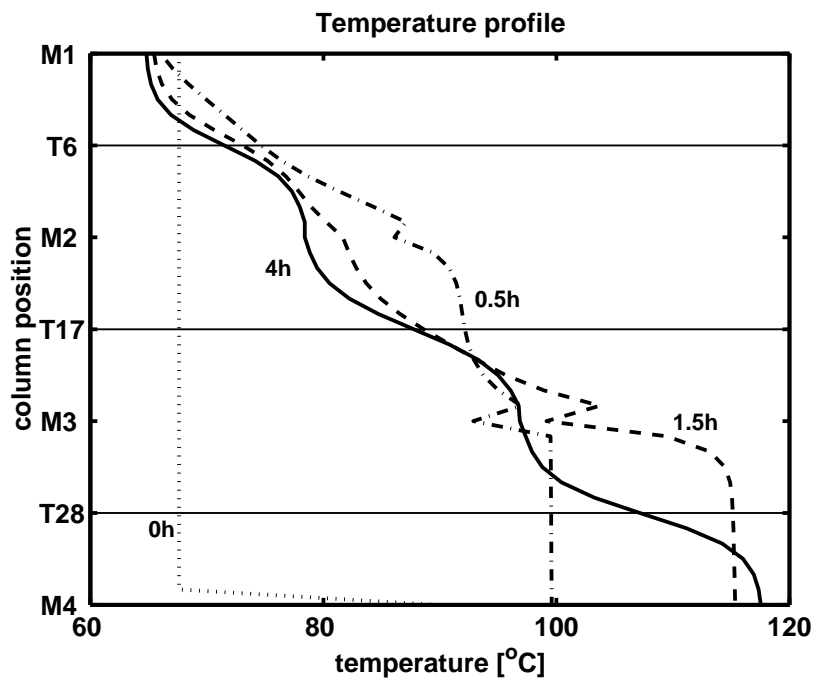


Figure 5.19: Tray temperature control with alternative start-up procedure, feed mixture z_{F2} : Temperature profile over column at $t = [0, 0.5, 1, 4]h$

5.5 Discussion

Simulations have shown that the initially by Hasebe *et al.* (1992) proposed procedure of constant vessel holdup performs poorly if feed disturbances are encountered. The system proposed by Hasebe with composition measurement and adjustment of the holdup to specify the existing three degrees of freedom is difficult to implement. Different feedback control strategies were investigated with control signals from primary (it e.g. gas chromatography) and secondary measurements (*e.g.* temperature). Primary measurements are available at a rather low frequency, *e.g.* gas chromatographs widely used in industries have a time delay in the order of $\theta = 0.2 h$ for an analysis of one sample of the here described type. Further, these instruments require a considerable amount of maintenance and are rather expensive to operate.

The implementation of control strategies based on direct composition as described in section 5.3.1 and 5.3.2 is not straightforward. Especially, the control scheme presented in section 5.3.1 is infeasible. The composition measurement is taken in the vessel, depending on the impurity measured the sign of the controller gain has to change during the course of operation. Applying single loop controllers where a frequent switching in the sign of the controller gain is required is infeasible at the best time consuming and require experienced operators.

The problem of sign-change of the controller gains is solved by moving the location of the composition sensor from the vessel to a tray in the column (see Figure 5.8). The location of the control tray was chosen from the composition profile over the column. At steady state primarily two components are present, such that a unique relation between controller gain and deviation from setpoint exists. Nevertheless, even if the scheme is feasible, the window when product compositions are initially satisfied is rather small, careful operation and exact composition measurement are necessary to avoid extensive energy consumption.

Instead of using tray composition as control signal and vessel composition as criteria for shutdown, temperature measurements are implemented along the column and applied to control the product compositions. The reflux flow is controlled by simple proportional controllers such that the desired products are accumulated in the vessels. By means of simulations it is shown that a level control for the intermediate vessels is not necessary, these levels are controlled implicit by the reflux to the section below the vessel.

Comparison of the strategies where the sensor for the control signal (either composition or temperature) is located in the center of the column shows that a similar holdup distribution when all product compositions are satisfied is achieved (see Table 5.7: holdup and composition tray composition control; Tables 5.9: compositions and Table 5.10: holdups for tray temperature control). From a practical point of view, the temperature control scheme is far more simple to implement and to operate.

The initial start-up procedure, where the liquid was distributed over the column, was inspired by the introductory example. This procedure is from a practical point of view not as favorable as the procedure where the feed is added to the reboiler. From a control point of view the start-up, with liquid feed added to the reboiler, is easier to perform. Applying this procedure avoid inverse responses of the controlled variables (temperatures) since the temperatures on the stages decrease monotonically towards the top during start-up. Further,

the simulation have shown that there are no significant differences in operation time, thus, the latter procedure is assumed to be the most favorable from a view point of a practical implementation.

5.6 Conclusions

Four different feedback control strategies for the multivessel batch distillation column are proposed and compared to each other. Temperature control with a control tray at the center of each section were found to be the most flexible (with respect to feed composition) and simple to implement control structure. Two different start-up procedures were investigated for the multivessel batch distillation column, both can be performed with the temperature control scheme. The composition measurement based structures require that the multivessel batch distillation column is started with a procedure where liquid is first distributed over the column, which will complicate the practical operation of a column considerable.

Bibliography

1. Barolo, M., G.B. Guarise, N. Ribon, S. Rienzi, A. Trotta and S. Machietto, "Some issues in the design and operation of a batch distillation column with middle vessel", Proc. ESCAPE-6, *Computers & Chemical Engineering*, Rhodes, Greece, May 1996
2. Bortolini, P. and G.B. Guarise, "Un nuovo metodo di distillazione discontinua; (A new method of Batch Distillation)", *Ing. Chim. Ital.*, Vol. 6, No. 9, Sep. 1970
3. Hasebe, S., B. Abdul Aziz, I. Hashimoto and T. Watanabe, "Optimal design and operation of complex batch distillation Column", *Preprint of the IFAC Workshop on Interaction between Process Design and Process Control*, London, 1992
4. Hasebe, S., T. Kurooka and I. Hashimoto, "Comparison of the Separation Performances of a Multi-effect Batch Distillation System and a Continuous Distillation System", *Proc. IFAC-symposium DYCORD'95*, Denmark, June 1995
5. Jacobsen, E. and S. Skogestad, "Multiple Steady States in Ideal Two-Product Distillation", *AIChE Journal*, Vol. 37, No. 4, Apr. 1991, pp. 499 - 511
6. Kister, H.Z.; "Distillation Operation", *McGraw-Hill*, 1990
7. Machietto, S. and L.M. Mujtaba, "Design and Operation Policies for Batch Distillation", Proc. NATO ASI on Batch Processing Systems Engineering, Anayla, Turkey, 1992
8. Mejdell, T.; "Estimators for Product Composition in Distillation Columns", Ph.d.-Thesis, The Norwegian Institute of Technology, 1990
9. Perry, H.P., Green,D., *Perry's Chemical Engineers' Handbook*, *McGraw-Hill Chemical Engineering Series*, 50th edition, 1984 Chapter 18
10. Robinson, C.S. and E.R. Gilliland, "Elements of Fractional Distillation", *McGraw Hill Book Company.*, New York, 4th ed., 1950

11. Skogestad, S., B. Wittgens, E. Sørensen and R. Litto, "Multivessel Batch Distillation"; *AIChE Annual Meeting, 1995*, Paper 184 i, Los Angeles, USA, 1995
12. Skogestad, S., B. Wittgens, E. Sørensen and R. Litto, "Multivessel Batch Distillation"; *AIChE Journal*, Vol. 43, No. 4, pp 971 - 978, 1997
13. SPEEDUP Release 5.4 User Manual, Prosys Technology Ltd., 1993
14. Sørensen, E. and S. Skogestad, "Optimal operating policies of batch distillation with emphasis on the cyclic operation policy", *Proc. Symposium PSE'94*, Kyongju, Korea, June 1994, 449-456
15. Sørensen, E., Studies on Optimal Operation and Control of Batch Distillation Columns, Ph.D. Thesis, The Norwegian Institute of Technology, 1994
16. Sørensen, E. and S. Skogestad, "Comparison of Inverted and Regular Batch Distillation", *Proc. IFAC-symposium Dycord'95*, Denmark, June 1995
17. Treybal, R.E., "A Simple Method of Batch Distillation", *Chemical Engineering*, Oct. 1970
18. Wittgens, B., Litto, R., Sørensen, E. and S. Skogestad, "Total Reflux Operation of Multivessel Batch Distillation", *ESCAPE-96, Comp. Chem. Engng.*, Vol. 20, S1041-1046, 1996

Notation

CC	Composition controller	
D	Distillate flow rate	$kmol/hr$
K	Controller gain	$kmol/h, kmol/(h\ ^\circ C)$
L	Reflux flow rate	$kmol/hr$
M	Molar holdup	$kmol$
M_{tot}	Total initial feed charge	$kmol$
N_c	Number of components	
N_s	Number of sections	
N_t	Number of stages per section	
N_{tot}	Total number of stages	
Q_b	Reboiler heat duty	
Q_c	Condenser heat duty	
T	Temperature	$^\circ C$
T_i	Temperature on tray i	$^\circ C$
TC	Temperature controller	
t	time	h
V	Molar vapor flow	$kmol/h$
x	Molar liquid composition	
y	Molar vapor composition	
z	Molar feed composition	

Greek Symbols

α	Relative volatility
Δ	Deviation
τ	Controller reset time $1/h$

Subscripts

b	Boiling point
F	Feed
i, j, k, l, m	Identifier
R	Reboiler
s	Controller Setpoint
t	Total number
tot	Total amount
0	Initial state
∞	Final state

Chapter 6

Comparison of Multivessel and Conventional Batch Distillation

Extended version of the following papers:

Wittgens, B. and Skogestad, S.;
Potential Energy savings of Multivessel Batch distillation,
presented at AIChE Annual meeting 1997, paper 34d

and

Wittgens, B. and Skogestad, S.;
Multivessel Batch Distillation - Potential Energy Savings,
DYCOPS-5, 5th IFAC Symposium on Dynamics and Control of Process Systems,
Corfu, Greece, June 8-10, 1998

Abstract

A multivessel batch distillation column is compared to a conventional batch distillation column, both columns are operated with a feedback control scheme. The comparison is performed in form of a case study, where in some cases we found that an increase in production rate up to 50 % is possible by using multivessel batch distillation instead of a conventional batch distillation column with similar column length. Besides the considerable reduction in energy usage, the main advantage with the multivessel batch distillation column is probably its much simpler operation compared to a conventional batch distillation column. Further, results on the maximum achievable separation and the influence of the chosen setpoint on the final batch time are presented.

6.1 Introduction

In chemical processing industries, separation of multi-component liquid mixtures into pure products is a task primarily performed by distillation. Dependent on the amount of feedstock to be processed, the choice has traditionally been either continuous or batch distillation. A new type of batch distillation column and operation strategy for separation of multicomponent mixtures was proposed by Hasebe *et al.* (1995) and has been further studied by the authors (Skogestad *et al.* 1997 and Wittgens *et al.* 1996), we refer to these papers for a more detailed review. The primary feature of the multivessel batch distillation column is that the energy required to separate the mixture is considerably less than in conventional batch distillation due to heat integration of several column sections. Hasebe *et al.* (1995) indicates that the energy efficiency of a multivessel batch distillation could be comparable to continuous distillation.

Although batch distillation generally is less energy efficient than continuous distillation, it has received increased attention in the last few years because of its simplicity of operation, flexibility and lower capital cost. For many years academic research on batch distillation was focused primarily on optimizing the reflux policy. However, in most cases the difference to the simple-minded constant reflux policy usually is small (*e.g.* Sørensen and Skogestad, 1994).

On a qualitative basis we compare conventional batch distillation columns (see Figure 6.1) with the multivessel batch distillation (see Figure 6.2) with respect to ease of operation and productivity (energy efficiency). Initial results on the economical potential of the new process are presented, the maximum attainable separation of the multivessel batch distillation column is investigated and the influence of the setpoint of the temperature controllers is presented. Finally the presented results are discussed and conclusions are presented.

6.2 Column configurations

6.2.1 Conventional batch distillation

The optimization of a conventional batch column (Figure 6.1) leads to an optimal control problem, for which problem formulation and numerical solution methods are not yet well established (Machietto and Mujtaba, 1992). Results from optimization studies have shown an increased performance of the column using an optimal reflux policy, compared to the conventional constant reflux policy or constant distillate composition policies time and energy savings in the order of 20 % dependent on the mixtures separated have been reported (Sørensen, 1994). Nevertheless, the implementation of an optimal reflux policy is not yet widely used in industries, while piecewise constant reflux policies are applied (Diwekar *et al.*, 1987). Industrial batch columns are operated often with a rather simple reflux policy *e.g.* the number of off-cuts are predefined and the reflux ratio is constant during operation. However, at least for multicomponent mixtures, this policy is difficult to implement, and one must often take off a large number of products, which are later, after composition analysis, blended to give the appropriate products. Also, it is not optimal to keep a constant reflux

ratio (e.g. high reflux ratio to fulfill the product specifications), so the production time may be much longer than is needed.

Another operation policy, which usually is better in terms of energy consumption (production time) is to use a feedback control scheme, which keeps the product composition at a desired value. In practice, composition may be difficult (time consuming) and expensive to measure, so we will here instead keep the temperature at a given position of the column constant, thus indirectly control the top product composition (see Figure 6.1). Change-over between products may take place when the reflux flow L increases above a predefined limit. At this time one normally needs to produce an off-cut fraction and one may, for example, when the next temperature setpoint is reached switch to the second product. This procedure is performed until $N_c - 1$ product fractions are withdrawn over top, finally, the last product is withdrawn from the reboiler.

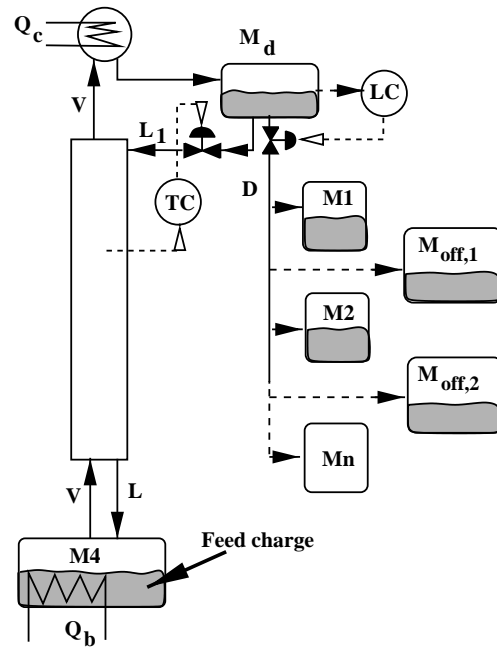


Figure 6.1: Conventional batch distillation, one component at a time over top

6.2.2 Multivessel batch distillation

For the separation of a mixture containing N_c -components, the multivessel batch distillation column consists of $N_c - 1$ column sections, reboiler, condenser/accumulator and $N_c - 2$ -intermediate vessels. The simplest strategy for operating the multi-vessel column, is the *total reflux operation* suggested by Hasebe *et al.* (1995) where the N_c product rates are set to zero ($D_i = 0$). There are at least two advantages with this multivessel column compared to conventional batch distillation where the products are drawn over the top, one at a time. First, the operation is simpler since no product change-overs are required during operation. Second, the energy requirement may be much less due to the multi-effect nature of the operation. For the total reflux operation of the multivessel column, a feedback control structure based on temperature controllers (see Figure 6.2) has been proposed by Skogestad *et al.* (1997). The idea is to adjust the reflux flow out of each of the upper $N_c - 1$ vessels by controlling the temperature at some location in the column section below. There is no explicit level control, rather the holdup, M_i , in each vessel is adjusted indirectly by varying the reflux flow to meet the temperature specifications and thus product quality requirements.

6.3 Simulation model

All the results in this paper are based on simulations using the dynamic model described in the paper by Skogestad *et al.* (1997). We have made a number of simplifying assumptions, such as constant molar flows, constant relative volatilities $\alpha_j = [10.2, 4.5, 2.3, 1]$. Assuming constant stage holdup, perfect level control and constant pressure simplify the column model considerably. We assume a linear boiling point curve, that is the tray temperature is the molar average of the boiling temperatures of the pure components ($T_i = \sum_{k=1}^{N_c} x_k \cdot T_{B,k}$ with $T_{B,k} = [64.7, 78.3, 97.2, 117.7]^\circ\text{C}$, the numerical values are chosen to be close to those of the system methanol, ethanol, n-propanol and n-butanol).

The linear boiling point curve assumption may seem very crude. However, we have performed simulations where temperatures are computed from *Raoult's* law for ideal mixtures, $p_{tot} = \sum_{j=1}^{N_c} x_j \cdot p_j^{sat}(T)$, and the *Clausius-Clapeyron* equation for the pure component vapor pressures, $p_j^{sat}(T) = \exp(-\Delta H_{vap,j}/R \cdot (1/T - 1/T_{b,j}))$, and the results show only minor deviations¹. The dynamic model is implemented using the SPEEDUP software package (Speedup, 1993).

6.4 Operation policies

6.4.1 Conventional batch distillation

Even though the separation of multicomponent mixtures by means of batch distillation is investigated for an extensive time, we did not find any simple operation procedures in the literature. In most of the available literature on operation of batch distillation, the reflux flow is considered as an optimization variable, the number of product cuts and off-cuts is specified a priori. From this, optimization problems considering the minimum time problem (minimum energy consumption) or maximum distillate recovery optimization problems can be formulated.

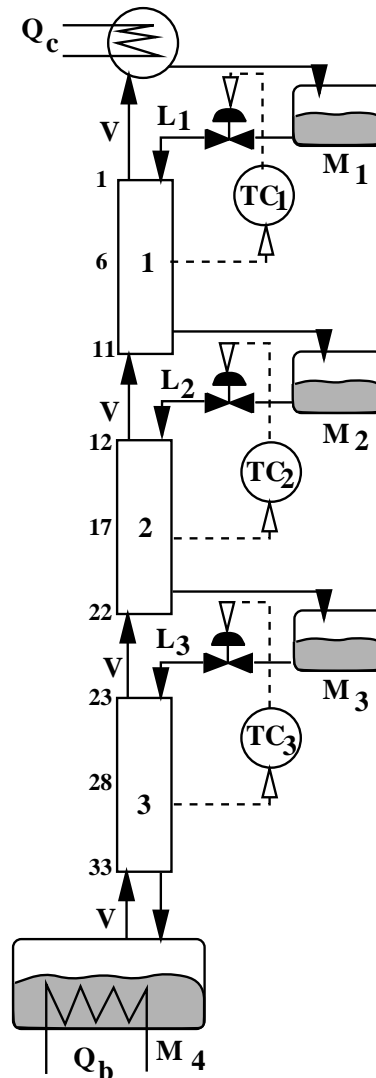


Figure 6.2: Multivessel Batch Column under feedback control

¹For a more detailed discussion we refer to Appendix D.

We decided a simple operation procedure based on a temperature measurement some stages below the column top. The procedure, is aimed at achieving for each product, an approximately constant overhead composition, somewhat better than its specification.

The feedback control strategy is based on the following ideas:

- A sensor is located a few stages below the column top such that a break-through of heavier components into the product is easily avoided. The setpoint is set to be somewhat above the boiling point of the product

$$T_{S,j}^i = T_{b,j}^i + \Delta T \quad (6.1)$$

where i is the stage location (counted from the top) and j is the index for the main component. The second term ΔT in Equation 6.1 accounts for the temperature increase along the column considering the location of the sensor below the column top. One may view ΔT to consist of the two terms $\Delta T^i = \Delta T_{composition}^i + \Delta T_{location}^i$, where $\Delta T_{composition}^i \approx (T_b^{heavy} - T_b^{product})x^{heavy}$ takes into account that we allow for some heavy component in the product. The second term $\Delta T_{location}^i$ takes into account that the temperature increases down the column. $\Delta T_{composition}^i$ can be computed beforehand, $\Delta T_{location}^i$ must be determined from either simulation or experiment.

- The change-over temperature $T_{off,j}$ for the collection of off-cut product j is determined from the boiling point of the next product fraction (product $j + 1$). We define:

$$T_{off,j}^i = T_{S,j+1}^i + \Delta T_{off} \quad (6.2)$$

where ΔT_{off} ensures that most of the component lighter than key component in the next product is removed from the column.

Operation of a conventional batch column with the above described policy to determine temperature setpoints as well as change-over temperatures is as follows:

1. Start-up from total reflux operation (not included in the simulation).
2. After establishing a composition profile, the temperature controller TC (see Figure 6.1) is activated and adjust the reflux L to keep the temperature on the control tray T^i at its setpoint $T_{S,1}^i$. If the reflux L reaches its maximum $L \geq L_{max}$, the collection of product 1 is finished.
3. During the next cycle, an off-cut fraction is withdrawn from the column. The column is operated off-line (feedback control deactivated) with a constant low reflux, L_{off} , until the change-over temperature $T_{off,1}^i$ (see Eq. 6.2) is reached.
4. Withdrawl of product 2 is performed, by activating the temperature controller which hold the temperature on the control tray at its given setpoint $T_{S,2}^i$ (see Eq. 6.1). Note that the change-over from off-cut 1 to product 2 is performed at a temperature *higher* than the desired setpoint for the withdrawl of product 2 that is: $T_{off,1}^i > T_{S,2}^i$. The latter

is to avoid that the lower initial temperature caused by light component remaining results in excessive amount of heavy component.

Again, collection of product 2 is finished when the maximum reflux is reached, $L \geq L_{max}$.

5. Off-cut 2 is withdrawn until temperature $T_{off,2}^i$ is reached, again slightly above the temperature setpoint of the third product fraction.

This cycling between production and off-cut withdrawal is performed until all products are produced. After the batch is finished, one may, based on composition analysis of the products and off-cut fractions, blend off-cuts into the products (especially if the off-cut is large) so that they exactly meet their specifications and to maximize the production rate. This was not done when computing the production rate given in Table 6.3.

6.4.2 Multivessel batch distillation

The operation of the multivessel batch column (see Figure 6.2) is described in detail by Skogestad *et al.* (1997). We assume the feed charge equally distributed over all vessels and the initial compositions on trays and vessels to be $x_i = x_F$ at the start of the simulations. The three PI-temperature controllers are activated immediately after start-up (*e.g.* total reflux operation), and the column is operated in this manner until the last of the four products reaches its specification. In practice, the column is operated under feedback control until the changes in reflux flows and temperature are small for a prespecified time.

6.4.3 Operation conditions

A summary of the operational conditions are given in Table 6.1, in Table 6.2 the column design² and the controller setpoints and changeover temperatures are presented.

The initial feed composition in the columns were chosen to

$$z_F = [0.25, 0.25, 0.25, 0.25] \quad (6.3)$$

The product specifications are given as lower bounds on the purity of the main component in all four products

$$x_{spec} = [0.98, 0.95, 0.95, 0.95, 0.98] \quad (6.4)$$

The columns operate with a constant vapor flow of $V = 10 \text{ kmol/h}$ and an initial feed charge which adds up to $F = 10 \text{ kmol}$ (the total holdup M_{tot} of the column consists of the vessel holdups and the tray holdup) with an initial feed composition z_F (see Eq. 6.3).

²For a more detailed discussion, see the appendix of this chapter and Appendix D.

Table 6.1: Summary of the initial conditions for multivessel and conventional batch distillation column

	Multivessel	Conventional
Number of components	$N_c = 4$	
Relative volatility	$\alpha_j = [10.2, 4.5, 2.3, 1]$	
Vessel holdups	$M_{i,0} = 2.5 \text{ kmol}$	$M_d = 0.0 \text{ kmol}$ $M_i = 0.0 \text{ kmol}$ $M_{off,i} = 0.0 \text{ kmol}$
Tray holdups (constant)	$M_k = 0.01 \text{ kmol}$	
Total initial charge	$M_{tot} = 10 + N_{tot}M_k$	
Initial reflux flows	$L_{i,0} = 10 \text{ kmol/h}$	
Vapor flow (constant)	$V = 10 \text{ kmol/h}$	

Table 6.2: Controller setpoints $T_{S,j}^i$ and changeover temperatures $T_{off,j}^i$ for fixed vapor flow $V = 10 \text{ kmol/h}$

column type	section length N_T	sensor location i	prod. M_1	off-cut 1	prod. M_2	off-cut 2	prod. M_3	off-cut 3
			$T_{S,1}^i$	$T_{off,1}^i$	$T_{S,2}^i$	$T_{off,2}^i$	$T_{S,3}^i$	$T_{off,3}^i$
conventional	15	3	67	82	80.5	100.5	99	113
	33	6	69	83.5	82	102.5	101	113
multi-vessel	11	6	71.5		87.75		107.2	
	15	8						
	19	10						

The location of the temperature sensor applied for feedback control of the conventional batch column is chosen to be at a distance of $0.2 N_T$ from the column top, the sensor is located on tray 3 for the column with 15 stages and 6 for 33 stages. For the conventional column equipped with 15 trays we choose $\Delta T \approx 2^\circ C$, in the case of 33 trays $\Delta T \approx 4^\circ C$, to account for sensor location and amount of heavy component in the product. The temperature offset to remove light component during off-cut production is for both columns chosen to be $\Delta T_{off} \approx 1.5^\circ C$. The boiling points of the products are computed to be $T_{b,j} = [64.97, 78.43, 97.23, 117.29]$, these temperatures are used to compute controller setpoints $T_{S,j}^i$ and changeover temperatures $T_{off,j}^i$ shown in Table 6.2. A PI-controller with gain $K_c = -0.5 \text{ kmol}/^\circ C$ and integral action $\tau_I = 0.05 \text{ h}$ is chosen. The reflux flow during production phase is $2 \leq L \leq 9.8 \text{ kmol/h}$ while during off-cut withdrawal the reflux flow is constant at $L_{off} = 5 \text{ kmol/h}$.

The sensor for the multivessel batch distillation column are located in the middle of each section. Controller setpoints are determined from $T_i^{S,j} = (T_{B,k} + T_{B,k+1})/2$, with $T_{B,k}$ as the boiling point of pure component k . The controller parameter are chosen to $K_c =$

$-0.25 \text{ kmol}/^\circ\text{C}$ and $\tau_I = 1h$. The reflux flow is controlled within the interval $5 \leq L \leq 15 \text{ kmol}/h$.

6.5 Results

In the presented work a conventional batch distillation with the proposed feedback operation policy and a multivessel batch distillation are compared with respect to energy consumption. We compare the energy usage in the sense of the net production rate defined as $(F - M_{off})/t_b$ for a given, fixed boilup $V = 10 \text{ kmol}/h$ $F = 10 \text{ kmol}$ as initial feed charge with a composition of $z_F = [0.25, 0.25, 0.25, 0.25]$, M_{off} as sum of off-cut and (if present) non-spec products and t_b as the batch time, which was required to achieve all of the product specifications (see Eq. 6.4). Further, we require that the impurities of the intermediate products N_c are distributed such that their ratio is $x_{N_c-1}/x_{N_c+1} \approx 1$.

Note, the batch time does not include charging of the column, preheating, start-up under total reflux and shutdown. Further, we assume that the composition measurement in the vessels is instantaneous for the presented simulations³.

The results are summarized in Table 6.3 and in Figures 6.3 and 6.4 we present the composition profiles, controlled temperatures in the column sections, reflux flow as well as the holdup in the product tanks for the considered operation policies.

6.5.1 Conventional batch distillation: Production rate

For the conventional batch distillation we note that the net production rate is not increased, when the number of stages is increased from 15 to 33. Of course, it should be possible to increase the production rate by adding stages, so the result illustrate the difficulty in operating conventional batch distillation, especially for multicomponent mixtures with off-cut. The increase in column length of the conventional batch column has opposing effects on the productivity. The product purities are increasing further above specification and batch time decreases, simultaneously the amount of off-cut D_{off} increases. The latter effect cancels the effect of batch time reduction, such that the production rate is unchanged, even though the column length increases.

Note that we have not blended the off-cut into the product. If we blend the combined off-cut product (all off-cut fractions are accumulated in one tank) into the four products to exactly meet the specifications, the net production rate of the conventional batch column would increase by less than 10 %.

6.5.2 Multivessel batch distillation: Production rate

For the multivessel batch distillation column the production of off-cut is negligible (actually, the remaining hold-up in the column sections could be seen as off-cut). The separation of the feed mixture is performed with considerable less time and thus energy consumption (see

³A gas chromatograph will have a time delay on the composition measurement of approximately 10 - 20 minutes, this delay will be equal for the presented simulations and is therefore omitted.

Table 6.3). Increasing the length of the column sections give some improvement in product quality, but since, at least one, of the components is at the specification, batch time decreases considerably.

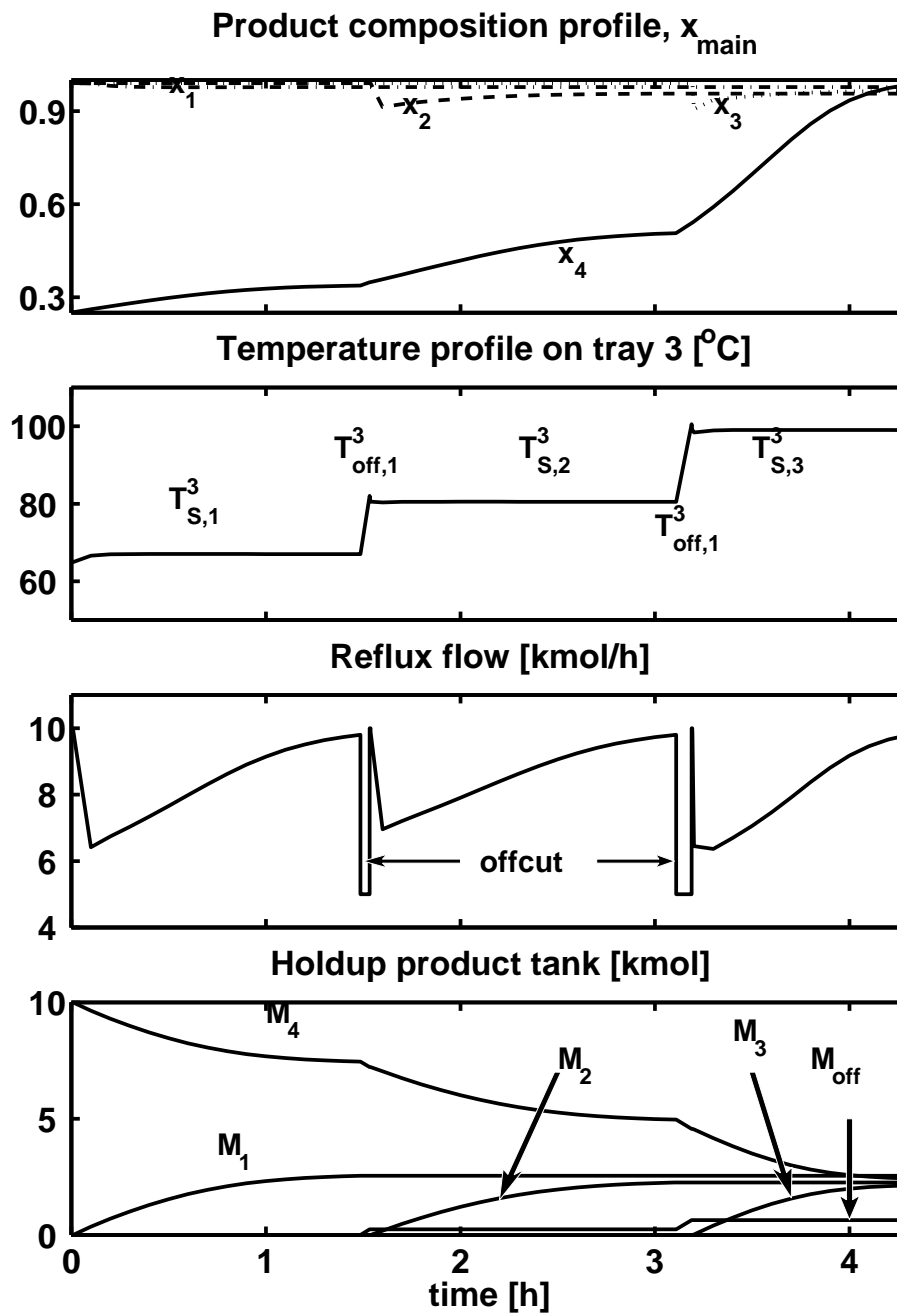


Figure 6.3: Product composition profile, controlled temperature, reflux flow and holdups of products for conventional batch distillation ($N_T = 15$)

For columns of identical length ($\sum N_T = 33$), the given separation consumes approximately 30 % less energy in the multivessel column compared to the conventional column.

Further, since no off-cut is produced, an increase of production rate in the order of 40 % was found. Increasing the length of the column sections of the multivessel column from 11 to 19 trays each, the production rate increases by approximately 40 %.

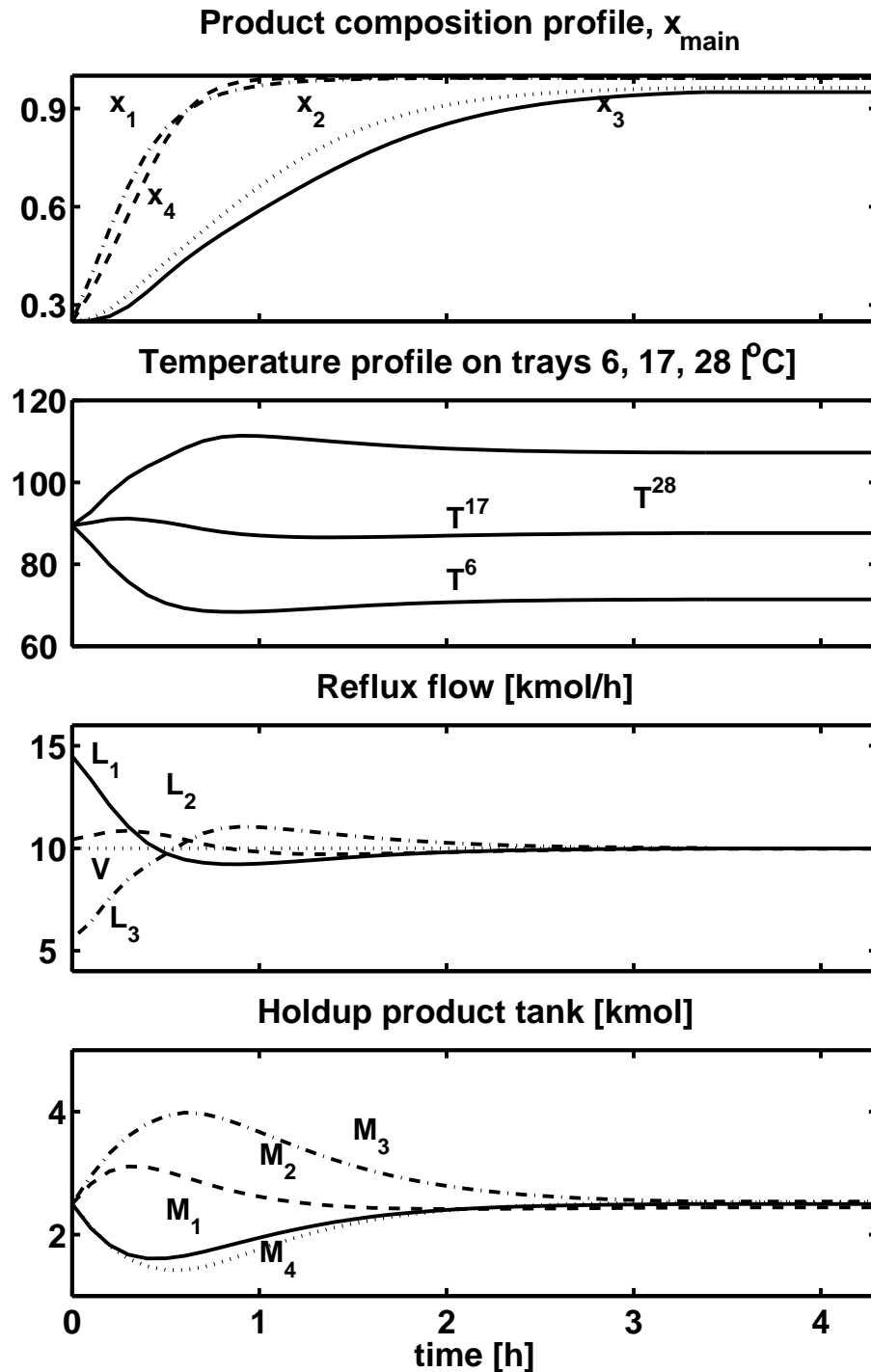


Figure 6.4: Product composition profile, controlled temperatures, reflux flows and holdups of products for multivessel batch distillation ($N_T = 3 \times 11$)

Table 6.3: Product composition and amount, batch time and production rate of batch distillation processes (fixed vapor flow $V = 10 \text{ kmol/h}$)

	N_T		product					t_b [h]	net production [kmol/h]
			M_1	M_2	M_3	M_4	M_{off}		
conventional batch	15	M [kmol]	2.54	2.26	2.13	2.43	0.64	4.31	2.17
		x_{main}	0.987	0.956	0.965	0.985			
	33	M [kmol]	2.68	1.99	1.89	2.28	1.15	4.01	2.17
		x_{main}	0.988	0.988	0.973	0.986			
multi- vessel batch	3×11	M [kmol]	2.50	2.44	2.54	2.52	0.0	3.38	2.96
		x_{main}	0.993	0.963	0.950	0.993			
	3×15	M [kmol]	2.51	2.44	2.56	2.49	0.0	2.48	4.03
		x_{main}	0.999	0.973	0.950	0.999			
	3×19	M [kmol]	2.52	2.45	2.55	2.49	0.0	2.33	4.29
		x_{main}	0.999	0.973	0.950	0.999			

6.5.3 Multivessel batch distillation: Achievable separation

The performance of the proposed control system will be investigated with respect to the influence of the number of stages on the final batch time and the achievable separation. We chose a column configuration with three identical sections, the initial conditions given in Table 6.1 and feed composition z_F as stated in Eq. 6.3. The separation is performed utilizing the feedback control structure presented in section 3 to ensure comparable performance of the columns. The simulation is terminated when either the product specifications (see Eq. 6.4) in all vessels are fulfilled or the derivative of all compositions is less than $dx/dt = 10^{-6}$, which is defined as steady state condition.

In Table 6.4 we present the maximal achievable product composition at steady state for a column with 7 to 25 stages per section. For columns consisting of three identical sections of $N_t \leq 11$, the desired product compositions are not achieved at steady state. By increasing the number of stages per section the achievable product quality improves.

Table 6.4: Steady state product composition as a function of number of stages per section

N_t	x_1	x_2	x_3	x_4
7	0.965	0.864	0.856	0.965
9	0.984	0.932	0.923	0.984
11	0.993	0.967	0.960	0.993
15	0.998	0.992	0.990	0.999
19	0.9997	0.9982	0.9974	0.9997
25	0.9999	0.9998	0.9997	0.9999

In Table 6.5 we present the steady state concentration of the main component in the ves-

sels. Increasing the number of stages from 11 to 15, reduces the batch time by approximately 25 %. A further extension of the column sections (from 15 to 19 or 25 trays) reduces the distillation time t_f only marginally.

From Table 6.5 we see that purification of the holdup in vessel 3 determines the final batch time (stop criteria is fulfilled). This is due to the chosen relative volatilities $\alpha_i = [10.2, 4.5, 2.3, 1]$, the ratios of $\alpha_2/\alpha_3 \leq \alpha_1/\alpha_2 \leq \alpha_3/\alpha_4$ such that the separation of component 2 and 3 is more difficult than the split of components 1 and 2 or components 3 and 4. To overcome this problem additional stages should be placed in the center section (section 2), alternatively we can adjust both the control tray location or the temperature setpoint.

Table 6.5: Final batch time as a function of number of stages and the product compositions

N_t	x_1	x_2	x_3	x_4	$t_f[h]$
11 (base case)	0.993	0.963	0.95	0.993	3.385
15	0.9969	0.971	0.95	0.999	2.470
19	0.9983	0.9723	0.95	0.9996	2.326
25	0.9987	0.9723	0.95	0.9999	2.274

6.5.4 Multivessel batch distillation: Influence of the controller setpoint

The design of a multivessel batch distillation column is, steady state product composition considered, closely related to the design of a binary distillation column. The proposed policy to determine the initial setpoints of the temperature controller is based on the following assumptions:

- each column section has a sufficient number of trays to perform a given separation problem
- the control tray is situated in the center of the column
- temperature setpoint is set to the average of the boiling point of the two pure components which will accumulate in the vessels adjacent to a section
- non-azeotropic mixtures are separated

As base case we consider the same set of temperatures given in Table 6.2 (third line). Based on this initial set we vary the temperature setpoints from a defined base case (Simulation 1, see Table 6.7) by $\pm 3^\circ C$ and investigate the influence on both separation efficiency and batch time. Note, we keep the control tray position in the center.

It has been shown that the batch time is determined on the separation of component 2 and 3 (see Table 6.5) and that the products in vessel 1 and 4 are above their specification (see Eq. 6.4), with a column length of 11 trays. In the here presented case study the center section has been extended from 11 to 15 stages, thus the column has a total for 37 stages. The number of additional stages is chosen such that the steady state compositions (see Table

6.6 for some examples) are $x_D \simeq [0.98, 0.98, 0.98, 0.98]$. This will give some freedom to adjust the temperature setpoints $T_{S,i}$, without compromising the product specifications (see Eq. 6.4). The remaining parameters of the column design are identical to those presented in Table 6.1. The column is operated with a feed mixture of $z_F = [0.25, 0.25, 0.25, 0.25]$, the initial feed mixture is distributed evenly over accumulator, intermediate vessels and reboiler, for control purposes PI-controllers are applied with setpoints given in Table 6.7.

Table 6.6: Simulations 1, 2, 3 and 5: Steady state data of multivessel batch column with $N_t = [11, 15, 11]$ trays, feed mixture z_F

		Vessel 1	Vessel 2	Vessel 3	Vessel 4	
Sim. 1	M_i [kmol]	2.515	2.474	2.471	2.540	
	x_1	0.993	0.016	0.0	0.0	
	x_2	0.007	0.979	0.009	0.0	
	x_3	0.0	0.046	0.985	0.007	
	x_4	0.0	0.0	0.063	0.993	
	x_l/x_h		0.35	0.14		
$t_\infty = 9.41h$						
	Sim. 2	M_i [kmol]	2.515	2.474	2.441	2.570
		x_1	0.993	0.016	0.0	0.0
		x_2	0.007	0.979	0.009	0.0
		x_3	0.0	0.046	0.988	0.013
		x_4	0.0	0.0	0.004	0.987
x_l/x_h			0.35	2.25		
$t_\infty = 9.41h$						
	Sim. 3	M_i [kmol]	2.515	2.474	2.499	2.512
		x_1	0.993	0.017	0.0	0.0
		x_2	0.007	0.979	0.009	0.0
		x_3	0.0	0.046	0.980	0.004
		x_4	0.0	0.0	0.012	0.996
x_l/x_h			0.40	0.75		
$t_\infty = 9.35h$						
	Sim. 5	M_i [kmol]	2.515	2.505	2.439	2.540
		x_1	0.993	0.016	0.0	0.0
		x_2	0.007	0.975	0.005	0.0
		x_3	0.0	0.088	0.989	0.007
		x_4	0.0	0.0	0.064	0.993
x_l/x_h			0.18	0.08		
$t_\infty = 9.43h$						

In Table 6.6 the steady state compositions, the time to achieve steady state (t_∞) and the impurity ratio for simulations 1, 2, 3 and 5 are presented⁴. Comparing Table 6.4 (third line) and 6.6 show that the steady state compositions in the intermediate vessels (M_2 and M_3) are changed by adding four additional trays in the center section of the multivessel batch distillation column.

⁴These simulations are chosen because of the shortest time to achieve the desired product compositions in all four vessels.

In Table 6.7 the applied temperature setpoints, the vessel compositions, vessel holdup and the batch time are presented. The batch time is defined to the time were all four product compositions are satisfied. For simplicity, the composition which determines the end of the separation is marked in **bold** face.

The influence of the variation of the setpoints (see Table 6.7) is summarized:

- Variation of one setpoint at a time:

From Table 6.7 we see that variation of the temperature setpoint of column section 3 (TC_3) compared to simulation 1 only has limited influence on the batch time. For simulation 2 were the temperature setpoint in the lower section is reduced while the setpoints of the upper and center section are kept constant, a reduction of the batch time by $\approx 2\%$ is observed. In simulation 3, TC_3 is increased and the batch time increase by 5 %.

Keeping the setpoints TC_1 and TC_3 in section 1 and 3 constant and decrease setpoint of TC_2 has results in an increase of the batch time by 17 %. Increase setpoint of TC_2 has no influence on the batch time. However, the increase in the setpoint results in that the composition specification in vessel 2 is achieved last instead of the specification in vessel 3 as in Simulation 2 and 3.

For simulations 6 and 7 an increase by at last 37 % is observed.

- Variation of two setpoints simultaneously:

For simulations 6 to 15, an increase in the final batch time is observed in excess of 25 % is observed.

In Figure 6.5 the temperature profile over the column for $t = t_f$ is presented for simulation runs 1, 2, 3 and 5. Similar to binary separations in a continuous column, changing one setpoint in a multivessel batch distillation moves the temperature profile up or down the column.

6.6 Discussion

Even though energy savings (in terms of shorter production time) are achievable when investigating a conventional batch distillation with feedback control we have to consider the added degree of complexity by implementing the presented operation policy. For the example studied in this paper, we achieved increases in production capacity of up to 98 % or equivalent, a reduction of energy consumption of approximately 50 % applying multivessel batch distillation instead of conventional batch distillation. Although the results for the conventional batch distillation column may be quite far from the optimal reflux policy, they are probably better than they can be expected from industrial practice. Note that a constant reflux policy, commonly used in industry, would yield significantly worse results.

Besides the considerable reduction in energy usage, the main advantage with the multivessel batch distillation is probably its much simpler operation compared to a conventional batch distillation column. It may be operated easily without operator intervention, whereas conventional batch distillation requires product and off-cut change-overs as well as adjustments of reflux or alternatively: temperature setpoints. It can be automated, *e.g.* using the

procedure proposed in this paper, but still operators would be needed for cases where something fails. Even though the above presented procedure finding temperature setpoints (see Eq. 6.1) in the column as well as the change-over temperatures (see Eq. 6.2) is a kind of intuitive, due to its simplicity, operation of multicomponent separation might be considerably less demanding.

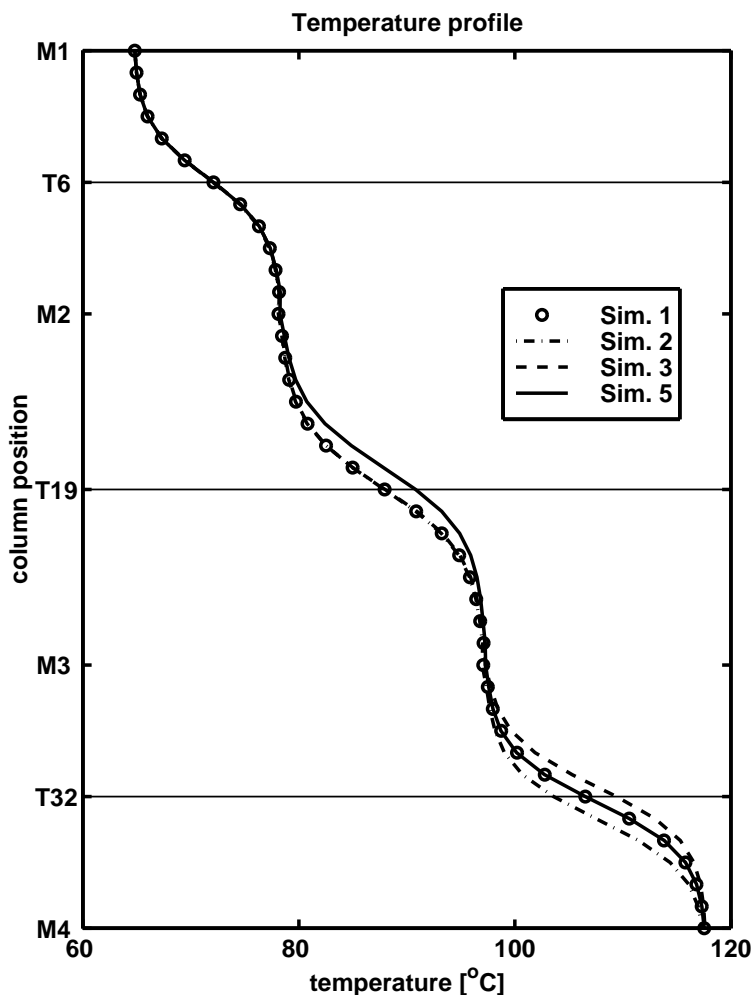


Figure 6.5: Tray temperature control: Temperature profile over column for simulations 1, 2, 3 and 5

As shown in Table 6.7 an increase of column length in the center section reduces both the batch time, as well as increases the product composition in the two intermediate vessels. The possible *over-purification* in the center section (steady state compositions considered) due to the longer column section results in a more robust separation process with respect to adjustment of the controller setpoint. In the worst case malfunction of the temperature sensor (off-set) will have only limited effect on the batch time for the given set of product specifications, provided the number of stages is sufficient.

Table 6.7: Influence of controller setpoints on product composition and final batch time for product compositions $x_{spec} \geq [0.99, 0.95, 0.95, 0.99]$

Sim.	Controller setpoint [$^{\circ}C$]			Product concentration				Batch time t_f [h]	
	TC_1	TC_2	TC_3		M_1	M_2	M_3		M_4
1	71.5	87.75	107.2	x_{main}	0.991	0.960	0.950	0.992	2.60
				x_l/x_h		2.49	1.46		
				M [kmol]	2.49	2.47	2.54	2.51	
Variation: one setpoint at a time									
2	71.5	87.75	104.2	x_{main}	0.991	0.957	0.950	0.984	2.54
				M [kmol]	2.48	2.47	2.56	2.54	
3	71.5	87.75	110.2	x_{main}	0.991	0.965	0.950	0.995	2.72
				M [kmol]	2.50	2.46	2.57	2.448	
4	71.5	84.75	107.2	x_{main}	0.992	0.979	0.950	0.992	3.14
		M [kmol]		2.52	2.39	2.57	2.53		
5	71.5	90.75	107.2	x_{main}	0.997	0.950	0.965	0.992	2.60
		M [kmol]		2.48	2.54	2.47	2.51		
6	68.5	87.75	107.2	x_{main}	0.997	0.950	0.980	0.993	3.58
				M [kmol]	2.42	2.56	2.48	2.54	
7	74.5	87.75	107.2	x_{main}	0.980	0.988	0.983	0.993	3.97
				M [kmol]	2.59	2.40	2.47	2.54	
Variation: two setpoints simultaneously									
8	68.5	84.75	104.2	x_{main}	0.992	0.950	0.960	0.986	3.26
				M [kmol]	2.42	2.50	2.52	2.56	
9		84.75	110.2	x_{main}	0.996	0.950	0.950	0.996	3.26
				M [kmol]	2.42	2.49	2.59	2.50	
10	68.5	90.75	104.2	x_{main}	0.997	0.950	0.990	0.987	3.96
				M [kmol]	2.43	2.60	2.41	2.57	
11	68.5	90.75	110.2	x_{main}	0.997	0.950	0.983	0.996	3.96
				M [kmol]	2.42	2.59	2.47	2.51	
12	74.5	84.75	104.2	x_{main}	0.980	0.991	0.974	0.986	3.84
				M [kmol]	2.59	2.36	2.49	2.57	
13		84.75	110.2	x_{main}	0.980	0.991	0.966	0.996	3.88
				M [kmol]	2.59	2.36	2.55	2.51	
14	74.5	90.75	104.2	x_{main}	0.980	0.984	0.9911	0.987	4.02
				M [kmol]	2.59	2.44	2.41	2.57	
15	74.5	90.75	110.2	x_{main}	0.980	0.984	0.983	0.996	4.04
				M [kmol]	2.59	2.43	2.47	2.51	

The design of the multivessel batch distillation column is more closely related to the design of a two product continuous distillation column than to the design of a batch distillation column. Slightly different ratios of the relative volatilities have a rather strong influence on the separation. The length of a column section has to be adjusted for a given separation problem. From the desired product compositions the number of stages above and below the control tray can be computed from steady state tray-by-tray computations. Alternatively, assumed that the number of trays is larger than required, the product compositions can be adjusted by variation of the temperature setpoint which in turn will move the temperature (composition) profile up or down the column. Note, care has to be taken for the separation in the middle section, two impurities are present such that moving the temperature setpoint of an intermediate section influence the steady state composition of both the adjacent vessels as shown in Table 6.6.

6.7 Conclusions

Conventional and multivessel batch distillation columns were compared in a case study with respect to the net production, a reduction of energy consumption of approximately 50 % were found. The main advantage with the multivessel batch distillation is probably its much simpler operation compared to a conventional batch distillation column. The simple minded procedure to set the temperature setpoints of the multivessel column to the mean of the boiling point of the two components to be separated proved to be rather effective, provided column sections are long enough. It is established that the length of a column section can be determined by simple steady state computations.

Bibliography

1. Bortolini, P. and G.B. Guarise, "Un nuovo metodo di distillazione discontinua (In Italian; A new practice of Batch Distillation)", *Quad. Ing. Chim. Ital.*, Vol. 6, No. 9, p. 150-159, 1970.
2. Diwekar, U.M., R.K. Malik and K.P. Madhavan, "Optimal reflux rate policy, Determination for Multicomponent Batch Distillation", *Comp. Chem. Eng.*, Vol. 11, pp. 629-637, 1987
3. Fenske, M.R.; *Ind. Eng. Chem.*, Vol. 24, p. 482, 1932
4. Gmehling J. and U. Onken, "Vapor-Liquid Equilibrium Data Collection", Vol. I, Part 2a, Dechema, Frankfurt, 1977
5. Hasebe, S.; T. Kurooka and I. Hashimoto, "Comparison of the separation performances of a multi-effect batch distillation system and a continuous distillation system", *Proc. IFAC-symposium DYC'D'95*, Denmark, June 1995.
6. Robinson, C.S. and E.R. Gilliland, "Elements of Fractional Distillation", *McGraw Hill Book Company*, New York, 4th ed., 1950

7. Shinskey, F.G., "Distillation Control", 2nd Edition, McGraw-Hill, New York, USA, 1984
8. Skogestad, S. Wittgens, B., and Sørensen, E., "Multivessel Batch Distillation", *AIChE Journal*, Vol. 43, No.4, p. 971, 1997
9. Sørensen, E. and S. Skogestad, "Optimal operating policies of batch distillation", *Proc. Symposium PSE'94*, Kyongju, Korea, June 1994, 449-456.
10. Wittgens, B., Litto, R., Sørensen, E. and S. Skogestad, "Total Reflux Operation of Multivessel Batch Distillation", *ESCAPE-96, Comp. Chem. Engng.*, Vol. 20, S1041-1046, 1996

Notation

D	Molar distillate flow	$kmol/h$
K_c	Controller gain	$kmol/(^{\circ}Ch)$
L	Molar reflux flow	$kmol/h$
LC	Level controller	
M	Holdup	$kmol$
N_c	Number of components	
N_i	Number of stages in section i	
R	Universal gas constant	$kJ/(kmolK)$
t	Time	h
t_f	Batch time	h
T	Temperature	$^{\circ}C$
T_B	Boiling temperature	$^{\circ}C$
TC_i	Temperature controller	
T_{off}	Changeover temperatures	$^{\circ}C$
V	Molar vapor flow	$kmol/h$
x	Molar liquid composition	
x_{spec}	molar product specification	
y	Molar vapor composition	
z_F	Molar feed composition	

Greek Symbols

α	Relative volatility	
ΔH_{vap}	Heat of vaporization	$kJ/kmol$
Δ	Deviation	
τ	Controller reset time	$1/h$

Subscripts

b	Boiling point
F	Feed
i, j, k, l, m	Identifier
off	Off-cut fraction
R	Reboiler
S	Controller Setpoint
t	Total number
tot	Total amount
0	Initial state
∞	Final state

Appendix: Estimation of column length

A possible method to determine the minimum number of theoretical stages in a section of the multivessel batch distillation column is based on the Fenske-equation (Fenske, 1932). Note that this relation is originally developed for a binary mixture in a continuous distillation column, but is here applied to a distillation column separating a multicomponent mixture. For continuous distillation the top composition, x_i , as “light” and the bottom composition, x_{i+1} , as “heavy” heavy key component will be constant. In general for batch distillation at least one of these compositions will vary with time. For the constant product composition policy of a conventional batch distillation column, *e.g.* x_i will be constant and x_{i+1} will vary. Application of this method to the closed operation of the multivessel batch distillation is possible since towards the end of separation the compositions will be constant.

Apply the Fenske-equation

$$\frac{x_i}{x_{i+1}} \Big|_{M_i} = \alpha_{i,i+1}^N \frac{x_i}{x_{i+1}} \Big|_{M_{i+1}} \quad (6.5)$$

with x_i and x_{i+1} in this section. The components will accumulate in vessel M_i (“distillate”) and M_{i+1} (“bottoms”), respectively.

Assuming constant relative volatilities and total reflux. Introducing the separation factor, S (Shinskey, 1984):

$$S = \frac{\left(\frac{x_i}{x_{i+1}}\right) \Big|_{M_i}}{\left(\frac{x_i}{x_{i+1}}\right) \Big|_{M_{i+1}}} \quad (6.6)$$

Combine equations 6.5 and 6.6 and apply data from to adjacent vessels (*e.g.* M_2 and M_3) the number of stages in a section can be computed from

$$N_T = \frac{\ln S}{\ln \alpha_{i,i+1}} \quad (6.7)$$

Given a set of product specifications, see Table 6.8 and the requirement that $\frac{x_{i-1}}{x_{i+1}} \approx 1$ the number of stages in each column section can be computed. Results from application of Eq. 6.7 are summarized in Table 6.9, the numerical values for the relative volatilities are chosen to be close to the chemical system methanol-ethanol-propanol-butanol.

Table 6.8: Specified vessel composition for design of the multivessel batch distillation column

Vessel	x_1	x_2	x_3	x_4
M_1	0.98	0.02	0.0	0.0
M_2	0.025	0.95	0.025	0.0
M_3	0.0	0.025	0.95	0.025
M_4	0.0	0.0	0.02	0.98

The multivessel batch distillation column operates under total reflux such that the minimum number of stages (see Table 6.9) is readily given from the most difficult separation. For the basic design of the multivessel batch distillation column, it is chosen to utilize sections of identical length, corresponding to the number of stages of the center section. For a conventional batch distillation column, operating with $L_{max} \leq 9.8 V$ the number of stages is increased by 40 %.

Table 6.9: Relative volatilities of the four component system and number of stages necessary for the given separation problem

	methanol-ethanol	ethanol-n-propanol	n-propanol-n-butanol
relative volatility $\alpha_{i,j}$	$\alpha_{12} = 2.31$	$\alpha_{23} = 1.96$	$\alpha_{34} = 2.30$
relative volatility $\alpha_{i,4}$	$\alpha_{14} = 10.4$	$\alpha_{24} = 4.5$	$\alpha_{34} = 2.30$
Fenske	$N_{T,1} \approx 8.99$	$N_{T,2} \approx 10.81$	$N_{T,3} \approx 9.03$

Chapter 7

Discussion, Conclusions and Future Work

7.1 Discussion

This thesis has addressed a number of different aspects of dynamics and operation of continuous and batch distillation columns. The research was a combination of simulation and experimental work were experiments were performed to verify simulation results. The research has been motivated by the need for a more thorough understanding on distillation columns dynamics.

Considering continuous distillation columns, the initial response to step changes in the manipulated variables has been investigated. In an iterative manner, experiments were performed on a pilot plant, parameters estimated and a simulation model was than updated. Those simulation results were than compared to experimental data. The resulting rigorous tray model gave rather good agreement with the performed experiments. From the analysis of the simplified model we see that even if we use simple dynamic models for the composition dynamics the hydraulic dynamics should still be considered and modeled in an appropriate manner. Especially care has to be taken to obtain good estimates for the hydraulic time constants and the liquid holdup on the stage. Studies on controllability or selection of control strategies of continuous high purity distillation which have applied the results were not performed. It could be argued that the performed simulations and experimental work should be applied in the area of control of continuous distillation columns, but research interests were redirected from continuous distillation to batch distillation.

Research was done on the operation of a novel batch distillation column including the development and experimental verification of a new control strategy which resulted in the first implementation of a multivessel batch distillation column. The thesis presents the verification of the proposed control strategy, including simulation studies which verify the feasibility of the process itself and experiments on a laboratory scale pilot plant which confirm the simulation results. The proposed control structure based on simple temperature measurements was compared to similar feedback structures with conventional input signals for composition controllers. Further, a procedure for feedback control of a conventional batch distillation column was developed, which proofed to be rather simple to implement and gave rather good

results. The operation policy of the conventional column was compared to the operation policy of the multivessel batch distillation column with respect to energy consumption and ease of operation.

The justification for using multivessel distillation instead of conventional batch distillation is to save energy, or equivalently, for a given heat input the batch time may be significantly shorter. Another advantage is the simple operation of the multivessel column under total reflux and it may be easier to operate the column close to optimum with the multivessel column. In conventional batch distillation the optimal operation may depend on the reflux policy and quite strongly on the use of off-cuts to achieve the desired product composition. However, conventional batch distillation enables the utilization of one process for quite different separation problems. On the other hand, in the multivessel batch column there are fewer degrees of freedom and this simplifies the operation considerably.

The implementation of the reflux policy and the switching between product and off-cut fractions require often an advanced control system or an experienced operator. In multivessel batch distillation there are fewer degrees of freedom in the design and operation of the unit. This allow for an close to optimal operation, provided the column sections are long enough.

One disadvantage with the multivessel column compared with the conventional batch distillation is that the column itself is more complicated. Also, whereas in a conventional batch column one only has to make decision on the length of one single column section, one has to decide on the number of sections and their length for a multivessel column. The design of the multivessel columns is therefore more closely linked to a specific feed mixture, in particular the relative volatility and the product specifications. Thus, the design process of a multivessel column is similar to the design of a sequence of continuous distillation columns.

Two start-up procedures were investigated, initially the liquid was distributed over the column and a second were liquid is fed to the reboiler. Simulation and experiment have shown that there are no significant differences in operation time for the two considered start-up procedures. Because of possible control limitations (inverse responses) for the first start-up procedure and from a view point of a practical implementation the latter procedure is assumed to be the most favorable.

It was found that the setpoint of the temperature controllers have some influence on the batch time. Nevertheless, simulations show that the simple minded procedure to chose the setpoint to equal the mean boiling temperature of the two components to be separated in a column section gave rather good results, again provided the column sections are long enough. Further, the investigation proofed that the design based on steady state tray-by-tray calculations is sufficient for a chemical system used in this case study.

7.2 Conclusions

The main results from the thesis are summarized below:

Chapter 2

The validity of a rigorous model of a trayed distillation has been demonstrated through the comparison of experimental and simulation results of the open-loop operation of the investi-

gated continuous distillation column. Analytical expression for the hydraulic time constants for liquid and vapor are developed based on the design data of a staged distillation column. It is fairly straight forward to generalize the results to other sieve tray distillation columns, since no for the investigated system specific correlations were utilized. The presented results demonstrate the importance of realistic modeled tray hydraulics for the proper operation of the process.

Chapter 3

A general multivessel batch distillation column is proposed which can be seen as a superstructure of previous proposed batch distillation columns. A new control strategy for the operation of the multivessel batch distillation column under total reflux is proposed and it is shown that the control scheme is easy to implement and operate. The simple proportional-only-controller apply temperature measurements in the column sections to temporarily adjust the reflux flows. It has been shown that the final product compositions are independent on the feed composition. A simple procedure to determine the setpoint is presented. For sufficient long columns it is possible to purify a multicomponent mixture in one separation step in a multivessel batch distillation column instead of separation of one component at a time from a given mixture in a conventional batch distillation column.

Chapter 4

The experimental verification of the previously presented simulation results are the main contribution presented in this chapter. Following the initial proposal for closed operation with indirect level adjustment based on temperature control, concerns were raised that this would not work in practice. The study was therefore performed to confirm experimentally the feasibility of the proposed method of operation. The experiments show very good agreement with the simulations, and confirm that the multivessel column can be easily operated with PI-controllers with temperature as input signal. For a given set of temperature setpoints, it is confirmed that the final product compositions are independent of the initial feed composition.

Chapter 5

The application of alternative control structures were investigated in a case study. The input signals to the single loop controllers were compositions from vessels and trays in the column. The performance of these schemes was considerable worse than the scheme based on temperature measurement, since long time delays in composition measurements strongly influence the control performance. It was found that the control scheme based on temperature measurements in the center of a column section gave the most favorable results with respect to batch time (energy consumption) and ease of operation.

Chapter 6

Conventional and multivessel batch distillation columns were compared in a case study with respect to the net production. A reduction of energy consumption of approximately 50 % were found when using a multivessel column instead of a conventional batch distillation column. The main advantage with the multivessel batch distillation is probably its much simpler operation compared to a conventional batch distillation column. The simple minded procedure to set the temperature setpoints of the multivessel column proofed to be rather effective, provided column sections are long enough. It is established that the length of a column section can be determined by simple steady state computations.

7.3 Future work

7.3.1 Continuous distillation

The initial response of a staged distillation column to step changes in the manipulated variables (reflux flow and reboiler heat input) have been considered in this thesis. It has been demonstrated that the dynamic behavior of a distillation column is strongly influenced on the hydraulics of liquid and vapor flows. Especially, for simplified models those should be estimated carefully to achieve appropriate results. The application of simulation models developed to describe the initial response of distillation columns (on the expense of the steady state behavior) should be investigated thoroughly for simulation studies concerning the selection of control structures. Especially if multivariable control or model based control is the aim of the study, simulation models with a correct as necessary description of the initial response are of vital importance.

Although the experimental and simulation results of this work are in good agreement, the generalization of these results will need further research. The presented work was performed on one single column such that the validity of the “tuning”-parameters of the simulation models have to be verified on other staged columns. Further assumptions made during the modeling process concerning the behavior of the liquid holdup on the sieve tray and down-comer, with respect to changes in liquid and vapor flow need further verification. Optical inspection was not possible in the available distillation column thus these assumption could not be verified yet. However, it would be worthwhile to consider building a distillation column in glass to investigate these effects in detail, especially verify which of the mentioned effects have the most extensive influence on the initial response.

7.3.2 Multivessel batch distillation

Although the results presented in this thesis on the temperature controlled multivessel batch distillation column are most encouraging, a number of questions are open for further research.

1. The total reflux operation may be generalized by also allowing withdrawal of products (continuous or discontinuous) from the vessels. It might be less optimal to operate the column with all vessels filled; considering that one of the vessels might have reached its product specification this vessel should be emptied. Emptying vessels which have reached their specification will reduce the composition time constant in this section, thus purification of the remaining column holdup will be simplified.

Additional to allow for product withdrawal during operation, adding feed to reboiler or intermediate vessels could be beneficial. In this way the multivessel column forms a “super structure” which has as special cases all previously proposed batch schemes. A systematic approach to determine possible feed or product flows during operation is needed for the multivessel batch distillation column to operate optimal with respect to energy consumption and product recovery.

2. It should be established for what type of mixtures and conditions the new multivessel batch column is most suited. The until now performed simulation work is performed with rather simple models (constant relative volatilities) such that the separation of *e.g.* azeotropic mixtures was not investigated. In this contents, a screening of the separation of azeotropic mixtures by means of an entrainer should be performed. The continuous recirculation of entrainer between vessels could facilitate the separation of an azeotropic mixture in one column, instead of two continuous columns with recirculation of the entrainer or the sequence of separation and entrainer regeneration in a conventional batch distillation column. However, an analytic approach for the screening procedure concerning the mixtures to be separated in this column configuration has to be found.
3. In this study the setpoints for the temperature controllers were set such that the temperature in the middle of the section equal the average of the boiling points of the components separated in that section. In general, this is most probably not optimal, especially if the requirements for product purities are very different. Research work to determine a procedure which finds the optimal setpoint for a given separation problem with a given column configuration has to be performed.
4. With the current policy, the operation of the multivessel batch distillation column is aborted when all product compositions are achieved. Research has to establish reasonable criterions for aborting the total reflux operation, that is, when is the improvement in product purity too slow to justify further operation, and how should this be detected. From a practical point of view some kind of composition measurement has to be used to determine the time when distillation can be stopped.
5. The start-up of the multivessel batch distillation column was performed in a kind of intuitive manner and could be seen as two extremes, either the liquid was added to the reboiler or distributed evenly over the intermediate vessels. In case of feed streams with identical components (*e.g.* number and type) but different initial composition it might be less economical to mix these feed streams, instead of distributing the individual feed charges according to their composition along the column. Some systematic approach is necessary to determine if a distribution of feed over the column is beneficial.

Additionally to the distribution of liquid over the column, more research has to be performed towards an automatization of the start-up. The development of an automatic start-up sequence which is event driven will result in a further simplification of the operation. However, the start-up of the experimental system proofed to be easy, provided liquid was fed to the reboiler. An optimization of the start-up procedure which is independent of the initial liquid distribution seams necessary to generalize the application of the column.

6. The aboved described research topics will be solved initially by simulations studies, which will need further experimental verification, even if the here presented experimental data show very good agreement with the performed simulations. The per-

formed experiments consider an ideal feed mixture such that operation of the column was rather easy. Simulations might show that more complex mixtures, like azeotropic or even hetero-azeotropic mixtures can be separate in this process. However, both simulation studies and their experimental verification should be performed before general conclusions for the application of the multivessel batch distillation column considering strongly non-ideal mixtures can be drawn.

Appendix A

Experimental facilities

The objective of the experimental work was to evaluate the theoretical simulation results and gain further insight on the complexity of the model required to describe the distillation unit sufficiently. This approach required iteration of the experimental and modeling phases. For this purposes a distillation column of the Department of Chemical Engineering, Norwegian University of Science and Technology (NTNU) was used. This column is a sieve tray distillation unit in pilot plant scale, the original pilot plant has been designed by Loe (1976) and has been modified later by Mejdell (1990).

The first part of the Ph.D. study was spent on rebuilding of the distillation column with redesign of several parts. The instrumentation was improved to enable a better comparison of experiment and simulation results. A PC based process control system, Paragon 500 from Intec Controls (Paragon, 1992) was implemented, interfaced to the existing equipment and tested. The flexibility of the control system enables the user to implement several different control structures and user written C-routines (MSC 6.0 Compiler, 1990).

A.1 Continuous distillation tower

The distillation column is equipped with eleven sieve trays, electrical heater, total condenser and reflux pump and preheater. A feed pump with feed preheater, back-up condenser, feed and product tanks complete the facility. A flowsheet of the unit is shown in figure A.1.

The entire unit is approximately 6 m high including the back-up condenser unit. The distillation column is about 3.5 meters high, the wall is build of 2 mm stainless steel and is with eleven sieve trays equipped. The distillation tower is operated at atmospheric pressure.

Due to safety regulations the entire unit, tank system and all piping is build of stainless steel. Further, the objective of the back-up condenser is to ensure that vapor is condensed if the cooler duty of the main condenser is insufficient alternatively in case of malfunction.

A.1.1 Tray design

The distillation column is build of 10 identical section, flanged to each other plus top and bottom section. The design of the sections is shown in figure A.2. Each section is 300 mm

high and has a diameter of 125 mm. Between the sections eleven sieve trays (figure A.3) with 75 holes of 2.7 mm diameter are installed.

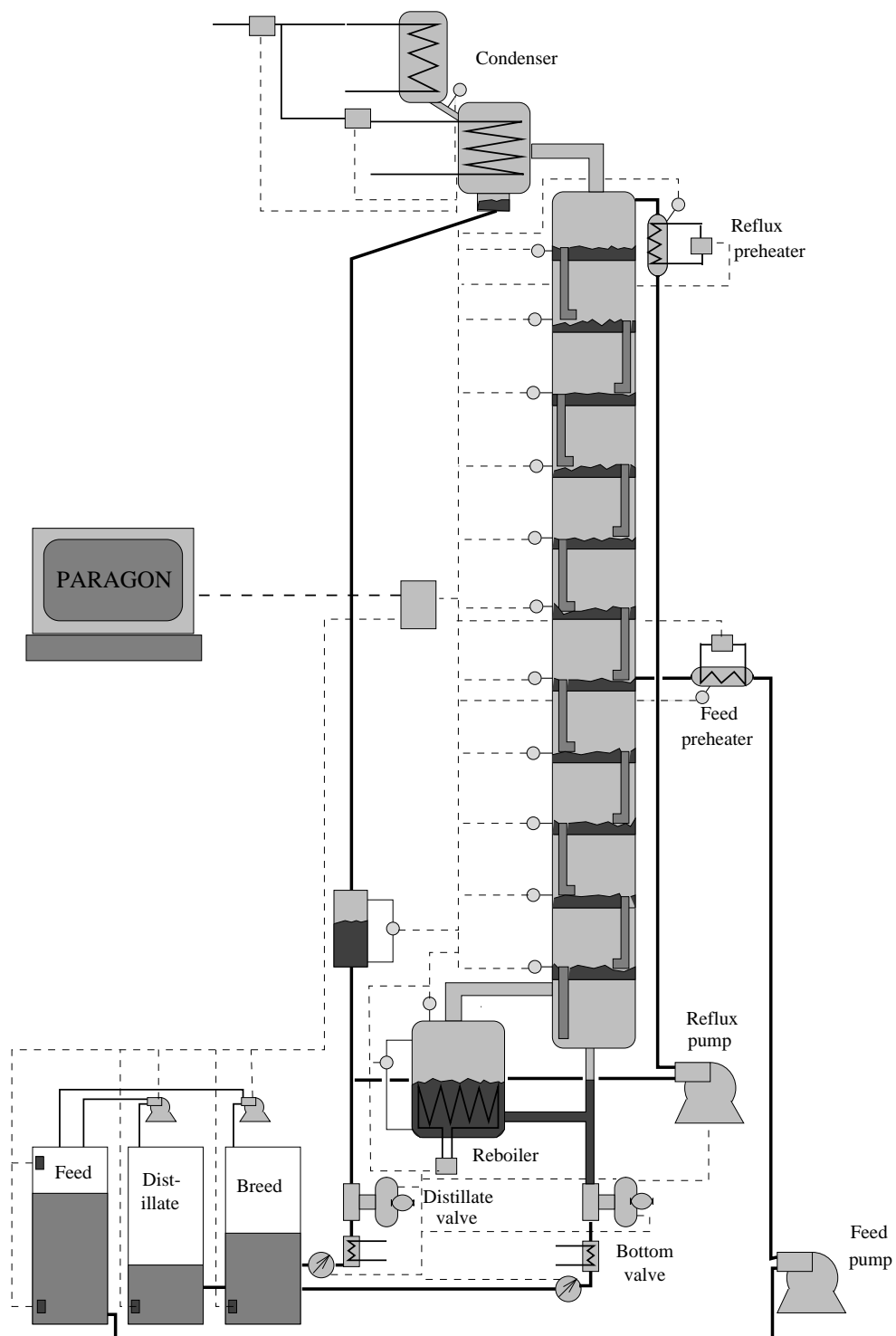


Figure A.1: Pilot plant scale distillation column

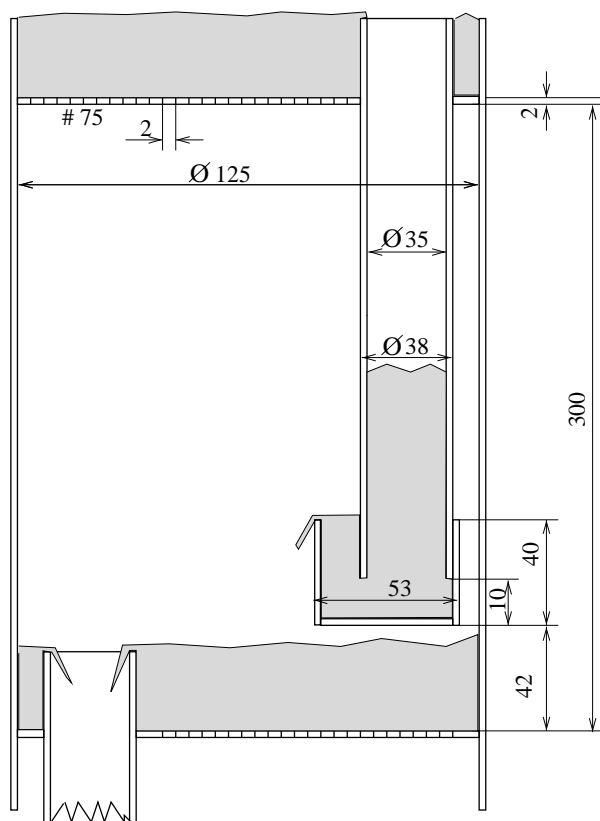


Figure A.2: Section design (measurements in mm)

The downcomer is designed as a combination of inlet weir for the tray and outlet weir for the tray above. The outlet weir height is 30 mm for all trays. The inlet weir is placed at the end of the downcomer and has a liquid seal of 30 mm with a total height of 40 mm. The reason for this design (Mejdell, 1990) is to increase the active area of the tower. These design meet recommendations from literature (Perry, *et al.* 1984) with respect to active area and percentage hole area, pressure drop and vapor speed in empty tower (see chapter 2). The design enables an operation with approximately 10 to 100 % of liquid flow and approximately 15 to 75 % of reboiler heat input without operational problems. Operational problems are mainly entrainment, weeping and flooding for the column and condenser overload. The possible maldistribution of the froth below the inlet weir is assumed to not have any measurable effect on the overall performance of the unit.

Each tray is equipped with a type K thermocouple, which is placed approximately 20 mm above the tray. The sensors are 150 mm long with a diameter of 1/16". The measuring point is not insulated, such that the time constant of the sensor is below 2 seconds for the chosen installation. The placement is chosen such that the thermocouple is still in the froth of the tray. The sensors are fitted to the column by fittings and tightened by Teflon packings to enable maintenance, *e.g.* recalibration.

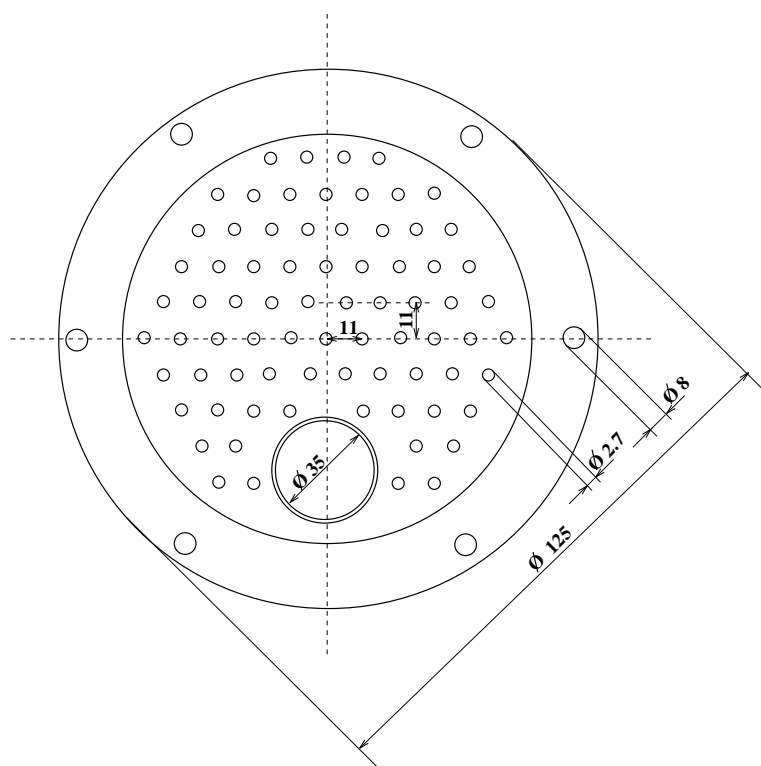


Figure A.3: Plate design (measurements in mm)

A.1.2 Reboiler

The bottom section, depicted in Figure A.4 connects the reboiler to the first tray of the column, such that the vapor inlet line enters above the outlet of the downcomer. This arrangement is chosen to avoid that droplets to be carried up by the incoming vapor flow.

The reboiler (see Figure A.4) is electrical heated with a maximum heat input of 15 kW, which is evenly distributed over 6 heating elements. The total volume of the reboiler is 12 liter, under normal operation approximately 4 liter are occupied by liquid. The reboiler is equipped with flanges to connect a differential pressure cell for liquid level measurement and two thermocouples. One thermocouple measures the liquid temperature in the liquid phase, the second is attached to the heating coil for safety reasons.

A.1.3 Total condenser and accumulator

The top (figure A.5) and bottom section (figure A.4) of the unit are designed to connect the distillation tower to reboiler and condenser, respectively.

The total condenser is divided into two parts, the main condenser (see Figure A.1) and the back-up condenser. The thermocouple is fitted into the vapor line between main and back-up condenser.

To avoid excessive subcooling of the condensed vapor a liquid seal in the bottom of the condenser is installed and some vapor passing through the seal will condense.

From the condenser the condensed liquid flows through a pipe to the accumulator. At steady state the approximately 1.5 l of the 2.5 l accumulator are occupied by liquid.

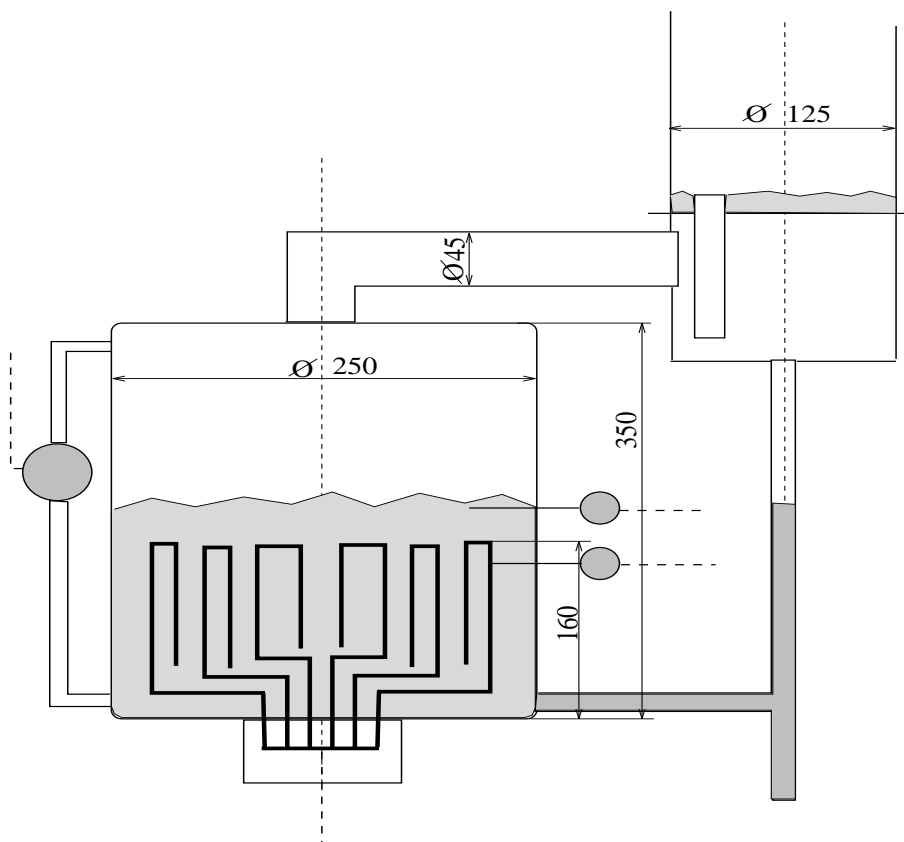


Figure A.4: Bottom section (measurements in mm)

A.1.4 Peripheral equipment

The reflux and feed flow is controlled by means of dosing pumps from Wallace & Tiernan, type G-50 plunger pump. The pumps are equipped with a constant speed motor drive with 1425 r.p.m. and variable stroke length which is adjusted by a servo motor. The flow is smooth to adjust from 0 to 1000 ml/min, the change from zero to full capacity takes approximately 1 minute. The reflux pump is controlled automatically while the feed flow is adjusted manually.

Reflux and feed preheater are equipped with 1.5 kW and 2.5 kW heating elements, respectively. The volumes of the heating elements are 250 ml for the reflux preheater and 700 ml for the feed preheater.

Reflux and bottom flow is controlled by air actuated needle valves, delivered by Foxboro.

The product streams are controlled by a cascade control arrangement of valve and flowmeter. To avoid temperature changes of the product streams, heat exchangers are installed between valve and product flow measurement. The heat exchangers are designed such that the outlet temperature is below 15°C. To adjust for viscosity changes of the product streams a

linear approximation of the viscosity as function of the composition is used. The flow is approximately 500 ml for the distillate valve and approximately 350 ml for the bottom valve when the control valve are fully open.

The product tanks and the feed tank are connected by two pumps, such that the products can be recirculated to the feed tank. The pumps are controlled by relay which act on the power supply of the pump.

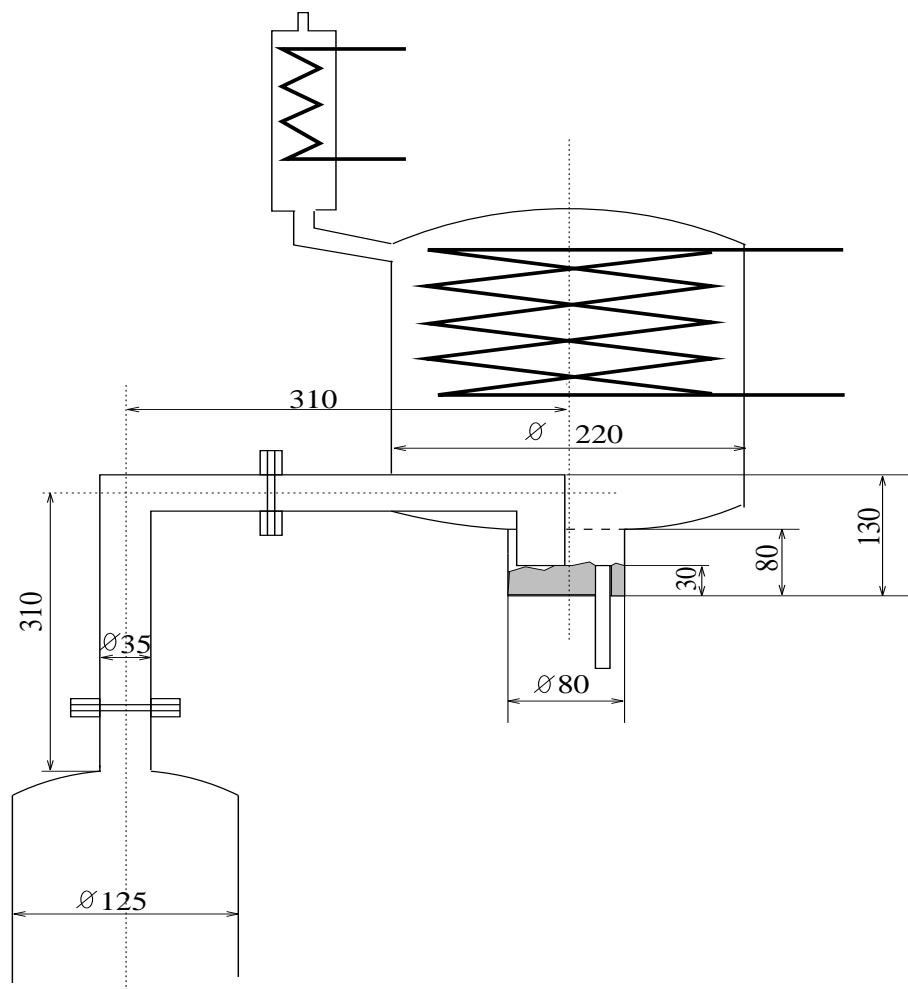


Figure A.5: Top section (measurements in mm)

A.1.5 Instrumentation

The distillation unit is equipped with 16 chromel-alumel thermocouples, where 11 are placed in the center of the trays, one each in reboiler, condenser and the preheaters further two elements were attached to the outer shell of the column. The thermocouples are connected to a Data Translation DT 756 terminal panel with cold junction compensation. The amplification of the signal is chosen to 200 times.

The temperature control of feed and reflux line is based on chromel-alumel thermocouples placed in the outlet of the preheater units. The outlet temperature of the preheater units

is controlled by single loop PI-controllers which send a digital signal to the control relay. The sample time is 2.5 seconds for the controller while the sending I/O-board executes at 0.1 second. The signal is routed to a relay which controls the power supply of the heating elements.

The temperature of the condenser is controlled such that the temperature in the vapor line (connection condenser and back-up condenser) is slightly lower than the dew point of the mixture to be condensed. The temperature control of the condenser is done by a solenoid valve which adjust the water flow through the cooling pipes.

The Foxboro product flow control valves are equipped with Foxboro TDC 3000 volt-to-current transmitters (0-10 V to 10-50 mA) and current-to-air actuators. The analog control signal to the valves is nominally from 0 to 10 Volt. To prevent the valves from damage, the allowed signals are constricted to 90 % of its maximum opening

The flow control of the reflux pump is done by a servo motor and a cascade type positioner. A control amplifier transforms the 0-10 Volt output signal of the computer to 4-20 mA signal to the servo motor.

Three Foxboro differential pressure cells are used to measure reboiler and accumulator liquid level and the total pressure drop from reboiler to condenser.

Two Turbo Messtechnik flowmeters are installed in the product lines. The media flows vertically upwards between the float and the measuring ring, the vertical position is of the float measured is proportional to the flow. The flow measurement is strongly influenced by pressure drop over the valve, temperature and the viscosity of the product streams. The correction of the viscosity is done by means of the software in the control system.

Two two-way solenoid valves are used for sampling of both product streams. The bottom sampling valve is installed in the connecting line between the lower tray and the reboiler. The top product sampling valve is placed in the reflux line behind the reflux pump. The valves are open for 0.5 seconds giving a sample volume of approximately 15 ml.

The feed tank is equipped with two level switches, indicating the maximum and lower tank level. The two product tanks are equipped with one level switch to indicate when the tanks are drained by the recirculation pumps. The pumps are started when the feed tank reaches its minimum level and stopped when the upper level of the feed tank is reached or both product tanks are drained.

All sensors of the distillation unit are connected to two Data Translation DT 2801-A data acquisition boards. The boards have each 16 serial ended analog input and 2 analog output channels, additional the boards feature two 8 channel digital I/O ports. These boards have two 12-bit A/D converters with a maximum of 13.7 kHz throughput. The analog digital conversion of the board for the temperature measurement is configured for an input signal range of 0 to 1.25 Volt giving a resolution of approximately 0.038°C.

The remaining board is configured for the sensors which have an 0 to 10 Volt output span. The digital conversion is chosen to cover an output range of 0 to 10 Volt.

Thermocouples in reboiler and the two preheaters are coupled to the safety system of the distillation unit. The thermocouple measures the temperature gradient (over time) on the surface of the heating elements. The temperature gradient on the heating element is used to shutdown the electrical power supply to reboiler and preheaters. Shutdown is activated for gradients $\frac{dT}{dt} > 5^{\circ}C/min$.

A.1.6 Data acquisition and control

The data sampling and control unit consists of a Areol PC-70 386-33 MHz personal computer and Epson LX-400 needle printer.

The control software is purchased from INTEC Controls Cooperation and is a Paragon 500 Version 1.32. The control system consists of a strategy and display builder for the development of monitor and basic control functions. A runtime routine and I/O hardware interface to execute the control task. An off-line historian module enables viewing and conversion of historical data into LOTUS 1-2-3 format (Lotus, 1989). Further data analysis is done in MATLAB (Matlab, 1999). The PARAGON 500 software (Paragon, 1989) allows for interfacing of User written Microsoft MSC 6.0a (MSC-compiler, 1990) routines. These routines are linked to the control system and enable the execution of more complicated tasks.

All measurements are sampled every second and read into the control program. Data conversion from analog to digital is performed by 12-bit A/D converters at the given sampling time. The digital signals are read into the control program by I/O hardware drivers written in MSC 6.0. Conversion of data from digital to a numerical representation is performed by the hardware driver. The analog signals are converted by third grade functions from rawdata to engineering units (*e.g.* Volt to °C) and afterwards used for control purposes. Filtering of the continuous signals is done by a second order filter with adjustable time constant. For temperature measurement a filter time from 0.03 to 0.1 minutes (2 to 6 samples) was chosen. After filtering the signals are routed to the blocks performing the control task.

The data logging routine of the data acquisition system (Paragon FS 502, version 2.32) from INTEC Controls Cooperation) is configured such that the average of the last five sample intervals is written to a buffer. When the buffer is filled up, the entire buffer is written to the hard disc of the computer. The logged input data are: the 11 tray temperatures, reboiler-, condenser-, preheater temperatures, liquid level in accumulator and reboiler, differential pressure, estimates of top and bottom product composition and the product flows. Analog output data which are logged are reboiler heat input, reflux pump position and product valve position. Additional to these signals the position of the sample valves is recorded.

An off-line routine is provide to convert the collected data set to WKS-format which can be loaded into *e.g.* LOTUS 1-2-3 format for further analysis. From this program the conversion of data to ASCII (tabular) or MATLAB format (tabular and graphics) is possible.

A.1.7 Control of manipulated variables

All functions of the operation of the distillation tower are controlled by the computer control system. The output signals to reboiler power supply, reflux pump position and the two product flow valves is updated once a second. The control signal send buy the computer is in the range of 0 - 10 Volts.

Different single control structures are implemented in one application. The default configuration is the LV-configuration, where the reflux flow (L) and the heat input to the reboiler (V) are the manipulated variables to control x_D and x_B , respectively. From this configuration the change to DV, (L/D)V and (L/D)(V/B) is possible by resetting switches which root the signals through the application. The single loop schemes use standard PI-controllers with

anti-windup and the bumpless transfer from manual to automatic control. Anti-windup is implemented such that the controller remains with maximum or minimum output signal and the integral part of the control algorithm is bypassed.

A.2 Multivessel batch distillation unit

A laboratory scale multivessel batch distillation unit was built to perform the experiments needed to verify the feasibility of the process and the proposed control feedback strategy. The objective was to make the apparatus as simple as possible, and to avoid auxiliary equipment such as reflux pumps. Therefore the column sections and intermediate vessels are placed on top of each other. The unit was built in glass and carefully insulated to reduce heat loss to the surroundings during operation. The apparatus is operated at atmospheric pressure.

The unit consists of a reboiler vessel (4 l volume), two intermediate vessels (1 l volume), and a condensate accumulator (1 l volume each). The four vessels are connected by three packed column sections of 420 mm length and 30 mm diameter which are filled with approximately 400 ml of double-wound wire mesh rings of 3 x 3 mm made from stainless steel by Normschliff. A flowsheet of the entire unit is shown in Figure A.6.

A.2.1 Instrumentation

Each column section is equipped with three type chromel-alumel-thermocouples placed in the center of the column cross section. One thermocouple each is placed 5 cm from the column ends and the third in the middle of the section. The sensors are 100 mm long with a diameter of 1/16". The measuring point is not insulated, such that the time constant of the sensor is below 2 seconds for the chosen installation. The sensors are fitted to the column by fittings and tightened by Silicone packings to enable maintenance.

The thermocouples placed in the middle of the columns are used to control the reflux from the vessel above by means of two-way solenoid valves (on-off) with an opening of 1.6 mm diameter, operated by solid-state relays. The reflux flow is estimated based on the control signal to the solenoid valve. The relation between opening frequency of the valve and liquid flow has been established by calibration. The reflux is introduced to the center of the column, slightly above the packing material.

Thermocouples are also placed in the intermediate vessels and in the reboiler. The reboiler temperature measurement gives an indication of the bottom product quality. A second thermocouple in the electrical heated reboiler is placed between heating mantle and glass vessel to avoid excessive surface temperatures. The temperature measurement of the intermediate vessels allows for the control of heating tapes fitted to the exterior surface of the vessels. The primary objective of these tapes is to compensate for heat losses in piping and vessels connecting the column sections.

Level measurements are not installed, a liquid leg is installed to enable the visual inspection of vessels and reboiler do give an indication of the liquid distribution over the column. During normal operation, level control is not necessary to control/influence the chosen reflux flow. In cases where the vessel volume decreases below a pre-specified minimum the reflux

is fixed to a minimum and the temperature-based reflux controller is overridden manually by the operator.

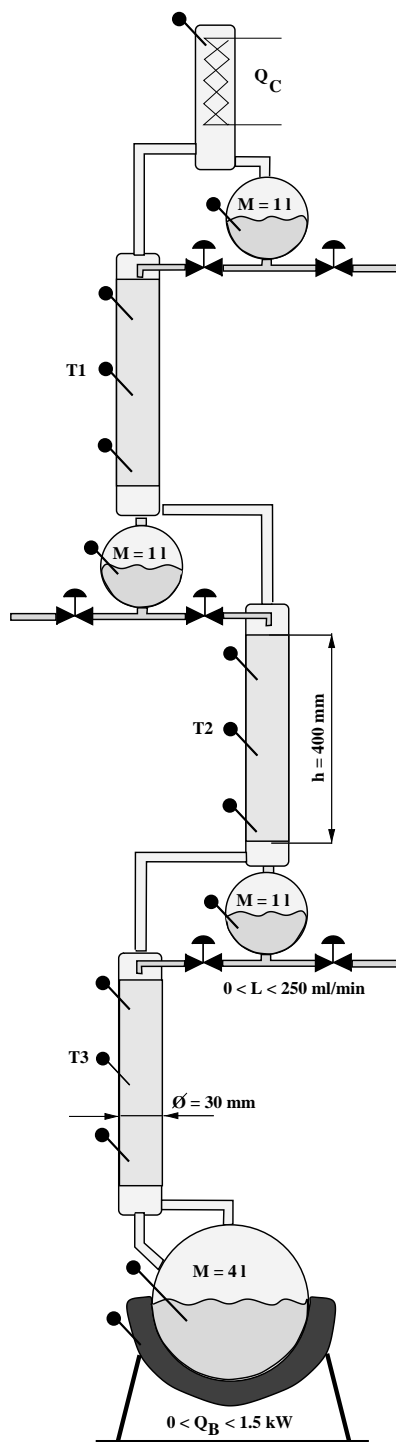


Figure A.6: Pilot plant scale distillation column

A.2.2 Control structure

The reflux into each section was used to control the temperature in the middle of the section below (as shown in Figure A.6). For simplicity the setpoint of the temperature controllers were set to the arithmetic mean of the boiling points of the two components to be separated in the section $T_{s,i} = \frac{1}{2} \cdot (T_{b,i} + T_{b,i+1})$. The chosen controller type for the experiments is a standard PI-controller, which were tuned to be rather slow to avoid excessive control action during start-up and in the presence of disturbances.

The thermocouple installed in the reboiler is used in conjunction with an external mounted thermocouple to adjust the heat input to the reboiler by controlling the temperature difference between reboiler and heating mantle.

A.2.3 Design and operation data

The multivessel batch distillation column is designed based primarily on the data available by Normschliff (1990). The data supplied by Normschliff are for the mixture of n-heptane/cyclohexane. These data are adjusted due to the differences in heat of vaporization, viscosity and density between the test mixture and the distilled alcohol mixture consisting of methanol, ethanol, n-propanol and n-butanol. The design process of the multivessel batch distillation column was strongly influenced by a rather unfavorable ratio between volume and surface (internal diameter of a column section of 30 mm), some adjustment of the design were made during the operation to avoid operational problems.

From the design information available from Normschliff (1990) (page 5.3.08), a maximum liquid load at total reflux of $L \approx 4.5 \text{ kg/h}$ with n-heptane should be possible to process in a column of 30 mm diameter. The viscosity at boiling point of n-hexane is of the order of $0.26 \leq \mu \leq 0.3$. The efficiency of the packing is determined by the vendor with a test mixture consisting of methylcyclohexane/n-heptane. For a column of 1 m length, filled with $3 \times 3 \text{ mm}$ wire mesh rings and an internal column diameter of 30 mm they 80 theoretical trays are specified for total reflux operation. At these conditions an average liquid holdup in the column of 75 ml was determined. Given a load of $L \approx 4.5 \text{ kg/h}$, a heat input in the order of $Q_B \approx 1 \text{ kW}$ and a vapor velocity in of $u \approx 1 \text{ m/s}$ were computed. The vapor velocity is rather high such that it was chosen to reduce the maximum allowed reboiler load during operation to $Q_{B,max} = 700 \text{ W}$ to avoid overload of the column.

Based on data from the vendor approximately 80 theoretical stages per meter packing are expected, for the multivessel batch column with 350 mm packing per column section this should be 28 trays. Assuming an efficiency of the trays in the order of 50 %, the separation a liquid mixture with a constant relative volatility $\alpha_{i,i+1} \approx 2$ should be feasible. Note, we assume a rather low efficiency due the rather short column sections.

The design of the column was verified in an initial experiment, an initial reboiler feed charge of methanol, ethanol, n-propanol and n-butanol (see Table A.1) shows that with a heat input (measured at the reboiler) of approximately $Q_b \simeq 500 \text{ J/s}$ the column operates without flooding in all three sections. Nevertheless the packing material in column 3 is wet, such that this reboiler duty is most probably the limit of operation without flooding. Liquid accumulation on the surface of the packing structure is assumed to be the first visible

indication that a packed column is approaching the flooding limit. The number of theoretical stages is computed based on the Fenske formula (see Appendix to chapter 6).

Table A.1: Initial feed charge and final product composition, $Q_B = 350W$

	component	methanol	ethanol	n-propanol	n-butanol
	$\alpha_{i,4}$	7.8	4.5	2.3	1
Feed	volume [l]	0.3	0.43	0.54	1
	holdup [mol]	7.39	7.36	7.22	10.93
	composition	0.225	0.224	0.220	0.332
Product	Vessel	M_1	M_2	M_3	M_4
	composition	0.96	0.93	0.94	0.96
	Number of theoretical stages between vessels	8 ± 1	10 ± 1	8 ± 1	

A.2.4 Data Acquisition and control

The sensors installed at the pilot plant are connected to a Data Translation DT 2801-A data acquisition board. The board is equipped with two 12-bit A/D converts and are operated at a sampling frequency of 1 Hertz.

The pilot plant is equipped with 16 thermocouples which are connected to a Data Translation DT 756-Y terminal panel with cold junction and a signal amplification of 200. The conditioning of the temperature measurements is performed by means of a second order polynomial by the control software.

The control software (Paragon FS 502, version 2.32) from INTEC Controls Cooperation is installed on a personal computer with 286 CPU. The control system consists of control strategy, operator display and I/O-hardware interface to communicate with the process. All analog signals are filtered by a filter with a time constant of 5 seconds for noise reduction. The data logging routine is configured such that the average of the last ten sample intervals is written to a buffer and later to the hard-disc for further analysis.

Reflux flow to the column sections is controlled based on temperature measurements from the center of each column section, the measurement is fed to a standard PI-controller (with bumpless transfer and anti-wind-up). The continuous control signal is transformed to a set of pulses, passed through a Data Translation DT2801 I/O-board to a solid-state relay which control the reflux flow by a solenoid valves (on-off) which operates at a frequency of 0.2 Hz.

The reboiler is controlled by a series of solid state relays, which control 4 independent heating coils installed in the heating cap. The distribution of heating elements **1** to **4** is shown in figure A.7. The control of the reboiler is configured such that the surface temperature of the heating elements is kept constant. The setpoint is fed to the PID-controller (see Fig. A.7) and based on the deviation, surface temperature and setpoint, a control signal is computed and send to the solid state relays. The heat input is controlled by relays by cutting the power

supply to the respective heating elements. A control signal of 50 % corresponds to equal time intervals were the heating element is *On* and *Off*.

Each element has a maximum effect of $Q_{max} = 275 J/s$. Elements **1** and **2** are interconnected and receive an identical signal from the relays (marked 100%). The thermocouple used to control the surface temperature is positioned near heating zone 2. Elements **3** operates at 50 % and **4** at 25 % of the load of element **1**, respectively. This scheme was chosen to avoid overheating of the heating elements installed in position 3 and 4 when the reboiler level decreases during operation. In Table A.2 we show how the reboiler duty is computed based on the control signal.

Table A.2: Energy input as function of control signal

control signal	energy input per element			total energy input
	1 & 2	3	4	
[%]	[J/s]	[J/s]	[J/s]	[J/s]
10	55	27.5	6.88	89.38
50	275	68.75	34.38	378.13
100	550	137.5	68.75	756.25

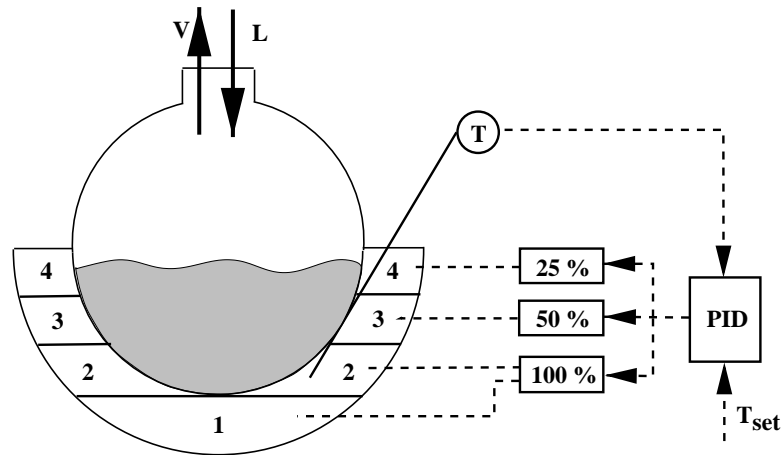


Figure A.7: Multivessel Batch Distillation: Reboiler control

A.3 Product composition analysis

For product composition analysis a Chrompack CP 9000 Gas Chromatograph with a Flame Ionization Detector (FID) and on-column injector is used. The gas chromatograph is equipped with a Chrompack CP-Wax 52 CB fused silica capillary column of 10 m length and 0.53 mm internal diameter. The stationary phase of the column is 0.42 μm thick the height of a theoretical plate for this column is $HETP_{min} = 0.446 mm$. The advantage of the wide bore

column is the considerable shorter analysis time for a sample. To avoid overloading of the capillary GC-column and the detector a dilution ratio of 1:1000 of sample and a solvent is chosen. Distilled water was chosen as a solvent, since the FID detector does not detect water, further organic impurities which can interfere with the measurement are not expected.

The operation parameters of the GC are the following:

	Gas	flows	inlet pressure
Carrier gas	Nitrogen	3 ml/min	200 kPa
Makeup gas	Nitrogen	27 ml/min	200 kPa
Detector	Air	200 ml/min	200 kPa
	Hydrogen	30 ml/min	200 kPa

Analysis of ethanol and butanol samples

The analysis program of the gas chromatograph was optimized for the analysis of ethanol and butanol, temperatures for the unit are set to:

Temperature injection port	230°C
Temperature detector	250°C
Oven temperature	100°C for 3.5 min followed by a ramp 50°C/min to 180°C
Final oven temperature	180°C for 5 min to clean/regenerate column

Analysis of methanol, ethanol, propanol and butanol samples

The samples drawn from the different vessels of the multivessel batch distillation column and a feed sample are analyzed. Operation parameters of the GC are:

Temperature injection port	240 °C
Temperature detector	250 °C
Oven temperature	40°C for 0.5 min followed by a ramp 10°C/min to 150°C
Final oven temperature	150 °C for 10 min to clean/regenerate column

Calibration procedure

Samples of approximately 60 ml are prepared, consisting of 50 ml main component, and approximately 2 ml of the impurities. As internal standard 2-pentanol (2 – *PeOH*, index *std*) is chosen, approximately 0.5 gr are added to the sample. The sample size is chosen to reduce errors during sample preparation.

This give a calibration where the main component is $x \approx 0.85$ on molar basis. Variations of the relative response factor are rather limited, even when the amount of main component is increased to $x \approx 0.98$. Known samples are analyzed, and the relative response factors are computed according to the following formula

$$RF = \frac{m_i}{m_{std}} \cdot \frac{A_{std}}{A_i} \quad (\text{A.1})$$

where index *std* denotes the internal standard and *i* the components to be analysed. The relative response factor is computed in this manner to reduce the influence of the injected amount (Note, we apply the area ratios and not the absolute area). The calibration is performed on mass basis and NOT on molar basis.

Response factors of methanol, ethanol, n-propanol and n-butanol relative to 2-pentanol (2 – *PeOH*) are computed to

$$RF = [2.2332, 1.4919, 1.1366, 1.0081, 1.0000] \quad (\text{A.2})$$

the standard deviation for this calibration method was determined to

$$RF_{std} = [0.0763, 0.0722, 0.0306, 0.0257, 0] \quad (\text{A.3})$$

from frequent recalibration.

Analyzing an unknown sample consists of the same steps, the total sample weight and the relative response factors are known. The mass of the impurities is determined by analysis and the mass of the main component is computed from a material balance over the sample.

Procedure for analysis

- The sample is filled into a vial, the net-weight of the sample (approximately 20ml \approx 15 – 16gr) is determined by a microscale and 0.2 g 2-pentanol (2 – *PeOH*) is added.
- 10 μ l of that sample is diluted in 5 ml of water, we choose water as solvent since the utilized FID-detector does not detect water, thus organic impurities from a solvent could be avoided.
- Injection of the sample into the injection port of the GC. The detector of the gas chromatograph is rather sensitive to overloading, such that a smaller amount of the heavier products (*e.g.* n-butanol rich fractions) like bottom product than top product (*e.g.* methanol rich fractions) was chosen to inject:

sample type	amount injected
feed	0.1 μ l
methanol	0.1 μ l
ethanol	0.08 μ l
1-propanol	0.07 μ l
1-butanol	0.05 μ l

After 10 samples, the column was regenerated at 200°C for 10 minutes to remove possible deposits of heavier components from the column.

The gas chromatograph is interfaced to a Commodore SX386 personal computer for data acquisition. The analysis program MOSAIC by Chrompack (Chrompack Mosaic, 1990) is used for basic analysis such as determination of the area-ratio of the two components. The final data analysis such as conversion of rawdata (area-ratio) to compositions is done with Matlab.

A.4 Distilled system

The chemical system distilled in the distillation columns have to fulfill the following requirements:

- The continuous distillation column consists of 11 sieve trays and the multivessel batch distillation column consists of sections approximately 8 trays each. High purity distillation requires a fairly high relative volatility.
- The mixture should not be toxic.
- Boiling temperature below 120 ° C for the higher boiling component due to safety considerations.
- Analysis of the product samples has to be uncomplicated.
- Fairly ideal behavior of the components during distillation, *e.g.* no azeotrop.
- At least one of the components should have a characteristic odor for a fast detection of leaks.

The above listed requirements are fulfilled by the system methanol, ethanol, n-propanol and n-butanol. In the continuous column high purity separations of ethanol/n-butanol and methanol/n-propanol are possible. The multivessel batch distillation column was operated with all four components. The properties of the systems are simulated using ASPEN - Properties Plus (Aspen Properties Plus, 1988-1999) and are compared to the pure component data given by Daubert and Dannert (1989) and Gmehling and Onken (1977). A collection of the most important thermodynamic data is presented in Table A.3

Table A.3: Thermodynamic data of components

component		methanol (1)	ethanol (2)	n-propanol (3)	n-butanol (4)
T_b	$^{\circ}C$	64.96	78.5	97.4	117.25
T_b	K	338.11	351.65	370.55	390.4
M	$kg/kmol$	32.04	46.07	60.11	74.12
ρ^{20}	kg/m^3	791	789	804	810
$\rho^{T_b^1}$	kg/m^3	745	747	764	772
$\rho^{T_b^2}$	kg/m^3	735	737	756	764
$\rho^{T_b^3}$	kg/m^3	714	717	736	745
$\rho^{T_b^4}$	kg/m^3	691	694	714	725
μ^{20}	$10^{-4} Pa \cdot s$	5.97	12.0	22.56	29.48
μ^T	$10^{-4} Pa \cdot s$	4.03 ⁵⁰	5.04 ⁷⁰	7.6 ⁷⁰	0.54 ¹⁰⁰
μ^{T_b}	$10^{-4} Pa \cdot s$	4.925	3.712	2.926	*
ΔH_{vap}^{20}	KJ/mol	37.4	42.2	47.35	52.2
$\Delta H_{vap}^{T_b}$	KJ/mol	35.0	38.7	41.22	43.14

* Not listed

The density of the alcohols are found in Hales and Ellender (1976). The viscosities of the components μ^{20} and μ^T are found in Weast (1978) while μ^{T_b} was extrapolated from Stephan (1988). The heat of vaporization of the components is found in Majer *et al.* (1985).

Bibliography

1. ASPEN PROPERTIES PLUS, "User Guide, Release 8", Aspen Technology, Inc., Cambridge, USA, 1988-1999
2. Chrompack MOSAIC "User Manual", Chrompack, The Netherlands, 1991
3. Daubert, T.E. and R.P. Danner, "Physical and Thermodynamic Properties of Pure Chemicals", Data Compilation, 1989
4. Gmehling, J. and U. Onken, "Vapor-Liquid Equilibrium Data Collection Organic Hydroxy Compounds: Alcohols", Chemistry Data Series, Vol. I, Part 2a, 1977
5. Halles, J.L. and J.H. Ellender, "Liquid Densities from 293 to 409 K of nine Aliphatic Alcohols, *J. Chem. Thermodynamics*, Vol. 8, pp. 1177-184, 1976
6. Heckenberger, T., "Thermal Conductivity and Viscosity Data of Fluid Mixtures", Chemistry Data Series, Vol X, Part 1, 1988
7. Loe, I. "Distillation Column Modeling, Dynamics and Control", Phd-Thesis, NTH-Trondheim, Norway, 1996
8. LOTUS 1-2-3 Release 3, "Reference Manual", Lotus Development Corporation, Cambridge, USA, 1989
9. Majer, V. and V. Svoboda, "Enthalpies of Vaporization of Organic Compounds", Chemical Data Series, Vol. 32, 1985
10. MATLAB, "High-Performance Numeric Computation and Visualization Software, Reference Guide", The MathWorks, Inc., Massachusetts, USA, 1992-1999
11. Mejdell, T., "Estimators for Product Composition in Distillation Columns", Phd-Thesis, NTH-Trondheim, Norway, 1990
12. Microsoft C 6.0a Optimizing Compiler, "Reference Manual", Microsoft Corporation, Redmont, USA, 1990
13. Normschliff, "Distillation Plants", 5.3 NGW, Wertheim, 1990
14. Normschliff, "Glass Plants and Components", Wertheim, 1994
15. "Paragon 500 Intuitive Software for Industrial Automation, User Manual", Intec Controls Corporation, Walepole, Massachusetts, USA, 1992
16. Perry, H.P. and D. Green (Ed.), "Perry's Chemical Engineers' Handbook", McGraw-Hill Chemical Engineering Series, 50th edition, 1984
17. Smith, J.M. and H.C. Van Ness, "Introduction to Chemical Engineering Thermodynamics", 4'th Ed, McGraw-Hill Chemical Engineering Series, 1987
18. Weast, R., (Ed.), "Handbook of Chemistry and Physics", 58th edition, CRC Press, 1977-1978

Appendix B

Obtain operational parameters of a distillation column

In this chapter, the experimental procedures to determine operational parameters of a continuous distillation column which describe the dynamics of a distillation column are presented. These experiments were used in an interactive manner to determine coefficients applied in the simulation models presented in chapter 2.

Experiments performed were step changes in reflux and vapor flow, tracer experiments, measurements of the pressure drop over the column and dumping experiments. From these experiments it was possible to find:

- Initial temperature responses
- Column holdup
- Hydraulic lag
- Residence time

The distillation column (see Figure B.1) used for the experiments is equipped with eleven sieve trays, an electrical heated reboiler and water cooled condenser. The feed and reflux are supplied by metering pumps, the temperature of these streams is controlled by electrical heater units. For a more detailed description we refer to appendix A.

The instrumentation of the column consists of thermocouples placed in the center of each tray, reboiler, condenser and the preheater units. The holdup of reboiler and condenser is measured by differential pressure cells. The feed and product tanks are equipped with level sensors to indicate draining or overflow of the tanks. The process is interfaced via a Hewlett-Packard TDC 2000 to a PC-based process control system by Intec Controls. The control system Paragon 500 is configured to sample at a frequency between 1 and 5 Hertz, depending on type of measurement and the experiments performed.

The tray numbering for the pilot plant is chosen from bottom to the top. The reboiler temperature is denoted (T_{reb}), the tray temperatures are from tray 1 (T_1) to tray 11 (T_{11}), counting from the bottom to the top, the temperatures of reflux, feed and condenser outlet are denoted (T_L), T_C and (T_F), respectively. The holdup in reboiler and accumulator are

denoted M_D and M_B , respectively, these holdups are measured in [l]. The pressure in the reboiler of the distillation column is measured in [mbar] and denoted p_{btm} .

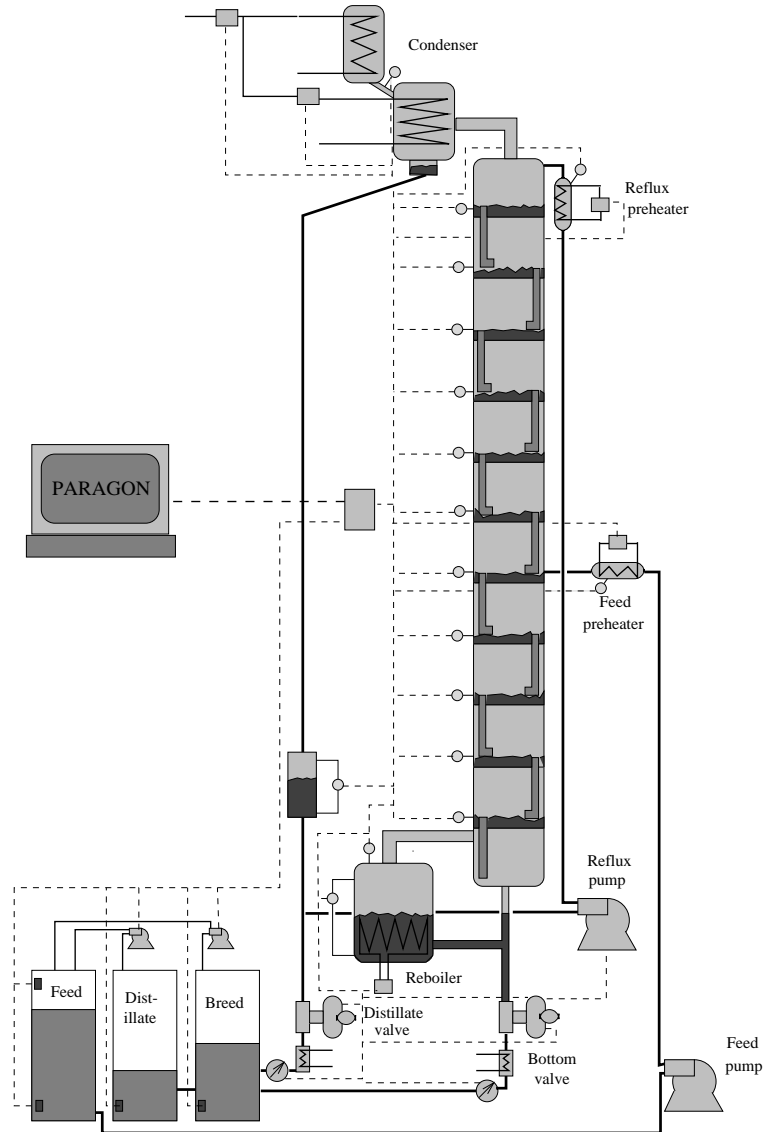


Figure B.1: Pilot plant scale distillation column

Note: In the here presented Appendix, the tray numbering of the continuous distillation column is from bottom to top, with the reboiler defined as “0”; this is in the opposite order compared to the data presented in chapter 2.

B.1 Initial temperature response

B.1.1 Definition of the initial time constant

The dynamics of a process can be determined from the response of the process to pulses or steps in the manipulated variables. If the process is linear and at steady state before the input is changed the process dynamics will be determined by a transient response experiment. In practice, it is difficult to ensure that the process is at rest, further measurement noise will corrupt the responses.

A step or pulse response can be obtained by the following procedure. When the process is at rest, the controller is set to manual and the control variable is changed rapidly to its new value. Examples of open loop step responses are shown in Figure B.2. Many properties of the process can be obtained directly from the recorded step response. The process in Figure B.2 (a) is stable whereas in Figure B.2 (b) an unstable process is presented. For a linear system the shape of the step response does not depend on the magnitude and direction of the input signal. Step response experiments are an easy way to characterize the dynamics of a given process due to its simple physical interpretation.

The time constant is defined as the time elapsed until a process adjust to a change in input, the value of the response reaches 63.2 % of its final value after one time constant.

The slope of the (normalized) response at $t = 0^+$ is equal to 1.

$$\frac{d[y(t)/y_\infty]}{d(t/\tau)} \Big|_{t=0^+} = e^{(-t/\tau)} \Big|_{t=0^+} = 1 \quad (\text{B.1})$$

Determine graphically the time constant of the first-order lag process is shown to the left (a) in Figure B.2. The transfer function of the process is:

$$G(s) = \frac{K}{1 + s\tau} e^{-\theta s} \quad (\text{B.2})$$

The initial time constant of a nearly capacitive process is shown to the right (b) in Figure B.2. A capacitive process with delay is described by:

$$G(s) = \frac{K}{\theta s} e^{-\theta s} \quad (\text{B.3})$$

the model is characterized by the gain K and the time delay θ . A reasonable good description of the process behavior is possible at time scale θ , the static (low frequency) behavior is not well defined.

B.1.2 Hydraulic time constant estimated from experiment

$$\tau_L = (\delta M_L / \delta L)_V \quad (\text{B.4})$$

The hydraulic time constant τ_L describe the dependency of the internal liquid flows dL on the manipulated variables dL_T . We assume constant molar flows and $dV = dV_T = \text{constant}$

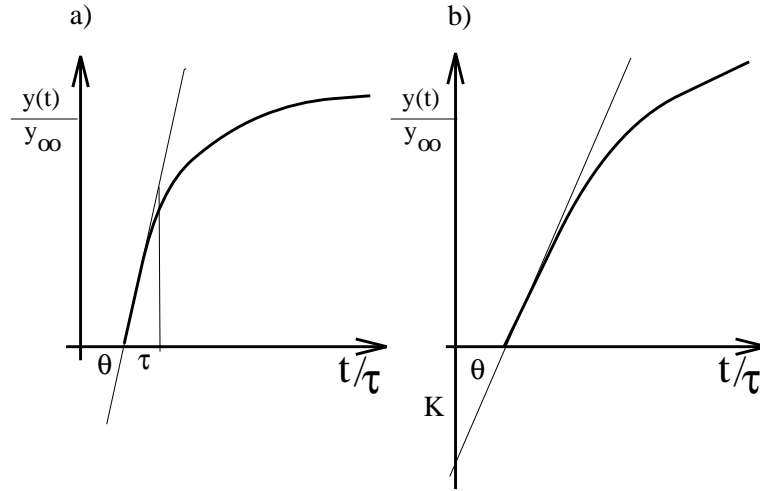


Figure B.2: Dimensionless response of a process to a step change in input, (a) first-order lag process, (b) almost pure capacitive process

(Rademaker *et.al*, 1975, Skogestad*et.al*, 1988). The numbering of the trays is from the top and down. The mass balance over tray i :

$$\frac{dM_i}{dt} = dL_{i-1} - dL_i \quad (\text{B.5})$$

and the tray hydraulics:

$$dL_i = \frac{1}{\tau_i} dL_{i-1} + \lambda dV \quad (\text{B.6})$$

insert the Laplace transform of Eq. B.5 into B.6 yields:

$$dL_i = \frac{1}{1 + \tau_L s} dL_{i-1} + \frac{\tau_L s}{1 + \tau_L s} \lambda dV \quad (\text{B.7})$$

rearrange this equation to

$$dL_i = \frac{1}{1 + \tau_L s} dL_{i-1} + \left(1 - \frac{1}{1 + \tau_L s}\right) \lambda dV \quad (\text{B.8})$$

repeated application of Eq. B.8 from the reboiler to the upper most tray (N trays) yields:

$$dL_B = \frac{1}{(1 + \tau_L s)^N} dL_T + \left(1 - \frac{1}{(1 + \tau_L s)^N}\right) \lambda dV \quad (\text{B.9})$$

were L_N denotes the liquid outflow response of the N^{th} -tray to a change in reflux. The response of the liquid flow on stage N is a cascade of first-order responses, one for each tray. Introduce the following approximation:

$$\frac{1}{(1 + \tau_L s)^N} \approx e^{-N\tau_L s} = e^{-\theta s} \quad (\text{B.10})$$

yields:

$$dL_N \approx e^{-\theta s} dL_T + (1 - e^{-\theta s}) \lambda dV \quad (\text{B.11})$$

From Eq. B.11 we can estimate the hydraulic time constant from the measurement of the delay between a change in external reflux until the liquid outflow of tray N changes $\theta_L \approx \tau_L N$.

Approximate the liquid time constant from experiment can be done by observation of the temperature response to increase in L_T . Observing the initial response (see Figure B.3) will indicate the time a reflux flow change needs to propagate through the column. Secondary effects, which are the changes of the liquid compositions on the trays will not be considered.

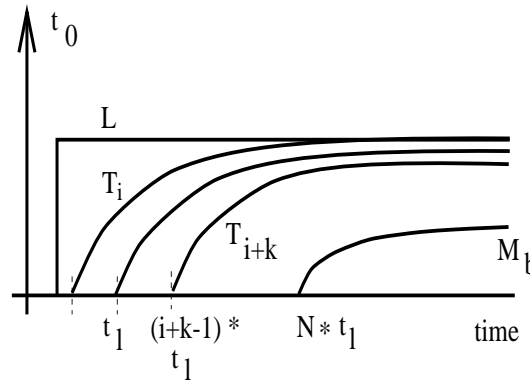


Figure B.3: Determination of the hydraulic time constant from measurement of the temperature responses of trays i and $i+k$

B.1.3 Experimental procedure to obtain the initial temperature response

A brief description of the experimental procedures is given. The time constants of the process are determined from experiments where step changes in one control loop are performed, while the other loop was not perturbed (*i.e.* the signal to the actuator was kept constant). The manipulated variables used are the control signal to reboiler heater and reflux pump. These manipulators set the heat input to reboiler and the volumetric reflux to the distillation column.

During the experiments the holdups of accumulator and reboiler are controlled by manipulation of distillate and bottom product flow, respectively. The responses are logged such that approximately 100 s prior to the step changed are recorded and approximately 1500 s afterwards.

The intention is to record the initial responses of temperatures on tray 3 and 9, bottom pressure and holdup in reboiler and accumulator. Trays 3 and 9 are chosen since these tray temperatures are most sensitive to step changes in the manipulated variables (see Figures *e.g.* B.12 and B.13). These tray temperatures will later on be used as input to the controllers of distillate and bottom composition. The influence of the reboiler heat input is largest on the temperatures in the bottom of the column, while a reflux change will primarily affect the upper part of the column.

For experiments where the product samples are taken, the shortest sampling interval of the product flow composition is in the range of 100 to 200 s. During the course of the experiments, the sampling interval is increased to avoid the analysis of an extensive number of samples.

The experiments performed are done with manual setting of reflux and reboiler heat input which corresponds to an open-loop LV-configuration. The column is operated at atmospheric pressure in the condenser such that a pressure control loop is not necessary.

Procedure: Experiment 1 to 4 The control of accumulator and reboiler holdup are done by PI-controllers acting on distillate and bottom flow, respectively. The control loops for the holdup are cascade loops with PI-controllers. The time constant of the secondary loop is approximately a tenth of the primary loop to ensure a reasonable response of the secondary controller.

Procedure: Experiment 5 to 7 For experiments 5 to 7 the holdups are uncontrolled, such that the hydraulics of the column is investigated.

At the end of the experiment, all control loops are placed into manual, until the measurements on tray temperatures and levels are stabilize, reboiler and reflux pump are shut down simultaneously as well as product valves are closed. This shut-down procedure is performed to determine the column holdup by measuring the change in reboiler and accumulator level.

B.1.4 Results initial temperature response

Experiment 1 to 4: Holdup controlled

The presented responses are for trays 3 and 9 as well as product compositions. Experiments 1 to 4 are performed with analysis of feed, top and bottom compositions. The control of reboiler and accumulator level is done automatically by means of distillate and bottom flow. The steady state data of experiment 1 to 4 before and after the step change are listed in Table B.1. The data are the average of at least 50 measurements prior to the step change. The final steady state is defined to be a time interval of 50 s approximately 300 to 900 s after the step change was introduced.

The experimental conditions, time constants and delay of experiments 1-4 are combined in Table B.2. The notation θ_{T9} indicates the time delay from a change in a manipulated variable (L or V) until the temperature on tray 9 starts to deviate from its former steady state. The entries in Table B.2 which are marked with (*) were not identified from the available data. Especially from the responses which are similar to an integrator it is difficult to determine the initial time constant (*e.g.* Exp. 2).

Table B.1: Steady state data from experiments 1 to 4

Variable	Dimension	Experiment 1		Experiment 2		Experiment 3		Experiment 4	
		t_0	t_f	t_0	t_f	t_0	t_f	t_0	t_f
time	s	0 - 110	500 - 550	180 - 230	500 - 550	310 - 360	700 - 800	190 - 247	520 - 575
T_{reb}	$^{\circ}C$	118.7298	118.5581	118.0258	118.1788	118.0849	118.0880	118.2272	118.2964
T_1	$^{\circ}C$	117.2862	117.0490	114.8678	116.1188	116.6216	116.4602	116.6483	116.8332
T_2	$^{\circ}C$	116.6627	116.0796	111.0827	114.0449	115.7771	115.3696	115.7738	116.2959
T_3	$^{\circ}C$	115.1178	114.0781	104.5306	109.9447	113.6465	112.6622	113.3564	114.7686
T_4	$^{\circ}C$	112.0872	110.2902	96.7197	103.1534	109.7096	107.7697	108.8267	111.6026
T_5	$^{\circ}C$	106.7461	104.3934	90.8374	95.8500	103.5823	101.1260	102.0704	106.0484
T_6	$^{\circ}C$	104.5680	101.3801	84.6928	88.6033	100.2453	96.7023	96.8826	102.7776
T_7	$^{\circ}C$	99.5559	95.6371	81.4463	83.1592	98.5549	95.0777	94.6838	100.4071
T_8	$^{\circ}C$	91.5876	88.1974	80.4206	81.1001	89.9089	86.6001	86.0642	91.6322
T_9	$^{\circ}C$	85.9345	83.8306	79.4533	79.8487	84.6381	82.6504	82.0784	85.5159
T_{10}	$^{\circ}C$	81.8198	80.8923	79.1158	79.2244	80.9016	80.0845	79.8665	81.3119
T_{11}	$^{\circ}C$	79.7862	79.5040	78.9100	78.9107	79.0376	78.8167	78.6863	79.1116
T_L	$^{\circ}C$	78.4134	77.1240	78.4155	77.6598	78.5842	78.6265	78.4821	78.5173
T_F	$^{\circ}C$	90.9424	90.9847	91.7870	91.0134	91.2657	91.2814	91.9647	91.8812
T_C	$^{\circ}C$	72.4826	75.1563	72.9242	75.4021	75.1444	74.9735	75.1292	74.8550
M_B	l	3.5096	3.5018	3.4715	3.3744	3.4745	3.6008	3.3883	3.3348
M_D	l	1.4950	1.4970	1.5003	1.5021	0.9798	1.0081	1.0059	1.0058
P_{b0m}	mbar	21.9330	20.1415	20.6588	21.7588	26.0066	26.5289	31.9728	31.5774
F	ml/min	250	250	250	250	250	250	250	250
D	ml/min	68.8065	45.8975	72.8670	93.9060	83.0608	66.7836	88.3149	115.3509
B	ml/min	145.8714	171.4858	143.4065	99.7371	115.8741	149.1091	123.5236	77.3160
L	ml/min	249.8474	249.8474	249.8106	249.8106	329.1896	382.7456	418.5046	382.8006
Q_B	kJ/s	3.7500	3.3000	3.6000	4.0500	4.5000	4.5000	5.4000	5.4000
x_B	mol/mol	0.00285	0.0036	0.0336	0.0152	0.0031	0.0065	0.0053	0.0020
x_D	mol/mol	0.9844	0.9873	0.9986	0.9996	0.9822	0.9875	0.9906	0.9864
z_F	mol/mol	0.4980	0.5040	0.5432	0.5349	0.5608	0.5620	0.5182	0.5203

The row denoted with time indicates the time intervals which are used to compute the initial and final steady state data.

Experiment 1, decrease in boilup

A step change is introduced in the reboiler heat supply from initial $Q_{B0} = 3.75kJ/s$ to $Q_{B\infty} = 3.3kJ/s$ at $t = 111s$. Since the initial response is of interest, the first 400 seconds

after the step change in the manipulated variable is displayed. Figure B.4 shows the product composition response to the reduction in reboiler effect. A decrease in reboiler effect give a lower purity of the bottom product and a higher purity of the top product.

Table B.2: Experimental conditions of experiments 1 to 4 and the experimental determined time constants and delays

		Exp.1	Exp.2	Exp.3	Exp.4
F	$\frac{ml}{min}$	250	250	250	250
z_F	$\frac{mol}{mol}$	0.50	0.54	0.56	0.52
T_F	$^{\circ}C$	91.0	91.0	91.2	92.0
T_L	$^{\circ}C$	77.0	78.0	78.5	78.5
step at	s	111	231	364	248
step in		Q_b	Q_b	L	L
L_0	$\frac{ml}{min}$	249.8	249.8	329.2	418.5
L_{∞}	$\frac{ml}{min}$	249.8	249.8	382.7	382.8
ΔL	$\frac{ml}{min}$	0.0	0.0	+ 52.8	-35.7
Q_{B0}	$\frac{kJ}{s}$	3.75	3.6	4.5	5.4
$Q_{B\infty}$	$\frac{kJ}{s}$	3.3	4.05	4.5	5.4
ΔQ_B	$\frac{kJ}{s}$	- 0.45	+ 0.45	0.0	0.0
x_D	$\frac{mol}{mol}$	0.9844	0.9988	0.9826	0.9909
x_B	$\frac{mol}{mol}$	0.0027	0.0225	0.0031	0.0055
K_{T3}		+ 2.23	+ 1.11	- 1.08	- 2.28
		$\frac{^{\circ}C \cdot s}{kJ}$		$\frac{^{\circ}C \cdot s}{ml}$	
θ_{T3}	s	26.9	11.6	26.5	40.5
τ_{T3}	s	69.8	26.7**	84.7	78.5
$\frac{d\Delta T_3}{dt}$	$10^{-2} \frac{^{\circ}C}{s}$	-1.48	+4.51	-0.87	+1.09
K_{T9}		+ 4.66	+ 0.88	- 2.04	- 5.22
		$\frac{^{\circ}C \cdot s}{kJ}$		$\frac{^{\circ}C \cdot s}{ml}$	
θ_{T9}	s	50.8	*	16.7	17.7
τ_{T9}	s	92.1	*	75.0	103.8
$\frac{d\Delta T_9}{dt}$	$10^{-2} \frac{^{\circ}C}{s}$	-1.48	*	-1.43	+0.97
$\theta_{P_{Btm}}$	s	3.8	1.5	*	*
$\Delta\theta_{\theta_{T3}-\theta_{T9}}$	s	23.9	*	13.8	22.8

* not possible to determine from data set; ** value rather inaccurate

$$\text{definition of } K = \frac{T|_{t=\infty} - T|_{t=0}}{Q_b|_{t=\infty} - Q_b|_{t=0}}$$

The initial responses to a step change in the reboiler heat supply is shown in Figure B.5. The time delay from the change in reboiler heat input until the temperature on tray 3 (-) reacts is $\theta = 23.7 s$ with an initial time constant of $\tau = 31.5 s$. The corresponding data for tray 9 (-) are a time delay of $\theta = 43.4 s$ with an initial time constant of $\tau = 76.8 s$.

Compare Figure B.4 and B.5 shows that the response of the tray temperatures is considerably faster than the product composition response. Appropriate control of a distillation column depends on measurements which are fast and reliable. Since the delay between step change and temperature change on tray 3 is about half the time compared to the composition change temperature as controlled variable will be preferable. Note that measurement delay due to composition analysis is not included, the samples were collected and analyzed off-line. On-line sampling will require a sampling range of approximately 20 - 25 minutes. For

a distillation column with an open-loop time constant in the order of 2 minutes this is not acceptable from a control point of view.

The initial response of the bottom pressure to the step change in the reboiler heat supply is shown in Figure B.6, we find $\theta = 3.8 \text{ s}$. The delay from reboiler load change to the temperature response on stage 3 is determined to $\theta_{T3} = 26.9 \text{ s}$ and on stage 9 to $\theta_{T9} = 50.8 \text{ s}$.

The product flows were under a rather sluggish tuned cascade control, such that a fast response of the product flow to the step in reboiler heat input is not expected. The bottom flow is changing approximately 52 s after the step in reboiler heat supply is performed. The distillate flow starts to change considerably at $t = 225 \text{ s}$, that is 114 s delayed. From the experiments where the product flows are under automatic control, we do not get any information on the hydraulics of the column.

Experiment 2, increase in boilup

The reboiler effect was increased from $Q_{B0} = 3.6 \text{ kJ/s}$ to $Q_{B\infty} = 4.05 \text{ kJ/s}$ at $t = 231 \text{ s}$. The increase in reboiler heat input gives a more pure bottom product (see Figure B.8), the composition of the top product is almost unchanged. The initial response of tray 3 to the step change in the reboiler heat supply is shown in Figure B.9 we found $\theta_{T3} = 11.6 \text{ s}$, $\tau = 26.7 \text{ s}$. The time delay and time constant on tray 9 to step change in reboiler effect are not determined (see Figure B.9) due to the shape of the response. The initial response of the bottom pressure to the step change in the reboiler heat supply is shown in Figure B.10, we found $\theta_{P_{btm}} = 1.5 \text{ s}$.

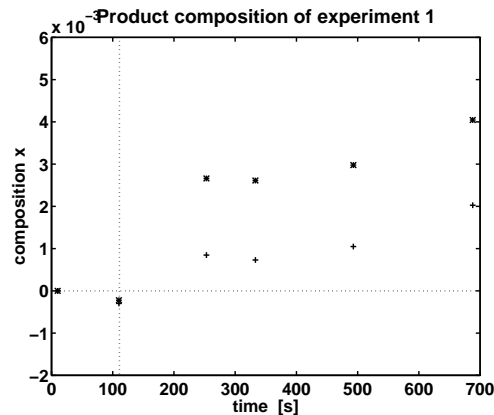


Figure B.4: Experiment 1, compositions of product samples, * distillate composition, + bottom composition

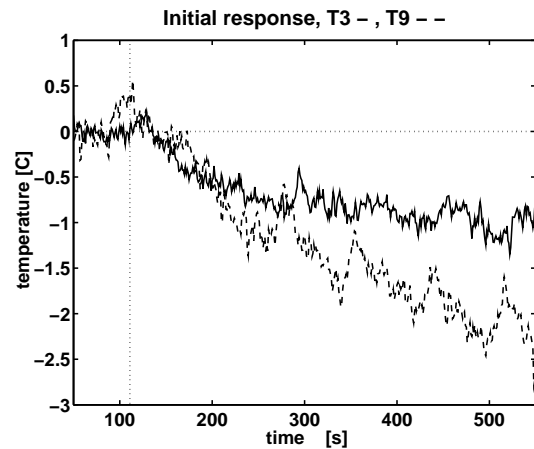


Figure B.5: Experiment 1, response of temperature on tray 3 and 9 to a change in reboiler effect, Step from 3.75 kJ/s to 3.3 kJ/s at $t = 111 \text{ s}$.

For the second experiment we have chosen to tune the cascade controllers faster compared to experiment 1. The response of the bottom flow follows immediately after the reboiler heat supply is considerably faster.

The propagation of the temperature profile in the investigated distillation tower during a step change is shown in Figure B.12 and Figure B.13. The temperature profile over the

column shows the movement of the zone of mass transfer for times $t = [200, 400, 600, 800]s$ due to the change in reboiler effect at $t = 231s$. From Figure B.12 we see that the tray temperature on tray 3 is particularly sensitive to a step change in reboiler effect. The temperature increases by approximately $6^{\circ}C$.

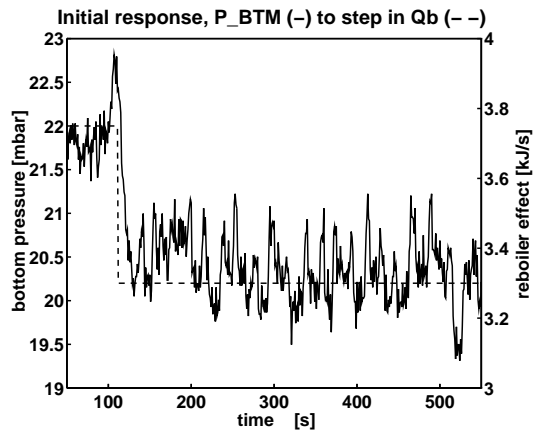


Figure B.6: Experiment 1, response of the bottom pressure to a change in reboiler effect at $t = 111 s$

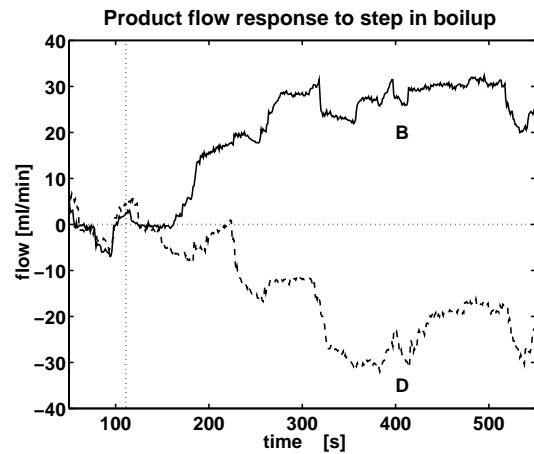


Figure B.7: Experiment 1, response of the product flows to a change in reboiler effect at $t = 111 s$

Figure B.13 shows the temperature responses on trays and reboiler, the time at which the boilup is incremented is marked by the vertical rule. The temperature on tray 3 follow a first order plus dead time type of response. The temperature at the opposite end of the column (trays 9 to 11) are almost constant despite the step change. The temperatures listed in Table B.1 as initial steady state is the average of the time interval $t = 180$ to $230 s$, the final steady state is chosen to be the average of the temperature from $t = 800$ to $850 s$.

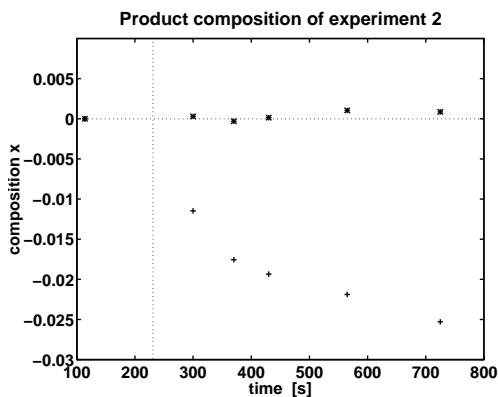


Figure B.8: Experiment 2, compositions of product samples, * distillate composition, + bottom composition

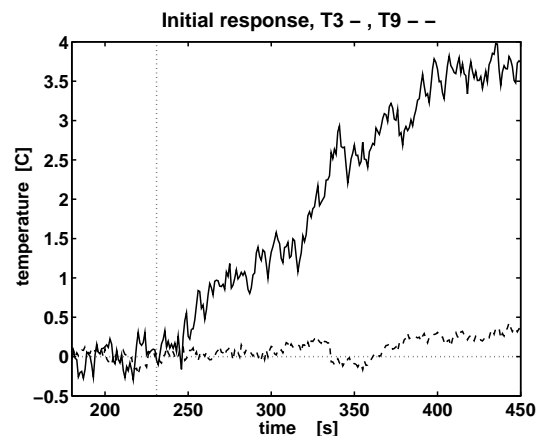


Figure B.9: Experiment 2, response of temperature on tray 3 and 9 to a change in reboiler effect. Step from $3.6 kJ/s$ to $4.05 kJ/s$ at $t = 231 s$

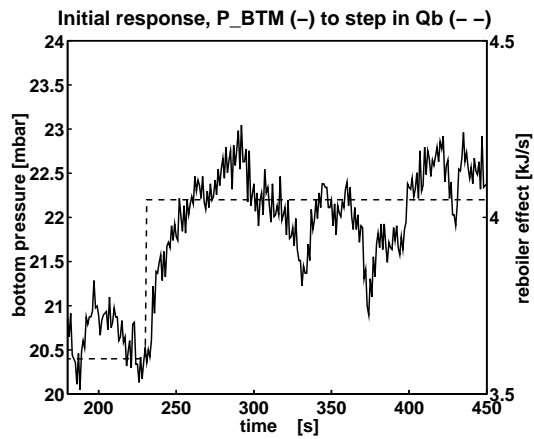


Figure B.10: Experiment 2, response of the bottom pressure to a change in reboiler effect

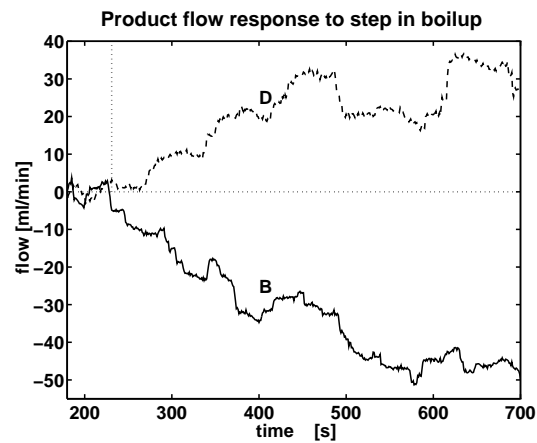


Figure B.11: Experiment 2, response of the product flows to a change in reboiler effect at $t = 231$ s

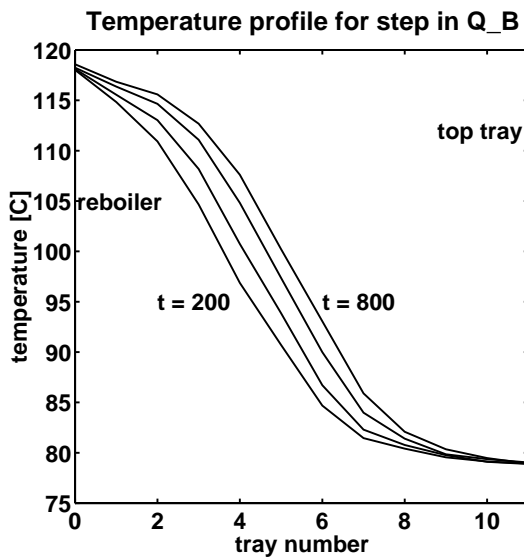


Figure B.12: Temperature profile over the distillation column for experiment 2, at $t = 231$ the boilup is increased from $Q_B = 3.6$ to 4.05 kJ/s (The numbering of the trays is from bottom to top, tray 0 is the reboiler)

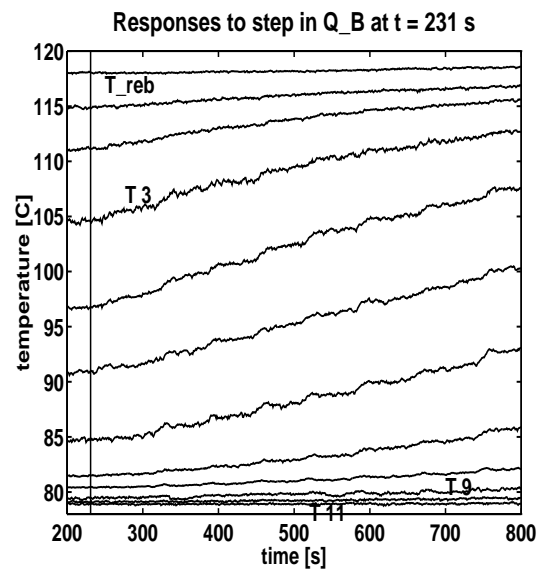


Figure B.13: Temperature responses for experiment 2, at $t = 231$ the boilup is increased from $Q_B = 3.6$ to 4.05 kJ/s (The numbering of the trays is from bottom to top, tray 0 is the reboiler)

Experiment 3, increase in reflux

The response of the product composition to a step change in reflux flow (on volumetric basis) is shown in Figure B.14. The reflux flow is changed from $L = 329$ to 383 ml/min at time $t = 364$ s. The analysis of the samples give a rather inconsistent response. As time increases, the distillate composition increases and the bottom purity decreases. The initial response of tray 9 to the step change in reflux flow at $t = 364$ s is shown in Figure B.15 we find

$\theta_{T3} = 26.5 \text{ s}$, $\tau_{T3} = 84.7 \text{ s}$ for tray 3 and $\theta_{T9} = 16.7 \text{ s}$, $\tau_{T9} = 75 \text{ s}$ for tray 9.

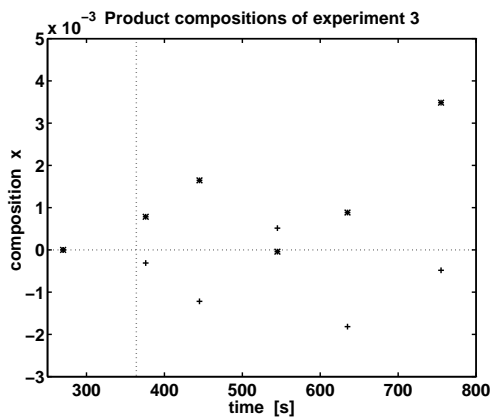


Figure B.14: Experiment 3, compositions of product samples, distillate * composition, + bottom composition

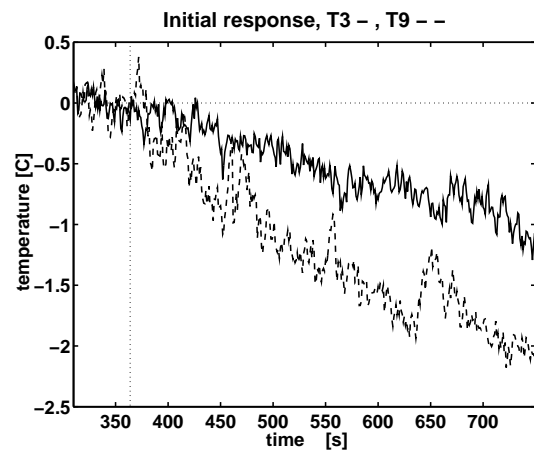


Figure B.15: Experiment 3, response of temperature on tray 3 and 9 to a change in reflux flow. Step change in reflux flow from 329.2 to 382.7 ml/min at time $t = 364 \text{ s}$.

The change in reflux flow do not have any measurable influence on the column pressure drop, see Figure B.16. A step change of approximately 60 ml/min reflux by constant boilup will increase the clear liquid height above weir by approximately $h_{ow} = 0.4 \text{ mm}$, this corresponds to an increase in pressure drop by $\Delta p = 0.028 \text{ mbar}$ which is not measurable with the available pressure sensor.

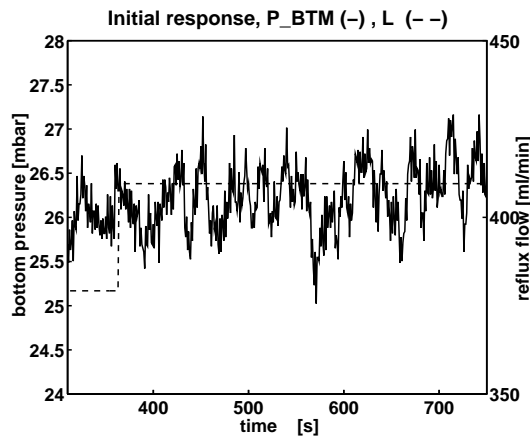


Figure B.16: Experiment 3, response of the bottom pressure to an increase in reflux flow

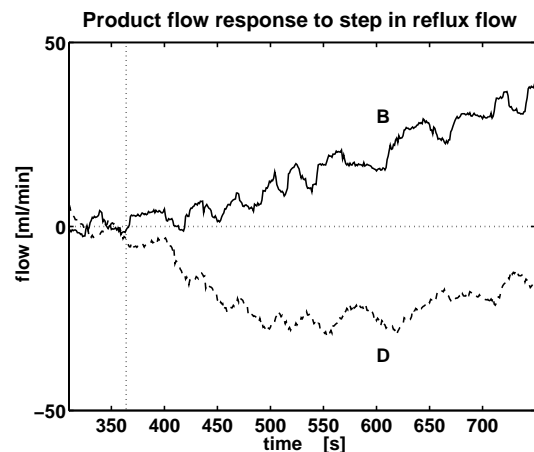


Figure B.17: Experiment 3, response of the product flows to a change in reboiler effect at $t = 364 \text{ s}$

The increase in reflux flow at $t = 364 \text{ s}$ results in a reduced distillate flow and increased bottom flow. The time needed for the additional reflux to reach the reboiler is rather difficult

to determine, since the estimation is considerably dependent on the speed of the bottom flow control loop. We see that the bottom flow response is delayed by approximately 100 s compared to the step in reflux flow.

The liquid flow dynamic of the distillation column is considerably faster than the composition dynamic. The temperatures on stages 3 and 9 are initially influenced by the liquid flow changes in the column and not by the change of composition on the tray above.

Experiment 4, decrease in reflux

The composition response to a decrease in reflux is shown in Figure B.18. The initial response of tray 9 to the step change in reflux flow is shown in Figure B.19, we found $\theta_{T3} = 40.5 \text{ s}$, $\tau_{T3} = 78.5 \text{ s}$ for tray 3 and $\theta_{T9} = 17.7 \text{ s}$, $\tau_{T9} = 103.8 \text{ s}$. The determination of the time constants (see Figure B.19) is rather difficult, since the process acts like a capacitive process instead of a first order process. As seen from Figure B.20, the column pressure drop is almost unchanged after the approximately 10 % step in reflux flow, product flows are presented in Figure B.21.

Experiment 5 to 7: Holdup not controlled

These second series of experiments is performed to determine the hydraulic lag throughout the distillation column. The experiments are performed without level control of both reboiler and accumulator. The steady state data for experiments 5 to 7 are presented in Table B.3 and in Table B.3 and B.4. The steady state data presented are the average of at least 50 measurements prior and after the step change. The liquid and vapor traffic in the system is increased compared to experiments 1 to 4 (see Table B.1).

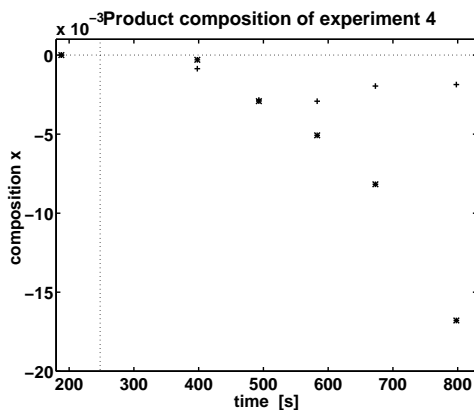


Figure B.18: Experiment 4, compositions of product samples, distillate * composition, + bottom composition

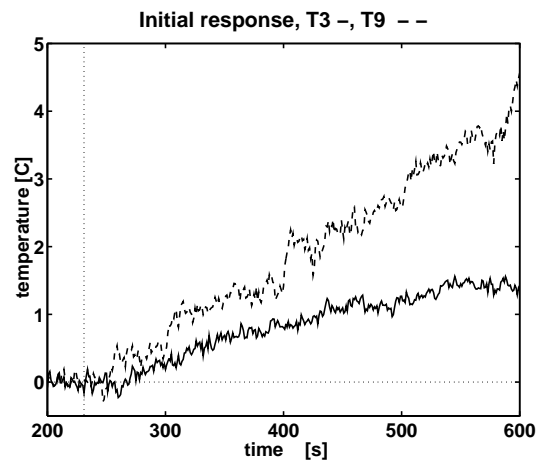


Figure B.19: Experiment 4, response of temperature on tray 9 to a change in reflux flow at $t = 248$ seconds from to 418.5 ml/min to 382.8 ml/min

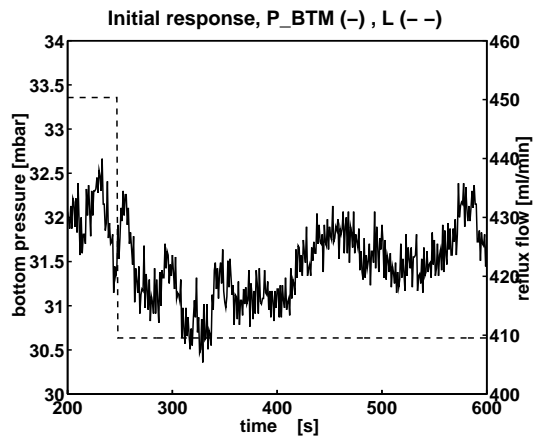


Figure B.20: Experiment 4, response of the bottom pressure to a change in reflux flow

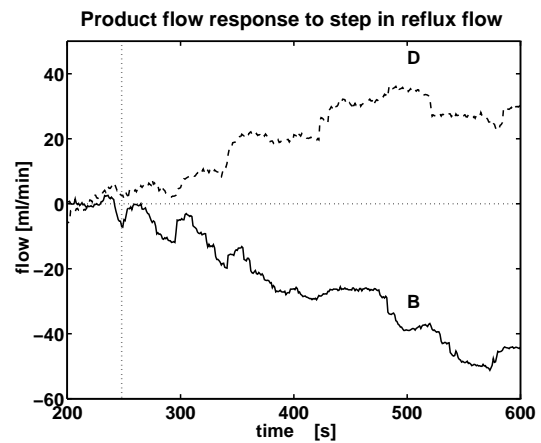


Figure B.21: Experiment 4, response of the product flows to a change in reboiler effect at $t = 248$ s

Table B.3: Experimental data of experiment 5 to 7

variable	dimension	Experiment 5		Experiment 6		Experiment 7	
		t_0	t_f	t_0	t_f	t_0	t_f
T_{reb}	$^{\circ}C$	118.6045	118.6336	118.7738	118.9800	119.8710	119.7464
T_1	$^{\circ}C$	117.1996	116.7045	117.4376	117.6355	117.8319	116.0682
T_2	$^{\circ}C$	116.6139	114.8309	117.2086	117.5027	116.8226	114.5664
T_3	$^{\circ}C$	114.9569	109.9427	116.7529	117.3282	113.4145	107.8200
T_4	$^{\circ}C$	110.7343	99.7791	115.6357	117.0800	107.6316	99.2418
T_5	$^{\circ}C$	98.8170	88.0182	110.3352	115.6045	99.2587	90.6255
T_6	$^{\circ}C$	90.0472	82.4473	103.3600	112.2018	91.8794	84.7627
T_7	$^{\circ}C$	83.6216	80.8209	93.7076	106.9482	86.0981	82.5382
T_8	$^{\circ}C$	81.0948	80.1255	84.6481	94.7482	82.3429	80.9600
T_9	$^{\circ}C$	79.7664	79.3145	81.4471	87.0918	80.7565	79.8818
T_{10}	$^{\circ}C$	79.1680	78.9800	79.7395	81.8515	79.6048	79.2909
T_{11}	$^{\circ}C$	78.8752	78.7882	78.9243	79.4509	78.9697	78.8791
T_L	$^{\circ}C$	78.6879	78.6336	78.5152	78.5600	76.9261	77.0336
T_F	$^{\circ}C$	91.0021	91.0531	91.7870	91.0892	90.9902	91.0254
M_B	l	3.8131	4.0573	3.33714	2.9882	4.0271	4.1618
M_D	l	1.6972	1.3200	1.8343	2.0918	1.9832	1.8109
L	ml/min	468.7094	557.2380	470.4976	470.4976	797.9228	883.8665
Q_B	kJ/s	5.7900	5.7900	6.4500	8.0250	11.2500	11.2500
F	ml/min	350	350	350	350	350	350
z_F	mol/mol	0.56		0.45		0.51	
P_{btm}	$mbar$	35.3		54.6		83.5	

For experiments 5 to 7 the position of the product valve is fixed by setting the distillate and bottom product flow controllers to manual. More extensive step changes are performed and the temperature responses of tray 3 and 9 as well as the level responses of reboiler and accumulator are presented. Pressure measurement are not recorded online since the sensor

was out of order, the level difference between reboiler and an open tube (ventilated to the atmosphere) connected to the bottom of the column is used to determine the pressure drop at the initial steady state.

In Table B.4 the main operational data, time delays, hydraulic lag and time constants are summarized. The entries in Table B.4 marked with (*) could not be determined from the experiments. The definition of the hydraulic lag in the distillation column is chosen such that the manipulator dynamics can be neglected, namely to the time difference from the initial deviation of the accumulator level until the reboiler level deviates. We assume the delay of the level sensors as negligible.

Table B.4: Experimental conditions of experiments 5 to 7, steps in reboiler heat input Q_b and reflux flow L and the experimental determined time constants as well as delays

		Exp. 5	Exp. 6	Exp. 7
F	ml/min	350	350	350
z_F	mol/mol	0.56	0.45	0.51
T_F	$^{\circ}\text{C}$	91.0	91.0	90.0
T_L	$^{\circ}\text{C}$	78.6	78.5	79.0
step at	s	75	86	161
step in		L	Q_b	L
L_0	ml/min	468.8	470.0	797.0
L_{∞}	ml/min	557.2	470.0	884.0
ΔL	ml/min	+ 88.4	0.0	+ 87.0
Q_{B0}	kJ/s	5.79	6.45	11.25
$Q_{B\infty}$	kJ/s	5.79	8.03	11.25
ΔQ_B	kJ/s	0.0	+ 1.58	0.0
K_{T3}		- 0.27 ⁺ $\frac{^{\circ}\text{C}\cdot\text{s}}{\text{ml}}$	+ 0.39 $\frac{^{\circ}\text{C}\cdot\text{s}}{\text{kJ}}$	- 0.29 ⁺ $\frac{^{\circ}\text{C}\cdot\text{s}}{\text{ml}}$
θ_{T3}	s	28.3	5.5	15.4
τ_{T3}	s	*	17.7	*
$\frac{d\Delta T_3}{dt}$	$10^{-2}\frac{^{\circ}\text{C}}{\text{s}}$	- 2.23	+ 2.15	- 2.42
K_{T9}		- 0.35 $\frac{^{\circ}\text{C}\cdot\text{s}}{\text{ml}}$	+ 0.18 ⁺ $\frac{^{\circ}\text{C}\cdot\text{s}}{\text{kJ}}$	- 0.58 $\frac{^{\circ}\text{C}\cdot\text{s}}{\text{ml}}$
$\frac{d\Delta T_9}{dt}$	$10^{-2}\frac{^{\circ}\text{C}}{\text{s}}$	- 0.63	+ 4.23	- 0.84
θ_{T9}	s	15.0	8.0	11.1
τ_{T9}	s	28.4	36.8 ⁺	61.6
$\Delta\theta_{\theta_{T3}/\theta_{T9}}$	s	13.3	3.0	4.3
θ_{M_D}	s	5.3	33.9	6.5
θ_{M_B}	s	23.1	3.9	22.3
$\Delta\theta_{M_B/M_D}$	s	17.8	30.0	15.8
τ_l	s	1.62	*	1.44

* not possible to determine from data set; + value rather inaccurate

$$\text{definition of } K = \frac{T|_{t=\infty} - T|_{t=0}}{Q_b|_{t=\infty} - Q_b|_{t=0}}$$

Experiment 5 and 7, increase in reflux

Inspecting the responses of experiment 5 and 7 (Figure B.22 and B.24), indicate that the temperature in the stripper section of the column responds like an integrator with some time delay to the step in reflux flow. From Tables B.3 and B.4 we see that the rather exten-

sive changes in the reflux flow results in a minor temperature change (first order plus dead time response with low gain) in the rectification section, T(9), and an extensive change in the stripper section, (T3) (almost capacitive response). The response of the (uncontrolled) reboiler level to a step increase in reflux flow is shown in Figures B.23 and B.25 for experiment 5 and 7, respectively. The response of the reboiler level in relation to the accumulator level is delayed by approximately 18 s (average of Exp.5 and 7). This is the time it takes the step change in reflux flow to propagate through the column. Apply the above presented definition we compute a liquid hydraulic time constant of approximately $\tau_l = 1.6s$.

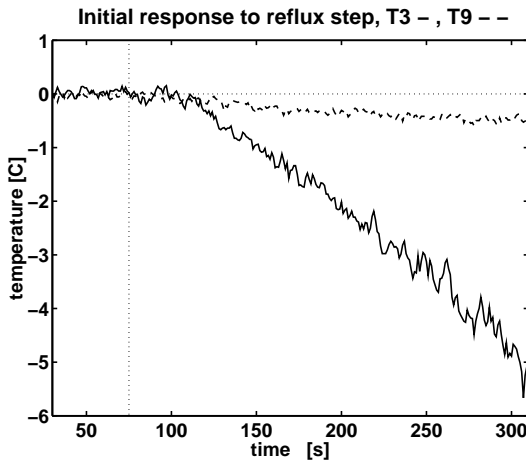


Figure B.22: Experiment 5, response of temperature on tray 9 (- -), tray 3 (-) to a step in reflux flow from 468.8 ml/min to 557.2 ml/min at time = 75 s

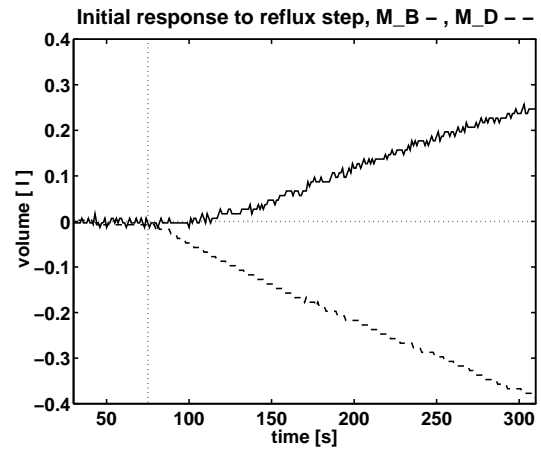


Figure B.23: Experiment 5, response of reboiler level to a step in reflux flow from 468.8 ml/min to 557.2 ml/min at time = 75 s

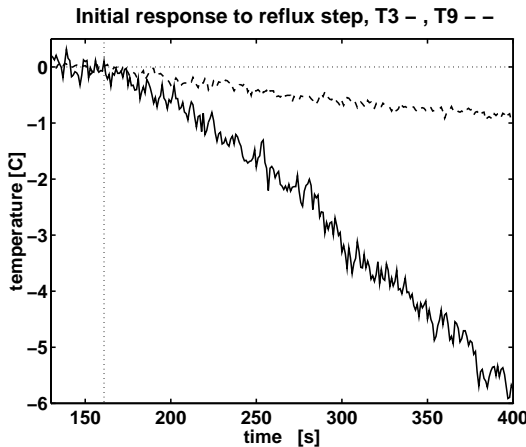


Figure B.24: Experiment 7, response of temperature on tray 9 (- -), tray 3 (-) to a step in reflux flow from 797 ml/min to 884 ml/min at time $t = 161$

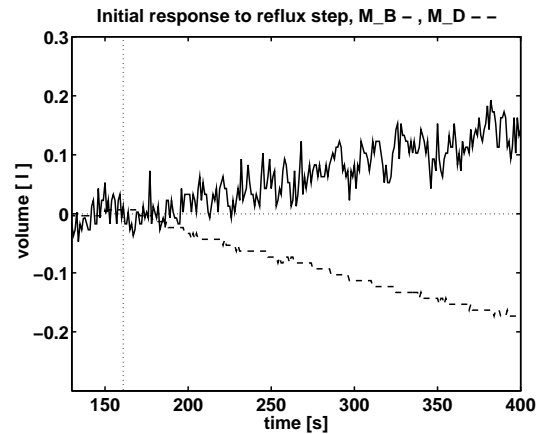


Figure B.25: Experiment 7, response of reboiler (-) and accumulator (- -) level to a step in reflux flow from 797 ml/min to 884 ml/min at time $t = 161$

Experiment 6, increase in boilup

Figure B.26 shows the temperature response of stages 3 and 9 for an increase in reboiler heat supply. The rather extensive step change in reboiler duty results in first a order response on tray 3, while the temperature on tray 9 does not level out. The change in holdups is shown in Figure B.27. For approximately 34 s after the step change is the accumulator level constant while the reboiler holdup decreases by 160 ml, this amount of liquid is stored inside the column. The increased pressure drop increases the downcomer backup, such that liquid is stored. At $t \simeq 120\text{ s}$ the velocity of holdup change is equal in reboiler and accumulator with a value of approximately 2.0 ml/s.

The initial change in the gradient of the reboiler level (see Figure B.27, approximately 10 s after the step change) indicates that liquid is pushed from the trays in the stripper section. At $t \simeq 112\text{ s}$ the gradient is changed a second time, indicating that liquid is pushed from the trays of the rectifying section. This wave reaches the reboiler (counting from the time the reboiler level starts to change) approximately 30 s after the initial decrease in reboiler level.

The total lag between increase in reboiler heat duty (electrically heated) and increase in accumulator level consists of the dynamic of the heating element, vapor transport through the column, dynamic of condensation in the condenser and a transport delay due to the piping connecting condenser and accumulator.

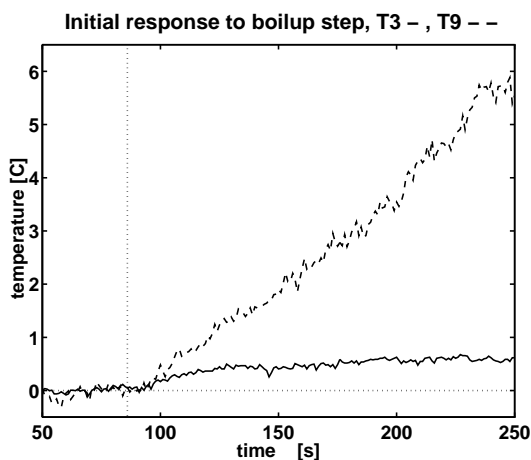


Figure B.26: Experiment 6 , response of temperature on tray 9 (- -) and tray 3 (-) to a step in reboiler heat input Q_b from 6.45 kJ/s to 8.03 kJ/s at time $t = 86\text{ s}$

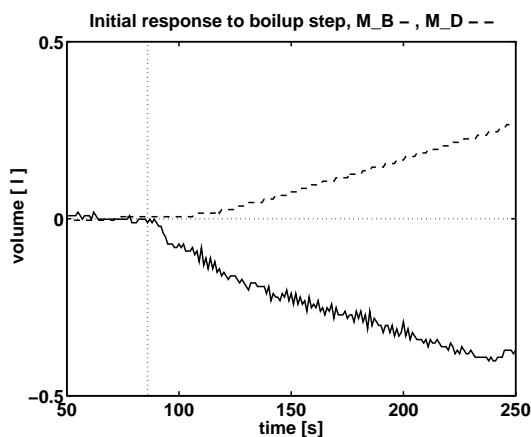


Figure B.27: Experiment 6 , response of reboiler (-) and condenser level (- -) to a step in reboiler heat input Q_b from 6.45 kJ/s to 8.03 kJ/s at time $t = 86\text{ s}$

B.1.5 Estimation of the tray holdup from initial temperature response

The estimation of the liquid holdup on a stage in a distillation column can be performed by measuring the initial temperature response to a step change in reflux ΔL or vapor flow ΔV .

Assumptions

The following assumption are necessary to develop a simple model of a staged distillation

column.

- OP1 thermal and mechanical equilibrium
- OP2 vapor holdup is negligible
- OP3 constant molar liquid holdup M
- OP4 equimolar flows (simplified/neglected energy balance)
- OP5 the local slope of the vapor-liquid equilibrium curve is $y_i = K_i \cdot x_i$. Since the here investigated system is fairly ideal we assume constant relative volatility (see Figure B.28):

$$\alpha_{12} = \frac{y_i (1 - x_i)}{x_i (1 - y_i)} \quad (\text{B.12})$$

such that the vapor composition is expressed by:

$$y_i = \frac{\alpha \cdot x_i}{x_i \cdot (\alpha - 1) - 1} \quad (\text{B.13})$$

For a small composition interval we define a local VLE, by:

$$y_i = K_{VLE,i} \cdot x_i \quad (\text{B.14})$$

- OP6 A third order function relating the stage temperature to liquid composition can be chosen to achieve a suitable fit of the experimental data.

$$T_i = 117.5 - 78.6 \cdot x_i + 65.3 \cdot x_i^2 - 25.7 \cdot x_i^3 \quad (\text{B.15})$$

For smaller composition intervals a piecewise linear relation between liquid composition and temperature, $x_i \leftrightarrow T_i$ can be assumed (see Figure B.29).

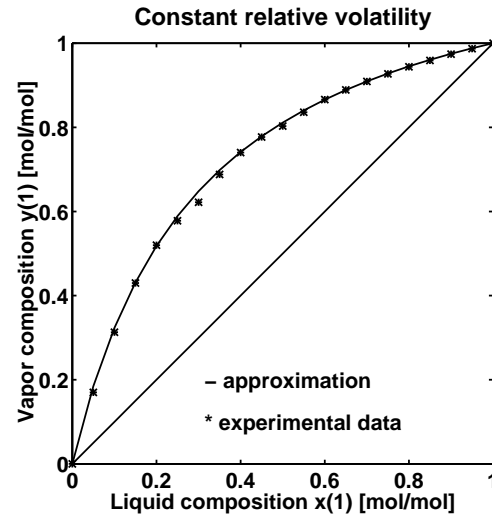


Figure B.28: Vapor-liquid equilibrium at 1 bar, assuming constant relative volatility with $\alpha = 4.3$, (Gmehling and Onken, 1977)

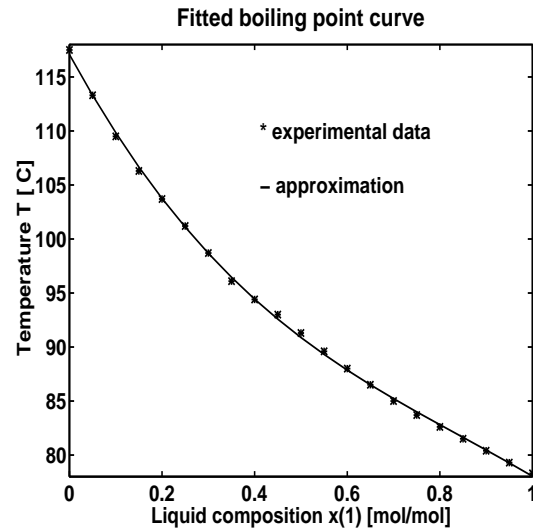


Figure B.29: xT -diagram for ethanol and butanol at $p = 1 \text{ bar}$ (Gmehling and Onken, 1977)

$$T_i = K_{T,i} \cdot x_i \quad (\text{B.16})$$

Further, the local slope of the composition/temperature relation is assumed to be identical for stages next to each other.

OP7 neglect heat losses

Stage model

The model of a stage consists of a material balance and a description of the vapor liquid equilibrium. From a mass balance over a stage it will be possible to estimate the liquid tray holdup under consideration of OP2.

$$dM_i/dt = L_{i-1} - L_i + V_{i+1} - V_i \quad (\text{B.17})$$

The material balance over a stage, consider OP3 and OP4, becomes

$$M dx_i/dt = L_i \cdot (x_{i-1} - x_i) + V_i \cdot (y_{i+1} - y_i) \quad (\text{B.18})$$

For a step change in L_i and V_i the internal flows are $L_i = L_i^o + \Delta L$ and $V_i = V_i^o + \Delta V$. Subtract the steady state solution from Eq. B.18 and consider the time immediately after the step change when the tray composition still is unchanged. This yields the following relationship for the initial slope as a function of ΔL and ΔV :

$$M \cdot \left(\frac{d\Delta x_i}{dt} \right)_{init} = \Delta L_i \cdot (x_{i-1}^o - x_i^o) + \Delta V_i (y_{i+1}^o - y_i^o) \quad (\text{B.19})$$

Apply assumptions OP5 and OP6 and rearrange Eq. B.19

$$\frac{M_i}{K_{T,i}} \cdot \left(\frac{d\Delta T_i}{dt} \right)_{init} = \Delta L_i \cdot \frac{1}{K_{T,i}} \cdot (T_{i-1}^o - T_i^o) + \dots \quad (\text{B.20})$$

$$\Delta V_i \frac{K_{V,i}}{K_{T,i}} \cdot (T_{i+1}^o - T_i^o)$$

From Eq.(B.21) it is possible to estimate the molar holdup M_i on a stage from observing the initial slope of the tray temperature to changes in reflux or boilup. Compute the stage holdup from the linear expression Eq. B.21 requires knowledge of the local correlation of $y_i = f(x_i)$ and $T_i = f(x_i)$ for each stage investigated, such that an *e.g.* table lookup for the vapor-liquid equilibrium is necessary. Determination of K can be performed from:

- from the initial temperature measurements on the tray we determine the liquid composition (see Eq. B.16)
- from the liquid composition we compute the vapor composition (see Eq. B.13)
- finally K is determined from Eq. B.14

B.1.6 Results tray holdup estimation

Based on the above presented estimation procedure the tray holdup of trays 3 and 9 in the distillation column is computed, the results are summarized in Table B.5

Table B.5: Holdup on trays estimated from temperature responses. Experimental conditions of experiments 1 to 7 converted to molar basis. (see Tables B.2 and B.4)

	Exp. 1	Exp. 2	Exp. 3	Exp. 4	Exp. 5	Exp. 6	Exp. 7
F	5.546	5.652	5.706	5.599	7.988	7.588	7.801
L_0	6.620	6.678	8.7151	11.135	12.466	12.498	21.193
ΔL	0.0	0.0	$+1.416$	-0.949	$+2.351$	0.0	$+2.314$
x_D	0.9844	0.9988	0.9826	0.9909	$0.99^{(1)}$	$0.99^{(1)}$	$0.99^{(1)}$
Q_{h0}	3.75	3.6	4.5	5.4	5.79	6.45	8.03
ΔQ	$+0.45$	-0.45	0.0	0.0	0.0	$+1.58$	0.0
x_B	0.0027	0.0225	0.0031	0.0055	$0.01^{(1)}$	$0.01^{(1)}$	$0.01^{(1)}$
Δh_{vap}	4.218	4.204	4.217	4.216	4.213	4.213	4.213
V_0	8.892	8.563	10.671	12.809	13.745	15.312	26.706
ΔV	-1.067	$+1.070$	0.0	0.0	0.0	$+3.751$	0.0
see Figure	B.5	B.9	B.15	B.19	B.22	B.26	B.24
T_2	116.6627	111.0827	115.7771	115.7738	116.6139	117.2086	116.8226
T_3	115.1178	104.5306	113.6465	113.3564	114.9569	116.7529	113.4145
T_4	112.0872	96.7197	109.7096	108.8267	110.7343	115.6357	107.6316
x_3	0.0363	0.2133	0.0592	0.0638	0.0387	0.0113	0.0629
y_3	0.1392	0.5383	0.2130	0.2266	0.1477	0.0466	0.2239
K_3	3.8405	2.5237	3.5971	3.5522	3.8126	4.1461	3.5611
$d\Delta T_3/dt$	-1.48	$+4.51$	-0.87	$+1.09$	-2.23	$+2.15$	-2.42
M_3	4.4183	4.1409	6.3872	3.9473	4.4612	3.3726	5.5284
T_8	91.5876	80.4206	89.9089	86.0642	81.0948	84.6481	82.3429
T_9	85.9345	79.4533	84.6381	82.0784	79.766	81.4471	80.7565
T_{10}	81.8198	79.1158	80.9016	79.8665	79.1680	79.7395	81.8515
x_9	0.6471	0.9282	0.6908	0.7906	0.9084	0.8191	0.8531
y_9	0.8874	0.9823	0.9057	0.9420	0.9771	0.9512	0.9615
K_9	1.3715	1.0583	1.3111	1.1915	1.0756	1.1612	1.1271
$d\Delta T_9/dt$	-1.48	$^{(2)}$	-1.43	$+0.97^{(3)}$	$-0.63^{(3)}$	$+4.23$	$+0.84$
M_9	5.4472	$^{(2)}$	3.7008	2.1659	2.2492	3.1852	3.0158

Remark:

⁽¹⁾ These product compositions are chosen to be at the nominal operation point of the column. The compositions of the product flows was not analyzed. The uncertain composition will give some uncertainty in the molar liquid and vapor flows in the column.

⁽²⁾ Initial temperature gradient could not be determined from the recorded data.

⁽³⁾ Initial temperature gradients were rather difficult to measure, due to extensive noise on the measurements, an error will be transferred to the holdup estimation.

Remarks on the estimation procedure

The method of estimating the stage holdup from the initial temperature response relies on the quality of the temperature measurement. The gradient on the initial response, $d T_i / dt$, is strongly influenced by the noise level on the signal, further the initial gradient is determined by graphical means from the recorded response.

During the estimation a number of assumptions were made:

- Neglecting the vapor holdup [OP2] in the column will not influence the estimation, since the vapor holdup in the here considered column will be considerably lower than 5 % of the liquid holdup.
- Assumption OP3 and OP4 have to be seen with respect to the experimental procedure. We assume that the liquid and vapor flow entering the column is stepped from its initial value to its final value. Because of the available equipment, an extensive change in a manipulated variable will result in a ramp of the manipulated variable to the control signal.

Further, we assume that the introduced step is transferred through the entire column as a step change. The introduced step will enter the first stage which is (composition dynamics considered) a mixing tank, thus some composition dynamics will be introduced. Since all the stages have an identical design, an n^{th} -order composition response will be seen on the stage on the opposite side of the column compared where the step is introduced. The hydraulic time constant of the column is much shorter than the composition dynamics, thus we assume that the introduced step change is travelling as a step change through the column.

- The constant molar holdup assumption [OP3] on the stage will be reasonable correct for liquid flow changes. An increased liquid flow will increase the height of liquid above weir which will lead to a marginal change of the tray holdup. The hydraulic time constant of a stage is measured to be in the range of 1.5 seconds (see Table B.2 and B.4), considerably shorter than the composition time constant, thus the liquid hydraulic is neglected and constant molar holdup in the column is assumed.

The flows entering and leaving the reboiler are sketched in Figure B.30. Rademaker (1975) assumes that the temporary liquid flow change is caused by liquid which is pushed from the trays. Initially the internal reflux flow is reduced (dashed line in Figure B.30, marked with L_B) until the downcomer backup and the pressure drop between stages balance again, then the liquid flow increases. Initially the reboiler holdup should decrease (due to more vapor leaving the reboiler and less liquid enters), then increases when the by vapor bubbles replaced liquid from the stages reaches the reboiler. The holdup on the sieve tray will be reduced, since the higher vapor flow reduces the froth density on the stages. The first increase in L_B is caused by liquid pushed from the sieve trays of the stripper section, while the second increase corresponds to liquid replaced in the rectifier section.

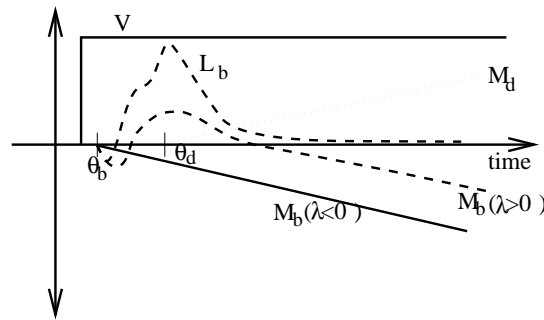


Figure B.30: Flow entering and leaving the reboiler for an increase in vapor flow, assuming that liquid is pushed from the stages

- The assumptions made concerning the vapor-liquid equilibrium (recall OP5) is fairly correct for the system ethanol-butanol, such that $K = y_i/x_i$ can be interfered from the liquid composition. The slope of the equilibrium curve for trays next to each other is shown in Table B.6 for experiments 1 and 3. The ratio of vapor to liquid composition, $K_i = y_i/x_i$, is changing by $\pm 10\%$ from stages 3 and 9 to the adjacent stages, respectively.

Table B.6: Slope of equilibrium curve, estimated from temperature profile

		Tray 2	Tray 3	Tray 4
Exp. 1	K	4.2264	3.9670	3.5204
Exp. 3	K	4.0747	3.7408	3.2171
		Tray 8	Tray 9	Tray 10
Exp. 1	K	1.6668	1.3366	1.1378
Exp. 3	K	1.5632	1.2693	1.1001

Nevertheless, even if there are some shortcomings of the proposed method, the estimation of the liquid holdup on the stages is possible and give a rather good indication of the liquid distribution between rectifying and stripping section.

B.2 Experiments to obtain the hydraulic time constant

B.2.1 Results

The liquid and vapor hydraulic is investigated by recording step responses of the manipulated variables reboiler heat input and volumetric reflux flow. The influence of variation of liquid density on the stages and heat of vaporization in the reboiler was minimized by distilling a mixture of $z_F = 0.95$ ethanol-butanol. The position of the product valve is fixed by setting the distillate and bottom product flow controllers to manual. Rather extensive step changes are performed to visualize the response of reboiler and accumulator level.

The column is operated open-loop such that the reflux pump position and the reboiler heat input are set manually. The conditions for experiments 8 to 10, further the time when the manipulated variable is changed and the measured delays are presented in Table B.7. The performed experiments include the increase and decrease of the manipulated variables reboiler heat input and volumetric reflux.

Table B.7: Experimental conditions of experiments 8 to 10, steps in reboiler heat input Q_b and reflux flow L and the experimental determined delays

		Exp. 8	Exp. 9	Exp. 10
F	ml/min	250	250	350
z_F	mol/mol	0.95	0.95	0.95
T_F	$^{\circ}C$	77.0	77.0	77.0
T_L	$^{\circ}C$	78.0	78.5	78.0
step in		L	L	Q_B
step at	s	284	645	1489
reset at	s	446	860	1550
L_0	ml/min	481.2	472.3	472.3
ΔL	ml/min	+ 89.5	-89.4	0
Q_{B_0}	kJ/s	6.0	6.0	6.0
ΔQ_b	kJ/s	0	0	+1.5
initial step				
θ_{M_D}	s	5.0	4.0	20.3
θ_{M_B}	s	24.9	34.1	4.4
$\Delta\theta_l$	s	19.9	30.1	15.9
τ_l	s	1.81	2.74	*
return step				
θ_{M_D}	s	5.4	3.0	25.3
θ_{M_B}	s	51.0	49.6	4.0
$\Delta\theta$	s	45.6	46.6	21.3
τ_l	s	4.15	4.24	*

* Not possible to determine

$$\tau_l = \Delta\theta_l / N_t \text{ with } N_t \text{ as the number of stages}$$

The magnitude of the reflux steps is identical for experiment 8 and 9 which were performed from approximately the same operation point, but in opposite directions. In Figures B.31 and B.32 we present the responses of the reboiler and accumulator level to changes in reflux flow. (Note that reflux and boilup are scaled to fit into Figure B.31 to B.33)

The delay of the accumulator level to the change in the control signal to the reflux pump is plotted in e.g. Figure B.31. The measured time delays, presented in Table B.7 differ considerably for experiments 8 and 9 for the initial reflux flow change. The delay between control signal change to the reflux pump and the response of the accumulator level is in the order of 5 seconds for an increase or decrease of the signal. These five seconds are caused by processing in the control and hardware unit (processing time of the computer, the dynamics of the reflux pump, a reciprocating metering pump, and the level sensor, dp-cell). The step signal from the control system to the reflux pump is transformed to a ramp with a gradient of 17 ml/s change, such that the step change of approximately 90 ml is completed after 6 s.

The rather extensive delay from the initial change of reflux until the reboiler level responds is caused by the combined effects of actuator dynamics and the liquid hydraulics of the sieve trays. From experiment 8 we estimate the average hydraulic time constant $\tau_l = \Delta\theta_l/N_t$ to be in the range of $\tau_l \simeq 1.8s$ for the increase in reflux flow, we estimated the actual change in accumulator level until the reboiler level changes, denoted $\Delta\theta$.

For the decrease in reflux (experiment 9) from a steady state operation point we determine a liquid delay over the column of $\Delta\theta_l = 30s$ which corresponds to a hydraulic time constant of $\tau_l \simeq 2.7s$. From Figure B.31, B.32 and Table B.7 we see that the delay for the reset of the reflux flow is between 15 and 25 seconds larger than for the increase. This error is caused by liquid which is still traveling downwards through the column after the reflux is reset. Thus we, conjecture that the most reliable method to estimate the hydraulic time constant by means of experiment is the increase in reflux flow, at constant reboiler heat supply.

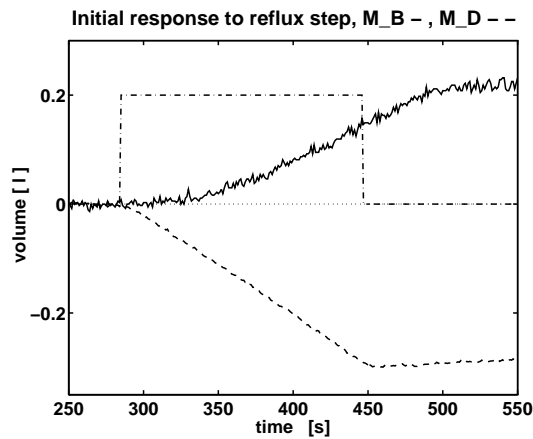


Figure B.31: Experiment 8, response of reboiler (-) and accumulator (- -) level to an increase in reflux flow (-.) from 481 ml/min to 570 ml/min at time $t = 284$ s

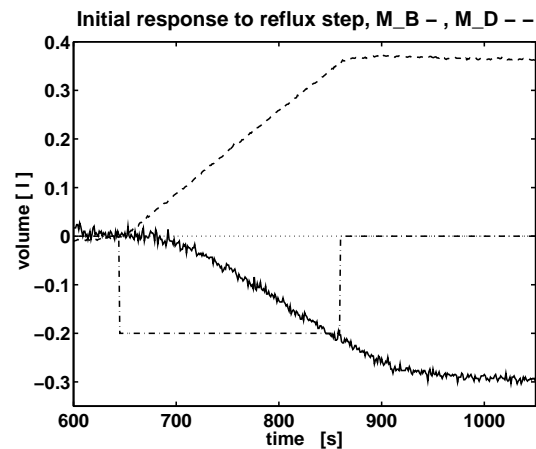


Figure B.32: Experiment 9, response of reboiler level to an decrease in reflux flow from 472 ml/min to 383 ml/min at time $t = 645$ s

Experiment (Exp. 10) was performed to investigate the action of an increase in reboiler heat input on the bottom level and accumulator level (see Figure B.33). The reboiler heat input is stepped from $Q_b = 6kJ/s$ to $Q_b = 7.5kJ/s$ at time $t = 1489$ s. The time elapsing from the increase of heat input until the reboiler level is changing is approximately 4.5 s. This delay is caused by the dynamics of the heating element and some delay due to transmission of the data inside the control system. The lag between the decrease in reboiler level until the accumulator level is changing is approximately 15.9 s for an increase in Q_B and 21.3 s for the case where the reboiler heat input is returned to its initial value. The increase of the heat input by 25 % does not initiate a temporary increase in liquid flow through the column due to pushing liquid from the sieve trays.

The level of the accumulator increases (dashed line in Figure B.33) even after the reboiler heat supply is decreased to its initial value. This is due to vapor entering the condenser after the reboiler effect is reset and the lag introduced through the piping between condenser and accumulator. The condenser is placed on top of the column while the accumulator is placed

on the floor near the reflux pump. The measured delays for increase and decrease in reboiler effect on the levels of accumulator and reboiler are rather similar. The delay for the vapor transport from reboiler through column, condenser and piping to accumulator is measured to be in the order of 17 s. Nevertheless, we do not have any possibility to distinguish the contribution of each single delay to the measured total delay.

Reset the reboiler duty to the initial value at $t = 1554$ s results in an increase of the reboiler holdup, which is caused by liquid returned from the column (see Figure B.33, at $t \geq 1550$ s). The increase of the liquid holdup is delayed by 5 s and liquid is dumped into the reboiler for approximately 22 s. That is, it takes 22 seconds until the excess liquid stored on tray 11 to reach the reboiler. This corresponds to an average hydraulic time constant for liquid of approximately 2 s for each stage. This time constant corresponds well with the hydraulic time constant estimated from Exp. 8 and 9 where the reflux flow is reduced or reset to its initial value.

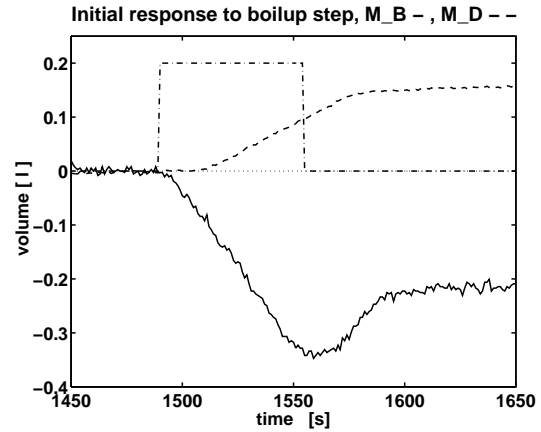


Figure B.33: Experiment 10, response of reboiler (-) and accumulator (- -) level to an increase in reboiler heat input from 6 kJ/s to 7.5 kJ/s at time $t = 1489$ s

The reduced heat input reduces the vapor flow through the column, which in turn decrease the differential pressure drop. The reduced differential pressure drop over a stage reduces the amount of liquid stored in the column. An opposing effect caused by the reduced vapor flow is an increase in froth density on the tray such that the liquid holdup increases. From this type of experiment we can not estimate exactly where the liquid is coming from. Some of the liquid has to be drained from the downcomer holdup.

B.2.2 Discussion

We find a significant difference between the experiments where we increase the reflux flow from a stationary operation point to experiments where *e.g.* the reflux flow is reset to its original value. This difference is caused by liquid flowing downwards. The experiments to investigate the column hydraulic have to be performed from steady state condition (composition and internal/external flows) with an increase in reflux. The experiments where the reflux is decreased give only limited information to determine the hydraulic time constant. The lag for an increase in reflux is about half the time measured for a decrease.

B.3 Experimental determination of the residence time

The residence time of a column is approximated by $\tau_{c,col} \simeq \theta_c$, this approximation is valid for long column where we can assume a plug flow like propagation of a heavy tracer through the column. We define θ_c to be the most extensive deviation in temperature on stage 1 with reference to the injection of tracer. Approximate the residence time $\tau_{c,col}$ by θ_c allows us to compute the volumetric liquid holdup of the column V_{Col} from $\theta_c \simeq \tau_{c,col} = V_{Col}/L$. Note we use the nominal reflux flow L to the column, since the injected tracer volume will increase the liquid flow through the column only temporarily.

The initial decrease in tray temperature is caused by liquid which is replaced on the stage above by the wave of liquid traveling through the column (see Figure B.36). This initial temperature reduction will correspond to the liquid hydraulic time constant. On most stages the reduction in temperature is rather limited, since the compositions on stages near to each other are similar. The hydraulic time constant τ_l can be estimated rather accurately from $\tau_l = \theta_{V_B}/N_t$ where θ_{V_B} denotes the time delay from tracer injection until the reboiler level increases and N_t is the number of trays. θ_{V_B} denotes the transport delay from the time of injection (initial temperature change on top stage) until the reboiler holdup V_B increases. The residence time of the accumulator and reboiler are computed from $\tau_c = V_i/L$. The transport delay through the pipe connecting accumulator, reflux pump and the upper most tray as well as column bottom to reboiler is $\theta_{L,pipe} = l_{pipe} \cdot A_{pipe}/L$.

B.3.1 Experimental procedure of tracer injection experiments

The residence time is investigated by operating a distillation column at total reflux. The mixture initially fed to the column was ethanol and butanol with a composition of approximately $z_F = 0.95$. The initial holdup of the accumulator and reboiler (after total reflux operation is established) is $V_D = 0.95 \text{ l}$, $M_D = 15.04 \text{ mol}$ and $V_B = 2.85 \text{ l}$, $M_B = 39.39 \text{ mol}$. The column is operated such that the reflux is adjusted to match the condensed vapor flow and keep the accumulator level constant. On tray 11 (the upper most tray) pure butanol with a temperature of 20°C is injected and the temperature responses on different trays to this pulse is recorded. The comparison of the recorded data is simplified by plotting the temperature deviations on the stages caused by the injected tracer.

B.3.2 Results

The conditions for experiments 11 to 13 are presented in Table B.8, further the times when the tracer reaches the trays are summarized. The time tags indicating when the tracer reaches the individual stages are determined graphically from the recorded data set. The time the tracer reaches a stage is defined as the time when the tray temperature *increases*. The initial temperature decrease is caused by liquid replaced on the stage above by the liquid wave traveling downwards.

The amount of tracer (butanol) injected is 200 ml (2.10 mol) in approximately 5 s. The butanol is injected onto the stage by means of a syringe through a fitting of the top pressure sensor. Since the injected liquid flows down the wall of the top stage, instantaneous mixing

of the liquid on the tray and the injected liquid will not occur. The energy needed to heat up the liquid is taken from the condensation of vapor, which can be seen by inspecting Figure B.35, where the accumulator level decreases due to condensation of vapor on stage 11. The experiments are performed with constant heat input to reboiler and volumetric reflux flow, such that the reduction in accumulator holdup has to be caused by the condensation of some vapor on stage 11.

Table B.8: Experimental conditions of experiments 11 to 13, measured time delays and computed transport delays

		Exp. 11	Exp. 12	Exp. 13
T_L	$^{\circ}C$	78.0	77.0	77.0
pulse at	s	75	94	255
L	ml/min	472	588	705
L	mol/s	0.125	0.155	0.186
Q_b^*	kJ/s	6.0	7.5	9.0
V^*	mol/s	0.145	0.181	0.218
Δp	mbar	29.82	32.96	47.08
$\theta_{T_{11}}$	s	0.0	0.0	0.0
$\theta_{T_{10}}$	s	10.0	10.0	11.0
θ_{T_9}	s	16.5	16.75	17.5
θ_{T_8}	s	21.5	20.0	22.5
θ_{T_7}	s	35.0	33.0	28.0
θ_{T_6}	s	57.0	49.0	41.0
θ_{T_5}	s	80.0	67.0	58.0
θ_{T_4}	s	108.0	86.0	76.0
θ_{T_3}	s	137.0	103.0	95.0
θ_{T_2}	s	164.0	127.0	112.0
θ_{T_1}	s	192.0	154.0	135.0
$\theta_{T_{Reb}}$	s	315.0	247.0	229.0
θ_{V_D}	s	9.7	10.8	13.3
θ_{V_B}	s	19.5	18.0	19.0
τ_l	s	1.77	1.66	1.73
τ_{c,V_D}	s	120.8	96.9	80.85
$\theta_{L,Dpipe}$	s	38.3	30.8	25.7
τ_{c,V_B}	s	362.3	290.8	242.5
$\theta_{L,Bpipe}$	s	27.95	22.44	18.71
θ_c	s	330.0	252.0	235.0
V_{Col}	l	2.59	2.47	2.76
V_{stage}	$10^{-3} l$	236	224	251

* estimated from control signal

Experiment 11

The distillation column is operated at total reflux, the initial temperature profile over the column shows a temperature of $80^{\circ}C$ on stage 1 decreasing to $78.5^{\circ}C$ on stage 11. Figure B.34 shows the propagation of butanol from the upper most stage 11 to the lowest stage of the column, stage 1, over a time interval of approximately 700 seconds after tracer injection (butanol).

Compare Figure B.34 and B.35 we see that the liquid hydraulics of the column is much faster than the composition dynamic, the reboiler level changes approximately 19.5 s after injection, while the temperature response on tray 1 reaches its maximum approximately 120 s later (Note, the different time scales). The constant reboiler level (at $t \geq 150$ s) indicates that all excess liquid (the injected amount) has reached the reboiler and the stage holdup are stable.

The “second” increase in stage temperature of stage 11 (in the interval $200 \text{ s} \leq t \leq 350 \text{ s}$) is due to butanol which was carried over to the condenser and is returned to the column. The combined residence time in the accumulator and the transport delay through the return pipe is approximately 140 s. This corresponds well to the time between injection of butanol and the second increase in temperature on tray 11 (see Figure B.36).

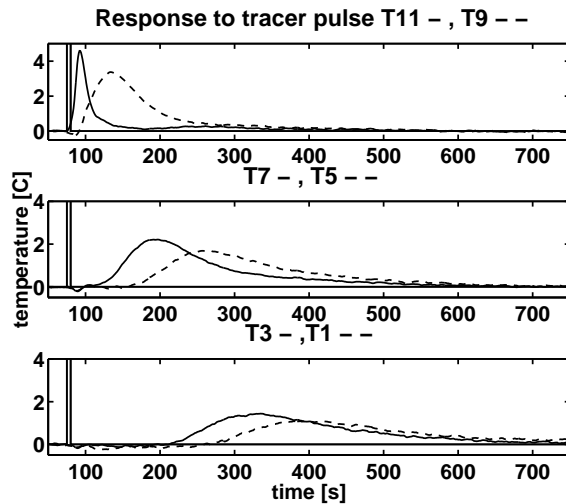


Figure B.34: Experiment 11, temperature deviations from average after injection of butanol on tray 11 at time $t = 75$ s

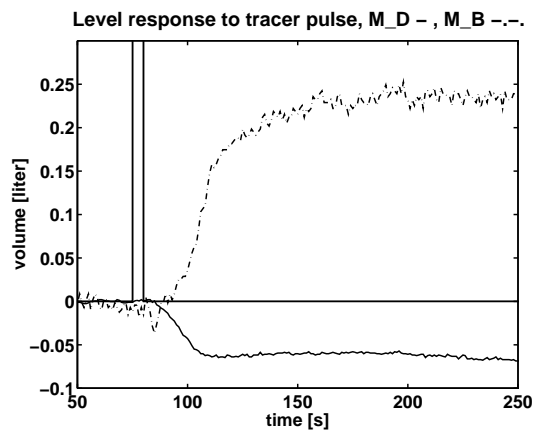


Figure B.35: Experiment 11, change in reboiler and accumulator holdup

The change in holdup of reboiler and accumulator is shown in Figure B.35. The reboiler level increases after approximately 19.5 s which give an estimated hydraulic time constant of $\tau_l = \theta_{V_B}/N_t \approx 1.77 \text{ s}$ per tray for this experiment (traveling over $N_T = 11$ trays and downcomer). The delay for the change in accumulator level is the order of 10 seconds which is due to the delay caused by the condenser dynamics and the transport delay through the piping between condenser and accumulator.

Figure B.36 is a magnified version of Figure B.34 and shows the injected pulse of a heavy tracer (butanol) and the temperature responses of stages 6 to 11. From Figure B.36 we see a reduction in temperature directly after the injection of butanol. The reduction in temperature is caused by liquid which is pushed from the stages above with a slightly lower temperature. The decrease in temperature is temporary and the initial decrease corresponds to the hydraulic lag of the stages. The temperature decrease on stage 1 is approximately 17 seconds after the injection of butanol, which corresponds to a hydraulic lag of 1.7 seconds. This corresponds well to the hydraulic lag determined from the reboiler level response to the tracer pulse. The reduction of temperature on stage 10 starts almost immediately after the injection

tion. This reduction is caused by the injection of 200 ml liquid (total tray volum in the order of 230 ml) and the condensation of vapor, such that weeping from tray 11 to 10 is expected. The initial and final bottom composition are estimated from measured temperatures in reboiler and tray 1. The initial reboiler temperature is $83.74^{\circ}C$, which corresponds to a liquid composition of $x_B = 0.76$, similar the composition on stage 1 is determined to $x_1 = 0.92$. The change in reboiler composition can be computed from an ethanol balance in the reboiler.

$$M_{Et,B} |_{t=300} = M_{Et,B} |_{t=75} + M_{inj} \quad (B.21)$$

The amount M_{inj} is estimated from the volume of butanol injected and the composition on stage 1. The molar holdup $M_{Et,B}$ can be computed from the volumetric holdup

$$M_{Et,B} = \frac{\rho \cdot V_B}{MW} \quad (B.22)$$

assume constant densities on stage 11 and reboiler to simplify the computation and rearranging the equation give

$$x_B |_{t=300} = \frac{\left(\frac{V_{B_{init}} \cdot x_{B_{init}}}{MW_{init}} \right) |_{t=75} + \left(\frac{V_{inj} \cdot x_1}{MW_1} \right) |_{t=75}}{\left(\frac{V_B}{MW_B} \right) |_{t=300}} \quad (B.23)$$

The initial reboiler volume is $V_B = 2.85 \text{ l}$. The entire injected volume of 200 ml (note we add liquid on stage 1) has reached the reboiler at $t = 300 \text{ s}$, such that the reboiler composition increases to $x_B |_{t=300} = 0.77$. Compare this to the composition estimated from the temperature measurement, the temperature of the reboiler at $t = 300 \text{ s}$ is $T_B |_{t=300} = 83.53^{\circ}C$ which corresponds to an estimated composition of $x_B = 0.769$. Note, we assume that ethanol rich liquid is replaced on tray 1, the butanol rich liquid has not reached tray 1 yet.

At $t = 700$ the temperature is constant in the reboiler, we can now compute the reboiler composition by exchanging 200 ml of ethanol with butanol such that the final reboiler composition is $x_B |_{t=700} = 0.744$. The composition estimated from the reboiler temperature is $x_B |_{t=700} = 0.742$. From the computed changes in reboiler composition we can see that the liquid which enters the reboiler in the time interval $90 \text{ s} \leq t \leq 150 \text{ s}$ is mainly liquid which is replaced on stage 1 (see Figure B.35).

The gradual increase in reboiler temperature from $t \geq 400 \text{ s}$ is due to the replacement of ethanol by butanol in the reboiler by the distillation process. Most of the heavier butanol has reached the reboiler at $t = 650 \text{ s}$, since from this time on the temperature on stage 1 is constant and has almost returned to its initial value. The temperature offset on the first stage

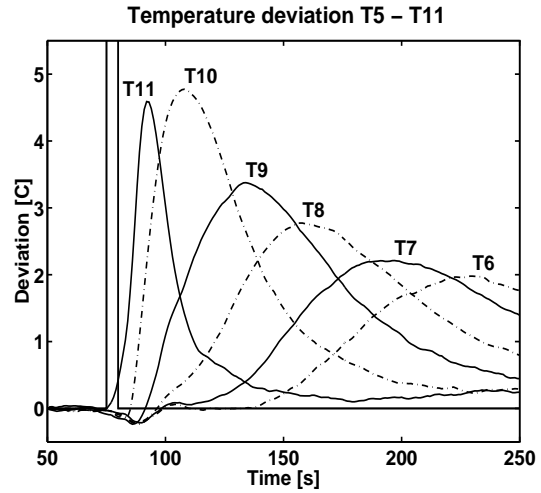


Figure B.36: Experiment 11, temperature deviation on stages 6 to 11

is due to the slightly changed composition of the reboiler, such that the vapor entering stage 1 has a higher butanol concentration than the initial.

Experiment 12 and 13 presented in Figures B.37 to B.40 are repetitions of Experiment 11 at different operation points. The temperature responses on the trays are similar in shape, nevertheless the peak of the responses is moved on the time axis due to slightly different tray holdups, internal vapor and liquid flows.

Experiment 12

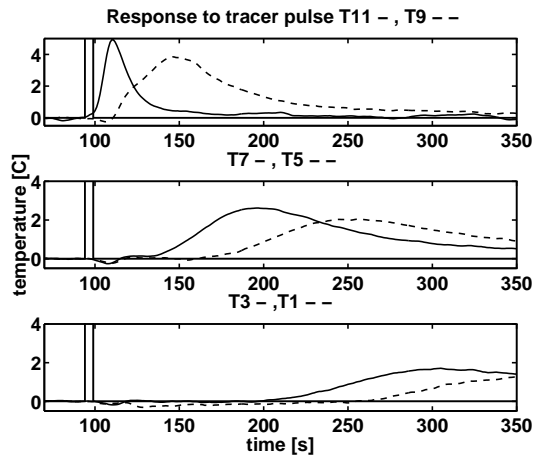


Figure B.37: Experiment 12, temperature deviations from average after injection of butanol on tray 11 at time $t = 94$ s

Experiment 13

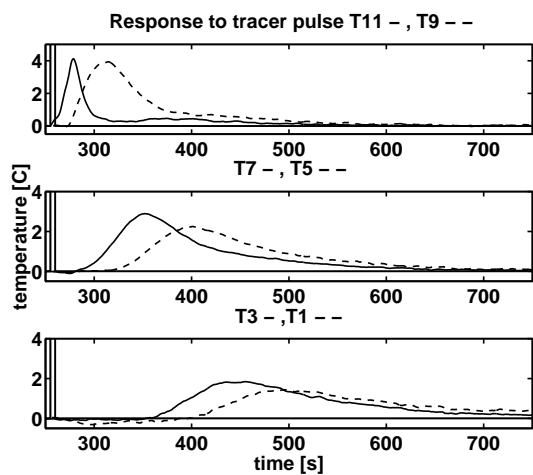


Figure B.39: Experiment 13, temperature deviations from average after injection of butanol on tray 11 at time $t = 255$ s

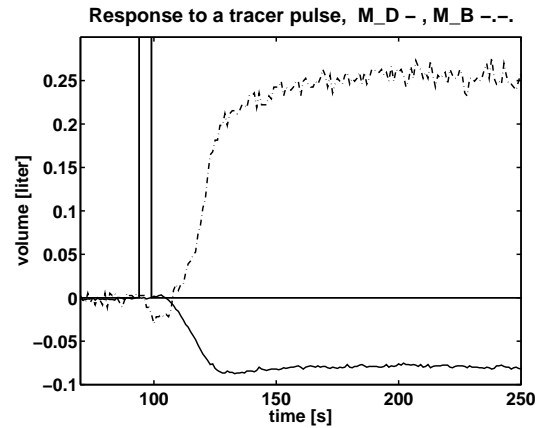


Figure B.38: Experiment 12, change in reboiler and accumulator holdup due to the injection of butanol on tray 11

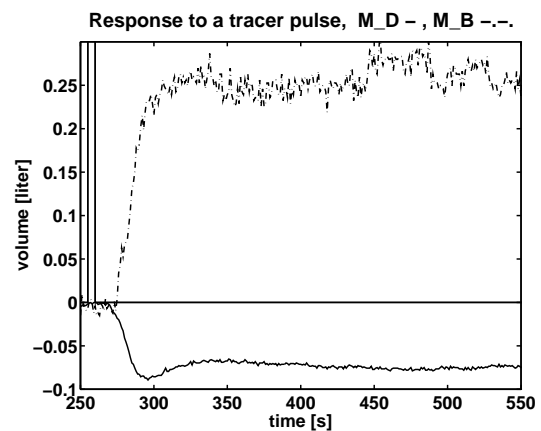


Figure B.40: Experiment 13, change in reboiler and accumulator holdup due to the injection of butanol on tray 11

B.3.3 Discussion of experimental procedure

The determination of the movement of the tracer wave will be influenced by the evaporation of some heavy tracer which will be “recycled” between stages such that we do not have a constant amount of tracer moving through the column. This recycling of tracer between stages will add to the effect of the mixing on the plate which transform the pulse to a normal distribution shaped wave. The assumption of a tracer plug flow is somewhat questionable as we move further down the column. This is further indicated by the increased tailing of the response as the distance to the point of injection increases. The gradual change from a pulse input to the upper most stage to a higher order liquid flow and composition response on the stages further down the column can be seen from Figure B.43. Further, recycling of some butanol through the condenser/accumulator unit can be seen from the second temperature increase on stage 11.

Different operation points were investigated and the manipulated variables (reboiler heat input and reflux flow) have a similar effect on the residence time, τ_c , on the stages. The increase in reflux flow reduce the residence time ($\tau_c = V_{stage}/L$) of each stage. The increase in vapor flow (equivalent to an increase in heat supply) will decrease the froth density Φ on the sieve tray, further the downcomer backup will increase due to an increase in differential pressure drop over the stage. Which one of these two effects is the dominating (decrease in froth density or increase in downcomer backup) is rather difficult to determine.

B.3.4 Modeling of tracer experiment

Modeling of tracer experiments can be performed by two different models, a series of mixing tank and a simple distillation model. The most simple method is to assume that the stages in a distillation column are modeled as continuous stirred tanks with a liquid flow entering and leaving. The liquid hydraulic is approximated by a first order response from liquid entering to the liquid leaving a stage. The second model will include the vapor flow in the column. This will introduce some recycling of heavy component from the stage below. The stage is modeled such that complete mixing in the liquid phase is assumed, the vapor phase is neglected. The vapor-liquid equilibrium is described by the assumption of constant relative volatility and constant molar flows are assumed. Further, the liquid holdup can be divided into tray and downcomer, we assume that only the liquid on the tray is in equilibrium with the vapor leaving the stage. The downcomer holdup is modeled as a mixing tank. In the fourth model we include a constant holdup mixing tank in front of the first tray. The remainder of the model is identical to the model with two holdups.

Experiment 11 is chosen as example to validate the different models against the experimental data. The simulations are performed in Matlab, with the operational parameters listed in Table B.9. Note that the total reflux operation and the assumption of constant molar flows result in slightly different molar flows in experiment and simulation. The simulation results presented are performed with the input values of Experiment 11, those are:

Feed flow	$F = 0 \text{ ml/min}$
Reboiler heat input	$Q_B = 6 \text{ kJ/s}$

External reflux	$L_T = 575 \text{ ml/min}$
Initial reflux composition	$x_{D,initial} = 0.9999$
relative volatility coefficient	$\alpha = 4.3$

Note: the reflux of the experimental system was subcooled, to balance the vapor flow and molar liquid flows of the simulation we adjusted the molar liquid flow (estimated from reboiler heat input, heat losses are neglected). The initial composition is $x = 0.95$ and the initial holdup is chosen to $M_B = 45 \text{ mol}$ and $M_D = 15 \text{ mol}$ for reboiler and accumulator, respectively, which corresponds to $M_B = 2.87 \text{ l}$ and $M_D = 0.947 \text{ l}$.

Table B.9: Initial operational parameters for simulation of Matlab models at $t = 75^- \text{ s}$

		CSTR	single holdup	divided holdup	two holdup, pre-mix
holdup on stages	mol	4	4	2+2	2+2
	liter	0.25	0.25	0.125+0.125	0.125+0.125
distillate composition	mol/mol	0.95	0.9999	0.9999	0.9999
bottom composition	mol/mol	0.95	0.9998	0.9673	0.9868
holdup accumulator	mol	0.0	15		
	liter	0.0	0.947		
holdup reboiler	mol	0.0	45		
	liter	0.0	2.842		
injected volume butanol	ml	200.48	200.38	200.15	200.05
	mol	2.110	2.109	2.106	
vapor flow	mol/s	0.0	0.1513		
initial reflux	mol/s	0.1523	0.1509	0.1513	
	ml/min	575.4	576.95	573.10	575.40

Mixing tanks in series

The distillation column is modeled as a series of mixing tanks for the tracer experiments. Approximate a distillation process by mixing tanks in series implies that we neglect the vapor liquid equilibrium on the stages and the vapor flow upwards, since we do not have countercurrent flows we can omit to model the accumulator. These assumptions remove the “feedback” of the vapor composition from tray lower than the one observed. The bottom product flow is the sum of external reflux flow, feed flow and injected tracer. For simplicity we present only the material balance over the feed tray, which is modeled with the following set of equations. The liquid flow leaving the tray:

$$\tau_l \frac{dL_i}{dt} = L_{i+1} + F - L_i \quad (\text{B.24})$$

the mass balance over the stage

$$\frac{dM_i}{dt} = L_{i+1} - L_i + F \quad (\text{B.25})$$

component balance:

$$M_i \frac{dx_i}{dt} = L_{i+1} (x_{i-1} - x_i) + F (z_F - x_i) \quad (\text{B.26})$$

The reboiler:

$$\frac{dM_B}{dt} = L_1 - (F + L_t) \quad (\text{B.27})$$

$$M_B \frac{dx_B}{dt} = L_1 (x_1 - x_B) \quad (\text{B.28})$$

The responses of the stage temperatures when butanol is injected into the “reflux” flow to the first stage (CSTR) is shown in Figure B.41. The “temperature wave” on the stage show the propagation of butanol through the sequence of tanks (see Figure B.41). The time axis is similar to the experimental data presented in Figure B.34 for the trays 1 to 9. In Figure B.42 we show the temperature responses of stages 8 to 11. The response on tray 11 is characteristic for a first order system which is subjected to a pulse shaped input and does not match the response of stage 11 shown in Figure B.34 (top). A hydraulic time constant of 2 s is included to account for the delay introduced through the stage design on the liquid flow. The injection of 40 ml/s butanol additionally to the initial reflux flow of $L = 9.58 \text{ ml/s}$ give a rather extensive change of the tray composition. In Figure B.43 the composition response of stages 8 to 11 is shown. In the CSTR model we assume $K = 0$ (that is no vapor liquid equilibrium), but as shown in Figure B.43, the rather extensive composition change on the trays question this approach (compare Figures B.34 and B.41).

Single holdup model

The residence time on the trays of a distillation column is investigated. The model used for the simulation consists of 11 trays plus accumulator and reboiler. The simulation was performed with a average composition of $x = 0.99$ throughout the column. The following assumptions were made:

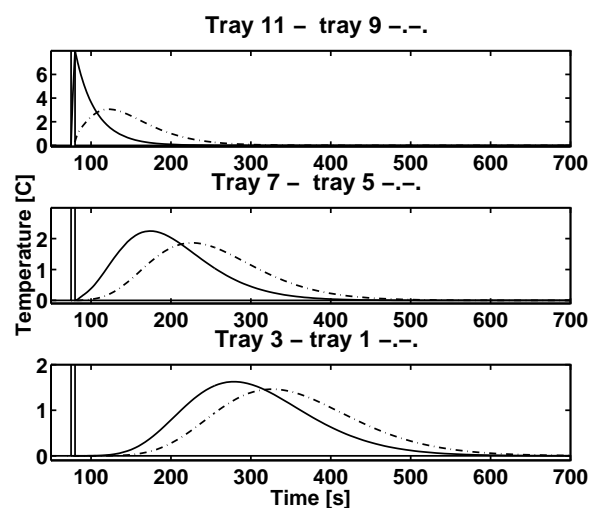


Figure B.41: Temperature responses of the CSTR-model

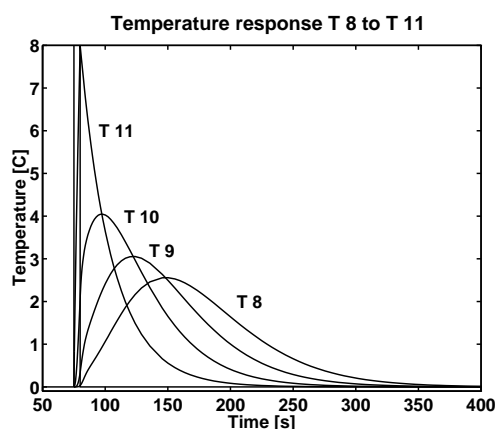


Figure B.42: Temperature responses of the CSTR-model for stages 8 to 11

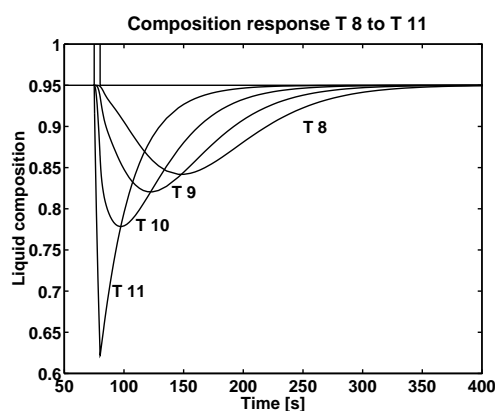


Figure B.43: Composition responses of the CSTR-model for stages 8 to 11

- vapor phase on the stages is neglected
- equimolar vapor and liquid flows (neglect energy balance)
- constant relative volatility α_{12}
- constant density of the liquid phase
- liquid flow leaving a stage is dependent on the flow entering the stage, modeled as a first order process
- total condenser and accumulator are modeled as one unit
- reboiler modeled as a theoretical stage

The model is implemented in MATLAB as a set of ODE's. The stage are counted from bottom to the top.

The accumulator model consists of mass and component balance:

$$\frac{dM_D}{dt} = V_t - D - L_{t0} \quad (\text{B.29})$$

$$M_D \frac{dx_D}{dt} = V_t (y_{11} - x_d) \quad (\text{B.30})$$

with L_{t0} as the nominal external reflux. The feed tray is modeled with the following set of equations. The liquid flow leaving the tray can be modeled by an ODE

$$\tau_l \frac{dL_i}{dt} = L_{i+1} + F - L_i \quad (\text{B.31})$$

which describe the liquid hydraulic. The mass balance over the stage assuming that the vapor flows entering and leaving are equal:

$$\frac{dM_i}{dt} = L_{i+1} - L_i + F \quad (\text{B.32})$$

component balance:

$$M_i \frac{dx_i}{dt} = L_{i+1} (x_{i-1} - x_i) + V_i (y_{i-1} - y_i) + F (z_F - x_i) \quad (\text{B.33})$$

The reboiler:

$$\frac{dM_B}{dt} = L_1 - B - V \quad (\text{B.34})$$

$$M_B \frac{dx_B}{dt} = L_1 (x_1 - x_B) - V (y_B - x_B) \quad (\text{B.35})$$

The hydraulic time constant is computed from the experimental data to an average of $\tau_l = 1.5$ s for each stage. The tray efficiency is set to $\eta = 0.85$ for all stages.

The responses composition and holdup responses of accumulator and reboiler to an injection of 200 ml butanol on tray 11 over the time interval $t = 70$ s to $t = 75$ s are shown in Figures B.44 and B.45. To take the condensation of vapor into consideration, the vapor flow leaving tray 11 is reduced temporarily by 50 %, this condensate is added to the nominal reflux and the injected amount of butanol.

Compare Figure B.35 and B.44 shows that the initial deterioration of the reboiler liquid holdup from the steady state agrees well for the experiment and the simulation. The gradient of the simulation results is slightly less than the one of the experimental data (Exp. 11). The difference is due to the modeling of the liquid hydraulic as first order processes in series. The temperature responses shown in Figure B.34 for Exp. 11 and Figure B.45 show reasonable good agreement with respect to the location of the response on the time axis. The magnitude of the response of the simulated results is approximately 50% of the experimental data for trays 1 to 10.

A limitation of the here presented model is the fact that the responses of the stages situated in the rectifier section are not matching the near symmetrical responses of interconnected mixing tanks on which the model is based. For a pulse input to a set of interconnected mixing tanks we expect symmetrical responses in each unit to an impulse. However, the injected amount of butanol is of a total of $M_{tracer} = 1.5$ mol, which is approximately 50 % of the liquid tray holdup. The nominal reflux flow is 0.14 mol/s, such that we get a short term increase in reflux by 300 % (from 0.14 to 0.58 mol/s).

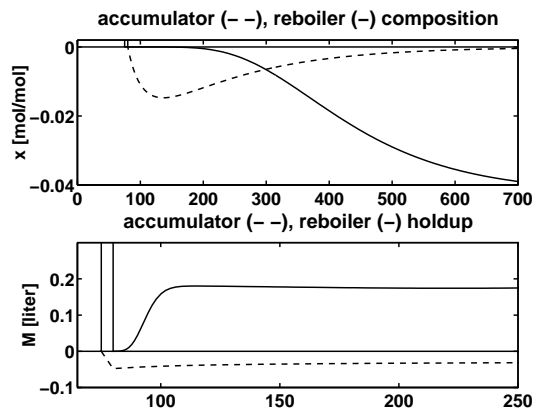


Figure B.44: Single holdup model: product composition, change in holdup of reboiler and accumulator for the simulation of Experiment 11

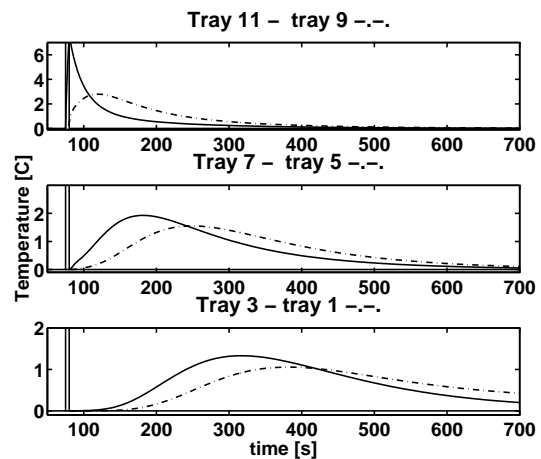


Figure B.45: Single holdup model: temperature responses of simulation of Experiment 11

Two holdup model

The modeling of the distillation tray can be improved by dividing the liquid holdup into tray and downcomer holdup. For this model we split the holdup such that half the liquid is on the tray and the rest in the downcomer. The hydraulics of the downcomer is neglected, such that we get one additional ordinary differential equation for each stage model. The mass

and component balances over the feed stage are identical to those of the one holdup model, except for the distribution of liquid. The component balance over the tray where the tracer (F, z_F) is injected:

$$M_i \frac{dx_i}{dt} = L_{i+1} (x_{d,i-1} - x_{t,i}) + V_i (y_{i-1} - y_i) + F (z_F - x_{t,i}) \quad (\text{B.36})$$

and the component balance over the downcomer:

$$M_{d,i} \frac{dx_i}{dt} = L_i (x_{t,i-1} - x_{d,i}) \quad (\text{B.37})$$

The total residence time of liquid on the stage is unchanged and the vapor is in contact with the liquid on the tray only, the vapor-liquid equilibrium is computed for the tray composition.

The liquid hydraulic and the temporary changes of the stage holdup for the two-holdup model is shown in Figure B.46. It is assumed that the downcomer holdup is constant and the entire change in stage holdup is on the tray. Further we assume that 80 % of the vapor is condensed in the period $t = 75$ to 80 s.

Comparing Figure B.34, B.45 and B.47 show that the magnitude of the temperature responses and position on the time axis are in good agreement. The split of the liquid holdup results in a more pronounced temperature response. The composition/temperature response is “delayed” due to the split of liquid holdup into tray and downcomer. Still there is some mismatch especially for tray 11. We expect a symmetrical response of the tray temperature to the liquid pulse. The simulated response (Figure B.47) show still a non-symmetrical response. In the simulation the liquid is added to the reflux flow, the tray is modeled as a perfectly mixed unit, such that effects due to mixing are neglected.

An improved two holdup model is developed due to the extensive mismatch between the temperature responses (primary concerning the shape of the response and not the magnitude)

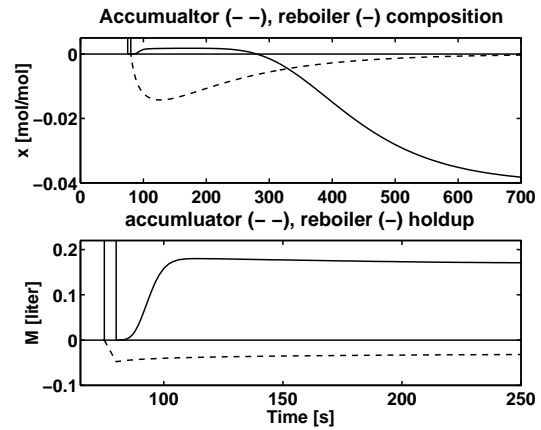


Figure B.46: Two holdup model: product composition and change in reboiler and accumulator holdup for the simulation of Experiment 11

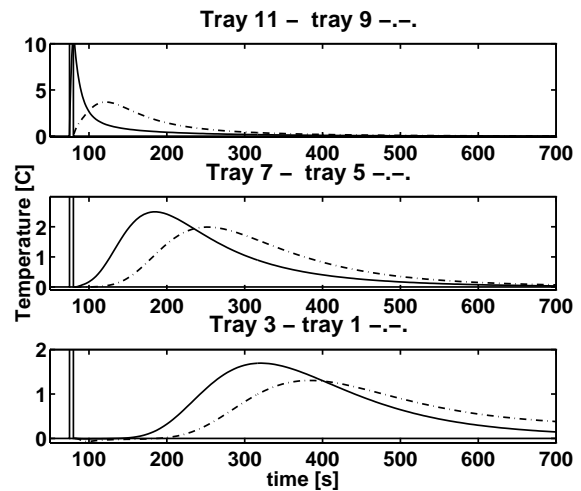


Figure B.47: Two holdup model: temperature responses of simulation of Experiment 11

of experiment and the simulation results. The injection of butanol is now done into a constant holdup vessel ahead of the upper most tray with a holdup of 2 mol (same as the tray holdup of a rectification tray). The additional lag is used to mimic the process of condensation and mixing of injected butanol, vapor and liquid on the top stage of the column. A hydraulic time constant of $\tau_L = 3s$ is chosen for this unit.

Compare Figures B.34 and B.48 show that the shape and the position on the time axis of the simulated responses are similar to the experimental data. The response of tray 11 is similar in the simulation and experiment.

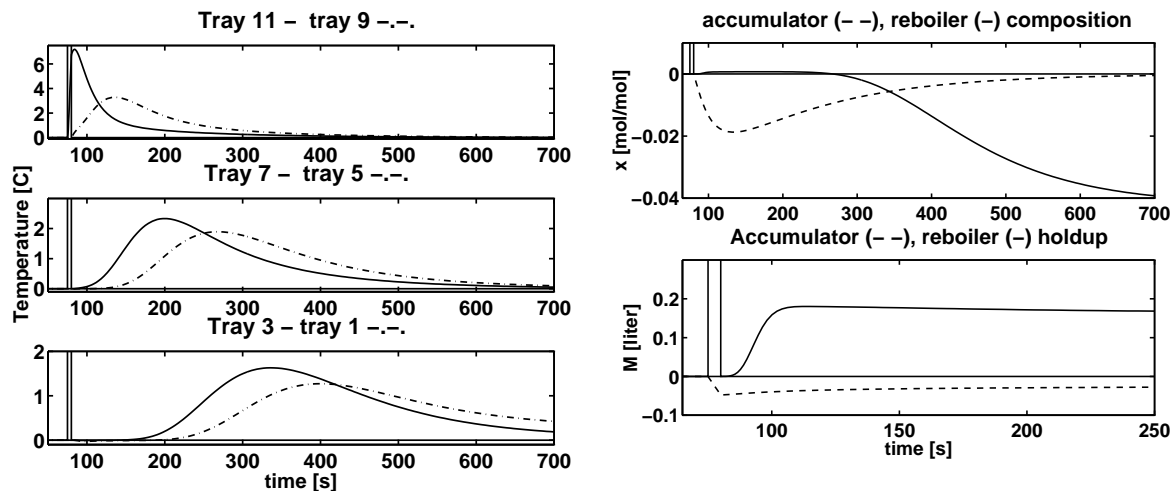


Figure B.48: Improved two holdup model: temperature responses of simulation of Experiment 11

Figure B.49: Improved two holdup model: holdup response Experiment 11

Remarks on the applied models:

We assume that all the vapor is condensed over a time period from $t = 75$ s to $t = 80$ s to heat the injected liquid, this condensed liquid is added to the internal reflux. The assumption of total reflux is implemented such that we compute the initial molar vapor flow, from this molar flow we compute the initial volumetric reflux (corrected for molecular weight), this volumetric reflux is then used throughout the simulation.

To account for the liquid delay through the column the hydraulic time constant is introduced. The liquid flow leaving the tray is responding like a first order response to the liquid flow entering the stage. Overall the liquid hydraulics is introduced primarily to model the liquid flows in the column correctly (response reboiler level to injected liquid), nevertheless there is some influence on the temperature response. The liquid hydraulics is modeled identically for all four models with a hydraulic time constant of $\tau_L = 1.5s$ the liquid flow through the column. The hydraulic time constant τ_l is estimated from experiment 11, where we determined the delay $\theta_{MB} \simeq 16s$ from butanol injection until the reboiler level increase.

Further mismatch can be caused by neglecting the energy balance and the vapor phase as well as the insufficient description of the liquid hydraulics of the column. The injection of the butanol causes a change of holdup on the trays, nevertheless the model does not include effects like the change in froth density caused by the temporarily injection of cold liquid.

B.4 Obtain column holdup

The holdup of a distillation column is of crucial importance for the composition dynamic of a distillation column, especially the distribution of the holdup influence the dynamic behavior of the column. The holdup of a distillation is determined by the following procedures:

- empty the column by dumping the liquid into the reboiler, vapor evaporating is collected in the accumulator
- compute the liquid holdup from pressure drop correlations

B.4.1 Dumping of the column

In Table B.10 results from different experiments are summarized. The data were collected after experiments for determination of step responses were finished. The procedure was as follows: When tray temperatures, holdups and product flows settled to a steady state, reflux and feed pump, reboiler heat supply and the product valves are shut down simultaneously. The holdup of reboiler and accumulator are recorded until these level out (approximately 20 minutes after shut down). The combined volume change of accumulator and reboiler give the total holdup of the column.

The increase in the accumulator volume is caused by liquid which is stored in the condenser and condenser seal during operation and due to evaporation of liquid from the column internals. Approximately 150 ml of liquid is stored during operation in the condenser and its seal, this amount is subtracted from the sum of holdup changes from accumulator and reboiler since the total column holdup is to be determined. The increase in reboiler holdup is caused by liquid stored on the sieve trays and downcomers which drains from the column into the bottom. It is assumed that all liquid which reaches the reboiler is from the liquid holdup on tray and downcomer.

Overall, the dumping experiments give a rather inconsistent picture of the dependency of liquid holdup in the column on reflux and heat input. From Table B.10 it is seen that the liquid holdup of the column increases rapidly when the total pressure drop exceeds approximately 70 mbar, which is found to be the limit of operation due to flooding.

B.4.2 Modeling of the column pressure drop

From the presented experiments it is not possible to determine the liquid distribution in rectifier and stripper section. Nevertheless, it is suggested to use pressure drop experiments to determine a suitable correlations for the liquid holdup on the stage, including estimation of the dry pressure drop over sieve tray, the height of clear liquid on the tray and the clear liquid height above the weir.

The pressure drop over the entire distillation column is caused by losses due to vapor flowing through the connecting pipes and through pressure drop over the stages in rectifier and stripper section. The pressure drop over a stage consists of dry and wet pressure drop. The dry pressure drop is caused by vapor passing through the perforation of the sieve tray.

Table B.10: Experimental determination of the column holdup by dumping of the column. Note that the experiment marked with (*) correspond to flooding.

ID	reflux flow	reboiler heat input	feed		pressure drop	change of		total* column
	$[ml/min]$	$[kJ/s]$	flow	composition		reboiler	accumulator	
	$[ml/min]$	$[kJ/s]$	$[ml/min]$	$[mol/mol]$	$[mbar]$	$[liter]$		
1	249.8	3.3	250	0.50	20.3	2.49	0.41	2.75
2	249.8	4.05	250	0.54	21.6	2.40	0.43	2.68
3	382.7	4.5	250	0.56	26.1	2.35	0.51	2.71
4	382.8	5.4	250	0.52	32.7	2.55	0.62	3.02
5	557.2	5.7	350	0.56	35.3	2.54	0.53	2.93
6	470.0	8.03	350	0.45	54.6	2.74	0.51	3.10
7*	884.0	11.25	350	0.51	83.5	3.48	0.64	3.97
14	660.1	6.4	250	0.53	50.9	2.53	0.46	2.84
15	391.8	3.7	250	0.53	27.5	2.29	0.54	2.68
16	409.5	5.4	250	0.52	32.5	2.34	0.55	2.74
17*	850.3	8.0	250	0.49	68.3	3.34	0.71	3.90
18	704.9	9.5	250	0.95	47.1	2.78	0.69	3.32
19	436.5	7.5	250	0.95	33.0	2.29	0.46	2.60
20*	888.9	7.6	400	0.95	75.6	3.76	0.61	4.22
21	659.2	9.7	250	0.49	53.6	2.31	0.46	2.62
22*	883.9	13.5	400	0.50	79.6	3.46	0.51	3.82
23	391.8	5.55	250	0.51	26.8	2.39	0.46	2.70
24	400.8	3.75	250	0.52	19.1	2.18	0.37	2.40
25	314.1	4.3	250	0.51	23.4	2.76	0.46	3.07
26	418.7	5.4	250	0.55	31.5	2.40	0.35	2.60

The areated liquid (static head) on the tray causes the wet pressure drop. We have chosen to neglect the residual pressure drop which is often mentioned in literature (*e.g.* Perry, 1984), since the proposed 12.5 mm of water is in the order of the wet pressure drop for a stage of the investigated column.

The experiments (*e.g.* dp1 and dp2) to determine the pressure drop of the distillation tower are performed with pure ethanol ($z_F = 0.99$) as feed. This procedure is chosen to eliminate the influence of changes in density in vapor, liquid phase and heat of vaporization in the reboiler. The control of the inventory is done automatically by adjusting the flow of distillate (accumulator) and the bottom flow (reboiler). The amount of reflux and heat input to the reboiler are set manually.

The design of the stages is identical in both rectifier and stripper section. To simplify the computations, constant molar flows throughout the column sections and constant liquid and vapor densities are assumed. The vapor flow is computed from the heat input to the reboiler

$$V = \frac{Q}{\Delta h_{vap}} \quad [m/s] \quad (B.38)$$

Since the column is fed with a mixture primary containing ethanol, we use the heat of va-

porization of ethanol $\Delta h_{vap} = 38.7 \text{ kJ/mol}$ at $T = 78.5^\circ\text{C}$. Heat losses to the surroundings from the column shell are neglected. The liquid flow through the column is computed from the control signals to the metering pumps for feed and reflux. The molar feed and reflux flows are computed under consideration of the temperature influence on the density.

We assume here that the influence of the entering feed and reflux on the vapor flow is negligible and subcooling is not that extensive that a considerable amount of vapor is condensed, the internal reflux L is identical to the external reflux L_T . The assumption of constant molar flows implies that the vapor velocity in both sections is constant. The temperature of feed and reflux is approximately 78°C , such that the assumption of neglected condensation of vapor on feed and upper most stage is reasonable.

One requirement to get a sufficient set of pressure drop data is to span the space of vapor and liquid flow over an as large as necessary interval. During the recording of the data negative flows of distillate and bottom product were necessary, these are the cases where: $V_T \leq L_T$ and $L_B \leq V_B$. The index T denotes the reflux to stage 11 and vapor from stage 11, respectively, while in the bottom section B denotes the liquid flow from stage 1 to the reboiler and the vapor flow from reboiler to stage 1, respectively. Feeding liquid directly to reboiler and accumulator to span the space for the pressure drop measurements introduce some errors on the results. The 'negative' bottom flow pumped into the reboiler has to be heated up from 20°C to the boiling point, this result in a lower vapor flow through the column which is computed from Eq. B.38. Due to the unfavorable influence of 'negative' bottom flow it is chosen to exclude these data from the estimation procedure. This phenomenon will not occur for 'negative' distillate flow, since the additional reflux is pumped into the accumulator. The reflux passes through a preheater before it enters the column.

Modeling pressure drop column-condenser pipe

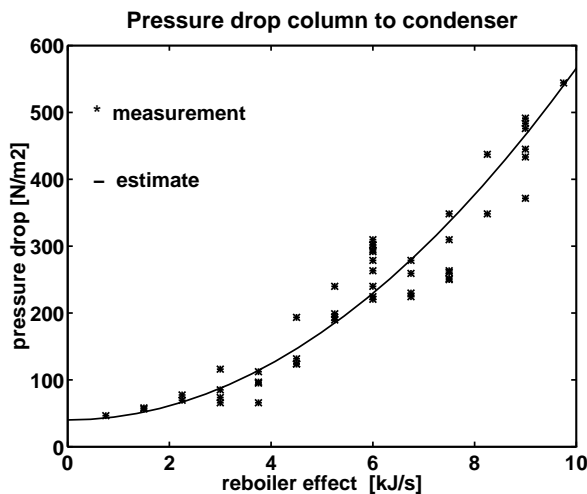


Figure B.50: Pressure drop in the pipe connection the distillation column and the condenser, '*' experimental data, '-' estimate

The estimate of the pressure drop is computed from a least square fit of the experimental data, the formula used is:

$$\Delta p_{pipe} = 40 + \frac{1}{2} \rho_V \left(f \frac{L_P}{D_P} + \zeta_t \right) u_{pipe}^2 \left[\frac{N}{m^2} \right] \quad (\text{B.39})$$

The fanning friction factor is estimated from Fig 5-28 in Perry Chemical Engineerings Handbook (1984), under consideration of the surface quality, the friction factor is estimated to $\epsilon/D_p = 1.2 \cdot 10^{-3}$, which give $f \simeq 0.005$. The dimensions of the connector pipe are $D_p = 38 \text{ mm}$, $L_p = 500 \text{ mm}$. The total friction loss factor is estimated to $\zeta_t \simeq 15$.

The constant in the equation covers not described/neglected effects in the liquid seal of the condenser inlet. The condenser is 'sealed' to the column by an approximately 5 mm liquid seal were the vapor has to pass through before it enters the condenser.

Computation of stage pressure drop

The pressure drop correlations presented here are taken from Coulson and Richardson (1985), Perry (1984) and Bennett(1983). These correlations are not necessarily the only found in literature, but are reasonable correct for the here investigated column.

Total pressure drop: The pressure drop over a stage is measured as the difference in pressure between two adjacent stages

$$\Delta p_{plate,i} = p_i - p_{i-1} \quad (B.40)$$

$$\Delta p_{plate} = \Delta p_{static} + \Delta p_{dry} \quad (B.41)$$

The pressure loss due to surface generation, Δp_{bubble} , is neglected compared to the equations listed in Coulson and Richardson (1985) or Perry (1984). The pressure drop due to bubble formation at the orifice is approximately $5 N/m^2$, which is less than the measurement accuracy. The 'residual pressure drop', Δp_R , as listed in literature (Perry, 1984) is neglected. The residual pressure drop is estimated from several authors to be equal to a pressure difference of 12.5 mm water. This liquid height corresponds to a pressure drop of $\Delta p_R = 123 N/m^2$ which is comparable to 50 % of the static pressure drop through the areated liquid.

Dry pressure drop: The dry pressure drop over the orifices of the sieve tray is estimated by

$$h_{dry} = \frac{K}{C_o^2} \cdot \frac{\rho_{mv}}{\rho_{ml}} u_h^2 \quad [mm] \quad (B.42)$$

The constant K in Eq. B.42 is for sieve plates given to $K = 51 [1000s^2/m]$ to give the correct dimension of the dry pressure drop h_{dry} in mm liquid. To convert the equivalent liquid height to the pressure drop we use:

$$\Delta p_{dry} = \rho_{ml} \cdot g \cdot \frac{h_{dry}}{1000} \quad [N/m^2] \quad (B.43)$$

introduce eq. B.42 into eq. B.43 give

$$\begin{aligned} \Delta p_{dry} &= \rho_{ml} \cdot \frac{g}{1000} \cdot \frac{51}{C_o^2} \frac{\rho_{mv}}{\rho_{ml}} \cdot u_h^2 \\ &= \frac{0.50031}{C_o^2} \cdot \rho_{mv} \cdot u_h^2 \quad [N/m^2] \end{aligned} \quad (B.44)$$

The velocity of the vapor through the orifices of the sieve tray is

$$u_h^2 = \frac{V_{in} \cdot MW_v}{\rho_{mv,in} \cdot A_{free}} \quad [m/s] \quad (B.45)$$

In Eq. B.45 the orifice coefficient is set to $C_o = 0.72$ (Coulson/Richardson, 1985) for a sieve tray 2.5 mm thick equipped with perforations of a diameter of 2.7 mm.

Clear liquid height above weir: The liquid hydraulic is determined by the amount of liquid above the weir. The height of clear liquid flowing over a weir is determined by a modified Francis weir formula for circular weirs (Perry, 1984).

$$h_{ow} = 44300 \cdot \left(\frac{L_q}{0.5 \cdot D_{weir}} \right)^{\pi_3} \quad [mm] \quad (B.46)$$

with the liquid flow L_q in $[m^3/s]$ and the exit weir diameter D_{weir} in $[mm]$. The liquid flow leaving the tray is computed from

$$L_q = \frac{L_{out} \cdot MW_l}{\rho_{ml}} \quad [m^3/s] \quad (B.47)$$

Note that we consider only 50 % of the exit weir circumference in Eq. B.46 as active weir length. This is due to the design with an circular exit weir placed near the column wall. The screened literature does not include any correlations which describe the distribution of liquid flowing over an off-center placed circular weir.

Froth density: The froth density ϕ can be expressed by

$$\phi = e^{(\pi_1 * K_s^{\pi_2})} \quad [] \quad (B.48)$$

The parameters π_i are determined empirically from experimental data to fit the pressure drop over a column section by known liquid and vapor flows in a least square sense (see Appendix B.4.3). The dimension of π_1 is $[(m/s)^{1/\pi_2}]$ to ensure a dimensionless froth density. The froth density on the tray depends on the velocity factor over the active tray area:

$$K_s = u_{active} \cdot \sqrt{\left| \frac{\rho_{mv,in}}{\rho_{ml,out} - \rho_{mv,in}} \right|} \quad [m/s] \quad (B.49)$$

Static pressure drop: The static pressure drop due to liquid stored on the tray is computed by :

$$\Delta p_{static} = g \cdot h_{cl} \cdot \rho_{ml} \quad [N/m^2] \quad (B.50)$$

Due to the rather small column diameter of 125 mm we neglect any hydraulic gradient over the tray (Bennett, 1983).

Estimation of clear liquid height: The clear liquid height (static head) on the tray can be computed by four different models, denoted **A** to **D**.

The liquid height h_{cl} on the tray is expressed by Bennett (1983):

$$h_{cl} = \phi \cdot \left(h_{weir} + C \left(\frac{q_l}{\phi} \right)^{\pi_3} \right) \quad [m] \quad (B.51)$$

with $C = 0.0327 + 0.0286 * e^{-0.1378 * h_{weir}}$ and h_{weir} in $[m]$. C is an empirical determined parameter, both to adjust the dimensions in Eq. B.51 and the flow of froth over the weir, q_l is the flow rate per unit length outlet weir in the dimension $[m^3/min * m]$. The computed liquid height on the tray h_{cl} has the dimension of $[m]$. Equation B.51 will be used in procedure **A** to describe the flow of a froth over the weir and to estimate the differential pressure over a stage.

The dimensions of Eq. B.51 are not that suitable for the investigated system. It is chosen to change the dimensions to SI-units and use a least square fit to adjust the coefficients π_i . We have chosen to use the exponent of $\pi_3 = 0.704$ to describe the flow over the circular weir as suggested in Perry.

$$h_{cl} = \phi \cdot \left(h_{weir} + C \left(\frac{L_q}{L_{weir} \cdot \phi} \right)^{\pi_3} \right) \quad [mm] \quad (B.52)$$

with h_{weir} in $[mm]$ and Q_l in $[m^3/s]$. π_i are empirical determined parameter, both to adjust the dimensions in Eq. B.52 and to adjust the liquid height on the stage. Equation B.52 will later on be denoted procedure **B**.

Note that the correlations in equations B.51 to B.52 for the computation of the liquid height are only functions of weir height, h_{weir} , vapor flow V_{in} and active tray area. Influence on the 'wet' pressure drop by the liquid flow is solely by the volumetric liquid flow L_q over the weir. In the here presented form is the liquid amount below weir primary dependent on the vapor flow through the tray. The influence of the liquid flow through the column is considered by the term $C \cdot \left(\frac{q_l}{\phi} \right)^{\pi_3}$. For the exit weir of the here investigated column C in Eq. B.51 is computed to $C = 0.0612$.

Possible simplifications of Eq. B.51 will include the application of the clear liquid height above weir as computed by Eq. B.46 instead of the volumetric flow rate over the outlet weir. Introduce this simplification opens for two different types of correlations. Based on the correlation of Bennett, such that

$$h_{cl} = \phi * \left(h_{weir} + C \left(\frac{h_{ow}}{\phi} \right)^{\pi_3} \right) \quad [mm] \quad (B.53)$$

with C as an empirical determined parameter to adjust the dimensions in Eq. B.53. The numerical value of C in Eq. B.53 is determined from experimental data of the investigated column. Equation B.53 will later on be denoted as procedure **C**.

The most simple form to describe the liquid height on the tray will be:

$$h_{cl} = \phi * \left(h_{weir} + \left(\frac{h_{ow}}{\phi} \right)^{\pi_3} \right) \quad [mm] \quad (B.54)$$

This simple prediction will be denoted procedure **D**.

In equations B.52 to B.54 we assume that clear liquid flows over the weir since a disengaging zone placed in front of the exit weir. Due to the design of the sieve tray, with the exit weir off center towards the column wall, we assume the 'active' weir length to be 50 % of the total length (see Eq. B.46).

The most correct form of equation to describe the liquid height on the tray will be a combination of correlations Eq. B.51 and B.54. Beside the correlations proposed by Bennett (1983) (see Eq. B.40 to B.49), correlations from Stichlmair (1978) and Lockett (1986) have been investigated too. Both, the correlations from Bennett (in its published form) and Stichlmair, overestimate the amount of liquid on the stage for the investigated system.

Remarks on estimation procedures

The application of pressure drop measurements as indication for the liquid holdup and its distribution on the tray is dependent on accurate measurements and correlations. The clear liquid height on the tray is dependent on the vapor flow (through the froth density) and the height of clear liquid above the weir.

The estimation of the coefficients in *e.g.* Eq. B.53 is rather sensitive to errors on the pressure drop measurement. The dry pressure drop is predicted by Eq. B.45 for each stage. The three parameters π_1 to π_3 describe the dependency of the holdup on vapor and liquid flow. The liquid holdup on the tray is very sensitive to these parameters, a wrong predicted froth density results in a considerable misprediction of the liquid holdup on the tray. The downcomer holdup depends mainly on the pressure drop over the stage (sum of dry and wet pressure drop) and the holdup under the inlet weir. An error in dry pressure drop of 1 mm will give an error of 1.1 ml, mispredicting the clear liquid height on the tray by 1 mm result in an error of 12.3 ml on each stage. The latter corresponds to approximately 5 % of the stage holdup and up to 10 % of the tray holdup. This shows the large sensitivity of this measurement on an exact prediction of the liquid height on the tray.

The design of the stages complicates the prediction further, with column diameter of $D_c = 125\text{mm}$ and a circular weir of length $L_w = 112\text{mm}$. It is a rather uncommon design, where the tray diameter and the length of the outlet weir are almost identical. The position of the outlet weir off-center towards the wall result in a rather complicated flow pattern on the tray. Due to the tray design is the clear liquid height above weir relative low (*e.g.*: $0.5 \leq h_{ow} \leq 1.5\text{ mm}$, see also Eq. B.46), even when we assume that only 50 % of the outlet weir length is active.

B.4.3 Parameter Estimation for the simulation model

Four different procedures to estimate the pressure drop over the stages in a distillation column are presented (see Appendix B.4.2). Procedure **A** is based on the original publication by Bennett (1983) which are presented in equations B.49. Procedure **B** is based on the same equations but the coefficients were determined by a least square optimization of the experimental data. In procedure **B** the coefficients are determined simultaneously for the rectifier and stripper section, taking the identical internal design of the stages into account. In procedure **C** (see Eq. B.53) we exchange the volumetric flow per unit weir length by the clear liquid height over weir which is computed from Eq. B.46. This will reduce the number of equations in a dynamic model where the modified Francis weir formula is used to describe the liquid hydraulic through the column. Simplify the correlations further leads to Eq. B.54, the results of this prediction are presented as procedure **D**, in **D2** the coefficients are computed for both sections separately.

The coefficients determined by a least square optimization of the experimental data to estimate froth density and clear liquid height on the tray are listed in Table B.11. Note that π_3 and C are not necessary for procedures D. The 3-d figures *e.g.* Figure B.51 show the

Table B.11: Coefficients of the correlations Eq. B.48, B.51, B.53 and B.54

Procedure	π_1	π_2	π_3	C
A	-12.55	0.91	2/3	0.0612
B	-14.50	0.38	0.704	15959
C	-14.88	0.27	0.704	45.49
D	-11.44	0.63	1.4	
D2R	-12.50	0.81	1.4	
D2S	-9.01	0.49	1.4	

pressure drop measurements over a stage in the rectification and stripping section of the investigated pilot plant. The actual measurements are marked with (*) and (o) for the rectifier and stripper, respectively. The surface which is drawn in the coordinate system of molar liquid and vapor flow and the pressure drop represents the estimation of the pressure drop based on the presented correlations. The advantage of the 3-d plots is that it is rather easy to see if the type of correlation is suitable. The deviations are plotted in an extra figure (see *e.g.* Figure B.53), where deviation for each experiment is shown. For simplicity we restrict the presentation of data to procedure **A** and **D**. Even though procedures **B** and **C** show some good results, those correlations were not used in the simulations, because of their considerable more complicated form.

Procedure A

Based on the correlations Bennet presented (Eq. B.40 to B.51). The coefficients chosen for both rectifier and stripping section given in Table B.11 marked with (A).

From Figure B.51 we see that the variation in liquid flow does only have a limited influence on the predicted pressure drop, which does not agree with the measured pressure drop. Overall the predicted pressure drop (surface in Figure B.51) over a stage in the rectifier (*) and stripper (*) section is far too high. (The measured data points which are lower than the predicted surface are hidden.) Rotate Figure B.51 such that we can inspect the dependency of the pressure drop on the vapor flow shows (see Figure B.52) that there is a rather extensive mismatch between predicted (—) and measured (*, o) pressure drop.

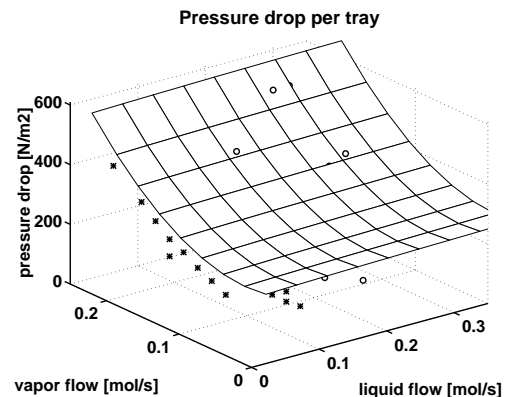


Figure B.51: Pressure drop over a tray in the distillation column, procedure **A**

Since the predicted pressure drop shows a rather constant offset (see Figure B.52) and the shape of the predicted pressure drop is similar to the observed values it is assumed that the liquid holdup on the tray is overestimated. We assume that the suggested type of correlation is reasonable and the amount of liquid stored on the tray under operation has to be reduced (this is the dependency of the liquid holdup on the vapor flow) to achieve a better fit.

The deviation between measurement and estimation is in excess of 50 N/m^2 this corresponds to a liquid height of approximately 7 mm, which is 30 to 70 % of the clear liquid height on the tray. The form of the froth density correlation (Eq. B.48) implies that for very low vapor flows ($K_s \sim 0$), the height of clear liquid on the tray equals the weir height plus the height of clear liquid above weir.

The error between the literature correlations and the measured values is presented in Figure B.53. This figure shows the extensive deviation in the prediction of the pressure drop. A deviation of approximately $\pm 20\%$ in the stripper (*) section and a deviation of maximum of 80% for the rectifier (o) section is observed.

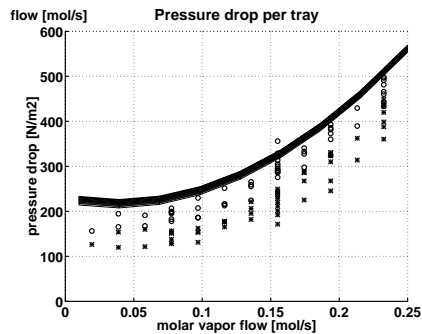


Figure B.52: Pressure drop over a tray in the distillation column, procedure A (rotation of Figure B.51)

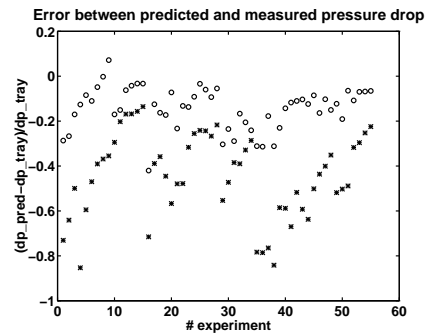


Figure B.53: Error between prediction and measured pressure drop, 'o' tray in stripper section, '*' tray in rectifier section, procedure A

Procedure D2

The most simple correlation to describe the clear liquid height on the tray is given in Eq. B.54. The results are presented in Figures B.54 to B.56. This correlation will be valid for a distillation tray where a calming zone is placed in front of the outlet weir. Predict the coefficients in Eq. B.48 separately for each section improves the prediction and reduces the offset significantly. We choose to do the parameter estimation separately due to the rather different liquid loadings on the stages.

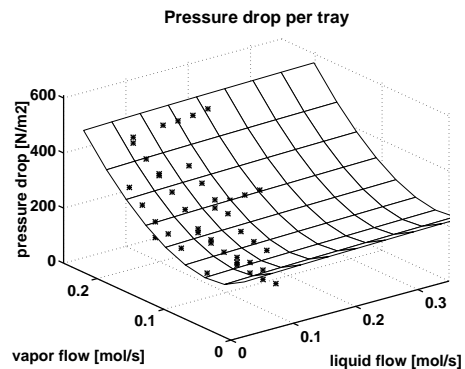


Figure B.54: Pressure drop over a tray in the rectifying section of the investigated distillation column, '-' estimated '*' measured pressure drop, procedure D2R

The deviation between estimation and measurement is shown in Figure B.56. The most extensive error (more than 15 %) are observed for experiments where a low vapor flow ($V \leq 0.02 \text{ mol/s}$) is used.

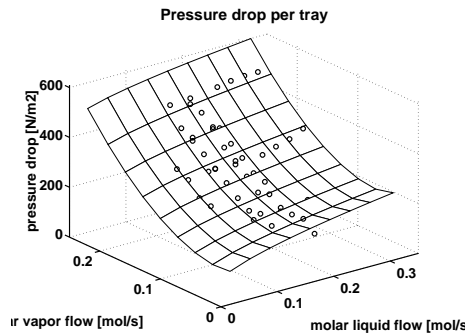


Figure B.55: Pressure drop over a tray in the stripping section of the investigated distillation column, '–' estimated 'o' measured pressure drop, procedure D2S

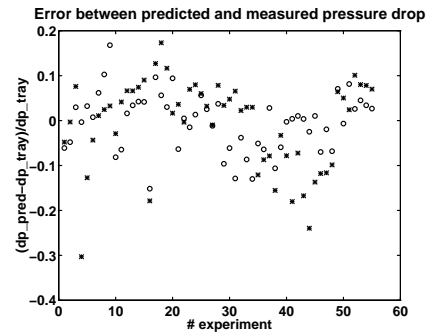


Figure B.56: Error of the improved correlation, 'x' tray in rectifier section, 'o' tray in stripper section, procedure D2

Discussion

The correlations developed by Bennett are based on experiments where the free tray area (hole area) is approximately 10 to 15 %, further the liquid and vapor load on the trays where several magnitudes higher than in the here investigated system. Due to these circumstances we have chosen to modify these correlations to allow a better prediction of the pressure drop and thus the clear liquid height on the tray. We adopt the equation for the froth density (Eq. B.48) and introduce the clear liquid height above the weir into the correlation to compute the clear liquid height on the tray.

B.4.4 Results

Column pressure drop prediction

The pressure drop over the distillation column, that is from the first tray to the condenser inlet is computed from correlations presented as procedure **D2** (see Table B.11). The total pressure drop over the column consists of the dry and static pressure drop of five and six stages of stripper and rectifier section. By applying Eq. B.40 to Eq. B.50 and Eq. B.48 to Eq. B.53 we are able to compute the pressure drop over the investigated distillation column.

The proposed correlations are compared to experimental data of the distillation of ethanol. The feed composition was $z_f = 0.95$, the reflux flow is chosen to 383 ml/min (0.1024 mol/s). Distilling ethanol has the advantage that the density of the liquid in the column will be constant and computation is slightly simplified. Apply procedure **D2** to the input data listed in table B.12 result in the pressure drop prediction shown in Figure B.57.

Evaluate the proposed correlation on experimental data (see Table B.10) of the distillation column is shown in Figure B.58. Overall the prediction of the pressure drop is sufficient when the coefficients determined from the distillation of ethanol are used to estimate the differential pressure over the distillation column.

Table B.12: Operational parameter of Experiment dp1 and dp2

		dp1	dp2
F_v	ml/min	374	225
F	mol/s	0.1068	0.0641
L_v	ml/min	385	385
L	mol/s	0.1024	0.1024
heat input	kJ/s	0.75 - 9.75	1.5 - 9.75

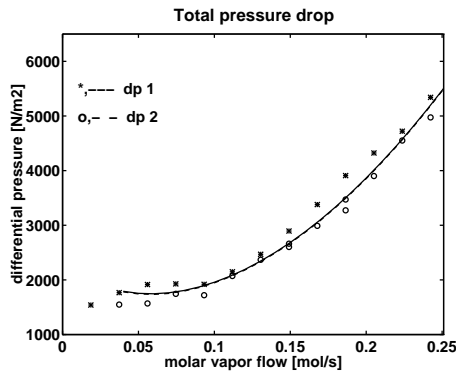


Figure B.57: Comparison of measured and estimated pressure drop for the distillation of ethanol, procedure D2

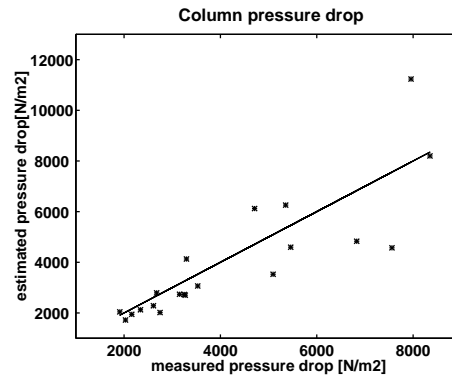


Figure B.58: Comparison of measured and estimated pressure drop, (*) measurement, (-) prediction based on procedure D2

The experiments with a measured pressure drop in excess 6500 N/m^2 were performed under conditions close to flooding (high liquid and vapor load). Even though flooding (rather fast increasing pressure drop) was not explicitly considered in the prediction of the pressure drop the prediction procedure, the estimated pressure drop over the column agrees rather good with the experimental data.

B.4.5 Holdup prediction

From the above presented procedures to predict the pressure drop, we are able to compute the liquid holdup in the distillation column. The measured pressure drop and the corresponding holdup in the distillation column determined by dumping are presented in Table B.13.

The differing vapor and liquid flows of the two sections are taken into consideration through the prediction of froth density (Eq. B.48) and liquid height above weir (Eq. B.46). The total pressure drop over the stage is proportional to the liquid backup in the downcomer. The total liquid holdup on a stage is thus, liquid on the tray, in the downcomer pipe and in the downcomer seal. Table B.13 shows the result of the holdup prediction for some of the performed experiments. The error in holdup prediction is in the order of $\pm 10\%$, but show increasing error as column loading increases.

The error between estimation and measured volumetric holdup is of the order of $\pm 10\%$ for procedure D2. The liquid holdup is somewhat underestimated for higher vapor and liquid

loads.

Table B.13: Column holdup by dumping of the column compared to estimated holdup.

Exp.	reflux flow	reboiler heat supply	feed		pressure drop	column holdup	
	$\frac{ml}{min}$	$\frac{kJ}{s}$	$\frac{ml}{min}$	z_F		dump.	D2
					[mbar]	[liter]	
1	250	3.3	250	0.50	20.3	2.75	2.88
2	250	4.05	250	0.54	22.3	2.68	2.77
3	380	4.5	250	0.56	26.1	2.71	2.74
4	382	5.4	250	0.52	32.7	3.02	2.67
5	557	5.7	350	0.56	35.3	2.93	2.69
6	470	8.0	350	0.45	54.6	3.10	2.66
7	800	11.25	350	0.51	83.5	3.97	2.98

B.4.6 Discussion

The prediction of the pressure drop and the total liquid holdup in the distillation column relies primarily on the correct prediction of the liquid height on the sieve tray. The liquid stored on the tray is primarily dependent on the vapor flow since vapor bubbles will replace liquid. Further will the liquid cross flow over the sieve tray influence the tray loading. The height of clear liquid above weir is computed from Eq. B.46 which is assumed to describe the liquid hydraulic well. The clear liquid height, h_{cl} on the stage is computed by Eq. B.54 and the froth density, ϕ from equation B.48. The error in the prediction of the liquid holdup over the whole column is in the order of ± 10 . The operation of a nearly flooded distillation column will not be considered later on in the dynamic simulation program.

B.5 Summary of experiments

Experiments 1 to 4 were performed with the level loops closed to maintain the material balance. The reflux pump and reboiler heat supply were under manual control. The signals to the manipulator were stepped such that reflux and vapor flow were increased and decreased in turn. The feed composition was near $z_F = 0.5$.

The experiments 5 to 7 were performed with a feed mixture of ethanol and butanol at a concentration near $z_F = 0.5$, while experiments 8 to 13 were performed with $z_F = 0.95$ to reduce effects of molecular weight and heat of vaporization.

In experiments 11 to 13 we injected a heavy tracer on the upper most stage of the distillation column operated at total reflux. The initial feed charge had a composition of $z_F = 0.95$. We determined the time delays for the tracer wave traveling through the column graphically and computed the hydraulic time constants.

Comparison step experiments (open loop), continuous operation The delay from a step change in reflux until the reboiler level starts to change is determined from experiments 5, 7 and 8 to be in the range of $15 \leq \theta_{M_B} \leq 20$ for an increase in reflux flow, this corresponds to a hydraulic time constant $\tau_l \simeq 1.6s$.

Reducing the reflux flow (Exp. 9 and reset Exp. 8) results in a time delay which is in the range of $30s \leq \theta_{M_B \leftrightarrow L} \leq 45s$, this difference is caused by liquid still traveling downwards liquid in the column towards the reboiler after the reflux pump control signal was reduced. The liquid flow from the column to the reboiler will remain on the initial level before it changes gradually due to the reduced reflux flow to the upper most tray.

The delay from increase/decrease of the reflux pump control signal until the accumulator level reacts is in the range of $4s \leq \theta_{M_D \leftrightarrow L} \leq 6s$. The response of the reboiler level to an increase in reboiler duty is delayed by $4s \leq \theta_{M_B \leftrightarrow Q_B} \leq 5s$. These delays are caused by processing time of the computer and the dynamics of reflux pump and reboiler heating elements, respectively.

The step experiments (7 and 10) performed to investigate the vapor hydraulics give a time delay from the increase of the reboiler heat input control signal until the accumulator level reacts in the range of $20s \leq \theta_{M_D \leftrightarrow V} \leq 35s$. From these experiments it is rather difficult to determine if the delay is caused by vapor traveling upwards through the column or due to the delay introduced by condenser and piping towards the accumulator. From Exp. 10 to 13 it is found that a disturbance in the top vapor flow, V_T , (some vapor is condensed by heating the injected tracer) result in a delay from top of the column to accumulator in the order of 10 seconds.

Comparison tracer experiments, total reflux Total reflux operation was used to preform experiments 11 to 13, with a reboiler effect varying from $6.0kJ/s \leq Q_B \leq 9.0kJ/s$ and a reflux flow of $470 ml/s \leq L_{vol} \leq 705 ml/s$. The delay of the responses of stages 1, 3, 5, 7 and 9 relative to the initial temperature increase on stage 11 is shown in Figure B.59.

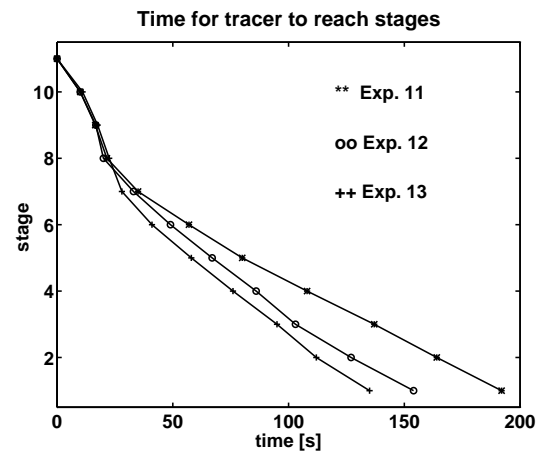
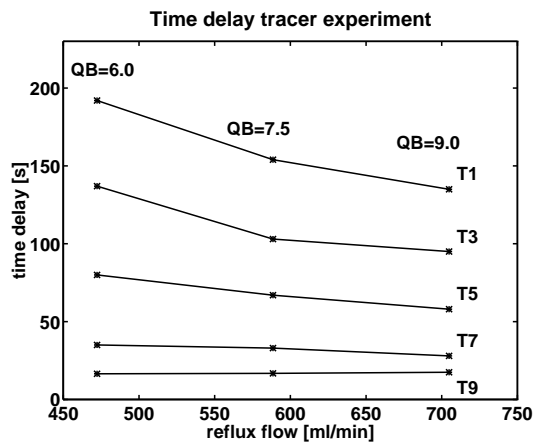


Figure B.59: Comparison of time delays for tracer experiment. Reference time is initial deviation on stage 11 to stages 1,3,5,7 and 9.

Figure B.60: Wave of tracer moving through the column (counting top-down)

The ratio of the increase in reflux and boilup is chosen such that we get an equidistant

increase of the manipulated variables reboiler heat supply and volumetric reflux flow. As can be seen from Figure B.59 we get an approximately linear dependency of the (composition) transport delay if both reflux and boilup are increased simultaneously. For a 20 % increase in reflux and vapor flow we get a residence time on the stages which is reduced (on average) by 20 % comparing Exp. 11 to 12; for an increase of 50 % the residence time decreases by 35 % (comparing Exp. 11 to 13).

The total time a tracer puls needs to travel through the column from stage 11 down to stage 1 is in shown in Figure B.60. It is rather difficult to determine the exact time at which the tracer reaches the stages 8, 9 and 10, since the upper most stages will be strongly influenced from the injected cold tracer. Effects influenceing the different composition responses in the rectifier and stripping section are due to liquid replaced by the tracer (200 ml injected is approximately the entire stage liquid holdup) immediate after injection and condensation of vapor which results in an increased tray loading which result in weeping, due to overloading of the upper most stage.

If we approximate the residence time of the column by the delay of the maximum temperature increase on stage 1 relative to stage 11 we can estimate the liquid holdup of the column. This is $\tau_{c,Col} \simeq \theta_c = V_{Col}/L$. Estimating the column holdup from this method give a holdup in the order of $2.4 l \leq V_{Col} \leq 2.8 l$ depending on the operation point. (This is, we assume a plug flow through the pipe) From the total liquid holdup we can compute the stage holdup (this is liquid on the sieve tray and stored in the downcomer) by $V_{stage} = V_{Col}/N_t$, such that the stage holdup is $V_{stage} \simeq 0.24l$.

Comparison step and tracer experiments

The principal differences of these two types of experiments make it rather difficult to compare the experimental data. The step experiments are performed such that the liquid flow is changed by less than 20 % from the initial reflux flow. The 'step' change is introduced as a ramp of 16 ml/s due to the dynamics of the metering pump supplying the reflux. The volume injected in the tracer experiment increases the reflux flow temporarily by more than 50 %, such that the composition time constant is considerably influenced by this increase.

The different methodology to perform the experiments require the definition of an appropriate reference time to allow for a comparison of the different experiments. To facilitate the comparison we have to account for the different effects which influence the hydraulic lag. For the step change we have to consider the influence of data transfer as well as reflux and reboiler dynamics and for the tracer experiment effects due to injection of the tracer liquid, subcooling and overloading on the stage. The hydraulic lag determined from the step experiments are determined from the time difference from the initial decrease of the accumulator to the initial increase in reboiler level. The tracer experiments are referenced to the initial temperature change on stage 11 to the increase in reboiler level.

Liquid hydraulics:

We compare first the experiments where the internal liquid flow is changed, either in form of a step of the signal to the reflux pump or by injection of a tracer. The experiment we are referring to are experiments 5, 7, 8 and 9 and the tracer experiments 11 to 13. To simplify the comparison of step and tracer experiment we present the essential data in Table B.14.

Experiments 8, 9 and 11 are performed at similar operation points but with different

operation strategies. Experiments 8 and 9 is the standard type of operation for a distillation column with feed and product flows. Experiments 11 to 13 are performed in the total reflux mode, such that there is no feed or product flows.

Table B.14: Comparison of liquid hydraulic

Experiment		5	7	8	9	11	12	13
Figure		B.23	B.25	B.31	B.32	B.35	B.38	B.40
F	ml/s	5.83		4.17		0.0		
z_F	mol/mol	0.56	0.51	0.95				
L_0	ml/s	7.81	13.3	8.02	7.88		9.8	11.75
Q_B	kJ/s	5.79	11.25	6.0			7.5	9.0
Exp. type		step				pulse of 5 s		
ΔL	ml/s	1.47	1.45	+1.49	-1.49	40.0		
θ_{M_D}	s	5.3	6.5	5.0	4.0	9.7	10.8	13.3
θ_{M_B}	s	23.1	22.3	24.9	34.1	19.5	18.0	19.0
referred to		accumulator level change				initial temperature change stage 11		
θ_l	s	17.8	15.8	19.9	30.1	19.5	18.0	19.0
τ_l	s	1.62	1.44	1.81	2.74	1.77	1.63	1.72

The time tags θ_{M_D} and θ_{M_B} for the step change change experiments are referred to the change of the reflux pump control signal until reboiler and accumulator level reacts. These for the tracer experiments are referred to the initial temperature deviation on stage 11. From Figure B.31 we see that the response of the accumulator level is delayed by approximately 5 seconds compared to the change of the reflux pump control signal. These 5 seconds are caused by the processing time of the computer system to change the controller output and the time elapsing to convert the electronic signal to a change in volumetric flow of the reflux pump. Further a change from 0 to 100 % (corresponds to 0 - 1000 ml/min) reflux flow takes approximately 60 s (this is a ramp with gradient 1000 ml/ 60 s = 16.7 ml/s). In Experiment 8 and 9 we change the reflux by $\simeq \pm 90 ml/min$, this change will be completed after approximately 6 seconds. We choose to approximate the ramp of the pump and the electronic processing by a delay consisting for processing/data transfer by a time delay of 5 seconds. The dynamics of the pump will be considered if the initial accumulator level change is used as reference for the step experiments.

Use the initial deviation of accumulator level as reference for the step experiments and the initial temperature deviation on stage 11 for the tracer experiments, the hydraulic delay is rather similar. The hydraulic delay from the upper most stage to the reboiler is denoted θ_l . The average liquid hydraulic time constant is computed to $\tau_l = \theta_{M_B}/N_t = 1.67s$ for each stage from experiments were the internal liquid flow is increased. These two methods (step on reflux and tracer injection) give consistant results. Note Exp. 9 is performed with a reduction in reflux flow, such that this result is not used.

Bibliography

1. Bennett, D.L., R. Agrawal and P.J. Cook, "New Pressure Drop Correlations for Sieve Tray Distillation Columns", *AiChe Journal*, Vol.29, No. 3, pp. 434-443, 1983
2. Coulson, J.M., Richardson, J.F., Sinnott, R.K., Chemical Engineering, Volume 6, Design, *Pergamon Press*, 1985
3. Lockett, M.J., "Distillation tray fundamentals", *Cambridge University Press*, 1986
4. Perry, H.P. and D. Green (Ed.), "Perry's Chemical Engineers' Handbook", *McGraw-Hill Chemical Engineering Series*, 50th edition, 1984 Chapter 18
5. Rademaker, O., J.E. Rijnsdorp and A. Maarleveld, "Dynamics and Control of Continuous Distillation Units", *Elsevier, Amsterdam*, 1975
6. Stichlmair, J., Grundlagen der Dimensionierung des Gas/Flüssig Kontaktapparates Bodenkolonnen, *Verlag Chemie, Weinheim, New York*, 1978

Notation

A	active area	m^2
C_0	discharge coefficient	
dp	dry pressure drop over tray	N/m^2
D	molar distillate flow	mol/min
	diameter	mm
F	molar feed flow	mol/min
	tracer flow	mol/min
g	standard acceleration of gravity	m/s^2
$G(s)$	Process transfer function	
h	molar enthalpy	$GJ/kmol$
h	height	mm
K	process gain	
	equilibrium constant	
K_s	dimensionless velocity	
L	molar liquid	mol/min
	length	m, mm
L_q	volumetric liquid flow	m^3/s
M	molar holdup of liquid	mol
MW	molecular weight	kg/kmol
N	number	
Q_b	heat input	kJ/s
q_l	flow rate per unit length	$m^3/(minm)$
p	pressure	Pa, bar, N/m^2
q	liquid flow	m^3/s

t	time	h, min, s
T	temperature	$^{\circ}C$
v	velocity	m/s
y_i	mole fraction of component i in vapor	
x_i	mole fraction of component i in liquid	
z_i	mole fraction of component i in feed	
	mole fraction of component i in tracer	

Greek Symbols

α	equilibrium constant	
Δ	deviation	
ϵ	surface roughness	mm
ρ_m	liquid mass density	kg/m^3
ρ	liquid molar density	$kmol/m^3$
π_i	empirical coefficient	
ϕ	froth density	
τ	time constant	s
θ	time delay	s
ζ	friction loss factor	

Subscripts

active	active tray area
apron	downcomer apron
B	bottom, reboiler
d,dc	downcomer
D	distillate
i	identifier
in	flow into the system volume
n	dummy index for number of components
l	liquid phase
out	flow out of the system volume
t	tray, total
v	vapor phase
0	initial state
∞	final

Appendix C

Linearized Tray Hydraulics

C.1 Tray hydraulics

The hydraulics of a distillation column is of crucial importance for the overall dynamic response. Models with a rigorous tray hydraulics tend to be very complex. In this section we use the simplified tray hydraulics which is proposed by Rademaker (1975) and Skogestad (1988). Simple expressions for the key parameters describing the hydraulics, namely the hydraulic time constant τ_l and the effect of vapor flow on liquid flow the vapor constant λ will be derived. For simplicity, the vapor holdup is neglected and constant molar flow is assumed $V_{in} = V_{out}$.

The liquid flow leaving the tray L_{out} equals L_{in} at steady state, dynamically it is affected by both vapor V_{in} and liquid L_{in} entering the tray. The liquid flow from the stage depends upon the liquid holdup and the impulse of the vapor flow characterized by the stage geometry and the loading condition. An increase in L_{in} will increase the holdup and gradually L_{out} , this time constant is denoted τ_l . A change in vapor flow V_{in} has no steady state effect on L_{out} , but may have an initial effect for $\lambda \neq 0$. The increased vapor flow will reduce the froth density on the tray which increases the froth height and such the froth flow leaving the tray. Simultaneously, an increase in V_{in} causes an increase in pressure drop between the stages. The increase in differential pressure increases the liquid backup in the downcomer which reduce temporarily the liquid flow L_{out} leaving the downcomer and thus reduce the liquid height on the tray h_{cl} below.

The sign and magnitude of λ depends on which of the two effects (increased downcomer backup or change in froth density) dominates, both effects are strongly dependent on the tray design. Since λ and τ_l are strongly dependent on stage geometry and column loading a different values may be found for the rectifying and stripping section.

$$dM = \left(\frac{\delta M_i}{\delta L_{out}} \right)_L \cdot dL_{out} + \left(\frac{\delta M_i}{\delta V_{in}} \right)_L \cdot dV_{in} \quad (C.1)$$

$$dM = \tau_L \cdot dL_{out} + \tau_V \cdot dV_{in} \quad (C.2)$$

Rademaker, 1975

$$dL_{out} = \left(\frac{\delta L_{out}}{\delta V_{in}} \right)_V \cdot dV_{in} + \left(\frac{\delta L_{out}}{\delta M} \right)_V \cdot dM \quad (C.3)$$

$$dL_{out} = \lambda \cdot dV_{in} + \frac{1}{\tau_L} \cdot dM \quad (C.4)$$

compare both equations give:

$$\lambda = \frac{\delta L}{\delta V} \Big|_{M_i} = - \frac{\left(\frac{\delta M_L}{\delta V} \right)_L}{\left(\frac{\delta M_L}{\delta L} \right)_V} = - \frac{\tau_V}{\tau_L} \quad (C.5)$$

It is assumed that the liquid flow, L_{out} , from a stage is directly affected through the vapor flow in, V_{in} , (indirectly through its effect on the liquid level) and by the holdup (mass) on the tray M . Linearizing this relation yields (Rademaker *et al.* 1975, Skogestad and Morari 1988)

$$\begin{aligned} dL_{out} &= \left(\frac{\delta L_{out}}{\delta V_{in}} \right)_M dV_{in} + \left(\frac{\delta L_{out}}{\delta M} \right)_V dM \\ &= \lambda dV_{in} + \frac{1}{\tau_L} dM \end{aligned} \quad (C.6)$$

Note that this relationship is assumed to hold dynamically. We want to obtain λ and τ_l from steady state relationships for the liquid holdup on the stage found from design data of the column. The liquid holdup can be expressed by the following relations $M = f(L, V, \Delta p)$ with pressure drop $\Delta p = f(L, V)$. Linearize these expressions and assume $L_{in} = L_{out}$ yields:

$$\begin{aligned} dM &= \left(\frac{\delta M}{\delta L_{out}} \right)_V dL_{out} + \left(\frac{\delta M}{\delta V_{in}} \right)_L dV_{in} \\ &= \tau_L dL_{out} + \tau_V dV_{in} \end{aligned} \quad (C.7)$$

Note that this equations only holds at steady state. After obtaining τ_l and τ_v we may express λ by

$$\lambda = - \frac{\tau_V}{\tau_L} \quad (C.8)$$

This follows by setting $dM = 0$ in equation C.6 and C.7 and rearrange to get $(\delta L_{out}/\delta V_{in})_M$.

For a physical explanation of λ we assume a constant liquid flow (no external change of reflux to the top tray). The liquid holdup on the tray has a negative slope with respect to V if λ is positive, this is an increase in vapor flow give an decrease in liquid holdup of each tray (decrease of froth density ϕ), excess liquid will be dumped on the next tray, assuming the downcomer level ($h_{dc} \approx h_{cl}$, Eq.: C.14) remains constant. The increase in vapor flow result in an temporarily increase in internal flow of liquid. (negative sign of λ = internal liquid flow is temporarily decreased while the tray holdup increases).

C.2 Estimation of hydraulic time constants from column design data

The liquid holdup distribution on the stage (tray plus downcomer) is shown in Figure C.1. In this section the vapor holdup on the stage is neglected, further all liquid holdup is in terms of clear liquid.

The liquid holdup depends on geometry, liquid and vapor flow. The liquid holdup of a stage can be split up into liquid on the tray M_{tray} and in the downcomer M_{dc} . The liquid holdup on the tray can be divided into liquid under, M_{uw} , and over, M_{ow} , weir. The holdup in the downcomer consists of the liquid in the seal pan M_{seal} (or behind the inlet weir), holdup due to hydrodynamic losses under the downcomer apron, M_{loss} , holdup due to dry pressure drop M_{dry} and the amount of liquid corresponding to the clear liquid height on the tray M_{dcl} . The liquid holdup in the seal pan is independent of the vapor or liquid flow. Since the height of clear liquid on the tray and the corresponding height of liquid in the downcomer (denoted h_{cl} in Figure C.1) depend equally on liquid and vapor flow, these holdups are combined to M_{cl} . To simplify the computation of the partial derivatives we combine the liquid holdups on the stage dependent on the vapor flow to M_{cl} and consider the liquid flow dependent part M_{ow} separately.

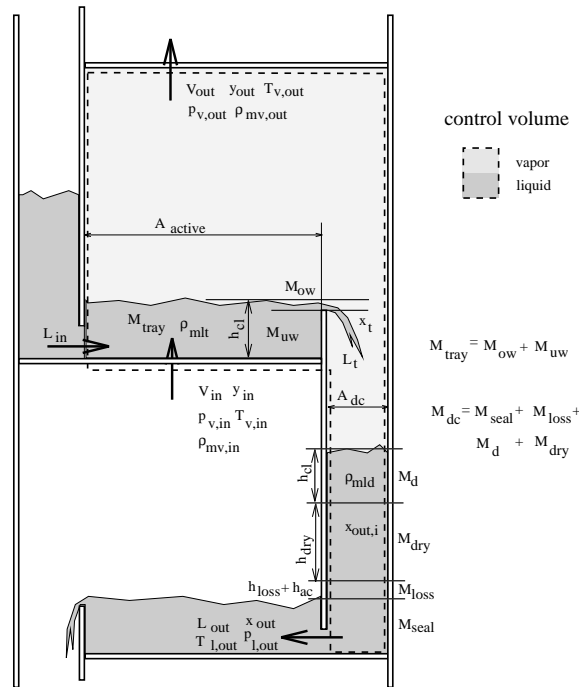


Figure C.1: Control volume on a stage

The holdup is related to geometry and flows by the flowing relations:

- liquid on stage corresponding to the clear liquid height $M_{cl} = f(L_{out}, V_{in})$

$$M_{cl} = M_{tray} + M_{dcl} \tag{C.9}$$

$$M_{tray} = M_{uw} + M_{ow} \quad (C.10)$$

$$M_{tray} = A_{active} \cdot \rho_l \cdot h_{cl} \quad (C.11)$$

$$M_{dcl} = A_{dc} \cdot \rho_l \cdot h_{cl} \quad (C.12)$$

$$M_{cl} = (A_{active} + A_{dc}) \cdot \rho_l \cdot h_{cl} \quad (C.13)$$

$$h_{cl} = \phi \left(h_{weir} + \left(\frac{h_{ow}}{\phi} \right)^{\pi_3} \right) \quad (C.14)$$

where the froth density ϕ is strongly dependent on the vapor flow

$$\phi = \exp(\pi_1 \cdot \left(u_{active} \cdot \sqrt{\frac{\rho_{mv}}{\rho_{ml} - \rho_{mv}}} \right)^{\pi_2}) \quad (C.15)$$

From equation C.14 we see that the liquid holdup under the weir M_{uw} primary depends on the vapor flow to the stage ($\phi \cdot h_{weir}$), while the liquid holdup above the weir ($\phi \cdot (h_{ow}/\phi)^{\pi_3}$) depends on liquid and vapor flow.

- liquid above weir, $M_{ow} = f(L_{out})$

$$M_{ow} = A_{active} \cdot \rho_l \cdot h_{ow} \quad (C.16)$$

with

$$h_{ow} = 44300 \cdot \left(\frac{L_{out} \cdot MW_l}{\rho_{ml} \cdot 0.5 \cdot D_{weir}} \right)^{0.704} \quad (C.17)$$

- liquid holdup in the downcomer due to dry pressure drop $M_{dry} = f(V_{in})$

$$M_{dry} = A_{dc} \cdot \rho_{ml} \cdot h_{dry} \quad (C.18)$$

$$h_{dry} = \frac{51}{C_o^2} \cdot \frac{\rho_{mv}}{\rho_{ml}} \cdot u_{hole}^2 \quad (C.19)$$

- liquid holdup due to the hydrodynamic loss under the downcomer apron $M_{loss} = f(L_{out})$

$$M_{loss} = A_{dc} \cdot \rho_{ml} \cdot h_{loss} \quad (C.20)$$

$$h_{loss} = \frac{\zeta \cdot v_{dc}^2}{g} \quad (C.21)$$

Assume constant flows over the tray we can express the hydraulic time constant of vapor τ_v and liquid τ_l of Eq.: C.7 by changes in liquid holdup on the stage.

$$\tau_V = \left(\frac{\delta M_{dry}}{\delta V} \right)_L + \left(\frac{\delta M_{cl}}{\delta V} \right)_L \quad (C.22)$$

$$\tau_L = \left(\frac{\delta M_{loss}}{\delta L} \right)_V + \left(\frac{\delta M_{ow}}{\delta L} \right)_V \quad (C.23)$$

Express the holdups with correlations C.10 to C.21 and linearize the nonlinear equations

- M_{cl} clear liquid on tray

$$\frac{\delta M_{cl}}{\delta V} = M_{cl} \frac{\phi(\ln\phi)^2}{V_{in}} \quad (C.24)$$

- M_{dry} liquid holdup in downcomer due to dry pressure drop over tray:

$$\frac{\delta M_{dry}}{\delta V} = 2 \frac{M_{dry}}{V_{in}} \quad (C.25)$$

- M_{loss} liquid height due to pressure drop under downcomer

$$\frac{\delta M_{loss}}{\delta L} = 2 \frac{M_{loss}}{L_{out}} \quad (C.26)$$

- M_{ow} liquid above weir

$$\frac{\delta M_{ow}}{\delta L} = 0.704 \frac{M_{ow}}{L_{out}} \quad (C.27)$$

Combine the equations C.24 to C.27 with C.22 and C.23 and we obtain:

$$\tau_V = 2 \frac{M_{dry}}{V_{in}} + M_{cl} \frac{\phi(\ln\phi)^2}{V_{in}} \quad (C.28)$$

$$\tau_L = 2 \frac{M_{loss}}{L_{out}} + 0.704 \frac{M_{ow}}{L_{out}} \quad (C.29)$$

$$\lambda = -\frac{\tau_V}{\tau_L} = -\frac{2M_{dry} + \phi(\ln\phi)^2 M_{cl} \frac{L_{out}}{V_{in}}}{2M_{loss} + 0.704 M_{ow} \frac{L_{out}}{V_{in}}} \quad (C.30)$$

The hydraulic time constant τ_l estimated from the rigorous model varies from $0.5 \leq \tau_l \leq 3$ and the vapor constant λ is varying from $-5 \leq \lambda \leq -0.5$. Estimate λ from equation C.30 will always give $\lambda \leq 0$.

C.3 Linearization of hydraulics

The liquid holdups on the stage (tray plus downcomer) are divided into:

- M_{cl} : clear liquid on tray and in downcomer, this is liquid under and above weir
- M_{dry} : liquid in downcomer due to dry pressure drop
- $M_{d,loss}$: liquid in downcomer due to flow resistance under downcomer apron
- M_{ow} : liquid on tray above weir

$$\tau_V = \left(\frac{\delta M_{dry}}{\delta_V} \right) |_L + \left(\frac{\delta M_{cl}}{\delta_V} \right) |_L \quad (C.31)$$

$$\tau_L = \left(\frac{\delta M_{loss}}{\delta_L} \right) |_V + \left(\frac{\delta M_{ow}}{\delta_L} \right) |_V \quad (C.32)$$

express the holdups with correlation and linearize:

- M_{cl} clear liquid on tray

$$M_{cl} = (A_T + A_D) \cdot \rho_l \cdot z_{cl} \quad (C.33)$$

$$z_{cl} = \phi \cdot \left(h_{weir} + \left(\frac{h_{ow}}{\phi} \right)^{\pi_3} \right) \quad (C.34)$$

$$\phi = e^{(\pi_1 \cdot K_s^{\pi_2})} \quad (C.35)$$

Table C.1: Parameters in the original Bennett formula and for trays in top and bottom section for the investigated distillation column.

	π_1	π_2	π_3
Bennett	-12.55	0.91	2/3
Rectification section	-9	0.5	1.4
Stripper section	-12.55	0.8	1.4

$$K_s = \frac{V_{in} \cdot MW_v}{A_{active} \cdot \rho_{mv}} \cdot \sqrt{\frac{\rho_{mv}}{\rho_{ml} - \rho_{mv}}} \quad (C.36)$$

$$\frac{\delta M_{cl}}{\delta V} \Big|_L = (A_T + A_D) \cdot \rho_l \cdot \frac{\delta z_{cl}}{\delta V} \Big|_L \quad (\text{C.37})$$

$$\frac{\delta z_{cl}}{\delta V} \Big|_L = \frac{\delta \phi}{\delta V} \cdot \left(H_{weir} + \left(\frac{h_{ow}}{\phi} \right)^{\pi_3} \right) + \phi \cdot \frac{\delta \left(\frac{h_{ow}}{\phi} \right)^{\pi_3}}{\delta V} \quad (\text{C.38})$$

$$\frac{\delta \phi}{\delta V} = \frac{\delta \phi}{\delta K_s} \cdot \frac{\delta K_s}{\delta V} \quad (\text{C.39})$$

$$\frac{\delta \phi}{\delta K_s} = \pi_1 \cdot K_s^{\pi_2} \cdot e^{(\pi_1 \cdot K_s^{\pi_2})} \cdot \pi_1 \cdot K_s^{\pi_2 - 1} \quad (\text{C.40})$$

$$\frac{\delta \phi}{\delta K_s} = \phi \cdot \ln \phi \cdot \pi_1 \cdot K_s^{\pi_2 - 1} \quad (\text{C.41})$$

$$\frac{\delta K_s}{\delta V} = \frac{MW_v}{A_{active} \cdot \rho_{mv}} \cdot \sqrt{\frac{\rho_{mv}}{\rho_{ml} - \rho_{mv}}} \quad (\text{C.42})$$

$$\frac{\delta K_s}{\delta V} = \frac{K_s}{V_{in}} \quad (\text{C.43})$$

$$\frac{\delta \phi}{\delta V} = \phi \cdot \ln \phi \cdot \pi_1 \cdot K_s^{\pi_2 - 1} \cdot \frac{K_s}{V_{in}} \quad (\text{C.44})$$

$$\frac{\delta \phi}{\delta V} = \frac{\phi \cdot (\ln \phi)^2}{V_{in}} \quad (\text{C.45})$$

$$\delta \left(\frac{u}{v} \right) = \frac{u' \cdot v - u \cdot v'}{v^2} \quad (\text{C.46})$$

$$\frac{\delta \left(\frac{h_{ow}}{\phi} \right)^{\pi_3}}{\delta V} = \frac{\delta \left(\left(\frac{h_{ow}}{\phi} \right)^{\pi_3} \right)}{\delta \phi} \cdot \frac{\delta \phi}{\delta V} \quad (\text{C.47})$$

$$\frac{\delta\left(\left(\frac{h_{ow}}{\phi}\right)^{\pi_3}\right)}{\delta\phi} = \frac{\frac{\delta h_{ow}^{\pi_3}}{\delta\phi} \cdot \phi - h_{ow}^{\pi_3} \cdot \frac{\delta\phi}{\delta\phi}}{\phi^{2\pi_3}} = \frac{h_{ow}^{\pi_3}}{\phi^{2\pi_3}} \quad (\text{C.48})$$

note h_{ow} is not a function of vapor flow

$$\frac{\delta\left(\left(\frac{h_{ow}}{\phi}\right)^{\pi_3}\right)}{\delta V} = \frac{\phi \cdot (\ln\phi)^2}{V_{in}} \cdot \frac{h_{ow}^{\pi_3}}{\phi^{2\pi_3}} \quad (\text{C.49})$$

$$\frac{\delta z_{cl}}{\delta V} \Big|_L = \frac{\delta\phi}{\delta V} \cdot \left(H_{weir} + \left(\frac{h_{ow}}{\phi}\right)^{\pi_3} \right) + \phi \cdot \frac{\delta\left(\left(\frac{h_{ow}}{\phi}\right)^{\pi_3}\right)}{\delta V} \quad (\text{C.50})$$

$$\frac{\delta z_{cl}}{\delta V} \Big|_L = \frac{\phi \cdot (\ln\phi)^2}{V_{in}} \cdot \left(H_{weir} + \left(\frac{h_{ow}}{\phi}\right)^{\pi_3} + \phi \cdot \frac{h_{ow}^{\pi_3}}{\phi^{2\pi_3}} \right) \quad (\text{C.51})$$

$$\frac{\delta z_{cl}}{\delta V} \Big|_L = \frac{\phi \cdot (\ln\phi)^2}{V_{in}} \cdot \left(H_{weir} + \left(\frac{h_{ow}}{\phi}\right)^{\pi_3} \left(\frac{\phi^{\pi_3} + \phi}{\phi^{\pi_3}}\right) \right) \quad (\text{C.52})$$

so far, no simplifications are introduced; inspecting Table C.1 $\pi_3 = 1.4$ further is in the range of $0.2 \leq \phi \leq 0.7$ give that $1.4 \leq \frac{\phi^{\pi_3} + \phi}{\phi^{\pi_3}} \leq 1.9$, further $0.5\text{mm} \leq h_{ow} \leq 3\text{mm}$ ($h_{weir} = 30\text{mm}$) such that neglecting the term $\frac{\phi^{\pi_3} + \phi}{\phi^{\pi_3}}$ will not have a large influence.

Neglecting the term $\frac{\phi^{\pi_3} + \phi}{\phi^{\pi_3}}$ leave us with:

$$\frac{\delta M_{cl}}{\delta V} = (A_T + A_D) \cdot \rho_l \cdot \frac{\phi \cdot (\ln\phi)^2}{V_{in}} \cdot \left(H_{weir} + \left(\frac{h_{ow}}{\phi}\right)^{\pi_3} \right) \quad (\text{C.53})$$

$$\frac{\delta M_{cl}}{\delta V} = M_{cl} \cdot \frac{\phi \cdot (\ln\phi)^2}{V_{in}} \quad (\text{C.54})$$

- dry pressure drop: M_{dry}

$$dp_{dry} = g \cdot \rho_{ml} \cdot h_{dry} \cdot 10^{-3} \quad (\text{C.55})$$

$$h_{dry} = \frac{51}{C_o^2} \cdot u_h^2 \cdot \frac{\rho_{mv}}{\rho_{ml}} \quad (C.56)$$

$$u_h = \frac{V_{in} \cdot MW_v}{\rho_{mv} \cdot A_{free}} \quad (C.57)$$

$$M_{dry} = A_D \cdot \rho_l \cdot \frac{dp_{dry}}{g \cdot \rho_{ml}} \quad (C.58)$$

$$\frac{\delta M_{dry}}{\delta V} = A_D \cdot \rho_l \cdot 10^{-3} \cdot \frac{\delta h_{dry}}{\delta V} \quad (C.59)$$

$$M_{dry} = A_D \cdot \rho_l \cdot 10^{-3} \cdot \frac{51}{C_o^2} \cdot \left(\frac{V_{in} \cdot MW_v}{\rho_{mv} \cdot A_{free}} \right)^2 \cdot \frac{\rho_{mv}}{\rho_{ml}} \quad (C.60)$$

$$\frac{\delta M_{dry}}{\delta V} \Big|_L = 2 \frac{M_{dry}}{V_{in}} \quad (C.61)$$

- $M_{d,loss}$ liquid height due to pressure drop under downcomer

$$M_{d,loss} = A_D \cdot \rho_l \cdot h_{d,loss} \quad (C.62)$$

$$d_{p,loss} = \rho_{ml} \cdot g \cdot h_{d,loss} = -\zeta \cdot \rho_{ml} \cdot v_{dc}^2 \quad (C.63)$$

$$v_{dc} = \frac{L_{out} \cdot MW_l}{\rho_{ml} \cdot A_{apron}} \quad (C.64)$$

$$h_{d,loss} = -\frac{\zeta}{g} \cdot \left(\frac{L_{out} \cdot MW_l}{\rho_{ml} \cdot A_{apron}} \right)^2 \quad (C.65)$$

$$\frac{\delta h_{d,loss}}{\delta L} \Big|_V = 2 \cdot \frac{h_{d,loss}}{L_{out}} \quad (C.66)$$

$$\frac{\delta M_{d,loss}}{\delta L} \Big|_V = A_D \cdot \rho_l \cdot \frac{\delta h_{d,loss}}{\delta L} \Big|_V \quad (C.67)$$

$$\frac{\delta M_{d,loss}}{\delta L} \Big|_V = A_D \cdot \rho_l \cdot 2 \cdot \frac{h_{d,loss}}{L_{out}} = 2 \frac{M_{d,loss}}{L_{out}} \quad (C.68)$$

- M_{ow} liquid above weir

$$M_{ow} = A_T \cdot \rho_l \cdot h_{ow} \quad (\text{C.69})$$

$$h_{ow} = 44300 \cdot \left(\frac{L_{out} \cdot MW_l}{\rho_{ml} \cdot 0.5 \cdot D_{weir}} \right) \quad (\text{C.70})$$

$$\frac{\delta M_{ow}}{\delta L} \Big|_V = A_T \cdot \rho_l \cdot \frac{\delta h_{ow}}{\delta L} \Big|_V \quad (\text{C.71})$$

$$\frac{\delta h_{ow}}{\delta L} \Big|_V = 0.704 \cdot 44300 \cdot \left(\frac{MW_l}{\rho_{ml} \cdot 0.5 \cdot D_{weir}} \right) \quad (\text{C.72})$$

$$\frac{\delta M_{ow}}{\delta L} \Big|_V = 0.704 \cdot \frac{M_{ow}}{L_{out}} \quad (\text{C.73})$$

C.4 Summary: Hydraulic time constants

Listing the changes in holdup as equivalent liquid heights

$$\tau_V = \left(\frac{\delta M_{dry}}{\delta V} \right)_L + \left(\frac{\delta M_{cl}}{\delta V} \right)_L \quad (\text{C.74})$$

$$\tau_L = \left(\frac{\delta M_{loss}}{\delta L} \right)_V + \left(\frac{\delta M_{ow}}{\delta L} \right)_V \quad (\text{C.75})$$

$$\frac{\delta M_{dry}}{\delta V} \Big|_L = A_D \cdot \rho_l \cdot 10^{-3} \cdot \frac{\delta h_{dry}}{\delta V} \Big|_L \quad (\text{C.76})$$

$$\frac{\delta M_{cl}}{\delta V} \Big|_L = (A_T + A_D) \cdot \rho_l \cdot \frac{\delta z_{cl}}{\delta V} \Big|_L \quad (\text{C.77})$$

$$\frac{\delta M_{d,loss}}{\delta L} \Big|_V = A_D \cdot \rho_l \cdot \frac{\delta h_{d,loss}}{\delta L} \Big|_V \quad (\text{C.78})$$

$$\frac{\delta M_{ow}}{\delta L} \Big|_V = A_T \cdot \rho_l \cdot \frac{\delta h_{ow}}{\delta L} \Big|_V \quad (C.79)$$

$$\tau_V = \rho_L \cdot \left(A_D \cdot 10^{-3} \cdot \frac{\delta h_{dry}}{\delta V} \Big|_L + (A_T + A_D) \cdot \frac{\delta z_{cl}}{\delta V} \Big|_L \right) \quad (C.80)$$

$$\tau_L = \rho_L \cdot \left(A_D \cdot \frac{\delta h_{d,loss}}{\delta L} \Big|_V + A_T \cdot \frac{\delta h_{ow}}{\delta L} \Big|_V \right) \quad (C.81)$$

$$\lambda = -\frac{\tau_V}{\tau_L} = \frac{10^{-3} \cdot \left(\frac{\delta h_{dry}}{\delta V} \right)_L + \left(\frac{A_T + A_D}{A_D} \right) \cdot \left(\frac{\delta z_{cl}}{\delta V} \right)_L}{\frac{A_T}{A_D} \cdot \left(\frac{\delta h_{ow}}{\delta L} \right)_V + \left(\frac{\delta h_{d,loss}}{\delta L} \right)_L} \quad (C.82)$$

in our case: $A_T \approx 10 \cdot A_D$, most influence by $\frac{\delta h_{dry}}{\delta V}$ and $\frac{\delta h_{ow}}{\delta L}$
express the linearized tray hydraulics on a holdup basis give:

$$\frac{\delta M_{dry}}{\delta V} \Big|_L = 2 \frac{M_{dry}}{V_{in}} \quad (C.83)$$

$$\frac{\delta M_{cl}}{\delta V} = M_{cl} \cdot \frac{\phi \cdot (\ln \phi)^2}{V_{in}} \quad (C.84)$$

$$\frac{\delta M_{d,loss}}{\delta L} \Big|_V = 2 \frac{M_{d,loss}}{L_{out}} \quad (C.85)$$

$$\frac{\delta M_{ow}}{\delta L} \Big|_V = 0.704 \cdot \frac{M_{ow}}{L_{out}} \quad (C.86)$$

$$\tau_V = 2 \frac{M_{dry}}{V_{in}} + M_{cl} \cdot \frac{\phi \cdot (\ln \phi)^2}{V_{in}} \quad (C.87)$$

$$\tau_L = 2 \frac{M_{d,loss}}{L_{out}} + 0.704 \cdot \frac{M_{ow}}{L_{out}} \quad (C.88)$$

$$\lambda = -\frac{\tau_V}{\tau_L} = \frac{2 \cdot M_{dry} + M_{cl} \phi \cdot (\ln \phi)^2}{2 \cdot M_{d,loss} + 0.704 M_{ow}} \cdot \frac{L_{out}}{V_{in}} \quad (C.89)$$

Applying the above given formulas, enable to estimate the hydraulic time constants given in Table C.2. The necessary data are the design data of a distillation column (given in chapter A) as well as reflux and feed flow, reboiler heat input and their respective perturbations.

Table C.2: Operational parameters determined from linearized tray hydraulics

	dim.	Exp. 1	Exp. 2	Exp. 3	Exp. 4	Exp. 5	Exp. 6
L	ml/min	250.0	250.0	380.0	450.0	470.0	470.0
ΔL	ml/min	0.0	0.0	+ 52.8	-35.7	+ 88.4	0/0
F	ml/min	250.0	250.0	250.0	250.0	350.0	350.0
Q_B	kJ/s	3.75	3.6	4.5	5.4	5.79	6.45
ΔQ_B	kJ/s	-0.45	+ 0.45	0.0	0.0	0.0	+ 1.58
p_{btm}	$mbar$	21.9	20.6	26.0	32.0	35.3	54.6
K_s	m/s	0.0160	0.0154	0.0192	0.0230	0.0247	0.0275
$H_{ow,t}$	mm	0.9163	0.9163	1.1141	1.3202	1.4290	1.4290
$H_{cl,t}$	mm	10.1386	10.4637	8.9102	7.7550	7.3665	6.6277
$M_{uw,t}$	mol	1.0383	1.0749	0.8777	0.7245	0.6685	0.5853
$M_{ow,t}$	mol	0.1032	0.1032	0.1254	0.1486	0.1609	0.1609
$M_{dry,t}$	mol	0.1605	0.1479	0.2311	0.3327	0.3825	0.4747
$M_{loss,t}$	$10^{-3} mol$	0.0581	0.0581	0.1012	0.1639	0.2052	0.2052
$\delta M_{cl,t}/\delta V$	s	-10.9513	-11.4629	-8.8136	-6.9254	-6.2712	-5.3333
$\delta M_{dry,t}/\delta V$	s	3.5001	3.3601	4.2002	5.0402	5.4042	6.0202
$\delta M_{ow,t}/\delta L$	s	1.5891	1.5891	1.4638	1.3629	1.3183	1.3183
$\delta M_{loss,t}/\delta L$	$10^{-3} s$	2.2635	2.2635	2.9878	3.8027	4.2554	4.2554
ϕ_t		0.3074	0.3182	0.2599	0.2145	0.1979	0.1733
$\tau_{l,t}$	s	1.5914	1.5914	1.4668	1.3667	1.3225	1.3225
$\tau_{v,t}$	s	-7.4512	-8.1028	-4.6134	-1.8852	-0.8670	0.6869
λ_t		4.6822	5.0916	3.1453	1.3794	0.6555	-0.5194
$H_{ow,b}$	mm	1.5272	1.5272	1.6902	1.8659	2.1564	2.1564
$H_{cl,b}$	mm	18.3793	18.6182	17.4453	16.4803	16.3245	15.6246
$M_{uw,b}$	mol	1.8973	1.9242	1.7738	1.6454	1.5951	1.5163
$M_{ow,b}$	mol	0.1719	0.1719	0.1903	0.2101	0.2428	0.2428
$M_{dry,b}$	mol	0.1605	0.1479	0.2311	0.3327	0.3825	0.4747
$M_{loss,b}$	$10^{-3} mol$	0.2479	0.2479	0.3306	0.4370	0.6605	0.6605
$\delta M_{cl,b}/\delta V$	s	-8.1108	-8.3594	-7.0565	-6.0912	-5.7450	-5.2334
$\delta M_{dry,b}/\delta V$	s	3.5001	3.3601	4.2002	5.0402	5.4042	6.0202
$\delta M_{ow,b}/\delta L$	s	1.2819	1.2819	1.2285	1.1784	1.1089	1.1089
$\delta M_{loss,b}/\delta L$	$10^{-3} s$	4.6768	4.6768	5.4012	6.2160	7.6341	7.6341
ϕ_b		0.5617	0.5697	0.5252	0.4871	0.4723	0.4489
$\tau_{l,b}$	s	1.2866	1.2866	1.2339	1.1846	1.1165	1.1165
$\tau_{v,b}$	s	-4.6107	-4.993	-2.8564	-1.0511	-0.3408	0.7868
λ_b		3.5836	3.8856	2.3150	0.8872	0.3052	-0.7047

C.4.1 Comparison: Experiment - Simulation

The behavior of vapor and liquid flows as well as the changes in holdup distribution during transient operation will be demonstrated. Step changes in the manipulated variables were performed and the responses of the models and the real process are compared. The responses are recorded for open-loop operation.

The response of vapor and liquid flows as well as the changes in holdup distribution during transient operation will be demonstrated. Step changes in the manipulated variables were performed and the responses of the models and the real process are compared. The volumetric reflux and the heat supply to the reboiler are set manually. Figure C.2 shows the response of the product composition to a step in reboiler heat input (Experiment 1, see Appendix B for experimental data).

The temperature profile of Experiment 1 with a reduction in heat supply and the rigorous model is compared in Figure C.3. Reasonable agreement between simulation and experiment has been found for the time interval $0 \leq t \leq 200$ s, for increasing times deviations between simulation and experiment is increasing.

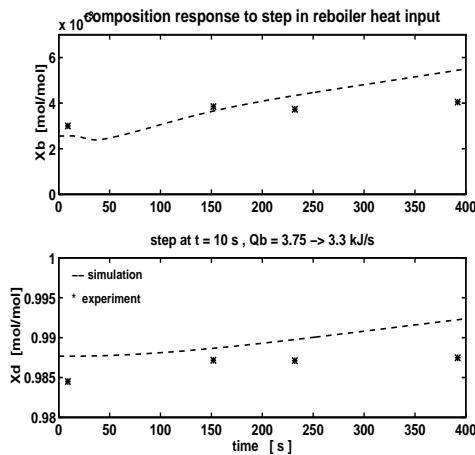


Figure C.2: Experiment 1: Composition response to step change in reboiler effect, (*) experiment, (—) simulation

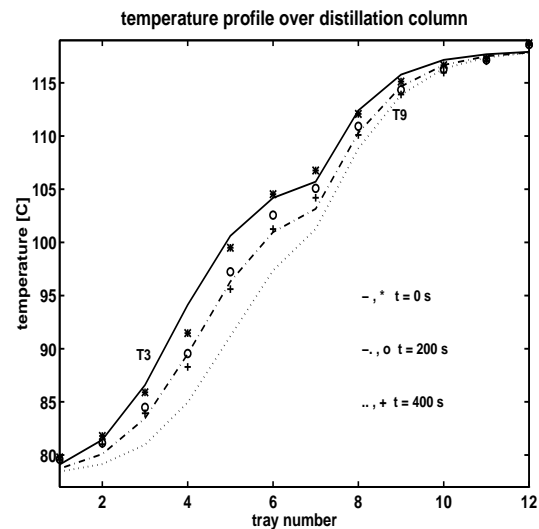


Figure C.3: Experiment 1: Temperature profile over distillation column, 1 = upper most tray of column, 12 = reboiler, (*) experiment, (—) simulation

Appendix D

Multivessel Batch Distillation, Modeling aspects

D.1 Introduction

In this section modeling aspects for the simulation studies for the evaluation multivessel batch distillation column are considered. The model applied for mass and composition balances is presented, further, three different methods to compute the tray temperatures, based on the liquid composition on the trays are considered. The chosen methods are: a) linear temperature curve, b) Clausius-Clapeyron approximation and c) the Antoine-equation. A reasonable correct computation of the temperature is necessary, since the proposed control structure is based on the assumption that a unique relation between the composition in the middle of a column section and the measured temperature exists.

The here presented simulations are performed to allow for the comparison of these models and to verify the applicability of the chosen temperature-composition relation. Further, the basic design of a multivessel batch distillation column for the separation of a four component mixture consisting of methanol, ethanol, 1-propanol and 1-butanol is presented.

D.2 Simulation model

D.2.1 Mass and Component Balance

The model used in the simulations is based on the following assumptions:

- constant relative volatility
- constant molar liquid holdups on the stages (liquid flow dynamics neglect)
- constant molar vapor flows V_i (energy balance neglected)
- constant pressure
- constant tray efficiency (100 %)

- negligible vapor holdup
- perfect mixing on all trays and in all vessels
- total condenser

The distillation column is modeled as a stack of stages (counted from the top) as shown in Figure D.1. Note that the vapor flow V does not pass through the intermediate vessels so these do not contribute to the number of theoretical stages.

The model for stage k in section i consists of a material balance for each component j (M_k is assumed constant)

$$M_k \frac{d x_{j,k}}{dt} = L_i (x_{j,k-1} - x_{j,k}) + V (y_{j,k+1} - y_{j,k}) \quad (\text{D.1})$$

The material balance for a condenser ($i = 1$) is

$$\frac{d (M_i x_{j,i})}{dt} = V y_{j+1,i} - L_i x_{j,i} \quad (\text{D.2})$$

and its mass balance

$$\frac{d M_i}{dt} = V - L_i \quad (\text{D.3})$$

For intermediate vessels (i)

$$\frac{d (M_i x_{j,i})}{dt} = L_{i-1} x_{j-1,i} - L_i x_{j,i} \quad (\text{D.4})$$

with

$$\frac{d M_i}{dt} = L_{i-1} - L_i \quad (\text{D.5})$$

where x_i is the composition in vessel i and $x_{j-1,i}$ is the liquid composition at the bottom of the section above. The liquid flow L_i leaving vessel i is set by a control valve.

The reboiler ($i = R$)

$$\frac{d (M_i x_{j,i})}{dt} = L_{i-1} x_{j,i} - V y_{j,i} \quad (\text{D.6})$$

where

$$\frac{d M_i}{dt} = L_{i-1} - V \quad (\text{D.7})$$

where again the vapor liquid equilibrium is described by Equation D.8.

The above presented models of stage, reboiler and condenser of the multivessel column are readily extended for a continuous columns, by adding a feed to the stage model, as well as product flow to condenser, D_i , and reboiler, B_i , respectively.

Additional to component (Eq: D.1), mass balances (Eq: D.3), and vapor-liquid equilibrium (Eq. D.8) equations to compute the temperature the boiling mixture are required.

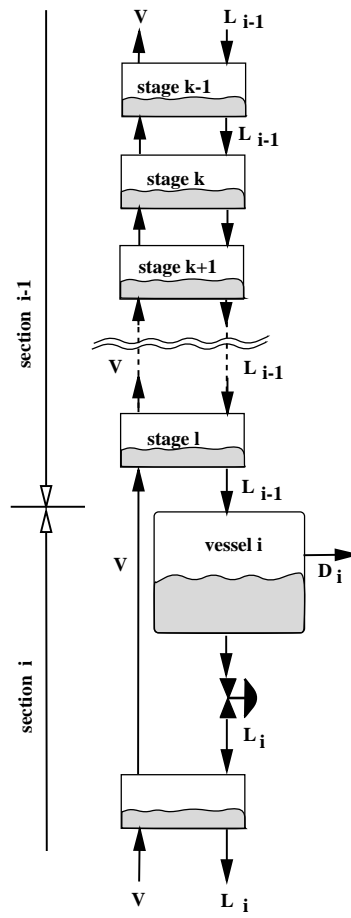


Figure D.1: Connection of trays and vessels for multivessel batch column

D.2.2 Vapor Liquid Equilibrium

The vapor liquid equilibrium data which were used to determine the value of the constant relative volatilities are shown in Figure D.2. From this plot, the relative volatilities given in equation D.13 for the binary systems are determined.

The vapor liquid equilibrium is described by

$$\alpha_{j,H} = \frac{K_j}{K_H} = \frac{y_{j,k}/x_{j,k}}{y_{H,k}/x_{H,k}} \quad (\text{D.8})$$

where H denotes the heaviest component in the mixture. The relative volatilities for the simulation studies were chosen to $\alpha = [10.2, 4.5, 2.3, 1]$, those data are close to the experimental data presented in chapter 4.

D.2.3 Thermodynamic model

For the computation of the boiling point of the liquid mixture three alternatives are chosen:

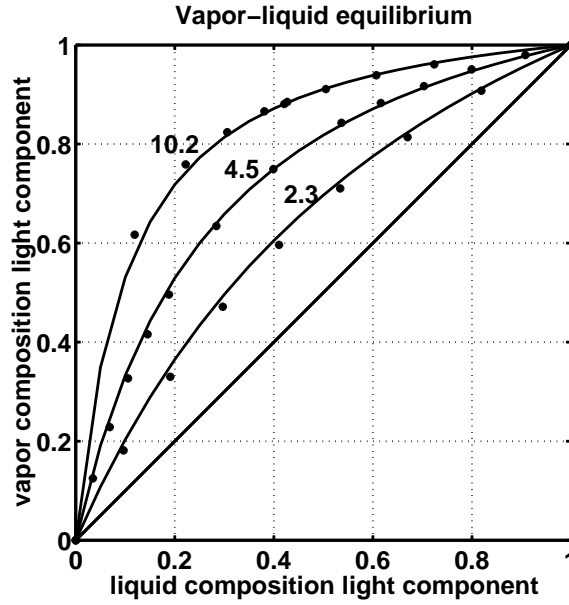


Figure D.2: Vapor-liquid equilibrium of the binary systems methanol-butanol ($\alpha \simeq 10.2$); ethanol-butanol ($\alpha \simeq 4.5$) and 1-propanol-1-butanol ($\alpha \simeq 2.3$)

- linear combination of concentration and the pure component boiling points

$$T_i = \sum_{j=1}^{N_c} x_{i,j} \cdot T_{b,j} \quad (\text{D.9})$$

where $T_{b,j} = [64.7, 78.3, 97.2, 117.7]^\circ\text{C}$

- the total pressure is computed from Raoult's Law for ideal mixtures

$$p_{tot} = \sum_{j=1}^{N_c} x_{i,j} \cdot p_j^{sat}(T) \quad (\text{D.10})$$

and the Clausius-Clapeyron equation for the pure vapor pressures is applied to compute boiling point of the mixture

$$p_j^{sat}(T) = \exp\left(-\frac{\Delta H_{vap,j}}{R} \left(\frac{1}{T_i + 273.15} - \frac{1}{T_{b,j} + 273.15}\right)\right) \quad (\text{D.11})$$

with the gas constant $R = 8.314 \text{ kJ/kmolK}$, the heat of vaporization of the components is chosen to $\Delta H_{vap,j} = [35.0, 38.7, 41.2, 43.14] \text{ kJ/kmol}$ and a total pressure of $p_{tot} = 760 \text{ mmHg} = 1013 \text{ mbar}$.

- the third alternative applies Raoult's law for the pressure computation and the Antoine equation to determine the boiling temperatures of the mixture

$$\log_{10} p_j^{sat}(T) = A - \frac{B}{T + C} \quad (\text{D.12})$$

with

Table D.1: Antoine parameters, for $p = 1013$ mbar

	A	B	C
Methanol	8.08927	1582.271	239.726
Ethanol	8.11220	1592.664	226.184
1-Propanol	8.37895	1788.020	227.438
1-Butanol	7.36366	1305.198	173.427

D.3 Comparison simulation models

Simulation models presented in section D.2 are compared to each other.

In the simulations we consider an equimolar feed mixtures $z_F = [0.25, 0.25, 0.25, 0.25]$. In all three presented simulations, the initial (at $t = 0$) vessel holdup is the same ($M_i = 2.5$ kmol) in all four vessels, and the initial composition in all vessels is equal to that of the feed mixture. In all simulations, the vapor flow is kept constant at $V = 10$ kmol/h. A summary of the column design data is given in Table D.2.

Table D.2: Summary of column data and initial conditions

Number of components	$N_c = 4$
Relative volatility	$\alpha_j = [10.2, 4.5, 2.3, 1]$
Number of stages per section	$N_i = 11$
Vessel holdups	$M_{i,0} = 2.5$ kmol
Tray holdups (constant)	$M_k = 0.01$ kmol
Total initial charge	$M_{tot} = 10.33$ kmol
Reflux flows	$L_{i,0} = 10$ kmol/h
Vapor flow (constant)	$V = 10$ kmol/h

For control purpose we applied proportional-only controllers $\Delta L = K_c \cdot (T_i - T_{s,i}) + L_0$ with control parameters given in Table D.3, the control tray is situated in the center of the column. For simplicity the controller setpoint is chosen to the average boiling point of the two components to be separated in a column section.

In Tables D.3 to D.6 the holdup and vessel compositions are presented for simulations performed with three different assumptions concerning the computation of the mixture boiling point temperature. In Table D.4 a linear boiling point curve is applied, whereas in Table D.5 Raoult's law and the Clausius-Clapeyron equation is used, finally in Table D.6 the Antoine equation is applied to compute vapor pressure of the pure component. The trajectories presented in Figure D.3 to D.5 show the vessel compositions (a), impurities (b), holdups (c), reflux flows (d) and tray temperatures (e) as a function of time.

Table D.3: Data for temperature controllers

	$T_{s,i}$ [$^{\circ}C$]	K_c [$^{\circ}Ch/kmol$]	L_0 [$kmol/h$]	location *
TC_1	71.5	-0.25	10	6
TC_2	87.75	-0.25	10	17
TC_3	107.2	-0.25	10	28

* stage no. from top of column

Table D.4: Vessel holdup and compositions, tray temperatures computed with linear boiling point curve, final batch time $t_b = 3.38 h$

	Vessel 1	Vessel 2	Vessel 3	Vessel 4
M [$kmol$]	2.499	2.441	2.538	2.522
x_1	0.993	0.019	0.0	0.0
x_2	0.007	0.963	0.041	0.0
x_3	0.0	0.018	0.950	0.007
x_4	0.0	0.0	0.009	0.993

Table D.5: Vessel holdup and compositions, tray temperatures computed with Clausius-clapeyron, final batch time $t_b = 3.42h$

	Vessel 1	Vessel 2	Vessel 3	Vessel 4
M [$kmol$]	2.495	2.444	2.539	2.522
x_1	0.993	0.020	0.0	0.0
x_2	0.007	0.962	0.041	0.0
x_3	0.0	0.018	0.950	0.007
x_4	0.0	0.0	0.009	0.993

Table D.6: Vessel holdup and compositions, tray temperatures computed with Antoine, final batch time $t = 2.91h$

	Vessel 1	Vessel 2	Vessel 3	Vessel 4
M [$kmol$]	2.509	2.484	2.515	2.492
x_1	0.991	0.017	0.0	0.0
x_2	0.009	0.954	0.033	0.0
x_3	0.0	0.029	0.950	0.005
x_4	0.0	0.0	0.017	0.995

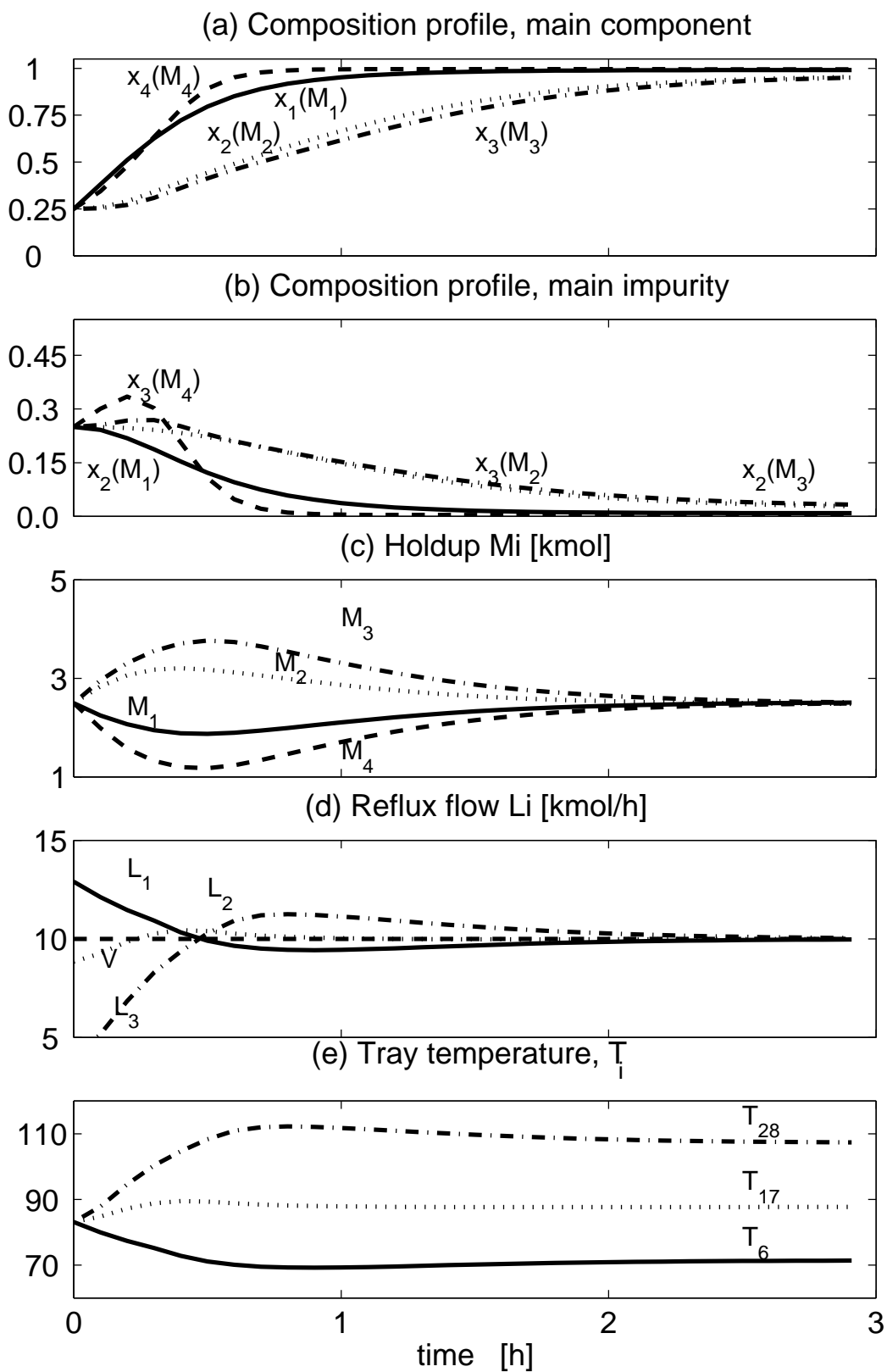


Figure D.3: Thermodynamic model: linear boiling point curve: Vessel compositions (a), impurities (b), holdups (c), reflux flows (d) and tray temperatures (e) as a function of time

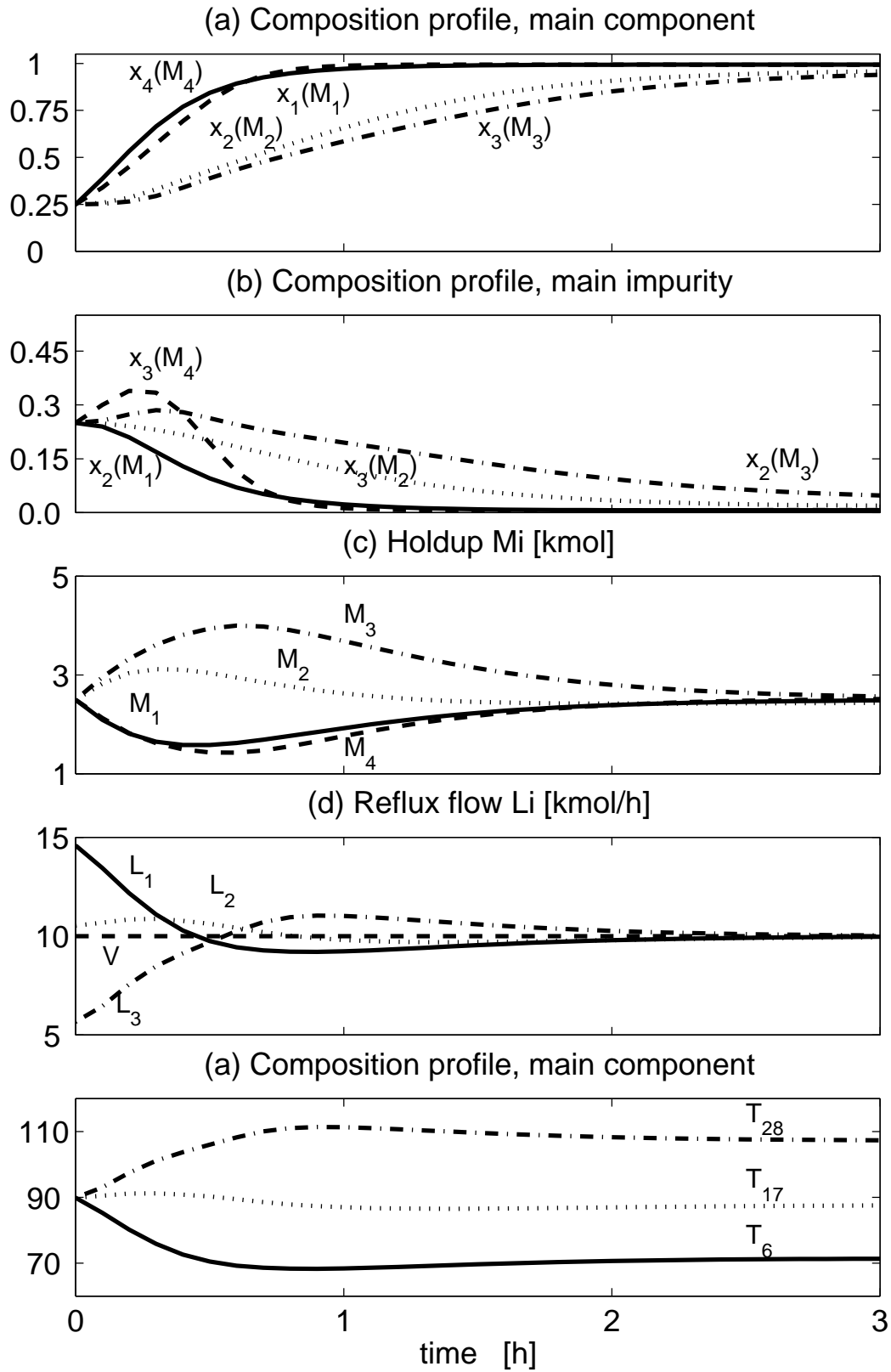


Figure D.4: Thermodynamic model: Raoult's law and Clausius-Clapeyron equation: Vessel compositions (a), impurities (b), holdups (c), reflux flows (d) and tray temperatures (e) as a function of time

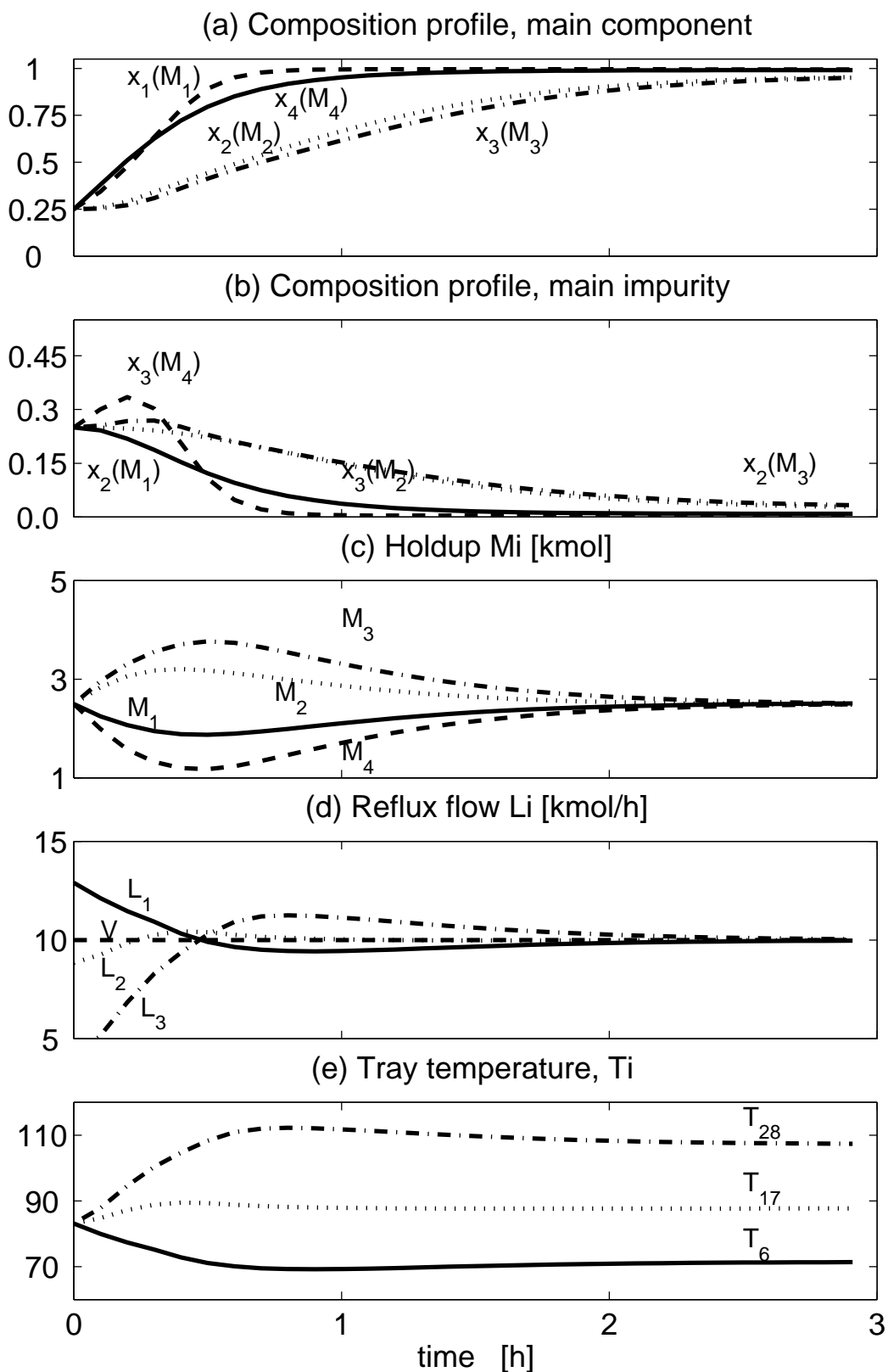


Figure D.5: Thermodynamic model: Raoult's law and Antoine equation. Vessel compositions (a), impurities (b), holdups (c), reflux flows (d) and tray temperatures (e) as a function of time

D.4 Design of the experimental system

The design of the distillation columns for this initial investigation is based on short-cut methods for the determination of the number of trays. Usually, short-cut methods are sufficient, provided good approximations of the relative volatilities of the components are available and the molar flows in the column can be assumed constant.

The determination of the number of stages is possible by two different methods, first based on McCabe-Thiele diagrams ¹, second by application of the Fenske equation to compute the minimum number of stages in a column. For the first method, we have chosen to combine impurities to one pseudo-component, whereas by applying the Fenske method only the main components present in a column section are used. For the experimental design of the multivessel batch we specify the concentration in reboiler and accumulator of the main component to be in excess of *e.g.*: 96 %, further the amount of impurities in the intermediate vessels is restricted to a sum of 7 %. Further, we specify that the impurity ratio $x_{k-1}/x_{k+1} \simeq 1$. A summary of the specified product compositions for the column design is given in Table D.7.

Table D.7: Specification of the product compositions for the pilot plant design

	vessel 1	vessel 2	vessel 3	vessel 4
composition	$x_1(M_1)$ ≥ 0.96	$x_2(M_2)$ ≥ 0.93	$x_3(M_3)$ ≥ 0.93	$x_4(M_4)$ ≥ 0.96
impurities	$x_2(M_1)$ ≤ 0.04	$x_{imp}(M_2)$ ≤ 0.07 *	$x_{imp}(M_3)$ ≤ 0.07	$x_3(M_4)$ ≤ 0.04
impurity ratio		$x_1/x_3 \simeq 1$	$x_2/x_4 \simeq 1$	

* the sum of impurities in vessel k is defined as $x_{imp}(M_k) = \sum_{j=1}^{j=k-1} x_j + \sum_{j=k+1}^{j=N_C} x_j$

The number of trays is determined based on the McCabe-Thiele-method (1925) for binary systems, assuming constant molar flows throughout the column and total reflux. Based on binary vapor-liquid equilibrium data (Gmehlin and Onken, 1977) the number of theoretical stages for operation under total reflux is graphical determined. In Figure D.6 we present experimental data of the vapor-liquid equilibrium of the binary systems methanol-ethanol (MeOH-EtOH), ethanol-1-propanol (EtOH-PrOH) and 1-propanol-1-butanol (PrOH-BuOH). Based on the McCabe-Thiele diagrams presented in Fig. D.6 we find that, under total reflux condition, we need at least 12 theoretical stages to fulfill the given specifications ². Simultaneously, for the binary separations of ethanol-propanol 9 stages are required and

¹The McCabe-Thiele method is not a short cut method if it is applied to a binary mixture, to facilitate the application of this method we introduced pseudo-components to reduce the separation problem to a binary separation. In column section one, primary methanol and ethanol are separated, in vessel 2 a concentration of approximately $x_{PrOH} = 0.05$ is allowed, in the determination of the number of stages we neglect these 5 % and assume that the composition of the vapor entering column 1 to be in equilibrium with the liquid holdup of vessel 2.

²Note that vapor is entering the column sections, the intermediate vessels are treated as mixing tanks without a vapor liquid equilibrium

for propanol-butanol at least 8 stages plus reboiler are necessary³.

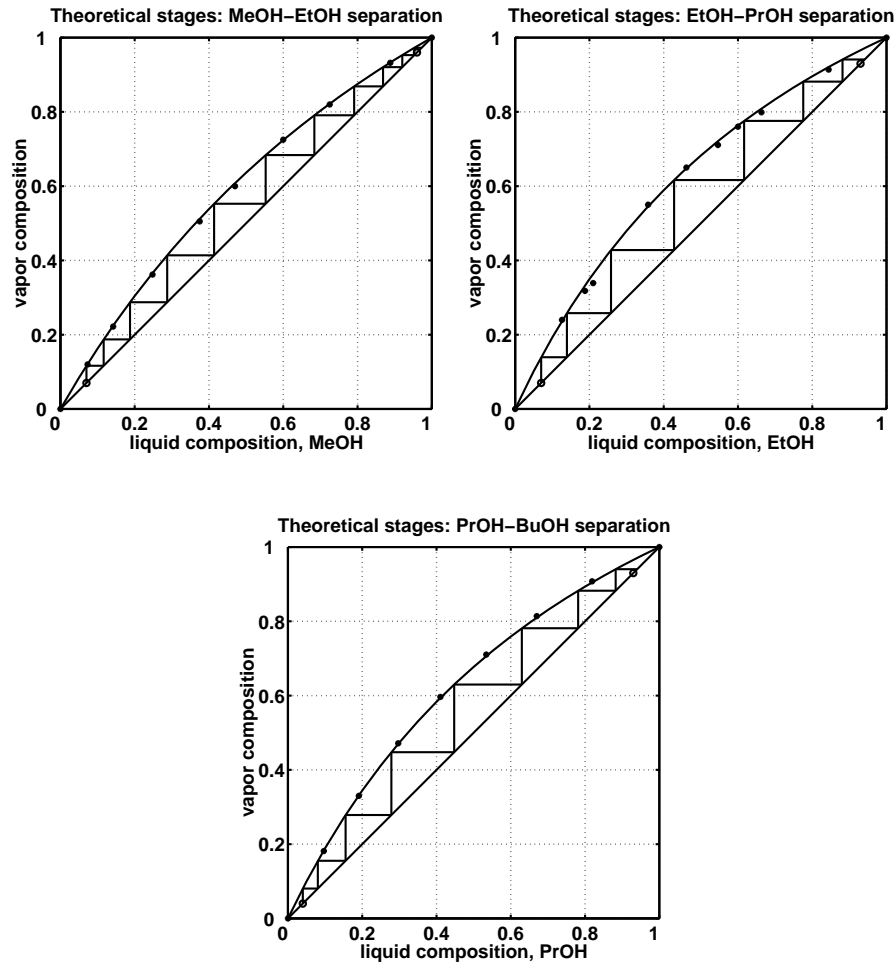


Figure D.6: Number of theoretical stages in a column section determined from the vapor liquid equilibrium for total reflux.

An alternative method is the estimation of the minimum number of theoretical stages based on the Fenske-equation

$$\frac{x_i}{x_j} \Big|_D = \alpha_{i,j}^N \frac{x_i}{x_j} \Big|_B \quad (\text{D.13})$$

assuming constant relative volatilities and total reflux. Introducing the separation factor, S (Shinsky, 1984):

$$S = \frac{\left(\frac{x_i}{x_{i+1}}\right) \Big|_D}{\left(\frac{x_i}{x_{i+1}}\right) \Big|_B} \quad (\text{D.14})$$

³We rounded the number of theoretical stages to the next higher integer.

Combine equations D.13 and D.14 and apply data from to adjacent vessels (*e.g.* D and B) the number of stages in a section can be computed from

$$N_T = \frac{\ln S}{\ln \alpha_{i,j}} \quad (\text{D.15})$$

Note that these equations are originally developed for a binary mixture in a continuous distillation column, but is here applied to a batch column separating a multicomponent mixture.

The resulting number of stages in each column section determined by the McCabe-Thiele method (see Figure D.6) and the Fenske-equation are summarized in Table D.8.

Table D.8: Relative volatilities of the four component system and number of stages necessary for the given separation problem

	methanol- ethanol	ethanol- 1-propanol	1-propanol- 1-butanol
relative volatility $\alpha_{i,j}$	$\alpha_{12} = 1.75$	$\alpha_{23} = 2.15$	$\alpha_{34} = 2.10$
relative volatility $\alpha_{i,4}$	$\alpha_{14} = 7.90$	$\alpha_{24} = 4.52$	$\alpha_{34} = 2.10$
McCabe-Thiele	$N_{T,1} \approx 12$	$N_{T,2} \approx 8$	$N_{T,3} \approx 8 + 1$
Fenske	$N_{T,1} \approx 11.53$	$N_{T,2} \approx 8.56$	$N_{T,3} \approx 8.7$

The multivessel batch distillation column operates under total reflux such that the number of stages is readily given from the vapor-liquid equilibrium data (see Table D.8), assuming a (primary) binary separation in each of the column sections (see Fig. D.6). Nevertheless, the number of trays have to be increased especially in the middle section, such that product qualities can be fulfilled. The assumption of binary separation is valid for the columns separating the lightest and next lightest as well as heaviest and next heaviest components. In the intermediate columns more than two components are present, such that the number of stages has to be increased.

Further, the assumption regarding a linear temperature curve has to be validated, in Figure D.7 experimental data (Gmehlin and Onken, 1977) and the computed temperature are compared. Deviations in temperature between these to models at an equimolar composition are $\Delta T_{dev} = \sum_i^{N_C} x_i \cdot T_{b,i} - T = [1, 2.2, 1.7]$ for the binary systems methanol-ethanol, ethanol-1-propanol and 1-propanol-1-butanol, respectively.

D.5 Discussion

The constant relative volatilities determined from the binary vapor liquid equilibrium data, with reference to the most heavy component (1-butanol) are applied in the simulation model primarily to allow for a convenient model formulation (see Eq. D.8). One might argue that the binary vapor-liquid equilibria for the binary systems MeOH-EtOH, EtOH-PrOH and PrOH-BuOH should be applied, as we used for the determination of the number of trays in the column sections of the pilot plant. The binary vapor liquid equilibrium data are $\alpha_{i,j} = [\alpha_{MeOH,EtOH}, \alpha_{EtOH,PrOH}, \alpha_{PrOH,BuOH}] = [1.7, 2.2, 2.1]$, combine these data

such that the heaviest component is used as reference, give $\alpha_{i,BuOH} = [7.9, 4.6, 2.1, 1]$. For the simulation studies we applied $\alpha_{i,BuOH} = [10.2, 4.5, 2.3, 1]$ where all components are directly related to butanol. It can be seen that the application of the two “set” of relative volatilities will only have influence on the split of methanol-ethanol. The difference will be in the shape of the response, the separation will be slightly slower and further the purity of the product will be less for a given number of stages because of the lower relative volatility between component 1 and 2. Nevertheless, consider the split of these two components simply by adjusting the number of trays the product purity will increase and the batch time will decrease.

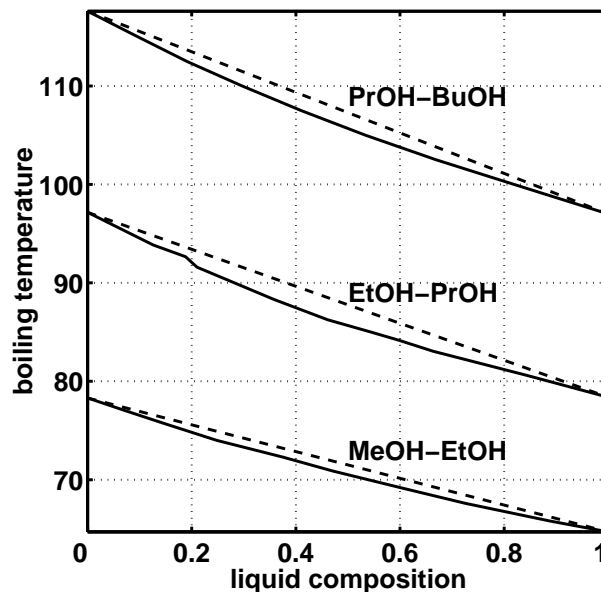


Figure D.7: Comparison linear temperature curve to experimental data

The above presented simulations are performed with different procedures to determine the boiling point of the mixtures along the column. The linear boiling curve assumption may seem very crude. However, comparison of the simulation performed with this assumption show only minor deviations from simulations performed with Raoult’s law for ideal mixtures and the Clausius-Clapeyron equation for the pure component vapor pressure. The Clausius-Clapeyron equation give reasonable results of the vapor-pressure relation over the temperature range from the triple-point to the critical point. For general use the Antoine-equation is preferred to approximate the vapor-pressure relation. Nevertheless, as can be seen from the above presented simulations, only minor deviations exist between the three models. The controlled temperature responses are close to each other, both in shape and time.

The constant molar flows flow assumption, see section D, has to be compared to a variation in heat of vaporization in the order of 20 % with respect to the heaviest component. Implementation of an energy balance in the model will have some influence on the dynamics, since a variation in the heat of vaporization, assumed adiabatic operation, result in a considerable change in molar flows throughout the column. This will have some influence on the duration of the separation, but not on the final product composition. The final product composition is

determined from the vapor liquid equilibrium. The final batch time of these simulations vary from $t_f = 2.91 h$ (see Table D.6 to $t_f = 3.42 h$ (see Table D.5; minor deviations are found for both vessel compositions and vessel holdups.

The design of the column based on the vapor liquid equilibrium of the binary systems is a simple and straightforward procedure, considering an ideal mixture. The number of stages determined by the two presented methods are rather close to each other.

D.6 Conclusions

The results show that the assumption of a linear boiling point curve for temperature computation give similar results compared to the more advanced simulations performed with Raoult's law and the Clausius-Clapeyron equation or the Antoine equation. For simplicity, the linear boiling point curve assumption is used for further simulations. The comparison of the modeling assumptions (constant relative volatilities and linear boiling point) to vapor-liquid equilibrium and bubble-point temperature of the experimental system show only minor deviations, such that the basic design of the experimental column presented in chapter 4, is made simulations with the data given in Table D.8.

For the presented simulations the dynamics and control of the multivessel batch distillation column are only slightly affected on the type of thermodynamic chosen. If the investigations are directed towards the design of a multivessel batch distillation column were a less ideal mixture is separated more rigorous thermodynamic relations should be applied to determine the length of the column sections, further optimization of the setpoints and vapor and liquid flow should be performed to achieve a minimum batch time.

For further research considering the multivessel batch distillation column, the following order of increasing complexity in the simulation model should be considered:

- Investigations on the start-up of the column:
A model with constant relative volatilities, with either $\alpha_{i,i+1}$ or $\alpha_{i,H}$ will be sufficient to determine a start-up procedure for the column with respect to practicability and minimum time consumption, assumed a rather ideal mixture is considered.
- For optimizations with respect to less ideal mixtures, the vapor liquid equilibrium could be described by:
 1. implement K-values, dependent on T and P
 2. implement K-values, dependent on T, p, x_i , y_i
- For investigations considering the application of the process for non-ideal mixtures, rigorous thermodynamics with mass, component and energy balance modeled as an UV-flash should be considered.

The above presented order of model complexity should be applied for research directed towards the application of the multivessel batch distillation column to separate mixtures with azeotropes and heteroazeotropes with the proposed feedback control structure.

Bibliography

1. Gmehling, J. and U. Onken, "Vapor Liquid Equilibrium Data Collection, 2 a, Organic Hydroxy Compounds: Alcohols", *Dechema Chemistry Data Series* Vol. 1, Part 2a, 1977
2. Shinskey, F.G., "Distillation Control", 2nd edition., McGraw-Hill, New York, 1984

Appendix E

Experiments: Multivessel Batch Distillation

In this chapter, some of the experiments performed during the development of the multivessel batch distillation column are presented. These experiments were performed to develop the multivessel batch distillation column from its initial design to working conditions, as well to improve the operation procedure. Note we present only a few of the performed experiments, a complete listing of experiments with the most important data is given in chapter 4. The process itself and the operation strategies are presented previously in chapter 4, the experimental set up is presented in chapter A, we refer to these chapters for more information.

E.1 Experiment 1

The experiment was started from an empty column and all liquid collected in the reboiler. The temperature of the system was $T = 20^{\circ}C$, such that approximately 0.5 h are used to heat up the reboiler charge and introduce vapor to the column. Reboiler duty at “steady state” (which is here defined as experiment termination) for the experiment performed 28.november.1995 is computed from a control signal $u = 4$ (40 % on) which corresponds to a heat input of $Q_b \approx 350J/s$.

The experiment is performed with PI-controllers ($K_C = 4.5ml/minK$, $\tau_I = 3.5min$) to achieve offset free tracking of the temperature in the columns. The PI-controller are necessary for a rather fast stabilization of the controlled temperatures in the column.

As soon as vapor was condensed the controllers of the valves were activated (see Figure E.2, bottom), the initial increase in temperature force the PI-controllers to open the valves ($t = 0.5 h$) and close them as soon as temperature stabilizes. The fast initial temperature increase is caused by (primary) methanol vapor entering the column, being condensed and recycled to the column.

This procedure is chosen as an initial operation strategy, vessels are filled up on start-up and liquid is introduced to the column section as soon as the controllers are activated. The experiment was performed with tracking of all setpoints (T1.2, T2.2 and T3.2) from the start and without a minimum reflux to the column sections. The final product composition of this

experiment is shown in Table E.1, we see that even if the temperature setpoint in column section 2 is achieved (see Figure E.1) we do not achieve the desired product composition. The desired product composition is in excess of $x = 0.95$ of the main component.

Initial feed charge Analysis of final product composition

Table E.1: Initial feed charge

component		methanol	ethanol	n-propanol	n-butanol
density	kg/m^3	791.4	789.3	803.5	809.8
molar weight	$kg/kmol$	32.04	46.07	60.11	74.12
$\Delta H_{vap}^{T_b}$	KJ/mol	35.0	38.7	41.22	43.14
volum	l	0.4	0.53	0.64	1.2
holdup	mol	9.88	9.08	8.55	13.11
composition		0.243	0.224	0.210	0.323

Table E.2: Final product composition

component	methanol	ethanol	n-propanol	n-butanol
Experiment 0: 27. november. 1995				
Vessel 1	0.982	0.016	0.002	0.000
Vessel 2	0.012	0.960	0.021	0.008
Vessel 3	0.003	0.041	0.924	0.032
Vessel 4	0.001	0.002	0.050	0.947
Experiment 1: 28. november. 1995				
Vessel 1	0.9693	0.0304	0.0002	0.0000
Vessel 2	0.4258	0.5473	0.0244	0.0025
Vessel 3	0.0017	0.0480	0.9432	0.0071
Vessel 4	0.0015	0.0021	0.0867	0.9098

Note: Experiment 0 was a training experiment, to achieve samples for GC-test and final test of equipment, no data logging during the experiment

Analysis of experiment 0 and 1 shows that even if all temperature setpoints in the column sections are satisfied, it does not necessarily mean that also the compositions in the vessels meet the product requirements. The temperature profile in column corresponds to simulation where we have an equal composition of the main component of $x \geq 0.9$ in the vessels. On contrary, experiment 1 result in a ratio of MeOH:EtOH = 1:1.

Problems during this experiment arise due to the accumulation of an excess of lighter components in accumulator and intermediate vessels. The reboiler was almost emptied when reflux (L_1) was recycled at $t = 1.5 h$. The step in temperature in vessel B at $t = 1.5h$ is

due to the manner vessel temperature control is performed, the heater is activated when a constant reflux flow is achieved.

The temperature responses in vessels 1 to 4 and in column section 1 to 3 is shown in figure E.1. We see that the temperature control of the vessels is rather noisy. Use the vessel temperature as indication for the composition is correct for a “primary” binary mixture, but will give a non-unique relation composition-temperature for a multi-component mixture.

The manipulated variables reboiler heat duty Q_b and the signal to the reflux control valves is shown in figure E.2. In Figure E.2 we present the manipulated variables reboiler heat duty Q_b [kJ/s] and the reflux flow control signals L_i (in % time the solenoid valve is open).

Discussion of experiment

From figure E.2 we find at steady state $t \geq 4.5h$ the valves are open for $L_{v,1} = 40\%$; $L_{v,2} = 25\%$; $L_{v,3} = 57\%$ of their cycle time. This is $L_{v,1} = 0.7 \cdot L_{v,3}$ and $L_{v,2} = 0.43 \cdot L_{v,3}$. From an estimation of the volumetric reflux flow, assuming constant molar liquid ($L_{m1} = L_{m2} = L_{m3}$) and vapor flow V in the column (total reflux operation at steady state) we expect to get a reflux on volume basis which is

$$L_{m,i} = \frac{\rho_{MeOH} * L_{v,MeOH}}{M_{MeOH}} = \frac{\rho_{EtOH} * L_{v,EtOH}}{M_{EtOH}} = \frac{\rho_{PrOH} * L_{v,PrOH}}{M_{PrOH}} \quad (E.1)$$

We expect to have one primary component and thus assume that we can neglect mixture effects and assume that the flow regimes in all three valves are identical. With the volumetric flow of $L_{v,MeOH} = L_3$ as basis, we expect that:

$$L_{v,PrOH} = \frac{\rho_{MeOH}}{\rho_{PrOH}} \cdot \frac{M_{PrOH}}{M_{MeOH}} \cdot L_{v,MeOH} \quad (E.2)$$

Due to the similar density of the components at boiling point $\rho_{MeOH}/\rho_{PrOH} \simeq 1$, by neglecting this influence we can estimate the liquid flow ratios.

$$L_1 = L_{v,PrOH} \simeq \frac{M_{PrOH}}{M_{MeOH}} \cdot L_{v,MeOH} = 1.88 \cdot L_{v,MeOH} \quad (E.3)$$

$$L_2 = L_{v,EtOH} \simeq \frac{M_{EtOH}}{M_{MeOH}} \cdot L_{v,MeOH} = 1.44 \cdot L_{v,MeOH} \quad (E.4)$$

During start-up from a cold column we primary have light components in the column sections (methanol and ethanol), these components have lower boiling points. The final product composition will be wrong when only the temperature in the column is observed, without observing the reflux flow ratio's lighter component will be accumulated/recycled in the lower sections (the reflux valves are closed initially until holdup is established) and not (as expected) accumulate in the upper vessels. This recycling of light component in the lower column sections enables the implementation of the temperature setpoints with low volumetric reflux flows, due to the low boiling point of the mixture.

Improvement of Experiments

- Avoid flooding in the column during start-up, if the column is (partially) flooded the separation efficiency will be reduced. Flooding towards the end of the separation is caused by the changing molecular weight of the mixture in the bottom. As composition x_4 increases and the vapor flow is kept constant, the column will be overloaded due to the increase in molecular weight.

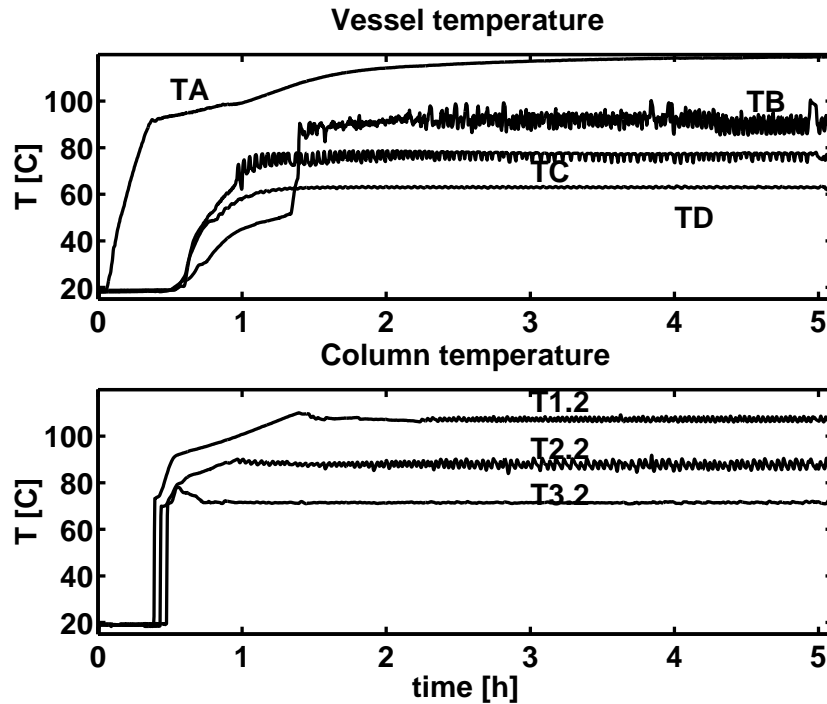


Figure E.1: Temperature responses, experiment 1

Flooding of the column is most likely when x_4 increases, since the mass flows are extensive ($M_{BuOH} = 2 \cdot M_{MeOH}$), such that the heat input has to be reduced over the course of the experiment. Further the viscosity of butanol (component 4) is larger compared to methanol, such that the flow regime in the column is changing due to a change in composition.

- Oscillations in liquid temperature out of vessels 2 and 3 is most probably caused by the chosen setpoint (should be well below boiling point of mixture). The setpoint should be set to the average of the column temperature above and below the vessel during start-up to avoid local boiler. Towards the end of the separation, the setpoint should be set such that $T_{set} = T_b - 1$. Additionally detune temperature controller, lower gain and increase integral time.
- Oscillations in temperature of vessel 2 are caused by combination of oscillations in reflux to column section 2 and oscillations in the heat input to vessel 3 as well as the chosen temperature setpoint in this vessel. Additional vapor is send into column 2 from vessel 2 which result in an increase in temperature at the sensor for $T_{2,2}$, give

an increase in liquid flow from the vessel above, such that more light component is recycled to the column. This in turn increase the amount of light component in vessel B, since the boiling point of the light component is lower and the mixture boiling point temperature in the vessel decrease. The controller will try to keep the temperature constant and increase the heat input. If we isolate this effect, the positive feedback in this loop will result in an unstable operation, since liquid will accumulate in the column (simultaneous increase in both liquid and vapor).

This effect is similar to the interactions in a one point control scheme of a continuous distillation column (LV-control), where the product composition is controlled by a temperature sensor in the center of the column and reboiler temperature/composition is kept constant.

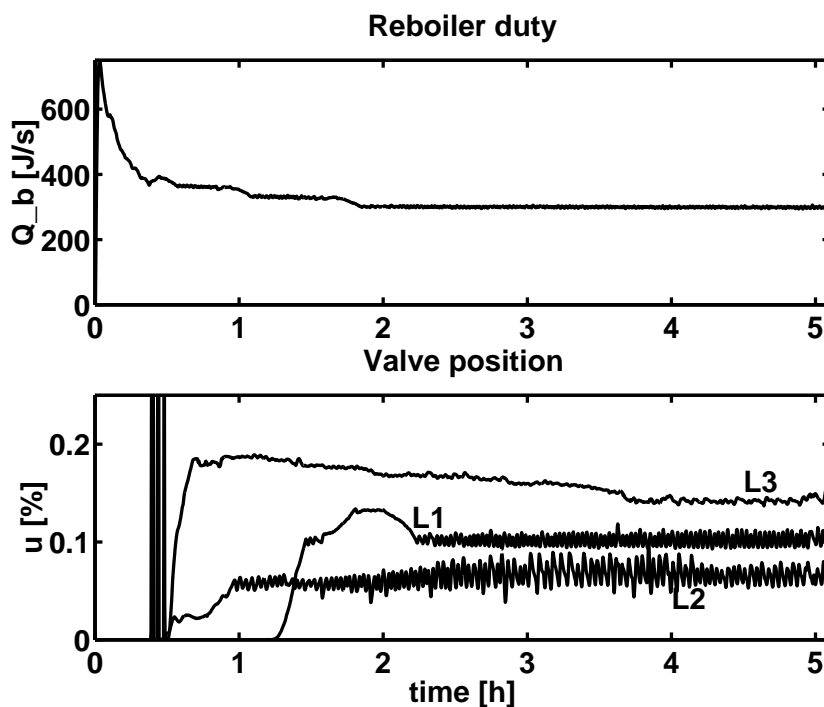


Figure E.2: Manipulated variables, experiment 1

- Oscillations in temperature $T_{2,2}$, L_2 and T_B match rather well from the frequency of oscillations, thus the reflux controller has to be detuned and the setpoint of the vessel temperature has to be adjusted to avoid an intermediate boiler.
- The increase in heavy component in the reboiler give an increase in heat of vaporization by approximately 22 % over time, if the vapor flow is assumed to be constant (on a molar basis) we have to have a higher energy input to the reboiler as x_4 increases. Nevertheless, the effect of viscosity and molecular weight enforce a reduction in heat input as butanol composition increases to keep the column operating.

The heat input is reduced over time due to the fact that the temperature difference between the reboiler surface and the reboiler holdup decrease over time. Adjust the

surface temperature setpoint such that $\Delta T = T_{surface} - T_4 = const$, thus by controlling the temperature difference between reboiler holdup and heating element surface we can adjust the vapor flow.

1. According to data provided by the vendor, it should be possible to operate at a reboiler duty of $Q_B \simeq 500 J/s$. Assuming constant heat transfer surface and coefficient, we should be able to increase the temperature difference at $t \rightarrow \infty$ to $\Delta T = 150^\circ C$. Previous experiments showed that this corresponds to an operation point close to flooding. Temporary increase in reflux at this operation point in the lowest column result in flooding.
 2. Keep the surface temperature of the reboiler constant, simultaneously the temperature inside the vessel is changing which result in a reduction in temperature difference from heating element to vessel. From the heat input $Q_B = V \Delta h_{vap} = UA \Delta T$, we are actually reducing the heat input during the experiment. Additionally the heat transfer zone (assumed inner surface covered with liquid) decreases which reduce the heat transferred to the system. This effect can be reduced by changing the control structure to control the temperature difference ΔT between reboiler holdup and heating surface, instead of controlling the surface temperature alone.
- Avoid accumulation of light component in column and emptying the reboiler by setting a minimum reflux.
 1. Set constant (minimum) volumetric reflux flow for all the reflux controllers and build up the levels in accumulator and intermediate vessel slowly, e.g: $L1 = L2 = L3$.
 2. Use reflux flow controller in the top section (separation of methanol and ethanol) to compute the flow based on the temperature measurement. During start-up we have primary methanol and ethanol in the column. Thus the liquid returned from vessel's above consist's primary of light component, to remove the lighter components we have to reintroduce the liquid into to the column, and not accumulate it for a considerable time (increase amount of light component) in the respective vessels. Light components accumulated in the lower vessels will increase the distillation time since the lighter component will be kept in the lower part and not transported towards the column top.

The volumetric flows from vessel 2 and 3 are computed based on the amount recycled from the accumulator. Based on the theoretical flows, we could use $L_3 = 1.88 \cdot L_3$ and $L_2 = 1.44 \cdot L_3$. This result in a start-up procedure similar to total reflux start-up of a conventional batch or continuous distillation column since the intermediate vessels are open and only a minor amount is kept back. Advantage from this procedure will be a more "controlled" establishing of the composition profile over the column. Also will the accumulation of light component in the intermediate vessels be reduced. Nevertheless, the filling of the intermediate vessels will require that we set the minimum reflux flow ratio of approximately 1 to achieve an accumulation of liquid in the intermediate vessels

Comparison experiment 1 and simulation

Differences between experiment and simulation:

- in simulation we have distributed liquid evenly over the vessels and reboiler, all compositions are identical and liquid at boiling point, this is we start the column “hot”
- we start the experiment from a cold column, all liquid with a temperature of $T = 20^\circ C$ collected in reboiler
- preheater for liquid in vessels are in operation after a constant reflux flow is achieved
- PI-controllers in experiment where the integral time is increased as time increases, final integral time $\tau_I = 20 \text{ min}$.

We primarily redistribute liquid inside the column according their boiling points. The maximum achievable steady state composition in the vessels is determined by the number of stages in each section. The split between components (pseudo-binary, lower than maximum achievable concentration) is determined by the choice of setpoint in the column section between vessels. Increase the setpoint will reduce the amount of light component in the lower vessel and simultaneously increase the amount of heavy component in the vessel above the sensor location.

Table E.3: Comparison experiment and simulation at final steady state

	Experiment				Simulation			
composition	0.243	0.224	0.210	0.323	0.25	0.25	0.25	0.25
initial charge	40.62 mol				10.33 kmol			
vapor flow	27.23 mol/h				10 kmol/h			
boilup	1.49 h				1 h			

Note: The vapor flow in the experiment is computed with an average heat of vaporization of $\Delta h_{vap} = 40 \text{ kJ/mol}$

Improvements on experimental procedure

- Control strategy changed such that minimum reflux 2 and 3 are dependent on the reflux to column section 1, chosen as default $L_{2,min} = 0.8L_1$ and $L_{3,min} = 0.8L_1$
- The position of temperature measurement in vessels has been moved to the pipe connecting vessel and control valve to give more stable measurement of the liquid temperature
- Temperature setpoint to the auxiliary heaters reduced to reduce possibility of an intermediate reboiler, the heating tapes are only used to compensate for possible heat losses.

E.2 Experiment 2, 06.december.1995

Experiment performed at 06.december.1995 with a heat input of $Q_b \simeq 450 J/s$. Experiment performed with “0.8 * total reflux” during start-up, reason for this is to establish simultaneously a composition profile over column and the vessel holdups. Reflux is out of vessels is necessary to ensure that light component are carried towards the column top and not be accumulated in the intermediate vessels. The policy would be slightly different if the vapor was passing through the vessel holdup and not as we build it is bypassed.

Experimental procedure

The reboiler was filled with approximately 2 l of an alcohol mixture containing methanol, ethanol, n-propanol and n-butanol. The entire mixture was fed to the reboiler. The controller of the reboiler was activated and the mixture was heated up. Vapor rising through the column is condensed in the condenser and an initial amount of approximately 100 ml is accumulated in vessel 1, reflux from vessel 1 to the uppermost column is introduced as soon as liquid is available. When the temperature in the center of section 1 ($T_{2,2}$) is close to the chosen setpoint, the controller is placed in automatic. The minimum reflux from reflux control valves L_2 and L_3 is set in relation to the flow computed by the controller which controls L_1 . During start-up we chose a minimum flow of 80 % to ensure that liquid holdup is build-up in vessel 2 and 3. The preheater of the vessels which compensate for heat loss are activated as soon as liquid is accumulated, the setpoints of the preheater control are chosen to be close to the temperature measured on top of each column section below the vessel.

When the temperature in the column section approaches their setpoint the controller are activated. The controller which set the reflux to the lowest and uppermost column section can be activated rather early. The temperature setpoints are chosen to be the arithmetic average of the expected components boiling points being separated in the column section. The controller for L_2 is placed in automatic when the column temperature at thermocouple $T_{2,2}$ is in excess of $81^\circ C$. Later we adjust the setpoint of this controller slowly until we achieve a temperature of $87.75^\circ C$.

During start-up of the column primarily methanol is evaporated and accumulated in vessel 1. The reflux introduced to column section 1 is accumulated in vessel 2 such that a rather high concentration of methanol in this vessel is observed. Recycle this liquid back to column section 2 reduces temperature in this section (due to the low boiling point of the accumulated methanol) which in turn reduces the reflux to the section such that more light component is accumulated in vessel 2. This problem of accumulating methanol in vessel 2 is effectively avoided by adjusting the minimum reflux to column section 2 based on the reflux in column section 1. We introduce light components to the column which is then transported upwards through the column. After stabilizing of the temperature the setpoint of the reflux flow controller is adjusted (in steps of app. $0.5^\circ C$) until the desired setpoint is reached.

In Figure E.3 and E.4 the temperature responses in vessels, column sections, reboiler heat input and reflux flow are shown.

Temperature response

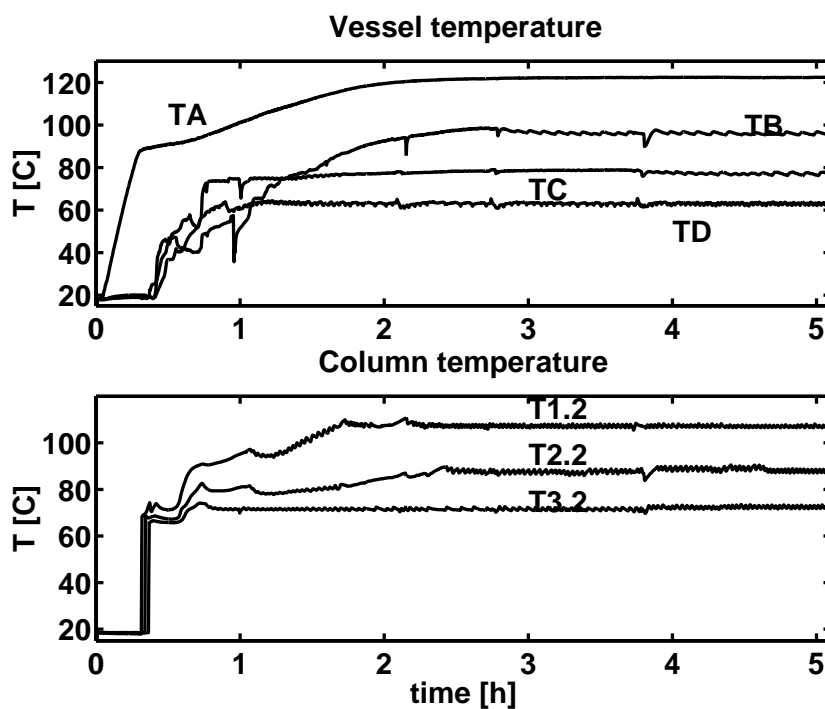


Figure E.3: Temperature responses, experiment 2

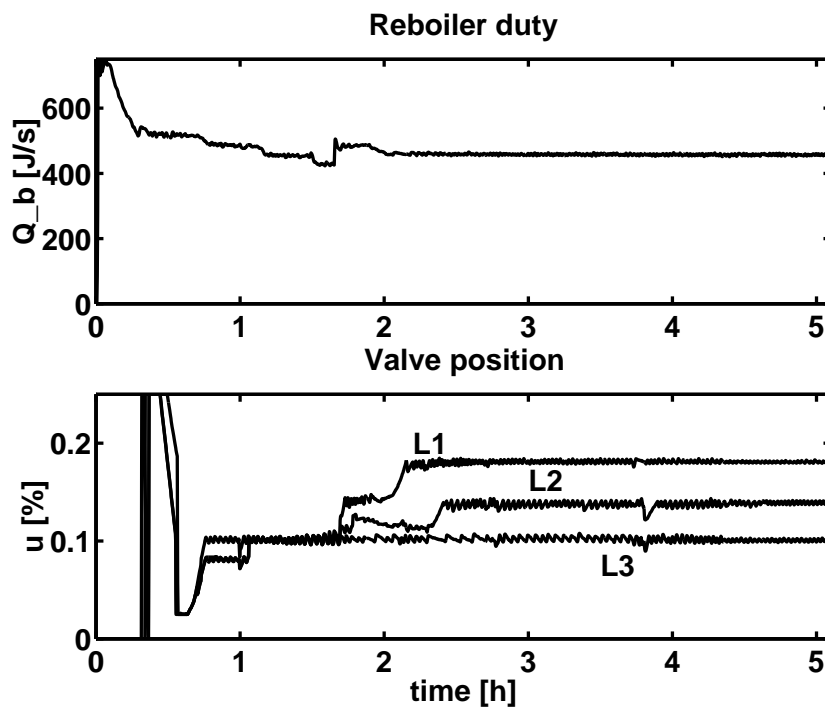


Figure E.4: Manipulated variables, experiment 2

Composition Analysis

At the start of the experiment the liquid was filled to the reboiler (vessel 4). The initial composition ($t = 0.0h$) and the composition in the vessels as a function of time are presented in Table E.2.

Table E.4: Product composition, experiment 2

	component	methanol	ethanol	n-propanol	n-butanol
		time = 0.0 h			
M4	Vessel 4	0.2667	0.1783	0.1548	0.4002
	volum [l]	0.5	0.5	0.55	1.70
	holdup [mol]	12.35	8.57	7.35	18.57
		time = 1.04 h			
M4 (reboiler)	Vessel 4	0.1005	0.1432	0.1943	0.5620
M3	Vessel 3	0.3497	0.3164	0.2370	0.0969
M2	Vessel 2	0.4223	0.4487	0.1276	0.0015
M1 (accumulator)	Vessel 1	0.8609	0.1368	0.0022	0.0001
		time = 2.04 h			
M4	Vessel 4	0.0016	0.0123	0.1250	0.8612
M3	Vessel 3	0.0362	0.2942	0.6480	0.0216
M2	Vessel 2	0.2001	0.7848	0.0151	0.0
M1	Vessel 1	0.9029	0.0969	0.0002	0.0
		time = 2.44 h			
M4	Vessel 4	0.0	0.0009	0.0818	0.9174
M3	Vessel 3	0.0049	0.1464	0.8340	0.0147
M2	Vessel 2	0.1430	0.8334	0.0236	0.0
M1	Vessel 1	0.9232	0.0768	0.0	0.0
		time = 3.44 h			
M4	Vessel 4	0.0	0.0004	0.0679	0.9317
M3	Vessel 3	0.0	0.1133	0.8769	0.0098
M2	Vessel 2	0.1191	0.8609	0.0201	0.0
M1	Vessel 1	0.9408	0.0592	0.0	0.0
		time = 5.09 h			
M4	Vessel 4	0.0	0.0	0.0662	0.9338
M3	Vessel 3	0.0	0.1073	0.8836	0.0091
M2	Vessel 2	0.0932	0.8856	0.0212	0.0
M1	Vessel 1	0.9399	0.0601	0.0	0.0

E.3 Experiment 3, 22. march. 1996

These experiment were performed after a retrofit of the column. Considerable increase in product purities has not been achieved, since the column length is only increased by 40 mm. On problem which was present earlier was the amount of vapor condensing on the column wall due to heat losses, increasing of the insulation from 30 to 60 mm reduced this problem.

The reboiler heat input was controlled by keeping the differential temperature between reboiler surface and liquid holdup constant. Initially the differential temperature was set to $T_s = 250^\circ C$ and has been changed gradually to $\Delta T = 150^\circ C$ as butanol concentration increases in the reboiler. The final temperature difference is rather close to the operation limit of the column and corresponds to a heat input of approximately 400 W. Note, no data were logged during the experiment performed on 18. march 1996.

Experimental procedure

- All liquid initially in reboiler
- PI-controllers in automatic with $K_c = 5ml/minK$, $\tau_I = 12min$
- Minimum reflux flows: $L_{2,min} = 1.2L_1$; $L_{3,min} = 1.1L_1$
- After heating up the reboiler hldup, the difference between reboiler holdup temperature and reboiler surface is reduced from $\Delta T = 250$ to $140 \sim 160^\circ C$

In Figures E.5 to E.6 the time responses of experiment Experiment 3 are shown. At time $t = 1.5$ h the lower column was close to flooding, to prevent the flooding and force the system back to normal operation, the reflux controller of this section was temporarily placed in manual. Simultaneously, the reboiler effect was reduced by adjusting the setpoint to the heater controller. At $t = 1.6$ h flooding has stopped and the controller was placed into automatic again. We see that the controller adjust reflux L_3 rather fast to a constant value. At $t = 4.9$ h product samples are drawn for off-line analysis. The distillation process was operated for approximately two more hours to investigate the influence of the distillation time on the final product composition.

The temporary reduction in reflux flow L_1 at $t = 1.4$ h was necessary since the column started to flood in section 3. After flooding had stopped, the reflux controller was placed in automatic again and stabilized the temperature in section 3 at the given setpoint of $T_{1.2,set} = 107.5^\circ C$. The temporary flooding of the column didn't have a noticeable influence on the final product composition (see Table E.5)

The final product compositions given in Table E.5 bottom show that the composition in vessels 2 and 3 at $t = 7.5h$ is similar to the composition measured at $t = 4.9h$. We have a slight increase in impurity in vessel 2 and 3. The disturbance add light components to the lower part of the column, which have to be moved upwards through the column. The amount of light impurities is increased in vessels C, while in vessel B both the amount ethnaol and butanol is increased.

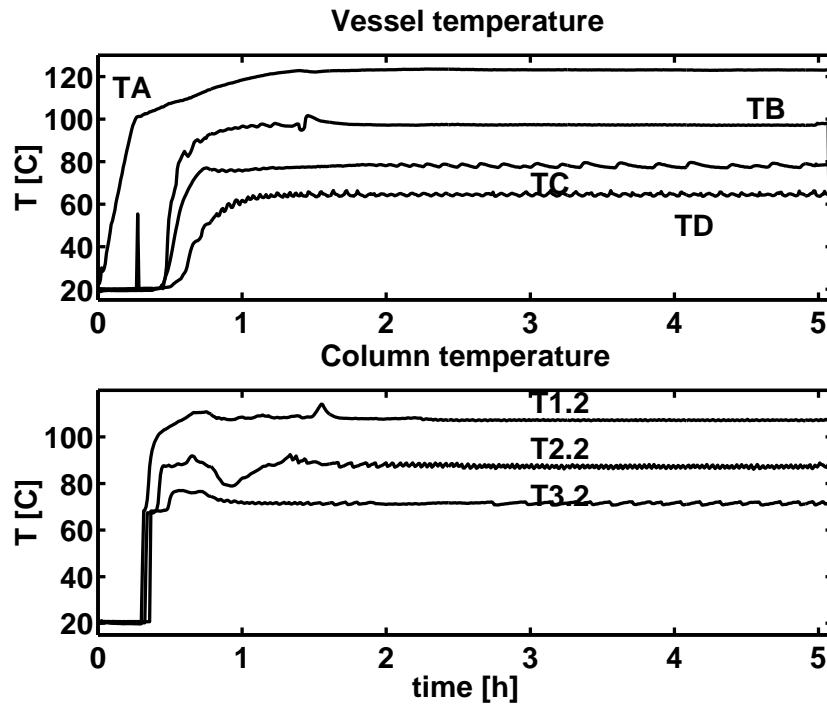


Figure E.5: Temperature responses, experiment 3

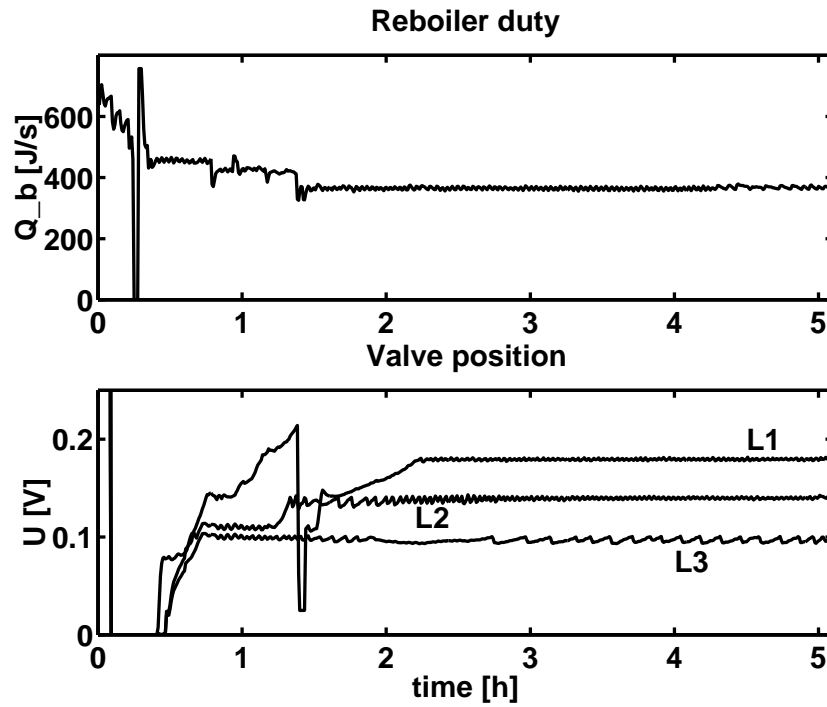


Figure E.6: Manipulated variables, experiment 3

Table E.5: Final product composition

component	methanol	ethanol	n-propanol	n-butanol
Experiment 18. march. 1996, t = 4.5 h				
Initial feed	0.250	0.188	0.190	0.372
Vessel 1	0.962	0.030	0.007	0.001
Vessel 2	0.062	0.906	0.028	0.004
Vessel 3	0.017	0.041	0.910	0.032
Vessel 4	0.011	0.018	0.050	0.921
Experiment 3, 22. march. 1996, t = 4.9 h				
Initial feed	0.201	0.153	0.211	0.435
Vessel 1	0.976	0.017	0.006	0.001
Vessel 2	0.040	0.915	0.045	0.001
Vessel 3	0.011	0.054	0.926	0.009
Vessel 4	0.001	0.002	0.087	0.910
Experiment 3, 22. march. 1996, t = 7.5 h				
Vessel 1	0.985	0.011	0.003	0.001
Vessel 2	0.063	0.909	0.028	0.001
Vessel 3	0.008	0.065	0.912	0.015
Vessel 4	0.001	0.001	0.070	0.928

From the analysis of these to experiments we see that the final product compositions in the vessels are similar even if we start from to different feed compositions (added 1-PrOH and 1-BuOH).

Remarks on experiments from 18. and 22. march 1996

- Frequent observation of flooding of the columns necessary, where column section 3 (bottom) is most exposed to flooding because of the increase in molecular weight and viscosity with time, caused by the increase in butanol concentration
- Condensation on the column walls was considerably reduced due to extra insulation
- Detuning of the vessel preheating reduced oscillations in column temperature

E.4 Experiment 4, 03. april. 1996

In experiment 4, the liquid feed was distributed over the column, 1.5 liter added to the reboiler and 500 ml were filled into each vessel. The experimental procedure was as follows:

- Setpoint for differential temperature in the reboiler was set to $\Delta T = 130^{\circ}C$ after start-up.
- Reboiler and preheaters were activated simultaneously.
- Reflux to column section 1 was controlled manually, reflux flows L_2 and L_3 are set equal to L_1 to ensure that the reboiler and none of the vessels run dry and overflow of intermediate vessels is avoided.

- Reflux controller set into automatic approximately 1 h after start-up

	K_C [ml/minK]	τ_I [min]
L_1	3.5	10 min
L_2	4.5	12 min
L_3	3.5	10 min

- Rather slow settling of column temperature $T_{2,2}$, the temperature was considerable below the setpoint, indicating too much ethanol in this section. The setpoint for the temperature controller of vessel 3 was increased from 95 to 97°C to remove ethanol from vessel (intermediate reboiler)

The final product composition product compositions are presented in Table E.6

Table E.6: Final product composition, experiment 4

component	methanol	ethanol	n-propanol	n-butanol
Experiment 4, 03. april. 1996, t = 6.8 h				
Initial feed	0.2656	0.1908	0.1984	0.3452
Vessel 1	0.9927	0.0061	0.0010	0.0001
Vessel 2	0.0863	0.9066	0.0062	0.0009
Vessel 3	0.0202	0.0594	0.9190	0.0012
Vessel 4	0.0019	0.0093	0.0528	0.9360

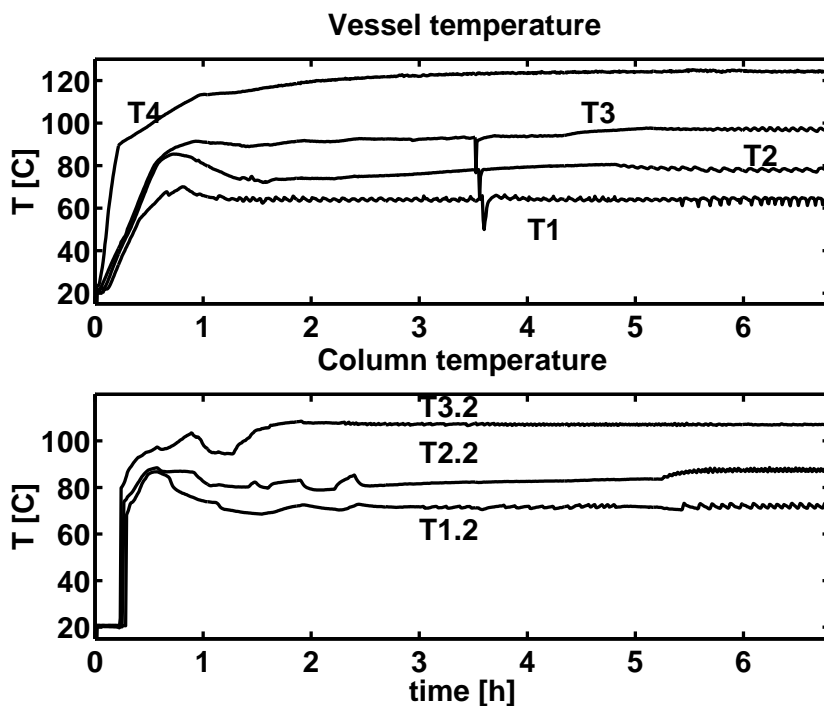


Figure E.7: Temperature responses, experiment 4

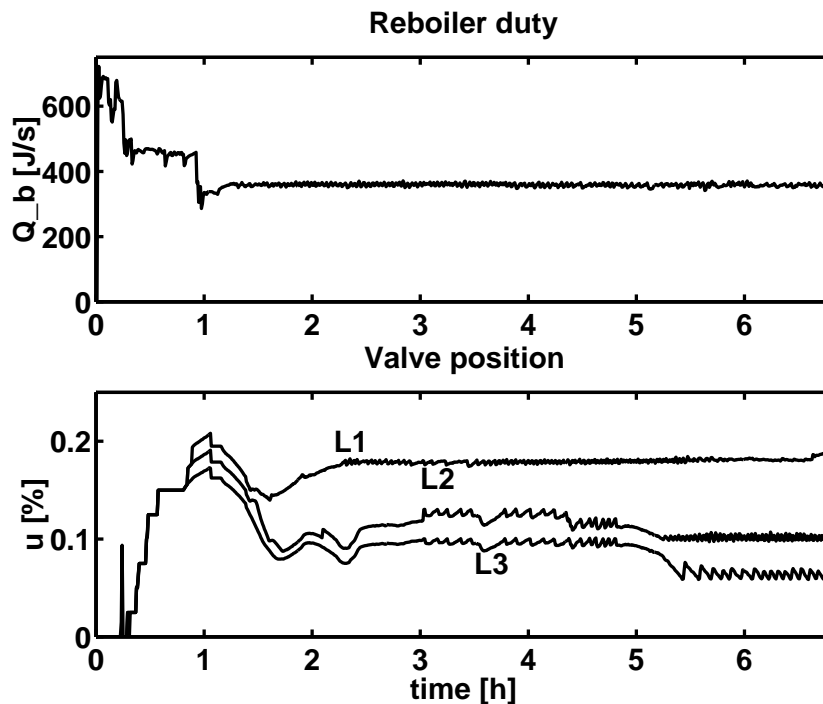


Figure E.8: Manipulated variables, experiment 4

Remarks on experiment 4

- Care has to be taken to avoid drainage of reboiler and overflow of vessels above → manual control of reflux during start-up
- Purification of products slightly slower compared to start-up from empty column were all feed is added to the reboiler.
- Subcooled liquid entering the column from the vessels will decrease temperature which inturn force the temperature controller to decrease reflux (positiv feedback).
- Process considerably more difficult to perform start-up from a column were liquid is distributed compared to start from empty vessels

E.5 Experiment 7, 04. october. 1996

Figure E.9 show the results for experiment 7. From Table 4.1 we see that the amount of the two intermediate components is much less than in experiment 12, such that a rather low holdup in intermediate vessels 2 and 3 are expected. Due to the large amount of light component, temperature T_1 in the uppermost column section (see Figure E.9, b) was initially so low that no reflux was recycled to the column. To avoid draining of the reboiler and ensure separation, reflux was therefore set manually at 25 ml/min in the time interval $0.0 \leq t \leq 0.3$ h (see Fig. E.9 d).

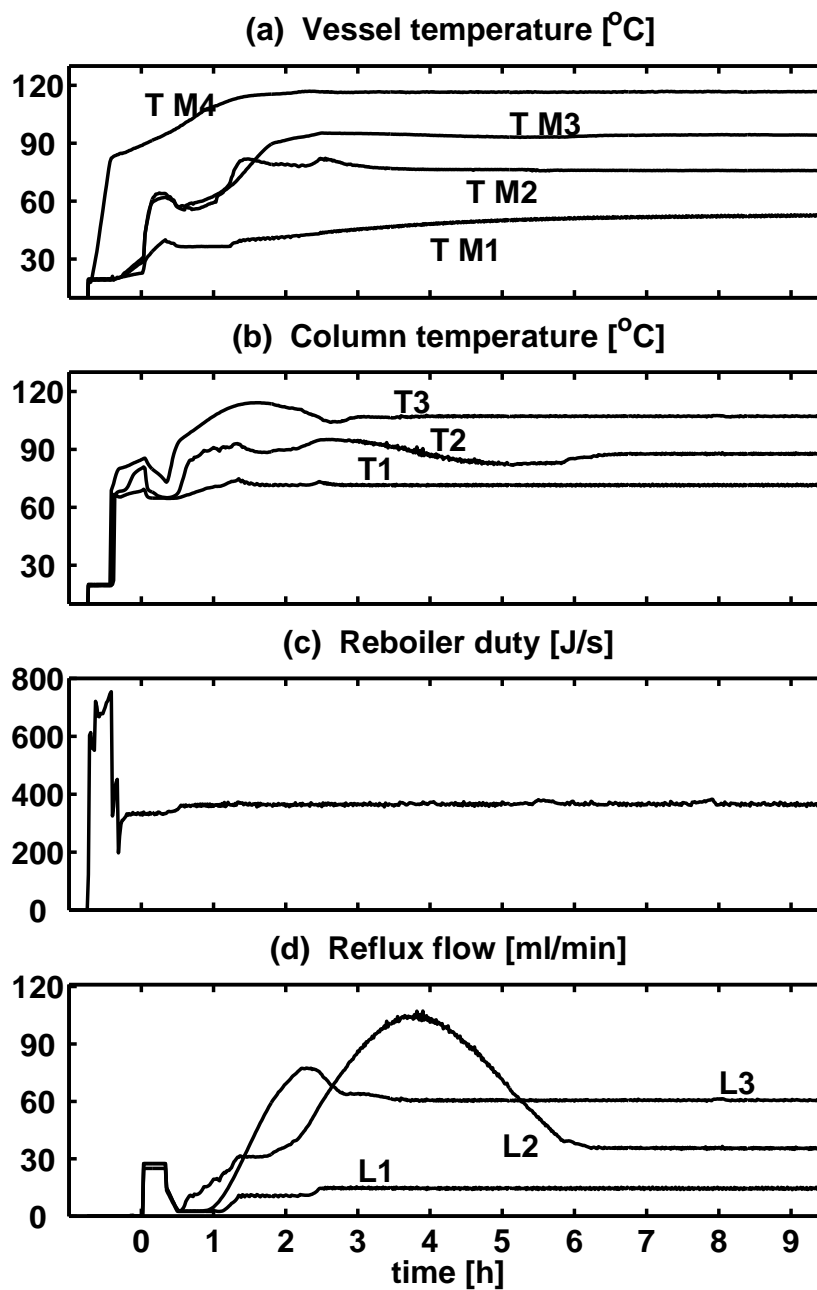


Figure E.9: Temperature responses in vessels (a), in column sections (b), reboiler heat input (c) and volumetric reflux flows as function of time recorded from experiment 7

The decrease in temperature in section 2 (T_2) and section 3 (T_3) at $0.1 \leq t \leq 0.5$, indicates that considerable amount of light components accumulated in the intermediate vessels during start-up, the manually controlled reflux flow returned the lighter components to the column section such that these are finally accumulated in the column top¹.

¹Note, that in the period from $0.5 \leq t \leq 1.5h$ the temperatures of vessel $M2$ and $M3$ are close to the steady state temperature of vessel 1 at $t \geq 8h$

In the period $2 \leq t \leq 4h$ vessel 2 was empty, such that control on temperature T_2 was lost and temperature T_2 increased. The experimental data show that the liquid flow $L_2 \geq L_3$, however since vessel 2 was empty we have to have $L_2 \leq L_1$ on volumetric basis ². Insufficient reflux flow allows heavier component to enter the column sections and accumulate in vessel 2 and 3, respectively. The temporary accumulation of heavier component in vessels 2 and 3 is indicated by the simultaneous increase in vessel temperatures $TM2$ and $TM3$. Due to insufficient separation during the period $2 \leq t \leq 4h$, considerable amount of time was used to establish stable flows and holdups in the column. The experiment was performed without operator intervention, after establishing constant reflux flows the column was operated for three more hours and samples of the products were withdrawn and analyzed.

E.6 Operation with three components

The flexibility of the multivessel batch distillation column was investigated by reducing the number of components from four to three, components present are methanol, ethanol and 1-butanol. Further, opening the reflux valve of vessel 3, liquid is not accumulated and a column twice as long as the design is achieved (consisting of two sections). This section consist of approximately twice as much stages, such that separation ethanol/1-butanol will improve.

Setpoint for butanol/ethanol split is set such that thermocouple in second column section is for control purposes. This thermocouple is placed in the middle of column 2, such that 75 % of column length (entire column 3 and half the column 2) are below this location. Assume a linear temperature profile between ethanol and butanol results that 75 % of the required temperature change (temperature difference $\Delta T = T_{b,BuOH} - T_{b,EtOH} = 39^\circ C$ has to be completed at this position, thus the temperature setpoint is set to $T_{2,2} = 88.5^\circ C$. During startup this setpoint will ensure rather fast accumulation of light components in the column. The start-up is performed with all liquid added to the reboiler.

Analysis of final product composition

Table E.7: Final product composition, three components, 26.april.1996

component	methanol	ethanol	n-butanol
Experiment 0204 26. april. 1996, t = 6.5 h			
Initial feed	0.4114	0.2853	0.3033
Vessel 1	0.9961	0.0029	0.0010
Vessel 2	0.0003	0.9500	0.0497
Vessel 4	0.0001	0.0376	0.9624

As can be seen from the product composition presented in Table E.7, the split between methanol and ethanol has improved considerably. Improving the split between ethanol and

²Note: the reflux flow is estimated based on the control signal to the solenoid valve, during time interval $2 h \leq t \leq 4 h$, the volumetric flow L_2 can not be greater than the reflux from column 1 which enters vessel 2, see Figure 4.1

butanol would be possible by reducing the setpoint of the temperature controller. Nevertheless, the experiment showed that the reduction in number of components is feasible, by just “recalculating” the temperature controller setpoint. On the contrary, when increasing the number of components a feasible operation procedure are still to be found.

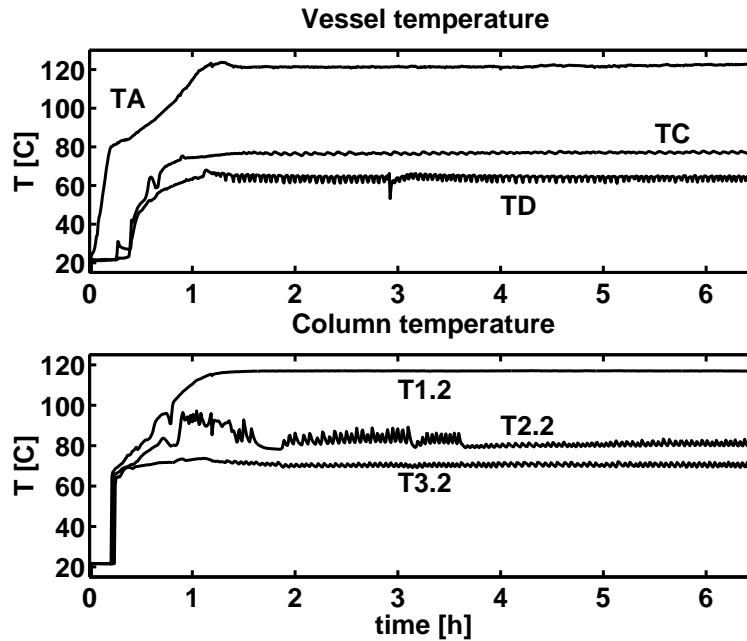


Figure E.10: Temperature responses, experiment 26/04-1996

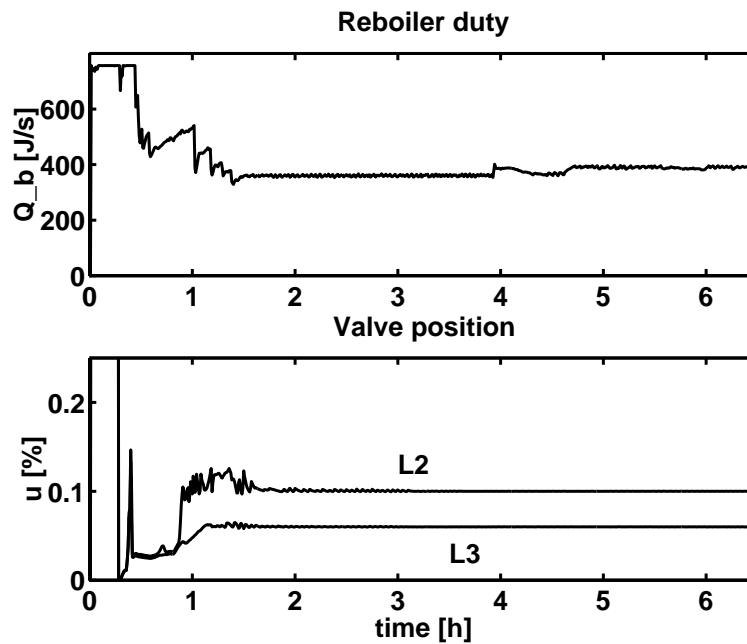


Figure E.11: Temperature responses, experiment 26/04-1996

Appendix F

Evaluation of Dynamic Models of Distillation Columns with Emphasis on the Initial Response

Bernd Wittgens and Sigurd Skogestad¹

presented at: DYCORN+ '95, 7 - 9 June 1995, Helsingør, Danmark

University of Trondheim, NTH,
Laboratory of Chemical Engineering,
7034 Trondheim, Norway

Abstract The flow dynamics (tray hydraulics) are of key importance for the initial dynamic response of distillation columns. The most important parameters are the liquid holdup, the liquid hydraulic time constant, and the constant representing the effect of a change in vapor flow on liquid flow. In the paper we present methods for determining these parameters experimentally, and compare the results with estimates from available correlations such as the Francis Weir formula.

Key Words: Distillation dynamics; Tray hydraulics

F.1 Introduction

The objective when deriving a model is to make it as simple as possible while at the same time matching the dynamics of the real system. The estimation of the dynamic parameters which determine the behavior of

the process is of crucial importance in the modeling process. For control purposes the most important feature of a model is to match the dynamic response at times corresponding to the desired closed-loop time constant. This means that if the dynamic model is to be used for evaluating and tuning the “fast”

¹Author to whom correspondence should be addressed,
phone: +47 7359 4154, fax: +47 7359 4080
E-mail: skoge@chembio.ntnu.no

loops on a distillation column (pressure loop, level loops, temperature profile “stabilization”) where the time constants are in the order of a few minutes or less, then a good model for the initial response is required and accurate steady state behavior may be less important.

Simplified models which simplify or neglect flow dynamics (tray hydraulics) and energy balance are often used for studies of distillation column dynamics and control. However, the applicability of such simple models for this purpose is often questioned by practitioners. This critique is indeed reasonable as one knows that the tray hydraulics are crucial in determining the initial dynamic response which is of key importance for control. Although the essential dynamics of a distillation column can be obtained from simplified models, the introduction of realistic and accurate hydraulic calculations allows to study the operability of a given system and the design and evaluation of complex control systems.

In the paper we consider detailed models of the tray hydraulics and use these to derive expressions for parameters that characterize the flow response. The most important parameters are the liquid holdup M_l , the hydraulic time constant τ_l , the parameter λ (denoted K_2 by many authors) for the initial effect of a change in vapor flow on liquid flow, the fraction of vapor on the tray and the pressure drop. These key parameters are also determined from experiments on our lab-scale column. The final goal of these studies is to see how detailed a dynamic model of a distillation column should be in order to be used for control purposes.

The literature on distillation dynamics is extensive so only a short overview will be given. In terms of experimental responses for tray columns we only mention the work of Baber et al. (1961, 1962).

Open- and closed loop experiments under automatic control were performed, additionally a linearized deviation model were presented and compared to the recorded transient responses. Perforated plates have been used extensively for liquid-vapor contacting in distillation columns, data for plate design has been published by *e.g.* Stichlmair (1978), Perry (1984) and Lockett (1986). Key parameters as *e.g.*: weeping, flooding and efficiency of sieve tray are influenced by the pressure drop which in turn is dependent on liquid and vapor flow as well as the tray design.

A detailed overview on recently published literature in the field of dynamics and control of distillation columns is given by Skogestad (1992). The survey includes the description of distillation models with rigorous and linearized tray hydraulics and a review of widely used simplifications. Rigorous models for distillation columns for nonlinear simulations are developed by *e.g.*: Gani *et al.* (1986) and Retzbach (1986). The work of Gani *et al.* is focused on the development of a general dynamic model including tray hydraulics and accurate prediction of the physical properties which is numerically robust. Further the influence of the simplifying assumption was investigated. The rigorous model of Retzbach is primarily developed for the nonlinear simulation of a multi-component mixture in a distillation column with side stripper. The tray hydraulic models applied by Retzbach are extensively described by Stichlmair (1978).

The paper is divided into 5 part. We present a detailed description of the rigorous stage model in section 2. The liquid holdup is divided into liquid on the sieve tray and downcomer. The dynamic model is implemented in the SPEEDUP simulation environment (1992) with a link to the ASPEN PROPERTIES PLUS data base for thermodynamic properties (1988) . The third part deals with

linearized tray hydraulics which simplify the dynamic model considerably. In the fourth section we present different methods to determine hydraulic parameters which describe the dynamic behavior of the system. These methods are based on experiments on our lab scale column or developed based on the rigorous stage model. Finally the results of the different methods are compared and conclusions are presented.

F.2 Tray Modeling

Tray models based on first principle consist of a large number of differential algebraic equations which may be solved simultaneously. Simulation of a staged distillation were the dynamics is described from first principles will enable a thorough investigation of the tray hydraulics. Changes in column design will influence the distribution of liquid on the stages and change the time constants of the system. A deeper insight in the hydraulics of a stage will reduce the possibility of designing a distillation column which is inherently difficult to control.

F.2.1 Rigorous Tray Model

In the rigorous model implemented in the SPEEDUP simulations each stage is divided into two liquid holdups (tray and downcomer) and one vapor holdup. Separated mass and energy balances for tray and downcomer are set up. The holdups are computed from the mass balances, the flows leaving the tray are determined from hydraulic correlations with pressure drop over the stage as driving force. The thermodynamic properties of the components are calculated by the ASPEN PROPERTIES PLUS (1988) package. The main difficulty in these simulations was to find the steady-state operating points

which match the performed experiments.

The design of a typical stage in a distillation column consisting of sieve tray, downcomer, inlet and outlet weir is shown in Figure F.1.

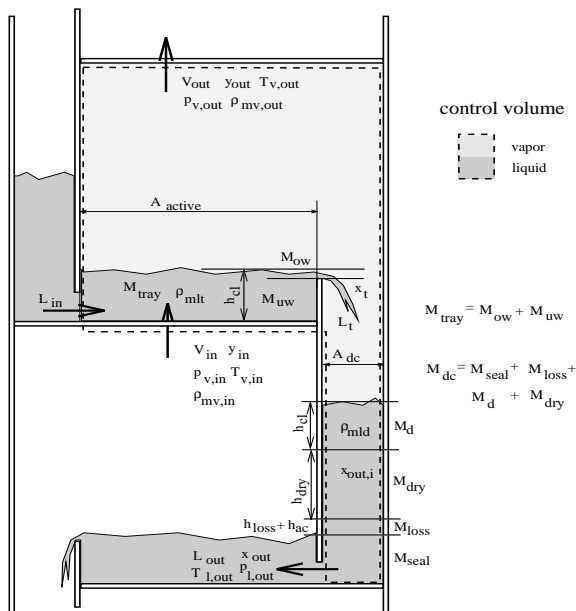


Figure F.1: Typical design of a staged distillation column with sieve tray and downcomer

Assumptions. The total holdup of the tray consists of liquid and vapor holdup. According to the geometry of the interior of the distillation column, see Fig. F.1, the liquid holdup on a stage is divided into liquid on the active tray area and liquid in the downcomer. The following assumptions are made:

- R1 two-phase system in thermal and mechanical equilibrium
- R2 perfect mixing in vapor and liquid phases
- R3 no heat losses to the surroundings
- R4 no heat of mixing
- R5 temperature dynamics of the column structure is neglected

Conservation of internal energy and constant volume of the system implies that the flash calculation is solved as an UV-flash.

Material and Energy Balance The balances presented are used throughout the whole distillation model, some modification are made for the reboiler and accumulator. The mathematical states are the component holdup M (both in vapor and liquid phase) on the stage and the internal energy. An in depth overview of these equations is given in Lockett (1983) and Stichlmair (1978).

The following set of equations is valid for a tray without feed, side draw and external heating or cooling.

$$\frac{dM_i}{dt} = V_{in} \cdot y_{in,i} + L_{in} \cdot x_{in,i} - V_{out} \cdot y_{out,i} - L_t \cdot x_{t,i} \quad (F.1)$$

The holdup of component i on the tray, this is liquid on the tray and vapor above tray and downcomer is

$$M_i = M_t \cdot x_{t,i} + M_v \cdot y_{out,i}; \quad (F.2)$$

The total molar holdup on the tray is given by

$$\sum_{i=1}^n M = M_t + M_v; \quad (F.3)$$

The energy balance of the tray

$$\frac{dU_t}{dt} = V_{in} \cdot h_{v,in} + L_{in} \cdot h_{l,in} - V_{out} \cdot h_{v,out} - L_t \cdot h_{l,t} \quad (F.4)$$

where the total internal energy is described by

$$U_t = M_v \cdot \left(h_{v,out} - \frac{p}{\rho_v} \right) + M_l \cdot \left(h_{l,out} - \frac{p}{\rho_l} \right) \quad (F.5)$$

A similar set of equations is applied to the downcomer material balance:

$$\frac{dM_{dc,i}}{dt} = L_t \cdot x_{t,i} - L_{out,i} \cdot x_{out,i} \quad (F.6)$$

$$M_d = \sum_{i=1}^n M_{dc,i} \quad (F.7)$$

the component balance:

$$M_{dc,i} = M_d \cdot x_{out} \quad (F.8)$$

the energy balance of the tray

$$\frac{dU_{dc}}{dt} = L_t \cdot h_{l,t} - L_{out} \cdot h_{l,out} \quad (F.9)$$

and the total internal energy of the downcomer

$$U_{dc} = M_d \cdot h_{l,out} \quad (F.10)$$

were we neglect the pressure dependent part. Note that there is no flash calculation performed on the downcomer holdup. The vapor composition is in equilibrium with the liquid on the tray and the vapor volumes of the tray and downcomer are combined. Due to this assumption a vapor flow from the downcomer to the tray can be neglected such that the overall system is somewhat simplified. Due to the assumption that the pressure is identical, both in the liquid phase of the tray and downcomer as well as the vapor phase the computation of the molar density is simplified.

Holdup Distribution. The liquid and vapor molar holdup a stage is related to the total tray volume V_t by:

$$V_t = M_t / \rho_l + M_v / \rho_v + M_{dc} / \rho_l \quad (F.11)$$

The molar volume of the liquid on the tray M_t and in the downcomer M_{dc} is computed by

$$M_t = h_{cl} \cdot A_{active} \cdot \rho_{l,t} \quad (F.12)$$

and

$$M_{dc} = M_{cl} + M_{dry} + M_{seal} = \underbrace{((h_{cl} + h_{dry} + h_{loss}))}_{h_{dc}} \cdot (A_{dc} + V_{seal}) \cdot \rho_{l,d} \quad (\text{F.13})$$

where V_{seal} is the volume of the downcomer seal. We assume no bubbles in the downcomer so h_{dc} is the height of clear liquid. The pressure drop over the downcomer (Perry *et al.*, 1984) from the surface of the liquid exiting the downcomer to the surface of the downcomer level is identical to the total pressure drop, Δp , over a plate (see Eq. F.20). The height h_{dry} is computed from the 'dry' pressure drop over the holes of the tray (see Eq. F.23). The flow under the downcomer apron is modeled by a nonstationary Bernoulli equation which considers losses due to friction and acceleration of the liquid under the downcomer apron.

Vapor-Liquid Equilibrium. The thermodynamic equilibrium of vapor and liquid is defined by

$$y_{eq,i} = K_i \cdot x_{out,i} \quad (\text{F.14})$$

with a K-value dependent on x, y, T, p . The composition of the vapor leaving the tray is computed by the Murphree tray efficiency coefficient

$$\eta_i = \frac{y_{out,i} - y_{in,i}}{y_{eq,i} - y_{in,i}} \quad (\text{F.15})$$

with $y_{eq,i}$ as the equilibrium vapor composition at given tray composition, temperature and pressure. It is assumed that liquid and vapor are perfectly mixed in their control volumes.

F.2.2 Tray hydraulics

The modeling of the tray hydraulic is based on empirical correlations selected from the

literature. Lockett (1986) and Stichlmair (1978) give an excellent overview over the different approaches. The chosen correlations are not necessarily the best available, but allow fairly accurate predictions and are easy to implement.

Clear liquid height. Consider the stage shown in Fig. F.1. Recall Eq. F.12 were the liquid holdup on the sieve tray, M_t , is defined with the active tray area, A_t , (excluding downcomer) and the clear liquid height h_{cl} . The clear liquid height is less than the actual height of fluid on the plate due to bubbles dispersed in the liquid. The fraction of liquid (froth density) in the fluid is denoted ϕ .

$$h_{cl} = \phi h_{weir} + h_{ow} \quad (\text{F.16})$$

We use the correlation presented by Bennett (1983) to compute the froth density ϕ

$$\phi = \exp(\pi_1 \cdot K_s^{\pi_2}); \quad (\text{F.17})$$

with the superficial velocity factor

$$K_s = v_t \sqrt{\rho_v / (\rho_l - \rho_v)} \quad (\text{F.18})$$

where $v_t = V_{in} / (A_t \rho_v)$ is the vapor velocity over the active tray. The parameters π_1 and π_2 are empirical constants. Bennett uses $\pi_1 = -12.55$ (in units consistent with the velocity factor K_s in m/s), and $\pi_2 = 0.91$ (dimensionless). We fitted new values to match pressure drop experiments and to get reasonable values for the liquid holdup.

Flow over outlet weir. The liquid flow, L_{out} , over the circular weir from the tray to the downcomer, is computed with a modified Francis weir formula (Perry *et al.*, 1984). Since the outlet weir is placed off center towards the column wall, the liquid height above the weir h_{ow} will not be constant. There are no existing correlations which deal with the converging flow over circular outlet

weirs in distillation column (Lockett, 1986). Taking the design into consideration, we choose to correct the weir length with a factor of 0.5.

$$h_{ow} = 44300 \cdot \left(\frac{L_{out}}{\rho_l \cdot 0.5 \cdot d_{weir}} \right)^{0.704} \quad (F.19)$$

We have here assumed that the liquid contains no bubbles as it passes over the weir, that is, h_{ow} is the clear liquid height of liquid over the weir (see Eq. F.16).

The actual height of fluid (mixture of vapor bubbles and liquid) on the tray is then h_{cl}/ϕ . If the computed froth height, $h_{cl}/\phi \leq h_{weir}$, the liquid flow leaving the tray is set to zero.

Pressure drop correlations. The pressure drop over a stage is measured as the difference in pressure between two adjacent stages

$$\Delta p = p_i - p_{i-1} \quad (F.20)$$

The total pressure drop Δp consists of the 'static' (wet) pressure drop through the areated liquid on the sieve tray and the 'dry' pressure drop through the holes of the tray, Δp_{dry} .

$$\Delta p = \Delta p_{static} + \Delta p_{dry} \quad (F.21)$$

The 'wet' pressure drop due to the height of clear liquid on the tray is

$$\Delta p_{static} = g \cdot \rho_l \cdot h_{cl} \quad (F.22)$$

According to Lockett (1986) the hydraulic gradient for sieve tray distillation column of small diameter (less than 0.5 m) is negligible.

Numerous correlations for the dry pressure drop are available (e.g.: Liebson *et al.* 1957) we have chosen:

$$\begin{aligned} \Delta p_{dry} &= \rho_{ml} \cdot \frac{g}{1000} \cdot \frac{51}{C_o^2} \frac{\rho_{mv}}{\rho_{ml}} \cdot v_h^2 \\ &= 0.965 \cdot \rho_v \cdot v_h^2 \quad (F.23) \end{aligned}$$

where $v_h = v_t A_t / A_h$ is the velocity through the holes [m/s].

The pressure loss due to surface generation, Δp_{bubble} , is neglected compared to the equations presented in Coulson (1983) or Perry (1984). The 'residual pressure drop', Δp_{resid} , as listed in literature (e.g. Perry (1984)) is neglected, since the suggested liquid height of 12.5 mm is comparable to the static liquid head on the sieve tray.

Summary of Holdup Distribution. The total liquid holdup on a stage is

$$M = M_t + M_{dc} \quad (F.24)$$

Here M_t is given by Equations F.12 - F.19. We have

$$M_t = \underbrace{A_t \rho_l \phi h_{weir}}_{M_{uw}} + \underbrace{A_t \rho_l h_{ow}}_{M_{ow}} \quad (F.25)$$

Note that ϕ depends on the vapor flow V whereas h_{ow} depends on the liquid flow L . We identify four contributions to the liquid holdup in the downcomer.

$$M_{dc} = M_{loss} + M_{cl} + M_{dry} + M_{seal} \quad (F.26)$$

1. Holdup which corresponds to the height of clear liquid on the tray plus the contribution from the corresponding "wet" pressure drop through the liquid on the tray above:

$$M_{cl} = A_d \rho_l 2h_{cl} = 2 \frac{A_d}{A_t} M_t \quad (F.27)$$

2. Holdup corresponding to pressure drop over the trays perforation ('dry pressure drop'), which from Eq. F.23 is

$$M_{dry} = \frac{A_d \cdot \Delta p_{dry}}{g \cdot MW_l} \quad (F.28)$$

3. Holdup due to pressure drop under the downcomer apron, M_{loss} . This term may usually be neglected.

4. Holdup of liquid in the downcomer seal, M_{seal} , which is independent of vapor and liquid flow.

F.3 Linear Tray Hydraulics

In order to obtain further insight into the tray hydraulics we shall consider the linearized approximation. Such a simple approximation may also be used in order to simplify dynamic simulations. For simplicity, the vapor holdup is neglected and constant molar flows are assumed.

It is assumed that the liquid flow, L_{out} , is a function of the liquid holdup, M and the vapor flow V_{in} (Rademaker *et al.* 1975, Skogestad *et al.* 1988). Taking the total differential of L_{out} then yields

$$dL_{out} = \underbrace{\left(\frac{\delta L_{out}}{\delta V_{in}}\right)_M}_{\lambda} dV_{in} + \underbrace{\left(\frac{\delta L_{out}}{\delta M}\right)_V}_{\frac{1}{\tau_L}} dM \quad (\text{F.29})$$

Note that this relationship is assumed to hold dynamically. The hydraulic time constant τ_L typically varies from 0.5 to 15 seconds. The vapor constant λ , representing the influence of V_{in} on L_{out} , typically ranges between -5 to +5 (Rademaker *et al.* 1975).

We want to obtain λ and τ_L from correlations for the liquid holdup M as a function of liquid and vapor flow given in Equations F.24 to F.28. The value of τ_L can be directly obtained from these correlations. To find λ we note that the total differential of M can be written

$$dM = \underbrace{\left(\frac{\delta M}{\delta L_{out}}\right)_V}_{\tau_L} dL_{out} + \underbrace{\left(\frac{\delta M}{\delta V_{in}}\right)_L}_{\tau_V} dV_{in} \quad (\text{F.30})$$

(this equation holds only at steady state). τ_L is always positive whereas τ_V may be either positive or negative.

Setting $dM = 0$ in equations F.29 and F.30 yields

$$\lambda = (\delta L_{out}/\delta V_{in})_M = -(\tau_V/\tau_L) \quad (\text{F.31})$$

Since both τ and λ depend on the tray loading, their values may be significantly different for the rectifying and the stripping section.

To derive analytic expressions for τ_L , τ_V and λ the holdup expressions in equations F.24 to F.28 are linearized:

$$\frac{\delta M_t}{\delta V_{in}} = A_t \rho_l \pi_2 \frac{\phi \ln \phi}{V_{in}} h_{weir} = \frac{M_{uw}}{V_{in}} \pi_2 \ln \phi \quad (\text{F.32})$$

$$\frac{\delta M_{dry}}{\delta V_{in}} = 2 \frac{M_{dry}}{V_{in}} \quad (\text{F.33})$$

$$\frac{\delta M_{loss}}{\delta L_{out}} = 2 \frac{M_{loss}}{L_{out}} \quad (\text{F.34})$$

$$\frac{\delta M_t}{\delta L_{out}} = 0.704 \frac{M_{ow}}{L_{out}} \quad (\text{F.35})$$

Equations F.32 to F.35 yield:

$$\tau_V = 2 \frac{M_{dry}}{V_{in}} + \left(1 + 2 \frac{A_d}{A_t}\right) \frac{M_{uw}}{V_{in}} \pi_2 \ln \phi \quad (\text{F.36})$$

$$\tau_L = 2 \frac{M_{loss}}{L_{out}} + \left(1 + 2 \frac{A_d}{A_t}\right) 0.704 \frac{M_{ow}}{L_{out}} \quad (\text{F.37})$$

Note that for our trays which have downcomers which exit above the liquid, we replace $2 \frac{A_d}{A_t}$ by $\frac{A_d}{A_t}$. It is important to note that τ_V and thus λ may be either positive or negative. A negative λ means that more liquid is stored inside the column when vapor flow is increased, resulting in a temporary reduction in liquid flow. The main cause for this effect is the increased pressure drop which increases M_{dry} . A positive λ means that *less* liquid is

stored inside the column when vapor flow is increased. At first this may seem unlikely. However, in tray columns it is quite common and is caused by a “swelling” (decrease in the froth density ϕ) which pushes liquid off the trays. For situations where $\lambda \geq 0$ an increase in vapor flow rate results in a decrease of liquid holdup on the tray. The liquid which is displaced on the sieve tray will be dumped on the stage below. If the change in ‘dry’ pressure drop is extensive enough (increase in h_{dry}) this excess liquid will probably be stored in the downcomer.

Numerical example We will discuss the experimental data later, but to illustrate the above procedure we shall compute the holdup distribution and hydraulic parameters for the top and bottom section for experiments no. 5 and 6.

The key data of the stage design are weir height $h_{weir} = 30$ mm and a ratio of downcomer to active tray area of $A_d/A_t=0.123$. With these data and the coefficients for Eq. F.17 presented in Tab. F.2 we compute the data presented in Tab. F.1. We have chosen to estimate the coefficients for Eq. F.17 for the rectifier and stripper section separately, since these sections have a rather different liquid load.

The column is operated with a feed of ethanol/butanol of composition $z_F = 0.5$ and a feed flow of 350 ml/min. The reboiler heat input is $Q_B = 5.79$ kW $\Rightarrow V = 0.142$ mol/s and $Q_B = 6.45$ kW $\Rightarrow V = 0.158$ mol/s for Exp. 5 and 6, respectively. The reflux is in both cases $L_T = 470$ ml/min = 0.096 mol/s. Note we assume constant molar flows through the column.

Table F.1: Numerical example, estimated data for experiment 5 and 6

parameter	dimension	Exp. 5		Exp. 6	
		top	bottom	top	bottom
		section			
Δp_{dry}	Pa/tray	199		247	
ϕ		0.20	0.47	0.17	0.45
h_{ow}	mm	1.43	2.16	1.43	2.16
M_{ow}	mol	0.16	0.24	0.16	0.24
M_{uw}	mol	0.67	1.60	0.59	1.52
M_{dry}	mol	0.38		0.47	
$\delta M_{cl}/\delta V$	s	-6.27	-5.75	-5.33	-5.23
$\delta M_{dry}/\delta V$	s	5.40		6.02	
$\delta M_{ow}/\delta L$	s	1.32	1.11	1.32	1.11
τ_L	s	1.32	1.12	1.32	1.12
τ_V	s	-0.87	-0.34	0.69	0.79
λ		0.65	0.31	-0.52	-0.70

The term $\delta M_{loss}/\delta L$ is in the order of $6 \cdot 10^{-3}$ s and can be neglected compared to the other terms.

These two experiments differ in the re-

boiler effect by approximately 10 %, but give entirely different results when the hydraulic parameters are computed. Note that the two contributions to τ_V : $\delta M_{dry}/\delta V$ (contribution

tion from change in downcomer holdup due to pressure drop) and $\delta M_{cl}/\delta V$ (contribution from change in tray holdup due to froth density) change in different directions when the heat input to the reboiler is increased. It is then clear that τ_V may easily change sign, and so may then $\lambda = -\tau_V/\tau_L$. For experiment 5 the absolute values of $\delta M_{dry}/\delta V \leq \delta M_{dry}/\delta V$ such that the liquid replaced on the sieve tray can not be stored in the downcomer. For experiment 6 the situation is such that the replaced liquid will be stored in the downcomer.

F.3.1 Linear flow relationships for column sections

In the following assume that the hydraulic parameters are equal for all trays in the top section (τ_{LT} and λ_T), and for all trays in the bottom section (τ_{LB} and λ_B). Consider a small deviation from steady state. With constant molar flows the material balance on a tray becomes

$$\frac{dM}{dt} = dL_{in} - dL_{out} \quad (F.38)$$

where the liquid flow leaving the tray is given from the linearized tray hydraulics (Eq. F.29)

$$dL_{out} = \lambda dV + \frac{1}{\tau_L} dM \quad (F.39)$$

Repeated combination of these equations yields the following expression for the change in liquid flow at the bottom of the column, L_B , in response to changes in reflux, L_T and boilup, V : (similar to Rademaker *et al.*, 1975, Skogestad *et al.*, 1988):

$$dL_B = g_L(s)dL_T + g_V(s)dV \quad (F.40)$$

where

$$g_L(s) = \frac{1}{(1 + \tau_{LT}s)^{N_T}} \frac{1}{(1 + \tau_{LB}s)^{N_B}} \quad (F.41)$$

$$g_V(s) = \lambda_B \left(1 - \frac{1}{(\tau_{LB}s + 1)^{N_B}} \right) + \frac{\lambda_T}{(\tau_{LB}s + 1)^{N_B}} \left(1 - \frac{1}{(\tau_{LT}s + 1)^{N_T}} \right) \quad (F.42)$$

The response of L_B to a change in reflux at the top, L_T is as expected a cascade of first-order responses, one for each tray. The response of L_B to a change in vapor flow, V , requires a more detailed derivation. Consider first a column with only one tray. We consider here the effect of a change in V only, so set $dL_{in} = 0$ in Eq. F.38. Taking Laplace transforms of equations F.38 and F.39 and combining yields $\frac{1}{\tau_L} dM = -\frac{\lambda}{\tau_L s + 1} dV$, and we get with one tray

$$dL_{out} = dL_1 = \lambda \left(1 - \frac{1}{\tau_L s + 1} \right) dV \quad (F.43)$$

For two identical trays we get in addition the change in liquid flow from the tray above, dL_{in} , which will be equal to dL_1 given above. dL_{in} will affect dL_{out} through a first order lag, so the total effect of a change in vapor flow with two trays is

$$dL_{out} = dL_1 + \frac{dL_1}{\tau_L s + 1} = \lambda \left(1 - \frac{1}{(\tau_L s + 1)^2} \right) dV \quad (F.44)$$

For a column with N identical trays we find

$$dL_{out} = dL_B = \lambda \left(1 - \frac{1}{(\tau_L s + 1)^N} \right) dV \quad (F.45)$$

For a column with a top and bottom section

$$dL_B = \lambda_B \left(1 - \frac{1}{(\tau_{LB}s + 1)^{N_B}} \right) dV + \frac{dL_{T,out}}{(\tau_{LB}s + 1)^{N_B}} \quad (F.46)$$

where $L_{out,T}$ is the liquid entering from the top section. It is itself caused by the increase in vapor, so

$$dL_{T,out} = \lambda_T \left(1 - \frac{1}{(\tau_{LTS} + 1)^{N_T}} \right) dV \quad (F.47)$$

and we derive the desired expression for $g_V(s)$.

Introduce the following approximations (which are good for long column sections)

$$\begin{aligned} \frac{1}{(1 + \tau_{LB}s)^{N_B}} &\approx e^{-\theta_B s}; \\ \frac{1}{(1 + \tau_{LTS})^{N_T}} &\approx e^{-\theta_T s} \end{aligned} \quad (F.48)$$

where $\theta_B = N_B \tau_{LB}$ and $\theta_T = N_T \tau_{LTS}$. Also introduce the total liquid lag from the top to the bottom $\theta = \theta_B + \theta_T$. Then we get from Eq. F.46 with $dL_T = 0$

$$dL_B \approx \lambda_B (1 - e^{-\theta_B s}) dV + \lambda_T (e^{-\theta_B s} - e^{-\theta s}) dV \quad (F.49)$$

In words, a step increase in boilup, dV , will result in an immediate increase in L_B equal to $\lambda_B dV$. This increase will last approximately for the time θ_B (which is the time it takes for a change in liquid flow to propagate through the bottom section), then the increase in L_B will change to the value $\lambda_T dV$ and it will stay at this value for an additional time θ_T . After approximately time $\theta = \theta_B + \theta_T$ the liquid flow L_B will change back to its original value.

F.4 Obtaining parameters from experiments

F.4.1 Liquid holdup

The liquid holdup on the stages determine the composition dynamics of the distillation col-

umn and influence the hydraulics of the system. The liquid holdup can be estimated from experiments and theoretical calculations.

i) Experimental dumping. The column is emptied by turning of the reflux and the heating. Liquid evaporated during this operation is collected in the accumulator. The combined holdup change of accumulator and reboiler is then the amount of liquid stored on the trays in the column during normal operation.

ii) Theoretical tray calculations using geometric data and correlations, see equations F.24 to F.28.

iii) Tracer experiments. One may inject a heavy component at the top of the column and measure the time it takes for the wave to move down the column. In general, the time constant for the composition response on a individual tray is $\tau_c = M_i / (L + KV)$, where we can set $K = 0$ for a heavy tracer, and the time constant (apparent delay) for N trays in series is approximately $N\tau_c$. We approximate $\theta_c \simeq N\tau_c$ such that we are able to estimate the column holdup from the measured delay θ_c .

iv) Experimental temperature responses. Measuring the initial temperature response to a step change in reflux ΔL or vapor flow ΔV enables the estimation of the liquid holdup.

The necessary assumptions are:

- OP1 vapor holdup is negligible
- OP2 constant molar liquid holdup M
- OP3 equimolar flows (simplified energy balance)
- OP4 the local slope of the vapor-liquid equilibrium curve is K_i
- OP5 local linear relation between liquid composition and temperature, $x = Tk_i$.

The material balance over a stage becomes

$$M dx_i/dt = L_i (x_{i-1} - x_i) + V_i (y_{i+1} - y_i) \quad (\text{F.50})$$

For a step change in L_i and V_i the internal flows are $L_i = L_i^o + \Delta L$ and $V_i = V_i^o + \Delta V$. Subtract the steady state solution from Eq. F.50 and consider the time immediately after the step change when the tray composition still is unchanged. This yields the following relationship for the initial slope as a function of ΔL and ΔV :

$$M \left(\frac{d\Delta x_i}{dt} \right)_{init} = \Delta L_i (x_{i-1}^o - x_i^o) + \Delta V_i (y_{i+1}^o - y_i^o) \quad (\text{F.51})$$

Apply assumptions OP4 and OP5 and rearrange Eq. F.51

$$M_i \left(\frac{d\Delta T_i}{dt} \right)_{init} = \Delta L_i (T_{i-1}^o - T_i^o) + \Delta V_i K_i (T_{i+1}^o - T_i^o) \quad (\text{F.52})$$

From Eq. F.52 it is possible to estimate the molar holdup M_i on a stage from observing the initial slope of the tray temperature to changes in reflux or boilup.

F.4.2 Liquid hydraulic time constant τ_l

The liquid hydraulic time constant can be determined experimentally by making a change in reflux and observing the delay in liquid response through the column.

- i) This delay may be observed from the response of the uncontrolled reboiler level, or
- ii) from the temperature responses inside the column.
- iii) τ_L may also be estimated theoretically from tray data (see Eq. F.37).

F.4.3 Vapor constant λ

The vapor constant λ represents the initial effect of a change in vapor flow on liquid flow from a stage. Experimentally we can obtain λ by the following means.

- i) From temperature responses. For example, for $\lambda \geq 1$ the effect of an increase in V will initially be counteracted by an even larger increase in L and we will observe an increase in tray temperature in the upper part of the column earlier than in the lower part.
- ii) From reboiler level response. Since $dM_B/dt = L_B - V$ we get from Eq. F.49 that for a unit step in vapor flow V (keeping the reflux flow constant $\Delta L = 0$), the slope of the response of M_B as a function of time will be approximately $(\lambda_B - 1)$ for the time θ_B , then equal to $(\lambda_T - 1)$ for the next time θ_T , and then remain at -1.
- iii) Estimate λ theoretically using hydraulic relationships such as Eq. F.36 and Eq. F.37.

F.5 Results

The distillation column is equipped with 11 sieve trays (numbered from the top) of 125 mm diameter. As compared what could be expected in an industrial column, the hole area of the trays is relatively small (A_h is about 5% of A_t), and the holdup in the downcomer is relatively large (about 50% of total holdup). Also, the downcomer design is different from that in Figure F.1 in that the downcomer ends above the liquid surface and has a quite large downcomer seal holdup.

The reboiler is a thermosyphon reboiler with a nominal holdup of 3.5 liters and equipped with electrical heating of a maximum effect of 15 kW. The total condenser is connected to an accumulator with a holdup of approximately 1.5 liters. The reflux and feed are fed to the column by metering pumps and

enter the column with a temperature approximately $2^{\circ}C$ below the boiling point.

Each tray is equipped with a thermocouple which is placed approximately 10 mm above the center of the tray. Below the lowest tray a pressure sensor is installed to measure the pressure drop over the column. The distillation column is interfaced to a computer system for data recording and control with a sampling frequency of 1 Hz.

The experiments were performed with mixtures of ethanol and butanol. For the theoretical estimation of holdups and time constants we assume constant density $\rho_l = 731.5 kg/m^3$ (Halles, 1976) and mole weight $MW_l = 60.1 kg/kmol$ corresponding to a 50/50 mixture. We also assume $\Delta h_{vap} = 40900 kJ/kmol$ (Majer, 1985).

F.5.1 Pressure drop

Experiments were performed to measure the pressure drop over the distillation column. Based on these measurements and applying equations F.16 to F.23 we compute by means of a least square approach the coefficients which were used in Eq. F.17. The estimation is performed separately for stripping and rectifier section. A comparison between experimental data and the estimated pressure drop is shown in Figure F.2.

The empirical parameters π_1 and π_2 for Eq.F.17 determined from the pressure drop measurements are presented in Tab. F.2.

Table F.2: Empirical parameters for Eq.F.17

	π_1	π_2
rectifier section	-24.17	0.73
stripping section	-7.05	0.61

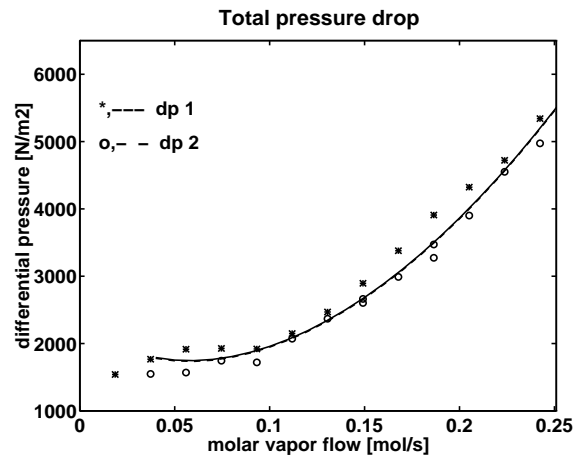


Figure F.2: Comparison of measured (*,o) and estimated (–) pressure drop over the distillation

F.5.2 Liquid holdup

Table F.3 lists experimental conditions and some results for experiments 2, 3 5 and 6.

i) The liquid volume determined by dumping the distillation column is denoted $V_{l,dump}$. The corresponding average tray holdup is denoted $M_{l,dump}$.

ii) The liquid volume estimated from pressure drop measurements is denoted $V_{l,\Delta p}$. It is found by measuring the differential pressure drop over the column and estimating the liquid holdup based on Eq. F.24 to F.28.

iii) We performed experiments with only ethanol in the column and used butanol as a heavy tracer. With reflux $L = 472$ ml/min the time for the butanol to reach the bottom was about 330 seconds (see Fig. F.3), corresponding to a liquid holdup of approximately 2.59 l.

The agreement between these three methods is good and gives a total column holdup of approximately 2.7 liter.

iv) We also used Eq. F.52 to estimate the holdup from the initial temperature response

on trays 3 and 9 to a step response in heat input Exp. 2 and Exp. 6 as well as in reflux Exp. 3 and Exp. 5. The temperature responses are shown in Fig. F.4 and F.5 for experiments 2 and 3, respectively. The corresponding estimated holdups (denoted M_3 and M_9) show large variations (see Tab. F.3) and are also different (mostly larger) from the values found above using dumping. The reason for the variations may be inaccuracy in determining the initial temperature derivative (see e.g. Fig.F.5). However, the deviation from the dumping experiments may also be because the assumptions for deriving Eq. F.52 do not hold. This is partly confirmed by the simulated responses (smooth

lines in the Figures) which are in good agreement with the experiments. The simulated responses are for the full model (with no assumption about constant molar flow *etc.*) using holdups which are in agreement with the dumping experiments.

Compare Exp. 2 to 6 and Exp. 3 to 5 shows that the quality of prediction increase for increasing step changes. The changes in experiments 5 and 6 are at least twice the step changes as in Exp. 2 and 3. Further we see that the estimated holdup varies largely for Exp. 2 and 3. Inspecting the results show that the holdup is very much overpredicted for the opposite side of the column were the step was introduced.

Table F.3: Data for holdup estimation for experiment 2, 3, 4 and 5

	units	Exp. 2	Exp. 3	Exp. 5	Exp. 6
F	ml/min	250	250	350	350
z_F		0.54	0.56	0.56	0.45
Δp	$mbar$	22.3	26.1	35.3	54.6
$Q_{t=0}$	kJ/s	3.60	4.50	5.70	6.45
ΔV	kJ/s	+0.45	0.0	0.0	+1.58
$L_{t=0}$	ml/min	249.8	382	468	470
ΔL	ml/min	0.0	+52.8	+88.4	0.0
$V_{l,dump}$	l	2.68	2.71	2.93	3.10
$V_{l,\Delta p}$	l	2.77	2.74	2.69	2.66
$M_{l,dump}$	mol	3.06	2.99	3.24	3.43
T_2	$^{\circ}C$	79.12	89.91	79.17	79.74
T_3	$^{\circ}C$	79.45	84.64	79.78	81.45
T_4	$^{\circ}C$	80.42	89.91	81.09	84.65
$d\Delta T_3/dt$	$10^{-2} \cdot ^{\circ}C/s$	+0.18	-1.43	-0.63	+4.23
M_3	mol	6.02	3.70	2.25	3.19
T_8	$^{\circ}C$	96.72	109.71	110.73	115.64
T_9	$^{\circ}C$	104.53	113.65	114.96	116.75
T_{10}	$^{\circ}C$	111.08	115.78	116.61	117.21
$d\Delta T_9/dt$	$10^{-2} \cdot ^{\circ}C/s$	+4.51	-0.87	-2.23	+2.15
M_9	mol	4.14	6.39	4.46	3.37

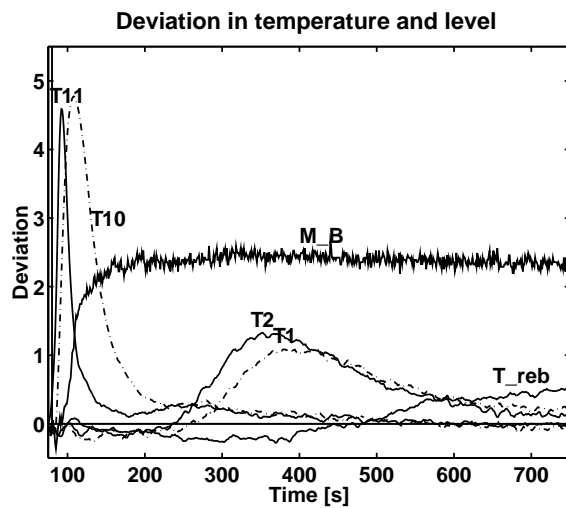


Figure F.3: Deviation in temperature of reboiler, T_{reb} and on stages 1,10, 11 and the reboiler level response due to injection of a heavy tracer.

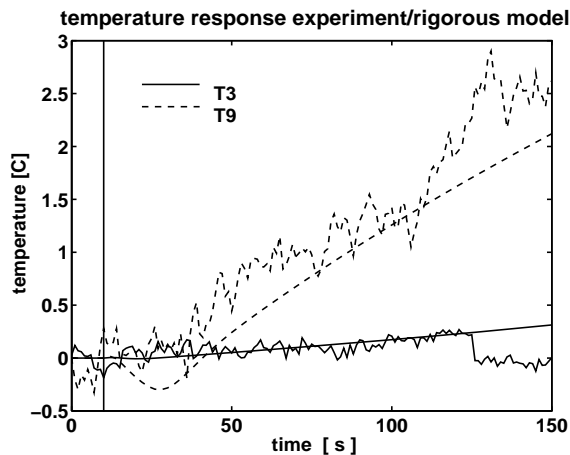


Figure F.4: Experiment 2. Initial response of temperatures on trays 3 and 9 to a step change in heat input at $t = 10$ s

F.5.3 Liquid hydraulic time constant τ_l

For the experimental determination of the hydraulic time constant, the level control of the inventory is placed into manual, such that the positions of the product valves are fixed. The

reboiler level will now primarily depend on the liquid flow to the reboiler and the vapor leaving it, although it should be noted that a fixed valve position not necessarily means that the liquid flow through the valve is constant.

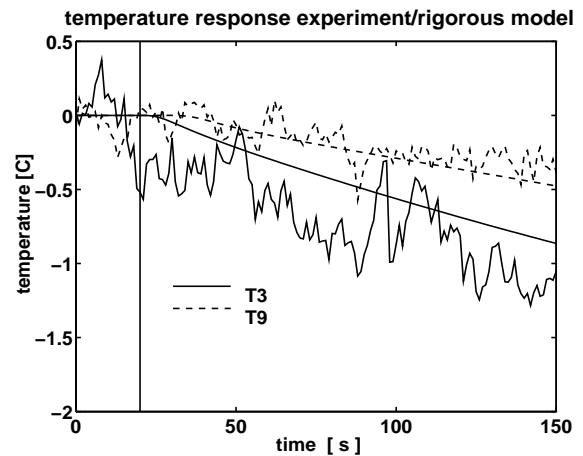


Figure F.5: Experiment 3. Initial response of temperatures on trays 3 and 9 to a step change in reflux flow at $t = 20$ s

Let us first consider experiment 5.

i) The hydraulic lag between the increase in reflux until the reboiler level changes is illustrated in Fig. F.6. We find $\theta = 23.1$ s from the change in reflux pump control signal to the initial level change of the reboiler, which give an average hydraulic time constant of $\tau_{LT} = 2.1$ s. The experimental response show a delay between the change in control signal and the change in accumulator level of 5.3 s. Consider the time difference from the initial accumulator level deviation until the reboiler changes which give a time delay of $\Delta\theta_l = 17.8$ s. From this delay we compute an average hydraulic time constant for each stage of $\tau_L = 1.62$ s.

ii) Using temperature measurements we find that the liquid delay between the temperature change on tray 3 and 9 is 12.7 seconds, which give an average hydraulic time constant of $\tau_L = 1.68$ s. For experiment 3 we find a delay

in the temperature change between the trays of 11.8 seconds which yields a hydraulic time constant of 1.68 s.

iii) Applying Eq. F.37 to the set of operational conditions of experiment 5 given in Table F.4 yields $\tau_{LT} = 1.32s$ and $\tau_{LB} = 1.11s$, which is approximately 2/3 of the experimental value. For experiment 3 we find from the temperature responses in Fig. F.5 an average hydraulic time constant of 1.83 s the estimated time constant is 1.46 and 1.23 seconds for the rectifier and stripper, respectively.

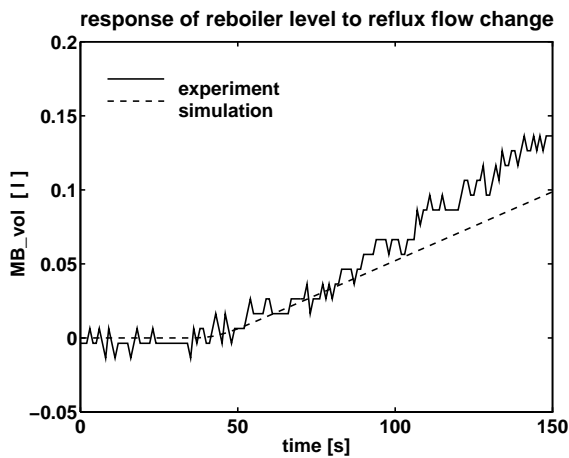


Figure F.6: Experiment 5. Response of reboiler level to a step in reflux flow at $t = 20$ s

We note from these and other results that the agreement between experiment and tray calculations is somewhat better for the level measurements if we consider the dynamics of the pump. Considering the dynamics in pump and sensor (see (i)) by re-defining the time horizon reduce the deviation between the different methods considerably. The computed value from the temperature measurement (ii) is strongly dependent on the quality of the signal to get a good approximation of the hydraulic time constant.

Table F.4: Experiments 3 and 5 for changes in liquid flows. Experimental conditions, measured time delays (θ), and hydraulic time constant (τ_L)

	units	Exp.3	Exp. 5
F	ml/min	250	350
z_F		0.56	0.56
$L_{t=0}$	ml/min	329.2	468.8
$L_{t=\infty}$	ml/min	382.7	557.2
$Q_{t=0}$	kJ/s	4.50	5.8
Θ_{T3}	s	16.7	13.3
Θ_{T9}	s	28.5	26
Θ_D	s	*	5.3
Θ_B	s	*	23.1
$\tau_{L,t}$ (Eq.F.37)	s	1.46	1.32
$\tau_{L,b}$ (Eq.F.37)	s	1.23	1.11

Still, it seems that the estimated values for τ_L from Eq. F.37 are too small. However, the rigorous simulations which are based on the same correlations show better agreement as is illustrated by comparing the experimental and simulated reboiler level in Figure F.6. The reason for the difference may be a somewhat more detailed tray model and effects of the energy balance which are also not included in the simple linear analysis leading to Eq. F.37.

F.5.4 Vapor constant λ

λ may be observed from the initial response to changes in the boilup as changes in the slope of the tray temperature or reboiler level as a function of time. From the temperature measurements for experiment 2 it is difficult to observe any change in the slope so one would expect λ to be close to 0. This does not agree with estimated values from tray calculations which yield λ equal to 5.1 and 3.8 in the top and bottom sections, respectively.

As seen from the simulated temperature on tray 9, this should yield an inverse response, which should be easy to observe in the bottom section (dashed curve in Fig. F.4).

From the level measurement for experiment 6 one can from Figure F.7 observe a change in the slope after about 10 s and then another change after about 35 s (from when the change in heat input was applied). This indicates that θ_T is about 25 s and θ_B is about 10 s. This is in reasonable agreement with experiment 5 which has the same initial liquid flow (see Table F.1). If we consider the slope of M_B as a function of time then one would from the experimental response in Figure F.4 expect λ_T to be about -1 and λ_B to be about -3.

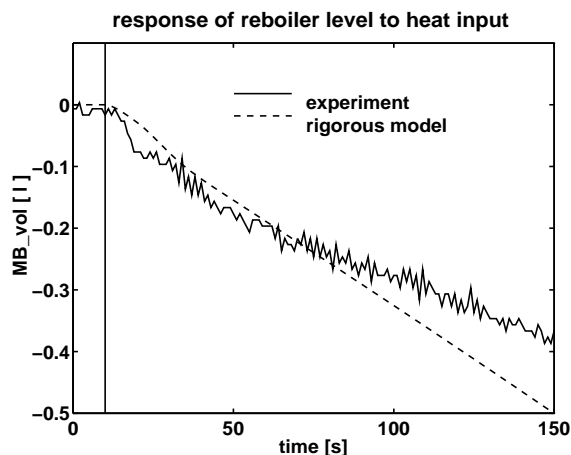


Figure F.7: Experiment 6. Response of reboiler level to a step in heat input at $t = 10$ s

Again, this does not agree very well with the estimated values of about -0.52 and -0.70, even if the sign λ_T and λ_B is correct. This deviation may seem very large, but the estimated values are very sensitive to small changes in the data. For example, consider Experiment 6 for which we estimate $\lambda_B = -0.7$. Recall from Eq. F.36 that λ has two contributions with different signs (see Table F.1). Both of these are very sensitive to the

value of the vapor flow. For example, the magnitude of the pressure drop term (which yields a negative contribution to λ) is proportional to V , while the froth density term (which yields a positive contribution to λ) may become less important as V is increased (because the froth density ϕ cannot be less than 0). For experiment 6, we obtained in Section 3 $\tau_{VB} = 6.02 \text{ s} - 5.23 \text{ s} = -0.70 \text{ s}$.

If we decrease the vapor flow by 20% then we find $\tau_{VB} = 4.812 \text{ s} - 6.32 \text{ s} = -1.51 \text{ s}$. τ_L is unchanged at 1.11 s, so we find that a 20% decrease in V changes the estimated value of λ_B from -0.70 to 1.35 such that an inverse response for the bottom section can be expected. On the other hand, an increase in vapor flow by 20% changes the estimated λ_B from -0.70 to -2.49, which is rather close to the experimental value of about -3.

F.6 Discussion and Conclusion

The agreement with the experimental responses and simulations using the detailed model were generally very good, except for the initial effect of changes in vapor flow (e.g., as expressed by the parameter λ). However, this was obtained only after considerable effort (including some parameter fitting) so in general we believe it is difficult to predict accurately the initial response of distillation columns based on only geometric data about the column and thermodynamic data. Two reasons are:

1. The correlations for estimating the tray holdups are empirical and do not seem very reliable. For example, this applies to the formula for estimating the froth density.
2. Even with a good model for estimating the tray holdups, the dynamic response, for example as expressed by λ , is very sensitive to small changes in the parameters.

This means that one cannot expect to be able to predict from tray data alone whether one will have an inverse response to changes in boilup.

In general, the inverse response is undesirable so one would like to have $\lambda < 0.5$. Fortunately, the models give us insight into how the tray design should be changed to achieve this. The reason for the undesired positive contribution to λ is the swelling due to bubbles. This effect seems difficult to avoid and is probably desirable to improve mass transfer. To make λ more negative one needs to increase the downcomer holdup as vapor flow is increased. This may be achieved by using a larger downcomer area or by increasing the pressure drop over the trays (e.g. by using smaller holes in the plates). Another alternative, which may be more attractive, is to use a packed column where liquid holdup generally increases with vapor flow, implying that λ is generally negative.

For control purposes one may want τ_L large as this increases the liquid lag from the top to the bottom of the column, and thus tends to decouple the dynamic response in

the two column ends. To increase τ_L one may increase M_{ow} by using a shorter outlet weir. Alternatively, one may increase the pressure drop under the downcomer to increase the term M_{loss} . For packed columns all the liquid contributes to the liquid lag, τ_L (as there is no holdup under the weir or in the downcomer), so although the liquid holdup in a packed column is generally smaller than in a trayed column, the decoupling effect from the liquid flow dynamics (as expressed by τ_L) may not be any less.

In conclusion, the dynamic simulations based on a detailed model gave good agreement with experimental responses, while it was found that simpler models based on constant molar flows and linear tray hydraulics gave quite large deviations. Better correlations are needed for predicting the holdup on the trays for the rigorous model. However, even with improved correlations one cannot expect to get accurate predictions of the flow behavior (e.g. λ) because of strong sensitivity to parameter changes. One will therefore in most cases need experimental data to validate the responses and possibly adjust parameters in the model for the tray hydraulics.

Bibliography

1. ASPEN PROPERTIES PLUS; User Guide; Release 8, Aspen Technology, Inc., Cambridge, USA, 1988
2. Baber, M.F., Edwards, L.L., Harper, W.T., Witte, M.D., Gerster, J.A.; Experimental Transient Response of a Pilot Plant Distillation Column, *Process Dynamics and Control*, 1961, **57**, No. 36, pp. 149-159.
3. Baber, M.F., Gerster J.A.; Experimental Transient Response of a Pilot Plant Distillation Column: Part II. Response to Liquid and Vapor Rate Perturbations, *AIChE Journal*, 1962, **8**, No.3, pp. 407-415.
4. Bennett, D.L., Agrawal, R., Cook, P.J., New Pressure Drop Correlations for Sieve Tray Distillation Columns,, *AIChE Journal*, Vol.29, No. 3, pp. 434-443, 1983
5. Coulson, J.M., Richardson, J.F., Sinnott, R.K., Chemical Engineering, Volume 6, Design, *Pergamon Press*, 1985

6. Gani, R., Ruiz, C.A., Cameron, T., A generalized Model for Distillation Columns - I: Model Description and Application, *Computers & Chemical Engineering*, Vol. 10, No. 3, pp. 181-198, 1986
7. Hales, J.L., Ellender, J.H., Liquid densities from 293 to 490 K of nine aliphatic alcohols, *J. Chem. Thermodynamics*, Vol. 8, pp. 1177-1184, 1976
8. Liebson, I., Kelly, R.E., Bullington, L.A., How to design perforated trays, *Petrol. ref.*, Vol. 36, No. 127, 1957
9. Lockett, M.J., Distillation tray fundamentals, *Cambridge University Press*, 1986
10. Majer, V., Svoboda, V., Enthalpies of Vaporization of Organic Compounds, *Chemical Data Series*, No. 32, 1985
11. Perry, H.P., Green, D., Perry's Chemical Engineers' Handbook, *McGraw-Hill Chemical Engineering Series*, 50th edition, 1984 Chapter 18
12. Rademaker, O., Rijnsdorp, J.E., Maarleveld, A., Dynamics and Control of Continuous Distillation Units, *Elsevier, Amsterdam*, 1975
13. Retzbach, B. Mathematische Modell von Destillationskolonnen zur Synthese von Regelungskonzepten, *VDI Fortschrittberichte*, Reihe 8: Mess-, Steuerungs- und Regelungstechnik, Nr. 126, 1986
14. Skogestad, S., Morari, M., Understanding the Dynamic Behavior of Distillation Columns, *Ind. & Eng. Chem. Research*, 1988, No. 10, Vol. 27, pp. 1848-1862
15. Skogestad, S., Dynamics and Control of Distillation Columns - A critical Survey, *IFAC-Symposium DYCORN⁺ '92*, Maryland, 1992
16. SPEEDUP Release 5.3 User Manual, *Prosys Technology Ltd.*, 1992
17. Stichlmair, J., Grundlagen der Dimensionierung des Gas/Flüssig Kontaktapparates Bodenkolonnen, *Verlag Chemie, Weinheim, New York*, 1978

Notation

A	area	m^2	L_i	molar liquid flow of component i	$kmol/h$
C_0	discharge coefficient		M	molar holdup	$kmol$
d	diameter	mm	MW	molecular weight	$kg/kmol$
F_i	molar feed flow of component i	$kmol/h$	N	Number of trays	
g	standard acceleration of gravity	m/s^2	p	pressure	bar, N/m^2
h	molar enthalpy	$GJ/kmol$	q	liquid flow	m^3/s
h	height	mm	T	temperature	$^{\circ}C$
K	equilibrium constant		v	velocity	m/s
k	constant		V	molar vapor flow	$kmol/h$
K_s	dimensionless velocity		Vol	volume	m^3
l	characteristic length	mm	$y_{eq,i}$	equilibrium molar fraction vapor	
			y_i	molar fraction of component i	

x_i molar fraction of component i
 z_i molar fraction of component i

Greek Symbols

Δ pressure drop N/m^2
 ρ_m liquid mass density kg/m^3
 ρ liquid molar density $kmol/m^3$
 ϕ froth density
 θ time delay s
 λ vapor constant
 τ time constant s
 π empirical parameter

Subscripts

a downcomer apron area
cl clear liquid

d, dc downcomer
dry parameter related to dry pressure drop
eq equilibrium composition
h hole area of the tray
i identifier
in flow into the system volume
n index for number of components
l liquid phase
loss hydrodynamic losses
out flow out of the system volume
ow over weir
seal seal pan of downcomer
stage stage consisting of tray and downcomer
t tray
tot total
uw under weir
v vapor phase
weir weir geometry